New pathophysiological concepts and potential therapeutic targets for oxidative phosphorylation disorders

New pathophysiological concepts and potential therapeutic targets for oxidative phosphorylation disorders

ISBN 978-90-8891-411-9
Cover design: Tony Houbrechts
Lay-out: An Voets
Printed by: Proefschriftmaken.nl

The studies described in this thesis were supported by IOP Genomics grant IGE05003, the Interreg IV program (project EMR.INT4) and the Kerry foundation and were performed within the CARIM School for Cardiovascular Diseases and the Faculty of Health, Medicine and Life Sciences of Maastricht University.

New pathophysiological concepts and potential therapeutic targets for oxidative phosphorylation disorders

Proefschrift

ter verkrijging van de graad van doctor
aan de Universiteit Maastricht
op gezag van de Rector Magnificus,
Prof. mr. G.P.M.F. Mols
volgens het besluit van het College van Decanen
in het openbaar te verdedigen
op 24 mei 2012 om 10.00u

door

An Mieke Voets
Geboren op 8 juni 1984 te Bilzen

Promotor
Prof. Dr. H.J.M. Smeets

Copromotor
Dr. I.F.M. de Coo

Beoordelingscommissie
Prof. dr. G. J. van der Vusse (UM) (voorzitter)
Prof. dr. H. H. W. Schmidt (UM)
Prof. dr. F. J. van Schooten (UM)
Prof. dr. B. Wieringa (Radboud UMC Nijmegen)

It won’t be soon before long
Maroon 5

Table of contents

Chapter 1

General Introduction

Oxidative phosphorylation disorders

Mitochondrial disorders are characterized by a broad spectrum of multisystem clinical features, sometimes clustered into a syndrome but more often not. They affect at least 1 in 5000 individuals and are associated with a deficiency of the oxidative phosphorylation (OXPHOS) system [1]. Therefore, they will be further referred to as OXPHOS disorders. Mitochondrial OXPHOS is essential for aerobic energy production in virtually all cells. During this process, oxidation of electron carriers nicotinamide adenine dinucleotide (NADH) and flavin adenine dinucleotide ($FADH_2$), reduced during metabolism of carbohydrates, fatty acids and proteins, drives the production of ATP. The OXPHOS system is composed of five complexes of which the subunits are encoded by both the mitochondrial and nuclear DNA (except for complex II, which is entirely encoded by nuclear DNA). Accordingly, OXPHOS disorders can be caused by mutations in both genomes. Because mitochondria are the main providers of energy, tissues with high energy demands are affected most often in OXPHOS disorders. These organs include the brain, heart, liver and muscle [2]. The consequences of pathogenic mutations can be tissue specific as different metabolic thresholds, depending upon the energy demand, apply for the different tissues [3]. However, this is not the sole factor involved and the mechanism behind the tissue specificity is not entirely clear. Thus, OXPHOS disease is usually multisystemic and the variety of clinical features includes, among others, encephalopathy, stroke, epilepsy, optic atrophy, deafness, neuropathy, myopathy, cardio-myopathy, exercise intolerance, diabetes and liver failure (figure 1.1) [4]. A few specific syndromes could be defined (table 1.1) but most often OXPHOS disease is not so well delineated [4]. Furthermore, there is most often no cure and the treatment options for even delaying OXPHOS disorders are limited.

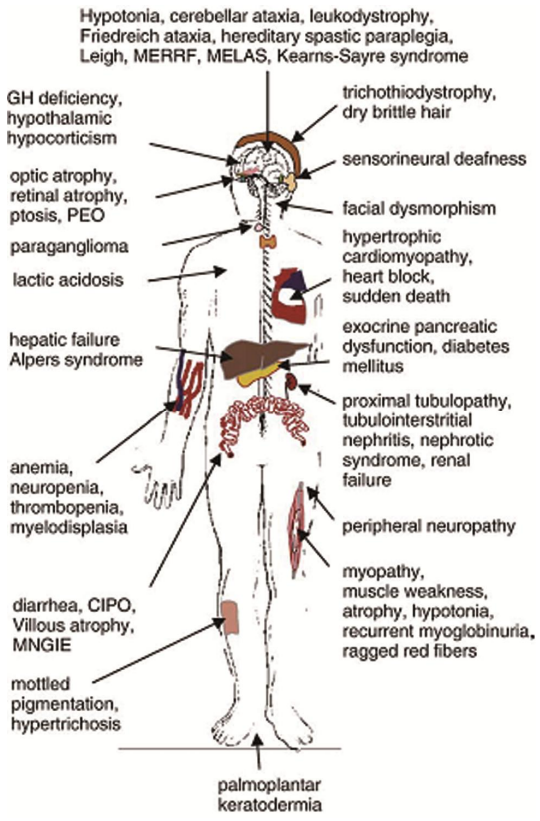

Figure 1.1. Potential clinical features associated with OXPHOS disease (adapted from [5])**.**

Table 1.1. Examples of common OXPHOS syndromes.

Syndrome	OMIM #	Genetic cause		Symptoms
		mtDNA	nDNA	
PEO (progressive external ophtalmoplegia)	258450 157640 609283 609286 610131 613077	Multiple heteroplasmic deletions	*POLG1*, *ANT1*, *TWINKLE*, *RRM2B*	Age of onset: between 20 – 50 years old External opthalmoplegia and bilateral ptosis often accompanied by proximal muscle weakness and exercise intolerance
MELAS (mitochondrial encephalomyopathy, lactic acidosis and stroke-like episodes)	540000	Heteropl. *MTTL1* (*3243A>G), *MTTQ*, *MTTH*, *MTTK*, *MTTS1*, *MTTS2*, *MTND1*, *MTND5*, *MTND6*		Age of onset: neonatal – 40 years Stroke-like episodes with seizures and/or dementia and ragged red fibers and/or lactic acidosis, often accompanied by diabetes mellitus, cardiomyopathy, external ophtalmoplegia, cortical blindness, cerebellar ataxia and retinitis pigmentosa
MERRF (myoclonus epilepsy with ragged red fibers)	545000	Heteropl. *MTTK* (*A8344G), *MTTL1*, *MTTH*, *MTTS1*, *MTTS2*, *MTTF*, *MTND5*		Age of onset: late childhood to adulthood Myoclonic seizures, cerebellar ataxia and myopathy, spasticity, dementia, hearing loss, optic atrophy, short stature and cardiomyopathy,
NARP (neuropathy, ataxia and retinitis pigmentosa)	551500	Heteropl. *ATP6* (*T8933G/C)		Age of onset: infancy or early childhood Developmental delay, retinitis pigmentosa, dementia, seizures, ataxia, proximal muscle weakness, mental retardation, sensory neuropathy and ragged red fibers
KSS (Kearns Sayre syndrome)	530000	Heteroplasmic rearrangements (deletions), *MTTL1*		Age of onset: before 20 years old retinitis pigmentosa, progressive external ophtalmoplegia (PEO) and the presence of at least one of the following: cardiac conduction block, elevated cerebrospinal fluid protein, or cerebellar ataxia

Pearson syndrome	557000	Heteroplasmic rearrangements (deletions)		Age of onset: neonatal Sideroblastic anemia and exocrine pancreas dysfunction, failure to thrive, lactic acidosis
LS (Leigh syndrome)	256000	*MTATP6* (*T8933G/C), *MTND2*, *MTND3*, *MTND5*, *MTND6*, *MTCO3*, *MTTV*, *MTTK*, *MTTW*, *MTTL1*	*NDUFV1*, *NDUFS1*, *NDUFS3*, *NDUFS4*, *NDUFS7*, *NDUFS8*, *NDUFA2*, *C8ORF38*, *C20ORF7*, *SDHA*, *BCS1L*, *COX10*, *COX15*, *SCO2*, *DLD*, *SURF1*, *TACO1*, *PDHA1…*	Age of onset: 3 months – 2years old Recurrent attacks of psychomotor regression with seizures, dystonia and brainstem dysfunction, lactic acidosis and hypotonia, ataxia, respiratory failure, retinitis pigmentosa and spasticity. Typical CT or MRI abnormalities with bilateral symmetric signal alterations in the basal ganglia, thalamus, midbrain and brainstem
LHON (Leber hereditary optic neuropathy)	535000	Homopl./heteropl. *MTND1* (*G4360A), *MTND4* (*G11478A), *MTND6* (*T14484C), *MTND2*, *MTND4L*, *MTND5*, *MTCO1*, *MTCO3*, *MTCYB*, *MTATP6*		Age of onset: midlife, mean 27 – 34 years old (range 1 – 70 years old) (Sub)acute, painless central vision loss, sometimes cardiac arrhythmia, non-specific myopathy, dystonia and ataxia
MNGIE (mitochondrial neurogastrointestinal encephalomyopathy)	603041		*POLG1*, *TP*	Age of onset: 20 – 50 years old Ptosis, progressive external ophthalmoplegia, gastrointestinal dysmotility (often pseudoobstruction), cachexia, diffuse leukoencephalopathy, peripheral neuropathy and myopathy
MDS (mitochondrial depletion syndrome)	609560 251880 612073		*DGUOK*, *MPV17*, *TWINKLE*, *TK2*, *SUCLA2*, *POLG1*	Age of onset: few weeks after birth Hepatocerebral form: early progressive liver failure and neurologic abnormalities, hypoglycemia and increased lactate in body fluids; Myopathic form: progressive generalized hypotonia, progressive external ophthalmoplegia, and severe lactic acidosis

AR = autosomal recessive, AD = autosomal dominant; * = primary mutations; adapted from [6].

Mitochondrial DNA

The mitochondrial genome is a double-stranded, circular molecule consisting of 16.569 base pairs and coding for 13 subunits of the OXPHOS complexes, two rRNAs and 22 tRNAs, required for mitochondrial translation (figure 1.2). The mitochondrial DNA (mtDNA) has a number of unique characteristics that discriminate it from nuclear DNA (nDNA).

- The mtDNA is polyploid. A mitochondrion contains five to ten copies of mtDNA and a cell can contain hundreds to thousands of mitochondria. All mtDNA molecules can be identical (homoplasmy) or mixtures of wild and mutant type base pairs can be present in a cell (heteroplasmy).
- mtDNA encoded genes do not have introns and several of them are overlapping. Less than ten percent of the genome is non-coding and is predominantly located in the displacement (D)-loop, involved in the replication and transcription of the mtDNA. Transcription of mtDNA can occur on both (heavy and light) strands, starting from the mitochondrial promotors, and produces polycistronic precursor RNA. This RNA is subsequently processed into individual tRNA, rRNA and mRNA molecules.
- mtDNA is maternally inherited.
- Replication of mtDNA is called relaxed as it is not connected to the cell cycle.
- mtDNA molecules lack histones and other protective proteins. In combination with its location nearby the reactive oxygen species (ROS)-producing OXPHOS system and less efficient DNA repair mechanism, this leads to higher mutation frequencies in mtDNA compared with nDNA.

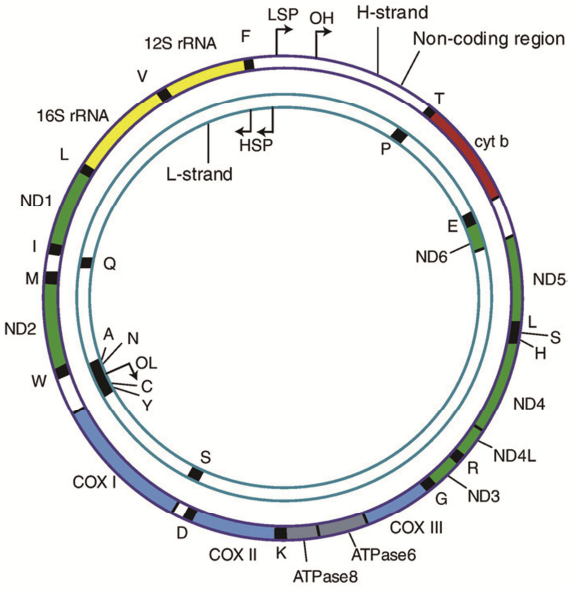

Figure 1.2. The mitochrondrial genome. Complex I (ND) genes are shown in green, the complex III *Cyt b* in red, complex IV (COX) genes in light blue, complex V (ATPase) genes in grey, rRNA genes in yellow and tRNA genes in black. Adapted from [7].

Clinically relevant mtDNA variations fall into five categories: 1) *de novo* or maternally inherited deleterious point mutations (mainly substitutions); 2) ancient adaptive polymorphisms that predispose individuals to disease in different environments; 3) single or multiple mtDNA deletions affecting multiple mtDNA encoded genes; 4) duplication of part of the mtDNA molecule [8] and 5) differences in mtDNA copy number, which when extremely decreased is called mtDNA depletion. These variations can occur separately or in combination (*e.g.* m.3243A>G and reduced mtDNA copy number [9]).

As a result of the exclusive maternal inheritance of mtDNA, OXPHOS disease due to mtDNA mutations is transmitted through the maternal lineage. The majority of pathogenic mtDNA variations are heteroplasmic, although a growing list of homoplasmic pathogenic mutations, including the more frequent occurring LHON mutations, exists. However, the variable penetrance of homoplasmic pathogenic mutations implies the presence of modifiers. Modifiers can be of mtDNA or nDNA origin and probably involve one or more polymorphisms that do not necessarily induce pathology on themselves [10]. For heteroplasmic mutations, a certain heteroplasmy threshold level is necessary before respiratory defects or tissue dysfunction become apparent, depending on the aerobic energy need of a tissue. Often, a higher proportion of mutant mtDNA will lead to a more severe biochemical defect and/or clinical phenotype [11], but an exact correlation is lacking [12]. When new mtDNA variants are identified in patients, a number of criteria (box 1) are checked to determine their pathogenicity. However, there are many examples of pathogenic mtDNA variants in literature that do not fit all of the current pathogenicity criteria, which particularly challenges the genetic counseling of families [13, 14].

Box 1. Pathogenicity criteria for mtDNA point mutations [14]

- Mutation must be present in patients and absent in controls
- Mutation must be found in different mitochondrial genetic backgrounds
- Mutation must be the best mtDNA candidate variant to be pathologic
- The percentage of the mutation must correlate with the phenotype
- Mutation must affect highly evolutionary conserved nucleotides
- Mutation must affect functionally important domains
- The transfer of the mutated mtDNA to another cell line must be accompanied by the transfer of the cell or molecular defect

Nuclear genes involved in oxidative phosphorylation

In contrast to the extensively studied and characterized mitochondrial genome, the list of nuclear encoded OXPHOS-related genes is less complete. Nuclear genes involved in OXPHOS function code for structural components of the OXPHOS complexes (*e.g. NDUFV1*, *NDUFS4*, *SDHA*), assembly factors of OXPHOS complexes (*e.g. SURF1*, *C20orf7*, *BCS1L*), factors involved in mtDNA replication and maintenance (*POLG1*,

TWINKLE, mtSSB) and proteins involved in the mitochondrial nucleotide balance (*ANT1*, *DGUOK*, *TK2*, *TP*, *SUCLA2*), mtDNA transcription (*e.g. POLRMT*, *TFAM*) and translation (*e.g. PUS1*, *EFG1*, *MRPS16*). Furthermore, there are also several nuclear genes that are indirectly related to respiration and energy production by mitochondria. This group includes genes coding for mitochondrial metalloproteases, mitochondrial import/export proteins, mitochondrial iron-storage proteins and proteins associated with mitochondrial fusion and fission. Mutations in these genes are associated, among others, with spastic paraplegia (*SPG7*), Friedreich's ataxia (*FRDA*), X-linked sideroblastic anemia and ataxia (*ABC17*) and optic atrophy (*OPA1*) [15].

Diagnostic strategy in suspected OXPHOS disease

Because of the variety in clinical manifestations of OXPHOS disease, diagnosis often requires a multidisciplinary approach. No single symptom is specific for OXPHOS disease or is able to distinguish it from other disorders, but when combinations of common chronic and unexplained symptoms (such as migraine, diabetes, deafness) occur, the possibility of OXPHOS disease should be considered [16, 17]. When clinical suspicion of OXPHOS disease arises, a number of investigations, including histochemical, biochemical and genetic analysis, can lead to the eventual diagnosis (figure 1.3).

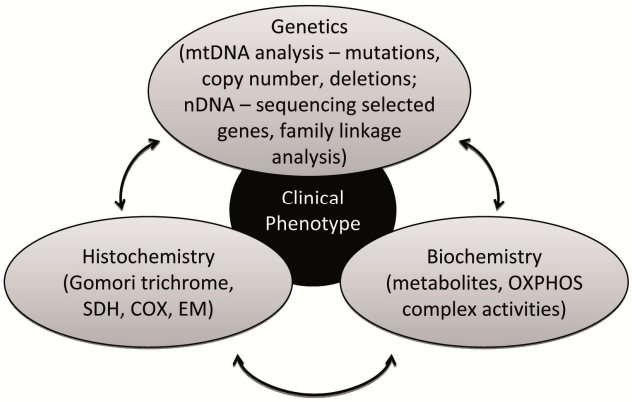

Figure 1.3. Diagnosis of OXPHOS disease needs a multidisciplinary approach. SDH = succinate dehydrogenase, COX = cytochrome C oxidase, EM = electron microscopy

Histochemical investigations

Histochemical assays are used to detect abnormal focal accumulation of mitochondria or low activity of respiratory chain enzymes in skeletal muscle biopsies. The red Gomori trichrome staining visualizes accumulation of focal subsarcolemmal mitochondria such as the so-called ragged red fibers (RRFs) which presumably denote a decrease of

energy production [18]. However, RRFs have also been described in healthy individuals and are only seldom observed in young children with mitochondrial disease, making interpretation by an expert necessary [17, 18]. Combined histoenzymatic reactions for succinate dehydrogenase (SDH) and cytochrome c oxidase (COX) typically result in a mosaic appearance of abnormalities but may be helpful in visualizing COX-negative fibers with mitochondrial proliferation (increased SDH staining). Histochemical investigations can provide additional evidence for a diagnosis of OXPHOS disease.

Biochemical assays

An initial biochemical examination in patients suspected of OXPHOS disease is a metabolic screening including the measurement of the metabolites lactate, pyruvate and alanine in blood, urine or cerebrospinal fluid and the measurement of organic acids in urine [16]. OXPHOS dysfunction leading to a disturbed oxidation ratio of NADH to NAD^+ results in feedback inhibition of pyruvate metabolism in the mitochondria. The excess pyruvate is transported back into the cytosol. Here it is metabolized into lactate or converted into alanine, which leads to an increase of these metabolites in body fluids [16]. The increase in the NADH/NAD^+ ratio or the reduced oxidation rate of $FADH_2$ may also lead to a metabolic arrest of the Krebs cycle leading to an increase and subsequent excretion of intermediates of the citric acid cycle in urine. Furthermore elevated levels of ethylmalonate and 3-methylgluconate are frequently found in mitochondrial patients [19]. However, due to the limited specificity of the initial screen, definite biochemical investigations are performed, preferably in a skeletal muscle biopsy or in fibroblasts when no muscle sample is available. Biochemical investigations in muscle may include the measurement of overall oxygen consumption, radio-labeled substrate oxidation or ATP synthesis by the OXPHOS system in fresh muscle biopsies and measurement of the activities of individual respiratory chain enzymes in frozen muscle homogenates. Assessing overall oxygen consumption, substrate oxidation and ATP synthesis in mitochondria require an intact mitochondrial membrane and is thus only applicable in fresh muscle biopsies [16]. The spectrophotometric assays of the activities of the individual complexes in muscle/fibroblast homogenates are based on the specific kinetic measurement of the velocity of the oxidation or reduction of the physiological substrates by the use of specific inhibitors of the individual complexes [18]. Interpretation of the individual complex measurements is rather difficult because there is only a narrow margin between control and patient ranges. Due to a large variation of absolute activities in samples which may be due to a large variation in the amount of mitochondria, the activity of the different complexes is expressed relative to the activity of another respiratory chain complex (usually complex II or IV) or citrate synthase. The severity of the enzyme deficiency is not necessarily linked to the severity of the clinical phenotype, therefore it is also important to detect even mild deficiencies. Furthermore, it is important that the different complexes or electron carriers are in a strict equilibrium for a sustained continuous and efficient substrate oxidation. Any imbalance can result in increased superoxide production or a decrease in respiration [18]. Available methods to measure superoxide production and its consequences are mainly based on HPLC analysis [20], probe (*e.g.* hydroethidine) oxidation [21, 22], mass spectrometry [23] and immunology [21].

Genetic analysis

In general, according to the clinical phenotype of a patient, a standard mtDNA analysis is performed first. This includes screening for common mtDNA point mutations (m.3243A>G, m.8344A>G, m.8993T>G/C and LHON mutations) in blood using restriction fragment length polymorphism (RFLP) analysis or pyrosequencing, which allow for the accurate quantification of heteroplasmy levels. Furthermore, the presence of mtDNA deletions in blood or muscle can be detected with long range PCR. The mtDNA copy number is determined by quantitave PCR (QPCR) and is represented by the ratio of the number of copies of a mtDNA-encoded gene (*e.g. 12S rRNA*) and the number of copies of a nDNA-encoded gene (*e.g. RNAP*). A decrease of the copy number below 35% of the copy number of age matched controls is called mtDNA depletion [24]. The detection of mtDNA depletion by QPCR and multiple mtDNA deletions by long range PCR warrant the screening of nuclear genes associated with mtDNA replication and/or the clinical phenotype. When the initial mtDNA analysis is negative, the whole mtDNA genome will be analyzed *e.g.* using the Affymetrix mtDNA resequencing chips (MitoChip), preferably in muscle samples. mtDNA variants detected by this method are usually confirmed by conventional Sanger sequencing. In the absence of pathogenic mtDNA mutations or based on the clinical phenotype, nuclear OXPHOS genes are being screened. In case the phenotype resembles that of patients for which a pathogenic mutation has been described previously (*e.g. POLG1*, *ANT*), the corresponding gene is screened by direct sequencing of the exonic regions. When no good candidate gene can be found in literature and multiple individuals of a family present a similar phenotype, linkage (single nucleotide polymorphism (SNP)) analysis can be performed to identify new candidate genes. Usually, this results in multiple candidate genes which are screened for mutations by direct sequencing. Recently, exome sequencing is used on itself or in combination with linkage studies to find pathogenic DNA variations in a high throughput manner [25]. Once a pathogenic mutation (mtDNA or nDNA) is identified, family members of the index patient will be examined and for mtDNA mutations, accurate heteroplasmy levels will be determined.

Pathophysiology

The clinical manifestation of OXPHOS disorders can occur immediately at birth, deteriorate progressively during life or be triggered by a number of events. These triggers of full-blown OXPHOS disease include viral infections [26, 27] and adverse effects of drugs, *e.g.* valproic acid induced liver failure in patients with mutations in *POLG1* [28], mtDNA depletion due to nucleotide reverse transcriptase inhibitors (NRTIs) for the treatment of human immunodeficiency virus (HIV) [29]).

There are a number of approaches to study the pathophysiology of OXPHOS disorders. In the past, pathophysiology was mainly studied in a ‘hypothesis-driven’ manner. A hypothesis was posed based on existing incomplete knowledge and tested in carefully designed experiments. Accordingly, the hypothesis could be falsified and rejected or supported by the data. At present, the use of ‘discovery-driven’ research is emphasized. This includes a systems biology approach, studying the interactions of

large numbers of molecules (DNA, mRNAs or proteins) that constitute the biological system and using data mining to generate (new) hypotheses by induction. High-density measurement technologies such as whole genome gene expression microarrays, high performance liquid chromatography and mass spectrometry are indispensible for this approach. Ultimately, the new hypotheses and theories that arise inductively should be tested in a 'hypothesis-driven' manner to lead to valid knowledge [30]. Finally, animal models have been very useful to study pathophysiology *in vivo* and to examine the effect of potential therapeutic or adverse drugs [31-35].

So far, research on OXPHOS pathogenesis has led to the identification of a number of biological processes that are assumed to play a role in OXPHOS disorders. Altogether, a dysfunctional OXPHOS system can increase the production of ROS [22, 36], can lead to abnormal mitochondrial fission/fusion [37] and a disturbed mitochondrial membrane potential [38] and will be unable to supply sufficient ATP to meet cellular needs (figure 1.4). Part of this ATP is necessary to fuel cellular import and export of key metabolites and inorganic ions such as calcium [39]. Eventually, increased oxidative stress, a dysfunctional mitochondrial membrane potential and impaired calcium homeostasis can culminate in apoptosis [40] (figure 1.4). In general, changes in oxidative stress and apoptosis co-exist with a deficiency of at least one OXPHOS complex [41-44], but the OXPHOS deficiency is not required for their involvement in the pathogenesis [45].

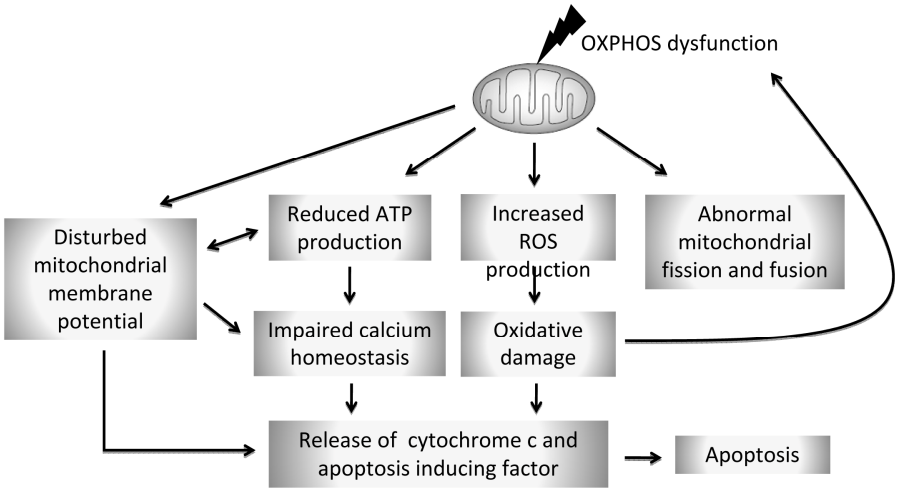

Figure 1.4. Physiopathological processes involved in OXPHOS disease.

Oxidative stress

Although ROS are generated by multiple other enzymes and processes in a cell, *e.g.* NADPH oxidases and lipid metabolism, it has been estimated that mitochondria produce most (~90%) of cellular ROS at complexes I and III [46]. In the process of oxidative phosphorylation, oxygen is consumed for the production of ATP. In physiological conditions, approximately 0.2% of the total consumed oxygen is

converted to ROS (superoxide anion and hydrogen peroxide). Any disturbance of the electron transport chain can increase the production of ROS [46]. Previously, ROS were considered to be merely harmful because of their capacity to oxidize DNA, lipids, carbohydrates and proteins [47]. Oxidation of these macromolecules will lead to mutagenesis [48], diminished functioning [49, 50] and loss of structural integrity [49]. However, ROS *per se* are not always a negative given. Nowadays, ROS are also believed to play a role as redox messengers in several signaling pathways leading to cellular adaptation, *e.g.* muscle fiber adaptation in response to both increased contractile activity and prolonged periods of muscle disuse [51].
To keep a balance between its role in signaling and toxic effects, ROS levels are tightly monitored and regulated by the antioxidant defense system. An overview of the most familiar contributors to the mitochondrial antioxidant defense system is depicted in figure 1.5. Superoxide ($O_2^{\cdot-}$) produced at sites from complex I and III will be dismutated to hydrogen peroxide (H_2O_2) by superoxide dismutase (SOD) in the mitochondrial matrix (Manganese (Mn) SOD) or cytosol (Copper/Zinc (Cu/Zn) SOD). Hydrogen peroxide can be converted by catalase (CAT) in the cytosol and the glutathione and thioredoxin detoxification systems in the mitochondrial matrix. Hydrogen peroxide that is not converted to water can lead to the formation of highly reactive hydroxyl radicals ($OH^{\cdot}$) through the Fenton reaction.

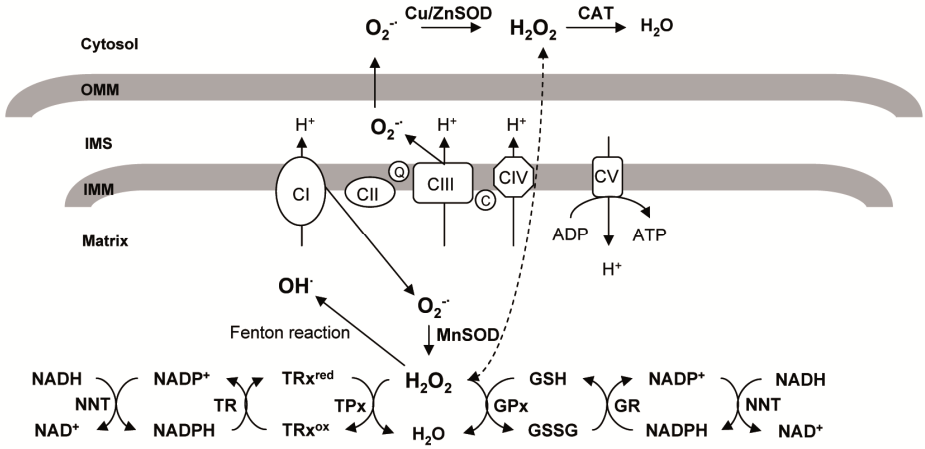

Figure 1.5. Mitochondrial antioxidant defense system. OMM = outer mitochondrial membrane, IMS = inner membrane space, IMM = inner mitochondrial membrane, GSH = reduced glutathione, GSSG = oxidized glutathione, GPx = glutathione peroxidase, GR = glutathione reductase, NNT = nicotinamide nucleotide transhydrogenase, TRx^{red}/TRx^{ox} = reduced and oxidized thioredoxin, respectively, TPx = thioredoxin peroxidase, TR = thioredoxin reductase.

Since OXPHOS disorders are characterized by disturbances in the electron transport chain, various studies have examined the role of oxidative stress in their pathogenesis (table 1.2). Although some addressed the question whether or not oxidative stress is actively involved in causing disease phenotypes, their results do not always

correspond. Several reasons can be given for this. First of all, some studies examined only two or three similar oxidative stress parameters. In order to get an impression of the oxidative status of a cell or tissue, three categories of parameters, *i.e.* ROS levels, antioxidant system levels and oxidative damage levels, should be documented. Especially the last read-out will give valuable information on how patients suffer from the consequences of oxidative stress. Another problem for comparing different experiments is the variety of protocols to measure one specific parameter, *e.g.* DNA oxidation can be determined by HPLC, ELISA, mass spectrometry, western blot and immunohistochemistry, each with its own advantages, disadvantages and limitations. Measurements with different protocols do not always give comparable results [47]. Finally, the examined tissue and the small sample size of the cohorts can also contribute to conflicting results. Conclusively, as can be appreciated from table 1.2, some OXPHOS disorders (MELAS, MERRF and NARP) show more evidence for the presence of oxidative stress and concomitant damage than others (*POLG1* and *SURF1* mutations). As there is no consensus, it is recommended to analyze a number of carefully chosen stress parameters, as indicated above, in parallel using the same methods in different OXPHOS disorders [52]. As a result, one will be able to compare the involvement of oxidative stress in each of those diseases and thus evaluate the relevance of antioxidant therapy.

Table 1.2 legend. The involvement of oxidative stress parameters (production, defense and damage) in different OXPHOS disorders as documented in literature.

↑ = increased, ↓ = decreased, N = normal, MnSOD = mitochondrial superoxide dismutase, CuZnSOD = cytosolic superoxide dismutase, GPx = glutathione peroxidase, GR = glutathione reductase, GST = glutathione S transferase, GSSG = oxidized glutathione, GSH = reduced glutathione, 8-OHdG = 8-hydroxy-2deoxy guanosine, 4-HNE = 4-hydroxynonenal, MDA = malondialdehyde

[+] F = fibroblasts, M = muscle, C = cybrids, Bl = blood, L = lymfocytes, My = myoblasts, Br = brain, Mi = mice

* p = number of patients, m = number of different mutations, cl = number of cell lines with different heteroplasmy percentage

Table 1.2. Overview of the role of oxidative stress in OXPHOS disorders (legend at page 21)

			Reactive oxygen species			Antioxidant defense system												Oxidative damage			
Phenotype or affected gene or OXPHOS complex	**Tissue[+]**	**n = ***	**Superoxide**	**Hydrogen peroxide**	**Hydroxyl radical (OH)**	**MnSOD activity**	**MnSOD expression**	**CuZnSOD activity**	**CuZnSOD expression**	**Catalase activity**	**Catalase expression**	**GPx activity**	**GPx RNA**	**GR activity**	**GST RNA**	**GST activity**	**GSSG/ GSH**	**8-OHdG**	**Lipid peroxides or aldehyde levels (hexanal, 4-HNE, MDA)**	**Protein carbonyls**	**Reference**
Complex I	F	21 p	↑/↓																		[22]
deficiency	F	10 p															N		N		[53]
	F	13 p	↑/↓				↑/N														[42]
	F	1 p				N		N													[54]
	C	3 p, 3 m	↑																	↑	[55, 56]
	F	3 p	↓		↑		↑												↑		[57]
	C	7 p, 3 m				↓	N	↓	N/↑	N		N/↓		↓			N (↑ in galact.)				[58]
	L	6 p	↑	↑		↑	↑	↑	↑/N	↓	↑	↓	↑	N	↑	N	N				[59]
Complex II deficiency	F	1 p				↑	↑	↑													[54]
Complex III deficiency	F	1 p				N		N													[54]
MERRF	F	3 p				↓	↓			↓	↓	N	N								[60]
	M	1 p					↑		↑								↑				[61]
	F	4 p		↑			↑				N		N								[62]
	C	1 p		↑		↑	↑	↑	↑	↑	N	↑							N	N	[36]
MELAS	M	2 p					↑		↑								↑				[61]
	C	1 p, 5 cl															↑		↑		[63]

	M	14 p	↑			N		N		N		N		N				↑	[21]
	My+Bl	4 p 17 p			↑		↑		N/↑										[43]
	Bl	1 p				↑		↑			↑								[44]
	Mi	2		↑	N/↑		N/↑		N		N								[64]
	M	1 p	↑																[65]
	Br	11 p				↓											↑		[66]
	C	1 p		↑	↑	↑	↑	↑	↑	N	↑							N	[36]
NARP	F	2 p			↑	↑	↑		N		N				N				[54]
	F	2			↑		↑												[67]
	C	?		↑	↑		N											↑	[41]
	C	1 m	↑	↑		↓		↑		↓	↑	N							[68]
SURF1	F	1 p			N		N												[54]
	M	8 p	↑			N		N		N		N		N				N	van Eijsden, unpublished
	M	3 p				↑		↑			↑								[44]
POLG	Mi	9		N													N	N	N	[33]
	Mi	?	N	N		N						N							N	[69]
	Mi	6															↑			[70]
CPEO	F	6 p			↑	↑			N	N	N	N								[60]
	F + M	8 p	↑	↑	↑	↑	N	N	N	↑	N	N					↑			[71]
	M	14 p				↑		↑							↑					[61]
	M	4 p				↑											↑	↑		[72]
	Bl	11 p													GSH ↓			↑		[73]
	C	1 p, 5 cl															↑	↑		[74]

Apoptosis

Mitochondria are at the crossroads of apoptosis (programmed cell death) regulation. The intrinsic mitochondrial apoptosis pathway can be initiated by a number of signals including DNA damage, growth factor deprivation and oxidative stress [75]. In short, mitochondrial outer membrane permeabilization leads to the release of soluble mitochondrial intramembrane proteins, such as cytochrome c, that trigger the proteolytic caspase cascade and cause inactivation of the electron transport chain [76]. Multiple studies have shown the involvement of apoptosis in muscle of patients with OXPHOS disorders (PEO [72, 77, 78], MELAS [45, 72, 78], MERRF [45, 78] and KSS [77]). However, patients with comparable phenotypes did not show equal signs of apoptosis in other studies [79-81]. Apoptosis was shown to be the central mechanism of tissue dysfunction in a mtDNA mutator mouse model (*POLG1* D257A knock-in) [33], but embryonic fibroblasts from transgenic mice with the same mutation were not more susceptible to undergo oxidative stress induced apoptosis than wild type mouse embryonic fibroblasts [69].

Altogether, the current results on the role of apoptosis in OXPHOS disorders are not straightforward and point to a dysregulation of apoptotic decisions rather than increased apoptosis on itself. One theory could be that damaged cells which should die, sometimes fail herein whereas some healthy cells become apoptotic without valid reason. This compromises physiological functions and could also favor replicative senescence [82].

Examples of pathophysiological models for OXPHOS disorders

In the next three paragraphs, three of the most frequent OXPHOS disorders will be described in more detail, including clinical phenotype, genetic cause and recent research on the molecular processes involved. Patients with isolated complex I (CI) deficiency, mitochondrial encephalomyopathy, lactic acidosis and stroke-like episodes (MELAS) patients and polymerase gamma (*POLG1*) patients represent three different disease classes *i.e.* defects in OXPHOS enzyme activity, mitochondrial protein translation due to a tRNA mutation and mtDNA maintenance, respectively. As a relatively high number of patients presents with these disorders, it is relevant to study their pathophysiology in order to improve their treatment options.

Isolated CI deficiency

CI deficiency leads to a number of clinical features including basal ganglia and/or brainstem lesions, respiratory abnormalities, muscular hypotonia, failure to thrive, seizures and lactic academia [83]. Most patients have a normal prenatal development and birth, but will develop symptoms within their first year of life, which are often fatal [38], or less severe symptoms later in life (*e.g.* Leber hereditary optic neuropathy [LHON]). CI deficiency is diagnosed when CI activity in muscle or skin biopsies is decreased compared to control specimen. Decreased CI activity can be caused by

mutations in both the mtDNA and nuclear genes, but often the genetic mutation leading to the deficiency cannot be identified [84].

LHON (table 1.1) is associated with multiple mtDNA mutations, but those most frequent are m.3460G>A, m.11778G>A and m.14484T>C in the *ND1*, *ND4* and *ND6* genes of CI, respectively [85]. LHON mutations are usually inherited and homoplasmic [86]. In mutant LHON cells CI redox activity has been shown to be normal or reduced [87, 88], but the interaction between CI and its ubiquinone substrate (CoQ) might have been affected by the three LHON mutations. This led to a decreased CI dependent ATP synthesis and the overproduction of ROS [85].

In case nuclear genes are involved, the reduced CI activity is primarily caused by lower levels of normal functioning CI instead of a decrease in intrinsic activity of the complex [89]. In resting fibroblasts of CI deficient patients, the overall cellular ATP levels were normal, which suggests that in the normal situation, ATP derived from glycolysis and/or residual CI activity is sufficient in fibroblasts. However, the same study showed that the reduced CI activity led to a depolarization of the mitochondrial membrane potential and reduced Ca^+ content in the endoplasmic reticulum (ER). The authors hypothesized that the ATP supply to the ER Ca^+ (SERCA) pumps was insufficient to maintain normal ER Ca^+ levels which probably influences cellular calcium homeostasis [39]. Furthermore, in CI patients it has been shown that residual CI activity was inversely correlated with the production of ROS (superoxide and superoxide-derived ROS) [22]. Notably, whenever a certain threshold of residual CI activity (and thus ROS production) is passed, mitochondrial morphology changed. In fibroblast cell lines with a relatively 'mild' CI deficiency, mitochondrial morphology was normal or even more elongated, whereas patient cell lines with a severe CI deficiency (and thus higher ROS levels) showed a fragmented mitochondrial morphology. These differences probably coincide with a decreased probability to compensate for increased ROS levels or ROS related damage [38]. An unbiased approach, such as gene expression analysis, will help integrating the current knowledge into a pathophysiological model that might be able to distinguish cause from effect.

MELAS

Although tRNA sequences comprise only a small fraction (~10%) of the mtDNA, more than half of the known pathogenic mtDNA mutations are found within the tRNA genes (MITOMAP database; www.mitomap.org/MITOMAP). The MELAS syndrome is the most common mitochondrial disorder and in 80% of the cases, patients carry the m.3243A>G mutation in the *tRNA Leu(UUR)* gene [90]. Clinical features associated with MELAS include recurrent strokes, CPEO, retinitis pigmentosa, optic atrophy deafness, dementia, extrapyramidal features ataxia epilepsy, myoclonus myopathy, cardiomyopathy, neuropathy, diabetes mellitus, gastrointestinal features (malabsorption and/or dysmotility), short stature and lipomata [11]. In a large patient cohort, a correlation could be observed between clinical features which occurred in >15% of the cases and the level of mutant mtDNA in muscle (n=111) but not in blood (n=73). A positive correlation with mutation percentage was identified for the frequency of recurrent strokes, dementia, epilepsy and ataxia, whereas an inverse correlation was detected for CPEO myopathy and deafness [11]. Another study could not find a

correlation between the percentage of mutated mtDNA and patient characteristics, which could be due to the smaller sample size (n=22). However, they did find a significant inverse correlation between the m.3243A>G mutant load and age of onset and CI activity [91]. Additionally, the m.3243A>G mutation percentage was positively correlated with hyperglycemia in diabetic patients [92].
The m.3243A>G mutation leads to incorrect tRNA processing and enzyme maturation due to disruption of the tertiary tRNA structure. Furthermore, the m.3243A>G mutation impairs taurine modification of the anticodon wobble position which is responsible for precise and efficient codon recognition [93, 94]. Eventually, mitochondrial translation is impaired because of a decreased steady-state of the normal aminoacylated tRNA [95]. The decreased protein synthesis rate will cause decreased enzyme activity and severe respiratory defects [90]. A gene expression study in muscle of symptomatic and a-symptomatic mutation carriers identified increased protein turnover, oxidative stress, apoptosis and complement activation [21]. In a-symptomatic carriers, the amount of protein regeneration and OXPHOS stimulation seemed sufficient to prevent the occurrence of symptoms. However, in symptomatic carriers, excessive protein damage presumably leads to termination of repair/adaptive processes and a switch to muscle regeneration, indicated by stronger complement activation [21]. A more in depth analysis of the oxidative stress (production, scavenging and damage) might be able to fine-tune the current model of MELAS pathogenesis.

POLG1 patients

DNA polymerase gamma (pol γ) is the only DNA polymerase involved in maintenance of the mtDNA and consists of a catalytic subunit and a homodimeric accessory subunit, encoded by the *POLG1* and *POLG2* genes, respectively [96, 97]. Over 150 mutations, which can be of a dominant or a recessive nature, have been detected in the *POLG1* gene (Human DNA Polymerase Gamma Mutation Database http://tools.niehs.nih.gov/polg/). Only recently, Euro and colleagues were able to cluster the recessive mutations into five distinct modules based on the recently solved crystal structure of the enzyme [98]. Mutations in *POLG1* are associated with a series of disorders such as PEO (table 1.1), Alpers-Huttenlocher syndrome, childhood myocerebrohepatopathy spectrum (MHCS) disorders, ataxia neuropathy spectrum (ANS) disorders, myoclonus epilepsy myopathy sensory ataxia (MEMSA) and sensory ataxic neuropathy with dysarthria and ophtalmoplegia (SANDO) [99, 100]. Additionally, *POLG1* mutations have been found to play a role in nucleoside reverse-transcriptase inhibitor (NRTI) [101] and valproic acid [28] toxicity and premature ovarian failure (POF) [102, 103].
Mutations in the exonuclease and polymerase domain of *POLG1* or combinations are associated with decreased mtDNA copy number in liver, muscle and fibroblasts of *POLG1* patients [104]. Decreased nucleotide insertion specificity [105], decreased catalytic activity [105], loss of interaction between the catalytic and accessory subunits [106] due to *POLG1* mutations have been observed *in vitro*. Furthermore, the accumulation of heteroplasmic mtDNA point mutations, which can [107] or cannot [108] stimulate mtDNA deletion formation, in skeletal muscle [107, 108] and cultured human cells expressing *POLG1* fusion proteins [109] have been reported. Whereas complete

knockout mice died prenatally [110], transgenic proofreading deficient mouse models (D257A *POLG1* knock-in) showed accelerated ageing phenotypes with increased levels of mtDNA point mutations without evidence for the involvement of oxidative stress [33, 34]. Human studies are limited to *in vitro* characterization of purified or recombinant enzymes [111], *in vivo* analysis of the functions of the pol γ protein and its domains in cultured cells [109] and large scale screening of mtDNA molecules in skeletal muscle and fibroblasts [104, 107, 108]. These studies point out a higher probability of accumulating mtDNA mutations and/or depleting mtDNA when *POLG1* is mutated. In addition, deficiencies in respiratory chain enzymes have been described in muscle of *POLG1* patients [112]. Up to now, the more integrative studies of POLG pathogenesis are performed solely in mouse. An unbiased top-down approach (*e.g.* whole genome gene expression) may help elucidating processes involved in human POLG pathogenesis. The obtained results will indicate if the same disease mechanisms apply for rodents and human beings.

Therapy in OXPHOS disorders

Although knowledge on OXPHOS disorders and their underlying pathological mechanisms is emerging, a cure remains unavailable for most of them. Treatment is usually based on preventing complications, minimizing disability (symptoms) and providing prognostic and genetic counseling [113]. Additionally, the use of certain medication might be contra-indicated in some OXPHOS disorders, *e.g.* valproic acid for the management of epileptic seizures in case of *POLG1* mutations [114]. Furthermore, the efficacy of other pharmacological agents is highly anecdotic. Nevertheless, various treatment cocktails of vitamins and cofactors (*e.g.* riboflavin, thiamine, folic acid, L-carnitine and creatine monohydrate, coenzyme Q10) are administrated to patients with OXPHOS disease because they are presumed harmless [114].
Recently, exercise-based therapies were tested for the treatment of OXPHOS disorders [115]. On the one hand, endurance training was shown to improve oxidative capacity in patients with mtDNA mutations but did not decrease the percentage of mutated mtDNA (so-called ‘gene shifting’) [116-118]. On the other hand, resistance training lead to muscle regeneration through the activation of satellite cells which did not harbor the mutant mtDNA [17]. After muscle regeneration, less muscle fibers contained the mutant mtDNA and initial studies showed improved biochemical activity [119, 120]. These preliminary results are encouraging for minimizing disability in patients with OXPHOS disorders.

Aim and outline of this thesis

The components of the OXPHOS system are encoded by both the mitochondrial and nuclear DNA. Mutations in genes encoding structural OXPHOS elements or factors involved in the maintenance or assembly of the OXPHOS system lead to a number of

diseases, in general referred to as OXPHOS disorders. The underlying pathological mechanisms of these diseases are not entirely understood and there is a lack of efficient therapies. The central aim of this thesis is to study the pathophysiology of a number of specific OXPHOS disorders and to create new models and identify new potential targets for therapeutic interventions. Therefore, microarray gene expression profiling was applied as an unbiased approach to find clues for biological processes that are affected by the individual diseases and that can be monitored or targeted by new therapeutic strategies. Additionally, oxidative stress has generally been considered to be an important pathogenic factor in OXPHOS disorders although the efficacy of antioxidant therapy is highly anecdotic. Hence, the involvement and extent of oxidative stress in a number of different OXPHOS disorders was interrogated. Characterized cell lines can be used as model systems to test compounds that have potential to ameliorate or slow down progression of the disease.

Altogether, the aim of this thesis is to create models or approaches to:

- Facilitate diagnostics of mtDNA-based OXPHOS disorders by determining the non-pathogenic variation of mtDNA in the general population.
- Gain knowledge on primary and secondary biological processes involved in OXPHOS disorders which have an impact on prognosis and therapy.
- Explore the extent to which different pathogenic mtDNA and nuclear DNA mutations induce oxidative stress and the consequences of this.

Chapter 2 describes the analysis of the mtDNA of 730 European subjects and presents novel data regarding the distribution of homoplasmic variants across the mtDNA. This comprehensive overview of mtDNA polymorphisms distinguishes between regions and positions which are likely not critical, pathogenic mutations targeting mainly conserved regions and regions containing no mutations at all. These data provide valuable information for evaluating the pathogenicity of mtDNA variants and counseling families. To improve prognosis and therapy options after genetic diagnosis, molecular disease pathways were identified in chapter 3 and 4 using microarray gene expression profiles in skeletal muscle of *POLG1* patients and fibroblast cell lines of complex I patients, respectively. Both chapters indicated a role of oxidative stress in OXPHOS pathology. Therefore, chapter 5 evaluated the effect of pathogenic mtDNA mutations (in *ND1*, *ND5* and *tRNALeu*) and mtDNA maintenance defects (*POLG1* mutations) on oxidative stress. This resulted in disease and patient specific signatures that indicate which parameter should best be used, *i.e.* oxidative damage, to evaluate which patients might benefit from antioxidant therapy. The cell line models of chapter 4 and 5 are now available for preliminary testing of the therapeutic effect of small compounds. The relevance of the results presented in chapter 2 to 5 in respect to the development of therapeutic strategies for OXPHOS disorders will be discussed in chapter 6.

References

1. Schaefer, A.M., et al., *The epidemiology of mitochondrial disorders--past, present and future.* Biochim Biophys Acta, 2004. **1659**(2-3): p. 115-20.
2. Wallace, D.C., *Mitochondrial DNA mutations in disease and aging.* Environ Mol Mutagen, 2010. **51**(5): p. 440-50.
3. Rossignol, R., et al., *Tissue variation in the control of oxidative phosphorylation: implication for mitochondrial diseases.* Biochem J, 2000. **347 Pt 1**: p. 45-53.
4. Montoya, J., et al., *Diseases of the human mitochondrial oxidative phosphorylation system.* Adv Exp Med Biol, 2009. **652**: p. 47-67.
5. Dimauro, S. and P. Rustin, *A critical approach to the therapy of mitochondrial respiratory chain and oxidative phosphorylation diseases.* Biochim Biophys Acta, 2009. **1792**(12): p. 1159-67.
6. Jacobs, J.A.M. The transmission and segregation of mitochondrial DNA mutations [PhD thesis]. Maastricht: Maastricht University; 2007.
7. Wanrooij, S. and M. Falkenberg, *The human mitochondrial replication fork in health and disease.* Biochim Biophys Acta, 2010. **1797**(8): p. 1378-88.
8. Pitchon, E.M., et al., *Patient with Fanconi Syndrome (FS) and retinitis pigmentosa (RP) caused by a deletion and duplication of mitochondrial DNA (mtDNA).* Klin Monbl Augenheilkd, 2007. **224**(4): p. 340-3.
9. Liu, C.S., et al., *Alteration in the copy number of mitochondrial DNA in leukocytes of patients with mitochondrial encephalomyopathies.* Acta Neurol Scand, 2006. **113**(5): p. 334-41.
10. Carelli, V., C. Giordano, and G. d'Amati, *Pathogenic expression of homoplasmic mtDNA mutations needs a complex nuclear-mitochondrial interaction.* Trends Genet, 2003. **19**(5): p. 257-62.
11. Chinnery, P.F., et al., *Molecular pathology of MELAS and MERRF. The relationship between mutation load and clinical phenotypes.* Brain, 1997. **120 (Pt 10)**: p. 1713-21.
12. Tuppen, H.A., et al., *Mitochondrial DNA mutations and human disease.* Biochim Biophys Acta, 2010. **1797**(2): p. 113-28.
13. Yarham, J.W., et al., *Mitochondrial tRNA mutations and disease.* Wiley Interdiscip Rev RNA, 2010. **1**(2): p. 304-24.
14. Montoya, J., et al., *20 years of human mtDNA pathologic point mutations: carefully reading the pathogenicity criteria.* Biochim Biophys Acta, 2009. **1787**(5): p. 476-83.
15. Zeviani, M., A. Spinazzola, and V. Carelli, *Nuclear genes in mitochondrial disorders.* Curr Opin Genet Dev, 2003. **13**(3): p. 262-70.
16. Janssen, A.J., J.A. Smeitink, and L.P. van den Heuvel, *Some practical aspects of providing a diagnostic service for respiratory chain defects.* Ann Clin Biochem, 2003. **40**(Pt 1): p. 3-8.
17. Rahman, S. and M.G. Hanna, *Diagnosis and therapy in neuromuscular disorders: diagnosis and new treatments in mitochondrial diseases.* J Neurol Neurosurg Psychiatry, 2009. **80**(9): p. 943-53.
18. Chretien, D. and P. Rustin, *Mitochondrial oxidative phosphorylation: pitfalls and tips in measuring and interpreting enzyme activities.* J Inherit Metab Dis, 2003. **26**(2-3): p. 189-98.
19. Kim, S.H., et al., *Mutations of ACADS gene associated with short-chain acyl-coenzyme A dehydrogenase deficiency.* Ann Clin Lab Sci, 2011. **41**(1): p. 84-8.
20. Passarelli, C., et al., *GSSG-mediated Complex I defect in isolated cardiac mitochondria.* Int J Mol Med, 2010. **26**(1): p. 95-9.
21. van Eijsden, R.G., et al., *Termination of damaged protein repair defines the occurrence of symptoms in carriers of the m.3243A > G tRNA(Leu) mutation.* J Med Genet, 2008. **45**(8): p. 525-34.

22. Verkaart, S., et al., *Superoxide production is inversely related to complex I activity in inherited complex I deficiency.* Biochim Biophys Acta, 2007. **1772**(3): p. 373-81.
23. Murray, J., et al., *Monitoring oxidative and nitrative modification of cellular proteins; a paradigm for identifying key disease related markers of oxidative stress.* Adv Drug Deliv Rev, 2008. **60**(13-14): p. 1497-503.
24. Nguyen, K.V., et al., *Molecular diagnosis of Alpers syndrome.* J Hepatol, 2006. **45**(1): p. 108-16.
25. Ng, S.B., et al., *Massively parallel sequencing and rare disease.* Hum Mol Genet, 2010. **19**(R2): p. R119-24.
26. Smeitink, J. and L. van den Heuvel, *Human mitochondrial complex I in health and disease.* Am J Hum Genet, 1999. **64**(6): p. 1505-10.
27. Hoefs, S.J., et al., *NDUFA2 complex I mutation leads to Leigh disease.* Am J Hum Genet, 2008. **82**(6): p. 1306-15.
28. Saneto, R.P., et al., *POLG DNA testing as an emerging standard of care before instituting valproic acid therapy for pediatric seizure disorders.* Seizure, 2010. **19**(3): p. 140-6.
29. Stankov, M.V., et al., *Mitochondrial DNA depletion and respiratory chain activity in primary human subcutaneous adipocytes treated with nucleoside analogue reverse transcriptase inhibitors.* Antimicrob Agents Chemother, 2010. **54**(1): p. 280-7.
30. van Beek, J.H., *Data integration and analysis for medical systems biology.* Comp Funct Genomics, 2004. **5**(2): p. 201-4.
31. Koene, S., et al., *Mouse models for nuclear DNA-encoded mitochondrial complex I deficiency.* J Inherit Metab Dis, 2010.
32. Fernandez-Ayala, D.J., et al., *Gene expression in a Drosophila model of mitochondrial disease.* PLoS One, 2010. **5**(1): p. e8549.
33. Kujoth, G.C., et al., *Mitochondrial DNA mutations, oxidative stress, and apoptosis in mammalian aging.* Science, 2005. **309**(5733): p. 481-4.
34. Trifunovic, A., et al., *Premature ageing in mice expressing defective mitochondrial DNA polymerase.* Nature, 2004. **429**(6990): p. 417-23.
35. Torraco, A., et al., *Mouse models of oxidative phosphorylation defects: powerful tools to study the pathobiology of mitochondrial diseases.* Biochim Biophys Acta, 2009. **1793**(1): p. 171-80.
36. Vives-Bauza, C., et al., *Enhanced ROS production and antioxidant defenses in cybrids harbouring mutations in mtDNA.* Neurosci Lett, 2006. **391**(3): p. 136-41.
37. Schon, E.A., et al., *Therapeutic prospects for mitochondrial disease.* Trends Mol Med, 2010. **16**(6): p. 268-76.
38. Distelmaier, F., et al., *Mitochondrial complex I deficiency: from organelle dysfunction to clinical disease.* Brain, 2009. **132**(Pt 4): p. 833-42.
39. Willems, P.H., et al., *Mitochondrial Ca2+ homeostasis in human NADH:ubiquinone oxidoreductase deficiency.* Cell Calcium, 2008. **44**(1): p. 123-33.
40. Norenberg, M.D. and K.V. Rao, *The mitochondrial permeability transition in neurologic disease.* Neurochem Int, 2007. **50**(7-8): p. 983-97.
41. Mattiazzi, M., et al., *The mtDNA T8993G (NARP) mutation results in an impairment of oxidative phosphorylation that can be improved by antioxidants.* Hum Mol Genet, 2004. **13**(8): p. 869-79.
42. Pitkanen, S. and B.H. Robinson, *Mitochondrial complex I deficiency leads to increased production of superoxide radicals and induction of superoxide dismutase.* J Clin Invest, 1996. **98**(2): p. 345-51.
43. Rusanen, H., K. Majamaa, and I.E. Hassinen, *Increased activities of antioxidant enzymes and decreased ATP concentration in cultured myoblasts with the 3243A-->G mutation in mitochondrial DNA.* Biochim Biophys Acta, 2000. **1500**(1): p. 10-6.
44. Di Giovanni, S., et al., *Apoptosis and ROS detoxification enzymes correlate with cytochrome c oxidase deficiency in mitochondrial encephalomyopathies.* Mol Cell Neurosci, 2001. **17**(4): p. 696-705.

45. Mirabella, M., et al., *Apoptosis in mitochondrial encephalomyopathies with mitochondrial DNA mutations: a potential pathogenic mechanism.* Brain, 2000. **123 (Pt 1)**: p. 93-104.
46. Balaban, R.S., S. Nemoto, and T. Finkel, *Mitochondria, oxidants, and aging.* Cell, 2005. **120**(4): p. 483-95.
47. Hawkins, C.L., P.E. Morgan, and M.J. Davies, *Quantification of protein modification by oxidants.* Free Radic Biol Med, 2009. **46**(8): p. 965-88.
48. Sekiguchi, M. and T. Tsuzuki, *Oxidative nucleotide damage: consequences and prevention.* Oncogene, 2002. **21**(58): p. 8895-904.
49. Bayeva, M. and H. Ardehali, *Mitochondrial dysfunction and oxidative damage to sarcomeric proteins.* Curr Hypertens Rep, 2010. **12**(6): p. 426-32.
50. Stark, G., *Functional consequences of oxidative membrane damage.* J Membr Biol, 2005. **205**(1): p. 1-16.
51. Powers, S.K., et al., *Reactive oxygen species are signalling molecules for skeletal muscle adaptation.* Exp Physiol, 2010. **95**(1): p. 1-9.
52. Giustarini, D., et al., *Oxidative stress and human diseases: Origin, link, measurement, mechanisms, and biomarkers.* Crit Rev Clin Lab Sci, 2009. **46**(5-6): p. 241-81.
53. Verkaart, S., et al., *Mitochondrial and cytosolic thiol redox state are not detectably altered in isolated human NADH:ubiquinone oxidoreductase deficiency.* Biochim Biophys Acta, 2007. **1772**(9): p. 1041-51.
54. Geromel, V., et al., *Superoxide-induced massive apoptosis in cultured skin fibroblasts harboring the neurogenic ataxia retinitis pigmentosa (NARP) mutation in the ATPase-6 gene of the mitochondrial DNA.* Hum Mol Genet, 2001. **10**(11): p. 1221-8.
55. Beretta, S., et al., *Leber hereditary optic neuropathy mtDNA mutations disrupt glutamate transport in cybrid cell lines.* Brain, 2004. **127**(Pt 10): p. 2183-92.
56. Sala, G., et al., *Antioxidants partially restore glutamate transport defect in leber hereditary optic neuropathy cybrids.* J Neurosci Res, 2008. **86**(15): p. 3331-7.
57. Luo, X., et al., *Excessive formation of hydroxyl radicals and aldehydic lipid peroxidation products in cultured skin fibroblasts from patients with complex I deficiency.* J Clin Invest, 1997. **99**(12): p. 2877-82.
58. Floreani, M., et al., *Antioxidant defences in cybrids harboring mtDNA mutations associated with Leber's hereditary optic neuropathy.* FEBS J, 2005. **272**(5): p. 1124-35.
59. Wani, A.A., et al., *Analysis of reactive oxygen species and antioxidant defenses in complex I deficient patients revealed a specific increase in superoxide dismutase activity.* Free Radic Res, 2008. **42**(5): p. 415-27.
60. Wei, Y.H., et al., *Oxidative stress in human aging and mitochondrial disease-consequences of defective mitochondrial respiration and impaired antioxidant enzyme system.* Chin J Physiol, 2001. **44**(1): p. 1-11.
61. Filosto, M., et al., *Antioxidant agents have a different expression pattern in muscle fibers of patients with mitochondrial diseases.* Acta Neuropathol, 2002. **103**(3): p. 215-20.
62. Ma, Y.S., et al., *Upregulation of matrix metalloproteinase 1 and disruption of mitochondrial network in skin fibroblasts of patients with MERRF syndrome.* Ann N Y Acad Sci, 2005. **1042**: p. 55-63.
63. Pang, C.Y., H.C. Lee, and Y.H. Wei, *Enhanced oxidative damage in human cells harboring A3243G mutation of mitochondrial DNA: implication of oxidative stress in the pathogenesis of mitochondrial diabetes.* Diabetes Res Clin Pract, 2001. **54 Suppl 2**: p. S45-56.
64. Li, J., et al., *Increased ROS generation and SOD activity in heteroplasmic tissues of transmitochondrial mice with A3243G mitochondrial DNA mutation.* Genet Mol Res, 2008. **7**(4): p. 1054-62.

65. Ishikawa, K., et al., *Increased reactive oxygen species and anti-oxidative response in mitochondrial cardiomyopathy.* Circ J, 2005. **69**(5): p. 617-20.
66. Katayama, Y., et al., *Accumulation of oxidative stress around the stroke-like lesions of MELAS patients.* Mitochondrion, 2009. **9**(5): p. 306-13.
67. Dassa, E.P., et al., *The mtDNA NARP mutation activates the actin-Nrf2 signaling of antioxidant defenses.* Biochem Biophys Res Commun, 2008. **368**(3): p. 620-4.
68. Wojewoda, M., J. Duszynski, and J. Szczepanowska, *Antioxidant defence systems and generation of reactive oxygen species in osteosarcoma cells with defective mitochondria: Effect of selenium.* Biochim Biophys Acta, 2010. **1797**(6-7): p. 890-6.
69. Trifunovic, A., et al., *Somatic mtDNA mutations cause aging phenotypes without affecting reactive oxygen species production.* Proc Natl Acad Sci U S A, 2005. **102**(50): p. 17993-8.
70. Lewis, W., et al., *Decreased mtDNA, oxidative stress, cardiomyopathy, and death from transgenic cardiac targeted human mutant polymerase gamma.* Lab Invest, 2007. **87**(4): p. 326-35.
71. Lu, C.Y., et al., *Increased expression of manganese-superoxide dismutase in fibroblasts of patients with CPEO syndrome.* Mol Genet Metab, 2003. **80**(3): p. 321-9.
72. Umaki, Y., et al., *Apoptosis-related changes in skeletal muscles of patients with mitochondrial diseases.* Acta Neuropathol, 2002. **103**(2): p. 163-70.
73. Piccolo, G., et al., *Biological markers of oxidative stress in mitochondrial myopathies with progressive external ophthalmoplegia.* J Neurol Sci, 1991. **105**(1): p. 57-60.
74. Wei, Y.H., et al., *Increases of mitochondrial mass and mitochondrial genome in association with enhanced oxidative stress in human cells harboring 4,977 BP-deleted mitochondrial DNA.* Ann N Y Acad Sci, 2001. **928**: p. 97-112.
75. Jin, Z. and W.S. El-Deiry, *Overview of cell death signaling pathways.* Cancer Biol Ther, 2005. **4**(2): p. 139-63.
76. Green, D.R. and G. Kroemer, *The pathophysiology of mitochondrial cell death.* Science, 2004. **305**(5684): p. 626-9.
77. Monici, M.C., et al., *Apoptosis in metabolic myopathies.* Neuroreport, 1998. **9**(10): p. 2431-5.
78. Ikezoe, K., et al., *Apoptosis is suspended in muscle of mitochondrial encephalomyopathies.* Acta Neuropathol, 2002. **103**(6): p. 531-40.
79. Fagiolari, G., et al., *Lack of apoptosis in patients with progressive external ophthalmoplegia and mutated adenine nucleotide translocator-1 gene.* Muscle Nerve, 2002. **26**(2): p. 265-9.
80. Sciacco, M., et al., *Lack of apoptosis in mitochondrial encephalomyopathies.* Neurology, 2001. **56**(8): p. 1070-4.
81. Otabe, S., et al., *Molecular and histological evaluation of pancreata from patients with a mitochondrial gene mutation associated with impaired insulin secretion.* Biochem Biophys Res Commun, 1999. **259**(1): p. 149-56.
82. Smeitink, J.A., et al., *Mitochondrial medicine: a metabolic perspective on the pathology of oxidative phosphorylation disorders.* Cell Metab, 2006. **3**(1): p. 9-13.
83. Nouws, J., et al., *Assembly factors as a new class of disease genes for mitochondrial complex I deficiency: cause, pathology and treatment options.* Brain, 2011.
84. Thorburn, D.R., et al., *Biochemical and molecular diagnosis of mitochondrial respiratory chain disorders.* Biochim Biophys Acta, 2004. **1659**(2-3): p. 121-8.
85. Lenaz, G., et al., *Bioenergetics of mitochondrial diseases associated with mtDNA mutations.* Biochim Biophys Acta, 2004. **1658**(1-2): p. 89-94.
86. Wong, L.J., *Pathogenic mitochondrial DNA mutations in protein-coding genes.* Muscle Nerve, 2007. **36**(3): p. 279-93.
87. Carelli, V., et al., *Biochemical features of mtDNA 14484 (ND6/M64V) point mutation associated with Leber's hereditary optic neuropathy.* Ann Neurol, 1999. **45**(3): p. 320-8.

88. Carelli, V., et al., *Leber's hereditary optic neuropathy: biochemical effect of 11778/ND4 and 3460/ND1 mutations and correlation with the mitochondrial genotype.* Neurology, 1997. **48**(6): p. 1623-32.
89. Valsecchi, F., et al., *Complex I disorders: causes, mechanisms, and development of treatment strategies at the cellular level.* Dev Disabil Res Rev, 2010. **16**(2): p. 175-82.
90. Finsterer, J., *Genetic, pathogenetic, and phenotypic implications of the mitochondrial A3243G tRNALeu(UUR) mutation.* Acta Neurol Scand, 2007. **116**(1): p. 1-14.
91. Mariotti, C., et al., *Genotype to phenotype correlations in mitochondrial encephalomyopathies associated with the A3243G mutation of mitochondrial DNA.* J Neurol, 1995. **242**(5): p. 304-12.
92. Laloi-Michelin, M., et al., *The clinical variability of maternally inherited diabetes and deafness is associated with the degree of heteroplasmy in blood leukocytes.* J Clin Endocrinol Metab, 2009. **94**(8): p. 3025-30.
93. Suzuki, T. and A. Nagao, *Human mitochondrial diseases caused by lack of taurine modification in mitochondrial tRNAs.* Wiley Interdiscip Rev RNA, 2011. **2**(3): p. 376-86.
94. Yasukawa, T., et al., *Wobble modification deficiency in mutant tRNAs in patients with mitochondrial diseases.* FEBS Lett, 2005. **579**(13): p. 2948-52.
95. Kirino, Y., et al., *Codon-specific translational defect caused by a wobble modification deficiency in mutant tRNA from a human mitochondrial disease.* Proc Natl Acad Sci U S A, 2004. **101**(42): p. 15070-5.
96. Chan, S.S. and W.C. Copeland, *DNA polymerase gamma and mitochondrial disease: understanding the consequence of POLG mutations.* Biochim Biophys Acta, 2009. **1787**(5): p. 312-9.
97. Ropp, P.A. and W.C. Copeland, *Characterization of a new DNA polymerase from Schizosaccharomyces pombe: a probable homologue of the Saccharomyces cerevisiae DNA polymerase gamma.* Gene, 1995. **165**(1): p. 103-7.
98. Euro, L., et al., *Clustering of Alpers disease mutations and catalytic defects in biochemical variants reveal new features of molecular mechanism of the human mitochondrial replicase, Pol {gamma}.* Nucleic Acids Res, 2011.
99. Wong, L.J., et al., *Molecular and clinical genetics of mitochondrial diseases due to POLG mutations.* Hum Mutat, 2008. **29**(9): p. E150-E172.
100. Milone, M. and R. Massie, *Polymerase gamma 1 mutations: clinical correlations.* Neurologist. **16**(2): p. 84-91.
101. Yamanaka, H., et al., *Novel mutation of human DNA polymerase gamma associated with mitochondrial toxicity induced by anti-HIV treatment.* J Infect Dis, 2007. **195**(10): p. 1419-25.
102. Pagnamenta, A.T., et al., *Dominant inheritance of premature ovarian failure associated with mutant mitochondrial DNA polymerase gamma.* Hum Reprod, 2006. **21**(10): p. 2467-73.
103. Blok, M.J., et al., *The unfolding clinical spectrum of POLG mutations.* J Med Genet, 2009. **46**(11): p. 776-85.
104. Ashley, N., et al., *Depletion of mitochondrial DNA in fibroblast cultures from patients with POLG1 mutations is a consequence of catalytic mutations.* Hum Mol Genet, 2008. **17**(16): p. 2496-506.
105. Graziewicz, M.A., et al., *Structure-function defects of human mitochondrial DNA polymerase in autosomal dominant progressive external ophthalmoplegia.* Nat Struct Mol Biol, 2004. **11**(8): p. 770-6.
106. Chan, S.S., M.J. Longley, and W.C. Copeland, *The common A467T mutation in the human mitochondrial DNA polymerase (POLG) compromises catalytic efficiency and interaction with the accessory subunit.* J Biol Chem, 2005. **280**(36): p. 31341-6.
107. Del Bo, R., et al., *Remarkable infidelity of polymerase gammaA associated with mutations in POLG1 exonuclease domain.* Neurology, 2003. **61**(7): p. 903-8.

108. Wanrooij, S., et al., *Twinkle and POLG defects enhance age-dependent accumulation of mutations in the control region of mtDNA.* Nucleic Acids Res, 2004. **32**(10): p. 3053-64.
109. Spelbrink, J.N., et al., *In vivo functional analysis of the human mitochondrial DNA polymerase POLG expressed in cultured human cells.* J Biol Chem, 2000. **275**(32): p. 24818-28.
110. Hance, N., M.I. Ekstrand, and A. Trifunovic, *Mitochondrial DNA polymerase gamma is essential for mammalian embryogenesis.* Hum Mol Genet, 2005. **14**(13): p. 1775-83.
111. Chan, S.S. and W.C. Copeland, *Functional analysis of mutant mitochondrial DNA polymerase proteins involved in human disease.* Methods Mol Biol, 2009. **554**: p. 59-72.
112. de Vries, M.C., et al., *Multiple oxidative phosphorylation deficiencies in severe childhood multi-system disorders due to polymerase gamma (POLG1) mutations.* Eur J Pediatr, 2007. **166**(3): p. 229-34.
113. Chinnery, P., et al., *Treatment for mitochondrial disorders.* Cochrane Database Syst Rev, 2006(1): p. CD004426.
114. Horvath, R., G. Gorman, and P.F. Chinnery, *How can we treat mitochondrial encephalomyopathies? Approaches to therapy.* Neurotherapeutics, 2008. **5**(4): p. 558-68.
115. Mahoney, D.J., G. Parise, and M.A. Tarnopolsky, *Nutritional and exercise-based therapies in the treatment of mitochondrial disease.* Curr Opin Clin Nutr Metab Care, 2002. **5**(6): p. 619-29.
116. Jeppesen, T.D., et al., *Aerobic training is safe and improves exercise capacity in patients with mitochondrial myopathy.* Brain, 2006. **129**(Pt 12): p. 3402-12.
117. Taivassalo, T., et al., *Endurance training and detraining in mitochondrial myopathies due to single large-scale mtDNA deletions.* Brain, 2006. **129**(Pt 12): p. 3391-401.
118. Jeppesen, T.D., et al., *Short- and long-term effects of endurance training in patients with mitochondrial myopathy.* Eur J Neurol, 2009. **16**(12): p. 1336-9.
119. Clark, K.M., et al., *Reversal of a mitochondrial DNA defect in human skeletal muscle.* Nat Genet, 1997. **16**(3): p. 222-4.
120. Murphy, J.L., et al., *Resistance training in patients with single, large-scale deletions of mitochondrial DNA.* Brain, 2008. **131**(Pt 11): p. 2832-40.

Chapter 2

Large scale mtDNA sequencing reveals sequence and functional conservation as major determinants of homoplasmic mtDNA variant distribution.

A.M. Voets, B.J.C. van den Bosch, A.P. Stassen, A.T. Hendrickx, D.M. Hellebrekers, L. Van Laer, E. Van Eyken, G. Van Camp, A. Pyle, S.V. Baudouin, P.F. Chinnery, H.J.M. Smeets

Mitochondrion 2011; 11: 964-972.

Abstract

The mitochondrial DNA (mtDNA) is highly variable, containing large numbers of pathogenic mutations and neutral polymorphisms. The spectrum of homoplasmic mtDNA variation was characterized in 730 subjects and compared with known pathogenic sites. The frequency and distribution of variants in protein coding genes were inversely correlated with conservation at the amino acid level. Analysis of tRNA secondary structures indicated a preference of variants for the loops and some acceptor stem positions. This comprehensive overview of mtDNA variants distinguishes between regions and positions which are likely not critical, mainly conserved regions with pathogenic mutations and essential regions containing no mutations at all.

Key words

MitoChip, mtDNA variants, distribution, pathogenicity

Introduction

Mitochondria are essential for the production of ATP, the main source of cellular energy, by the process of oxidative phosphorylation (OXPHOS). Part of the enzyme complexes involved are encoded by the mitochondrial DNA (mtDNA). The human mtDNA consist of 16,569 base pairs and contains 13 OXPHOS protein encoding genes, two ribosomal RNA genes and 22 tRNA genes [1]. It is generally considered that the mtDNA has a higher mutation rate compared to the nuclear DNA (nDNA) which is thought to be due to a combination of less extensive repair mechanisms, the lack of protective histones and closer proximity to a major source of mutation-inducing agents, i.e. the reactive oxygen species (ROS) [2]. The mtDNA is present as multiple copies within the mitochondria of each cell and altered nucleotides can be present in either the homo- or heteroplasmic state [3]. Not long ago it was generally accepted that the most deleterious pathogenic mutations were heteroplasmic, while homoplasmic variants were less severe risk factors or neutral polymorphic variants [4]. However, recent work has revealed a growing list of pathogenic homoplasmic mtDNA variants [5, 6], and most common pathogenic mutations are also present in the general population but usually far below the threshold level for phenotypic expression [7]. This presents a particular challenge when novel genetic variants are detected in patients with mitochondrial disease - conventional criteria cannot reliably determine which variants are phenotypically neutral, and which are actually causing disease. This is especially the case for variants in the protein coding genes and the tRNA genes, the latter compromising more than half of the published pathogenic mtDNA mutations [4, 8]. Pathogenic rRNA have been described to lesser extent, implicated in for example hearing loss [9]. A number of criteria and tools have been described to facilitate the classification of variants [10, 11], but a final conclusion regarding the pathogenicity of a certain variant is not always easy to achieve.

The availability of techniques to generate mutation and/or sequence information of complete mtDNA genomes at a rapid pace has opened new possibilities for the detection and classification of variable and conserved parts of the mtDNA, based on large data sets of mtDNA sequences [12-17]. So far these studies have not been consistent on the frequency and distribution of variants in the mtDNA, both in human and mice. Some report specific hotspots for positions that are altered [11], while others show a more random distribution of variants across the mitochondrial genome [18]. Therefore, we chose to analyze the mtDNA in a large population of 730 European individuals with one technology. We applied the GeneChip® Mitochondria Resequencing array from Affymetrix (MitoChip) as a fast and reliable method to detect homoplasmic variants in the mtDNA [9, 13, 19]. As different approaches to analyze MitoChip data have been described with different sensitivity and specificity for the detection of mtDNA variants [19-21], we had to optimize our procedure. The study cohort contained 218 patients with mitochondrial symptoms, who could also carry pathogenic mutations in the mtDNA, which would create a risk of incidentally including non-neutral variants in the analysis. To minimize this risk we systematically checked all variants identified in this group for pathogenicity. All pathogenic and potentially

pathogenic mutations, identified in 30 patients, were excluded from analysis and only polymorphisms and, based on the scoring system, predicted benign variants were included. This, together with the size of the entire cohort in majority of individuals with no mitochondrial disorders, prevents that the analysis is influenced by inclusion of pathogenic mutations. In our paper, we present novel data regarding the distribution of homoplasmic variants across the mtDNA and we provide clues to help distinguish neutral (homoplasmic) variants from highly deleterious pathogenic mutations in the tRNA genes.

Material and methods

DNA extraction

Total cellular DNA was isolated from muscle or blood from 730 subjects (supplementary table 2.1) according to standard procedures. Of these, 400 subjects were inhabitants with age-related hearing impairment from a residential village of Antwerp (Belgium), between 54 and 66 years old, invited through population registries [22]. A total of 218 subjects were patients with a variety of mitochondrial symptoms and ages between 0 and 50 years, referred to the Clinical Genetics department in Maastricht (the Netherlands). For those subjects, the pathogenic or likely pathogenic mutation, when found, was added to supplementary table 2.1 and was not included in the further analysis. The remaining 112 subjects (with age from 54 to 75) were sequential admissions to the Critical Care Unit in Newcastle upon Tyne (United Kingdom). This cohort had an identical haplogroup distribution to the background population from the same geographical region, and thus is considered to be a random sample of individuals living in the North East of England [23]. All known or likely pathogenic mutations (supplementary table 2.2) in the entire cohort were excluded from the analysis.

MitoChip and experimental procedure

GeneChip® Mitochondria Resequencing 2.0 Arrays (Affymetrix, Santa Clara, CA, USA) were used to determine the sequence of the 730 DNA samples. In short, the entire mtDNA was amplified using the Expand Long Template system (Roche, Almere, the Netherlands) in 2 fragments (A and B) of 8207 bp and 8545 bp in length, with an overlap of 183 bp. The primers for fragment A were forward primer [5'-cgttccagtgagttcaccct-3'] and reverse primer [5'-ggtaagaagtgggctagggc-3'], and for fragment B forward primer [5'-taaacctagccatggccatc-3'] and reverse primer [5'-tgtggctaggctaagcgttt-3']. PCR products were purified using the QIAQuick PCR cleanup kit (Qiagen). Equimolar amounts of the amplified fragments A and B were pooled and fragmented, labeled and hybridized on a pre-hybridized GeneChip according to the GeneChip CustomSeq Resequencing Array Affymetrix protocol. Chips were washed and stained on the GeneChip fluidics station 450 (Affymetrix) using the preprogrammed wash and stain protocol (Mini_DNAARRAY_WS5_450). The chips were scanned using the Affymetrix GeneChip scanner 3000 creating CEL files for subsequent analysis.

Data analysis

After generation of the cell intensity (CEL) files by GeneChip® Operating Software 1.4 (GCOS 1.4), raw sequence data was obtained by the GeneChip® Sequence Analysis Software 4.1 (GSEQ 4.1, Affymetrix) and Sequence Pilot – module SeqC (JSI medical systems) according to the flow chart depicted in figure 2.1. GSEQ uses an objective statistical framework, based upon the ABACUS algorithm [24] to assign base calls to each position which meets quality criteria in the mitochondrial genome, based on consistent calls of both strands. GSEQ analysis was performed using the haploid model with quality score threshold (QST) 3. SeqC automatically uses all previously made analyses as controls for the actual samples and therefore is able to anticipate the shape of every peak in the software output. Dissimilarity scores are calculated for every peak and are a measure for the deviation of the peak areas from the statistical average. A warning is displayed for any peak with an abnormal high dissimilarity score. The SeqC software was used with the standard parameters. The eventual mtDNA sequences were compared with the revised Cambridge reference sequence to list all homoplasmic variants.

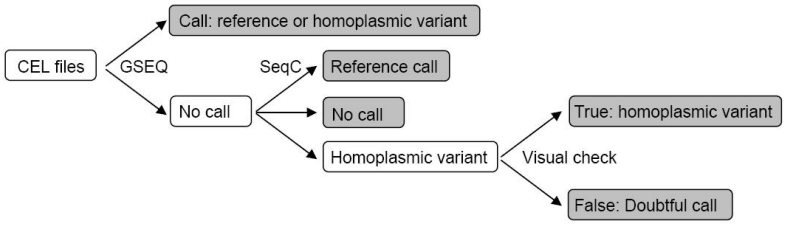

Figure 2.1. Data analysis flow chart.

The haplogroups were determined according to the presence or absence of the haplogroup variants listed in supplementary table 2.3. The best fitting haplogroup was assigned. The sequences of the seven species used for examining conservation of the mitochondrial genes were derived from NCBI: H. sapiens NC_012920; C. lupus NC_002008.4; B. taurus NC_006853.1; M. musculus NC_005089.1; R. norvegicus NC_001665.2; G. gallus NC_001323.1; D. melanogaster NC_001709.1. A filtered list of pathogenic tRNA and protein mtDNA mutations was created from a list of disease associated mtDNA mutations in the MITOMAP database (www.mitomap.org/MITOMAP, supplementary table 2.2). Variants of which the pathogenicity status was listed in Mitomap as ‘unclear’, ‘polymorphism’, ‘synergistic’, ‘conflicting reports’, ‘secondary’, ‘haplogroup marker’ or ‘warrants further study’, or was ‘unconvincing’ in the corresponding publication were not included. All inherited pathogenic mutations (Mitomap ‘confirmed’) were included. For the remaining variants (Mitomap ‘reported’), a pathogenicity score was calculated for the tRNA and protein coding mutations according to a checklist. For protein coding genes, the scoring system described previously [25] was used. Additionally, the conservation of the variant position (mtSNP http://mtsnp.tmig.or.jp/mtsnp/index_e.shtml; Alamut, Interactive Biosoftware) and the effect of the variant on polarity, protein structure/function (PolyPhen http://genetics.bwh.harvard.edu/pph/; SIFT http://sift.jcvi.org/www/

SIFT_BLink_submit.html; InterProScan http://www.ebi.ac.uk/Tools/InterProScan/; UniProt http://www.uniprot.org/ uniprot/; TMHMM http://www.cbs.dtu.dk /services/TMHMM/; MSOP http://npsa-pbil.ibcp.fr/cgi-bin/npsa_automat.pl?page= npsa_sopm.html) were evaluated. For the tRNA genes, another scoring system was used [11]. Additionally, the conservation of nucleotide and the effect of the variant on secondary or tertiary interactions (Mamit-tRNA http://mamit-trna.u-strasbg.fr/) within the tRNA molecule were evaluated. For all variants, the presence of the variant in general databases (mtSNP, mtDB http://www.genpat.uu.se/mtDB/, OMIM, PubMed, Google) was checked. Variants that were scored definitely or highly likely pathogenic were included in the list of pathogenic mutations and excluded from further analysis. Correlation between the number of variants and the variant intensity of guanine (G) residues in the protein coding genes was analyzed using the linear regression function of SPSS.

Results

Analysis of the entire mtDNA sequence in 730 subjects

The mtDNA of 730 subjects was sequenced using the MitoChip and sequences were compared with the revised Cambridge Reference Sequence (rCRS). Because of the lower sensitivity and specificity of the MitoChip for the detection of heteroplasmic variants [19], the analysis was restricted to homoplasmic variants. After analysis with GSEQ, 1.3 % (standard error 0.03) of the 16544 nucleotides in the 730 samples gave a no call. The main reason was a low signal, a repetitive sequence or a C-stretch in one of the two strands (data not shown). These regions were predominantly located in the D-loop of the mtDNA and less in the protein and RNA coding genes. The D-loop was excluded from the analysis. The distribution of no calls was not homogeneous and some genes (e.g. *ATP8*) showed a significantly higher percentage of nucleotides that were not called than others (e.g. *ND4L*) (table 2.1). Therefore, to reduce the number of bases with a no call, Sequence Pilot – module SeqC was used for the positions that were not called by GSEQ. Additional variants called by SeqC were checked visually. Variants scored by SeqC were only called confirmed when both forward and reverse strand clearly showed the mutant and no wild type peak. When a wild type peak was visible on one of the strands, the variant call from SeqC was depicted as ‘doubtful’. When both GSEQ and SeqC could not call a position, it remained a ‘no call’. SeqC analysis decreased the percentage of no calls from 1.096 to 0.001 (excluding the D-loop) without adding many extra different homoplasmic variants or doubtful calls. The distribution of the no calls over the different genes was more homogeneous (table 2.1). Five randomly chosen additional SeqC variants were conventionally sequenced and confirmed (data not shown).

Table 2.1. Results of variant and 'no call' analysis using the GSEQ and SeqC analysis pipeline.

Gene	GSEQ analysis			SeqC analysis [a]			
	# different variants	# no calls	% ntds with no call[b]	# different variants	# no calls	% ntds with no call	# doubtful calls
ATP6	89*	16809	3.381	91*	68	0.014	8
ATP8	26*	9276	6.139	27*	3	0.002	2
CYB	115	10615	1.274	115	9	0.001	6
COI	129	8245	0.732	130	4	<0.001	3
COII	53	9473	1.897	57	11	0.002	2
COIII	69	3442	0.601	71	0	0.000	9
ND1	95	9344	1.338	96	5	<0.001	16
ND2	113	10518	1.383	114	16	0.002	53
ND3	45	1383	0.548	45	2	0.001	10
ND4	112	9126	0.907	114	15	0.001	10
ND4L	29	228	0.105	29	1	<0.001	2
ND5	185	15900	1.202	187	3	<0.001	12
ND6	51	6562	1.712	55	1	<0.001	174
TRNF	2	329	0.635	2	2	0.004	0
TRNV	1	4	0.008	1	0	0.000	1
TRNL1	1	1	0.002	1	0	0.000	0
TRNI	4	322	0.639	4	2	0.004	0
TRNQ	3	58	0.110	4	0	0.000	3
TRNM	3	104	0.210	3	0	0.000	0
TRNW	4	19	0.038	4	0	0.000	0
TRNA	4	29	0.058	4	0	0.000	1
TRNN	0	1	0.002	0	0	0.000	0
TRNC	9	3	0.006	9	0	0.000	0
TRNY	2	8	0.017	2	0	0.000	0
TRNS1	2	353	0.711	2	1	0.002	23
TRND	3	244	0.492	3	0	0.000	4
TRNK	2	35	0.068	2	0	0.000	1
TRNG	4	26	0.052	4	0	0.000	0
TRNR	3	579	1.220	3	1	0.002	20
TRNH	5	23	0.046	5	2	0.004	0
TRNS2	2	255	0.592	2	0	0.000	0
TRNL2	2	163	0.314	2	0	0.000	2
TRNE	5	0	0.000	5	0	0.000	0
TRNT	16	96	0.199	16	0	0.000	0
TRNP	0	75	0.151	0	0	0.000	0
RNR1	38	3340	0.480	39	0	0.000	0
RNR2	79	3852	0.338	80	5	<0.001	5
Total analyzed[c]	1317	123582	1.096	1341	150	0.001	394

Table 2.1 legend

[a]Positions which were not called by GSEQ analysis were analyzed with the SeqC software and newly identified variants were checked visually. When the SeqC call was wrong, the position was recorded as a 'doubtful call'.

[b]Average percentage of nucleotides that were not called for 730 subjects (total number of no calls/[length of the sequence x 730 subjects] x 100)

[c]The mtDNA sequence was analyzed from position 577 to position 16023.

* *ATP6* and *ATP8* have 8 variants in common

Characterization of variants in the mtDNA

General features of the variants identified

A total of 12,063 homoplasmic variants (average 16.5 variants per subject) were detected relative to the rCRS, of which 1,341 (average 1.8 per subject) were different variants at 1,321 (average 1.8 per subject) different positions in the mtDNA (supplementary table 2.4). The large amount of total variants is due to the presence of European haplogroup variants which were present in a high proportion of the subjects (haplogroup and number of subjects: H 307, U 99, K 59, HV 52, J 64 and JT 73; supplementary table 2.1). The haplogroup distribution was comparable among the three cohorts (supplementary table 2.5), pointing to a generally European population, and therefore the three cohorts were merged for further analysis. Furthermore, to minimize confounding by the haplogroup variants, variant numbers mentioned in the analyses are based on the 1,341 different variants.

Table 2.2. Overview of observed variants by nucleotide.

Observed number of variants[a]						**Number of nucleotide[b]**	**Variant Intensity[c]**
ref\var	A	G	C	T	Total		
A	-	383	23	19	425 (32%)	4785 (31%)	1.03
G	228	-	7	2	237 (18%)	2017 (13%)	1.35
C	31	13	-	239	283 (21%)	4810 (31%)	0.68
T	13	16	367	-	396 (30%)	3833 (25%)	1.19
Total	272	412	397	260	1341	15446	

[a] Observed number of different variants according to the revised Cambridge Reference Sequence (rCRS)

[b] The number of nucleotide x in the mtDNA excluding the displacement loop (position 577-16023)

[c] Variant intensity is calculated as follows: (observed number of variants nucleotide x/total number of nucleotide x)/(total number of variants/total number of nucleotides)

The observed frequency of variants for each of the different nucleotides (A, C, G, T) according to the rCRS are shown in table 2.2. Variants changing nucleotide A were most frequent. To correct for differences in the total number of the four nucleotides in the mtDNA regions tested, the variant intensity [26] was calculated. This variant intensity corrected for the presence of the nucleotide in the mtDNA (excluding the D-

loop) by comparing this value with the prevalence of all variants in the entire mtDNA (excluding the D-loop) (formula: [number of variants nucleotide x/total number of nucleotide x]/[total number of variants/total number of nucleotides]). The variant intensity is depicted in table 2.2 and is increasing in the order C<A<T<G. Although nucleotide G showed the smallest number of variants, it had the highest variant intensity.

Protein coding variants

The number of variants in the different protein coding genes was assessed (figure 2.2A). After correction for the length of the gene, differences in the prevalence of variants could be observed. On average, 10.4% of the nucleotides in the protein coding genes showed a variant in one of the 730 subjects (0.104 variants/base pair) While *ATP6*, *ATP8* and *ND3* showed the highest number of variants, *COI*, *COII* and *ND4* contained fewer variants per base pair. These differences were mainly due to differences in variant numbers on codon position 1 and 2 (figure 2.2A). In general, it was observed that the number of variants at codon position 1 (0.070 variants/base pair) and 2 (0.036 variants/ base pair) was lower compared with the 3rd position (0.192 variants/base pair) (figure 2.3). Codon position 3 variants predominantly consisted of synonymous amino acid changes, whereas codon position 1 showed only a small proportion of synonymous variants and codon position 2 variants consisted entirely of non-synonymous variants.

The frequency of Cs (lowest variant intensity) or Gs (highest variant intensity) in the sequence of the genes (all positions or only third codon positions) could not explain the discrepancy in the number of variants between the different genes (data not shown). However, there was a significant ($p = 0.004$) correlation between the number of variants and the variant intensity of G in the protein coding genes (figure 2.2B). *ND6* was not included in the analysis as this gene is transcribed from the L-strand and the G content differs from the H-strand. To check for a role of evolutionary conservation in the distribution of the variants, *COI* (low number of variants/bp) and *ATP6* (high number of variants/bp) were examined in more detail in seven species (H. sapiens, G. gallus, C. lupus, B. taurus, M. musculus, R. norvegicus and D. melanogaster). Whereas more than half of the nucleotides in the *COI* gene were conserved in seven species, approximately half of the variants were located at positions conserved in less than four species (figure 2.4A). In contrast, the *ATP6* sequence was less well conserved (figure 2.4A) but the preference of the variants for the less conserved positions in *ATP6* was lower compared with *COI* variants (figure 2.4A). However, no such difference could be observed when only the third codon positions were analyzed (figure 2.4B). The same trend in sequence conservation was shown for *COII* and *COIII* (low number of variants/bp) and *ATP8* and *ND3* (high number of variant/bp) but the preference of variants for less conserved first and second positions between the genes was less discriminating (supplementary figure 2.1). The 67 pathogenic mutations that passed our filter were all, except for five deletions, located on first and second codon positions and were mainly targeting highly conserved positions (57/67 conserved in at least 6 species; supplementary table 2.2).

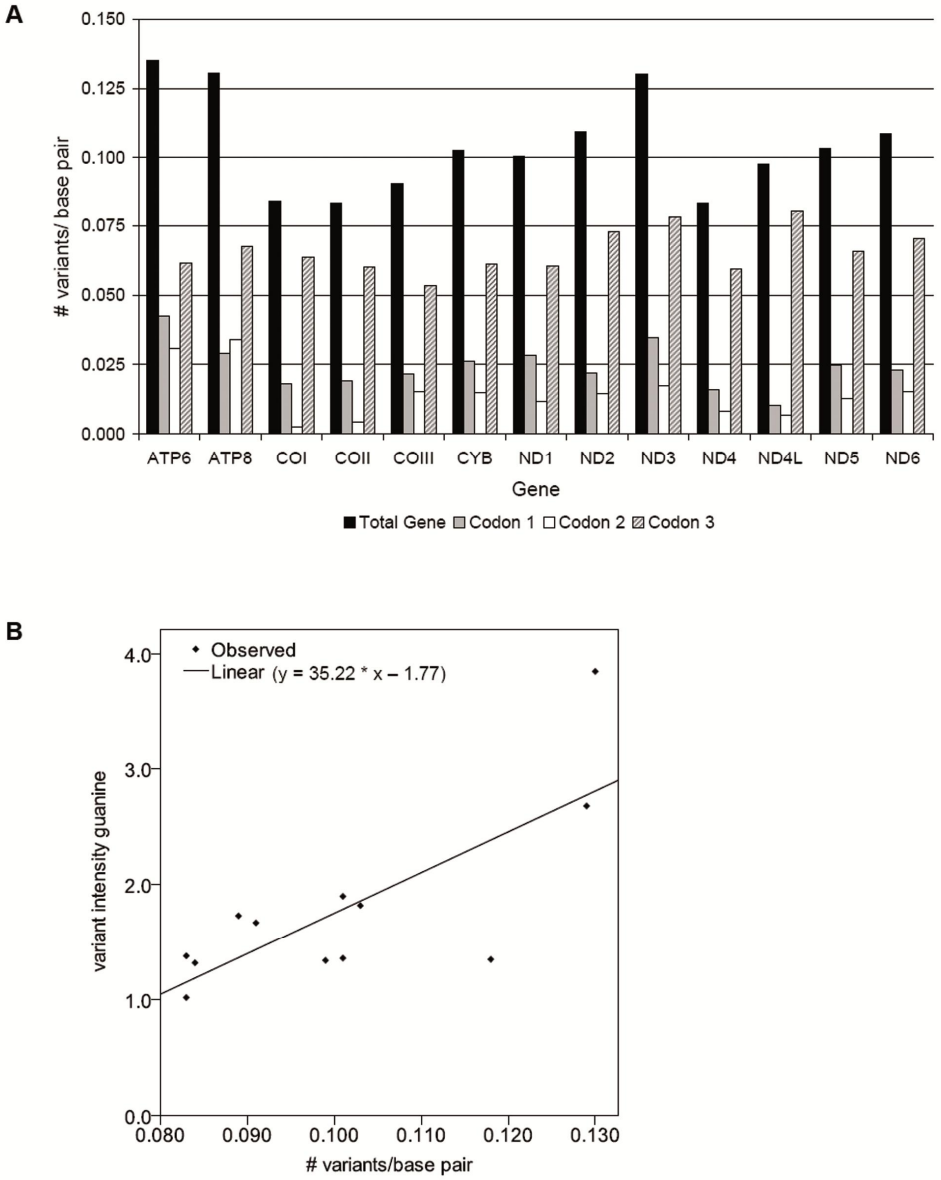

Figure 2.2. Variant distribution by protein coding gene. A The observed number of variants in the whole cohort is expressed as the number of variants per base pair to correct for the length of the genes and is shown for the total gene as well as for the three different codon positions. **B** Significant ($p = 0.004$) correlation between the number of variants and the variant intensity of guanine in the protein coding genes (excluding ND6).

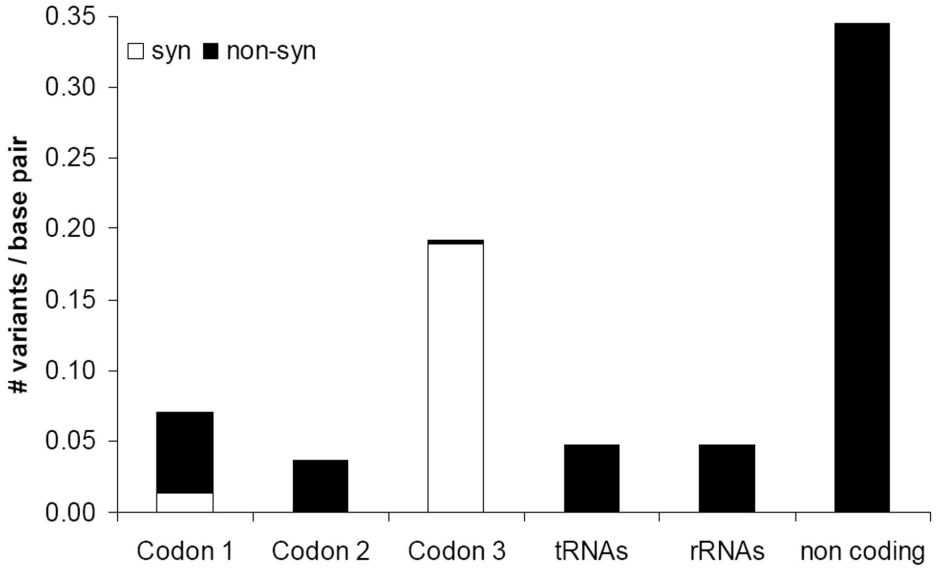

Figure 2.3. Variant distribution in protein coding genes by codon position, tRNA and rRNA genes and non-coding nucleotides. The observed number of variants in the whole cohort is expressed as the number of variants per base pair of each sequence type. The proportion of synonymous and non-synonymous variants is indicated.

tRNA variants

In the 730 samples, only 78 different homoplasmic tRNA variants were detected. On average, 5.3% of the positions showed a variant in one of the 730 subjects (0.053 variants/base pair), in between the rate observed for codon positions 1 and 2 of the protein coding genes (figure 2.3). The location and positional conservation of these variants were compared with a list of known pathogenic tRNA mutations (supplementary table 2.2) to detect discriminating characteristics (table 2.3). For the homoplasmic variants, approximately half (52%) of the variants were located in the loops of the tRNA whereas only 32% of the pathogenic mutations were located here. Homoplasmic variants were representing, among others, poorly conserved mismatch to Watson–Crick base pair (WC) changes and both poorly and highly conserved mismatch to mismatch changes in the tRNA stems, which were not present among the pathogenic mutations. While three pathogenic mutations changed WCs into severe mismatches (not A·C, C·A, G·U or U·G) on conserved positions, no homoplasmic variants caused such changes. Furthermore, when examining the conservation of the base pairing (conserved WC, G·U or mismatch base pairs), pathogenic mutations predominated in conserved base pairs compared with the homoplasmic variants (34/90 pathogenic mutations versus 7/78 homoplasmic variants).

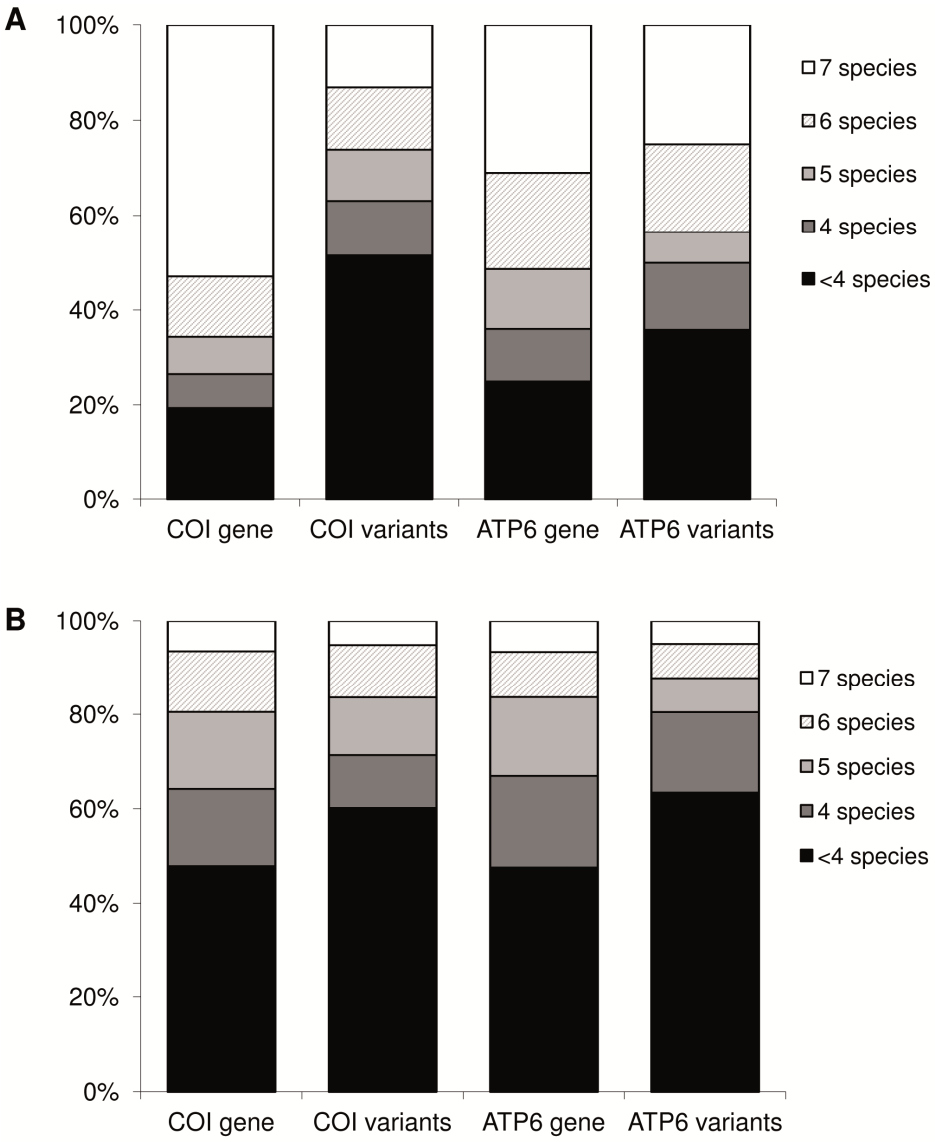

Figure 2.4. Conservation of total gene sequence and variant positions in *COI* and *ATP6* for all codon positions (A) and third codon positions (B). The human sequence of both genes was aligned with the sequence of six other species: G. gallus, C. lupus, B. taurus, M. musculus, R. norvegicus and D. melanogaster.

Table 2.3. Location and conservation characteristics of homoplasmic tRNA variants and pathogenic tRNA mutations.

			homoplasmic variants		pathogenic mutations[c]	
Location	**Change[a]**	**Positional conservation[b]**	**total # (%)**	**# conserved pairing[d]**	**total # (%)**	**# conserved pairing[d]**
loop		<100%	37 (47)		11 (12)	
		100%	4 (5)		18 (20)	
stem	MM>WC	<100%	13 (17)	2	0 (0)	
	MM>WC	100%	1 (1)	1	2 (2)	1
	MM>MM	<100%	3 (4)		0 (0)	
	MM>MM	100%	1 (1)		0 (0)	
	WC>mMM	<100%	16 (21)	1	31 (34)	13
	WC>mMM	100%	3 (4)	3	25 (28)	20
	WC>sMM	<100%	0 (0)		0 (0)	
	WC>sMM	100%	0 (0)		3 (3)	
Total			78	7	90	34

Underlined data represent types of variants only present in the homoplasmic variants or pathogenic mutations group

[a] MM>WC = mismatch base pair to Watson-Crick base pair (WC)
MM>MM = mismatch base pair to another mismatch base pair
WC>mMM = WC to a mild mismatch base pair, mild mismatch base pairs are A·C, C·A, G·U and U·G
WC>sMM = WC to a severe mismatch base pair, severe mismatch base pairs are all mismatch base pairs excluding A·C, C·A, G·U and U·G

[b] as determined in 31 mammalian mitochondrial genomes [27]

[c] see supplementary table 2.3 for detailed list

[d] conserved pairing: 100% conserved WC or >90% G·U and U·G as determined in 31 mammalian mitochondrial genomes [27]

Finally, a heat map of all 22 tRNA secondary structures was generated according to the tRNA numbering to examine positional differences between homoplasmic variants and pathogenic mutations in more detail. In this way, the homoplasmic variants and pathogenic mutations in all tRNA molecules could be visualized in one figure (figure 2.5). Homoplasmic variants were located more often in the tRNA loops (except for the anticodon) and some positions of the acceptor stem compared with the pathogenic mutations (figure 2.5A and B). Again, it is clear that pathogenic mutations in the stem almost always cause WC to mismatch changes while a significant proportion of homoplasmic variants represents mismatch to mismatch or mismatch to WC changes (figure 2.5A and B). It can be observed that pathogenic mutations are dominating the anticodon, the anticodon stem, the D stem and part of the acceptor stem of the tRNAs (figure 2.5C).F

Figure 2.5

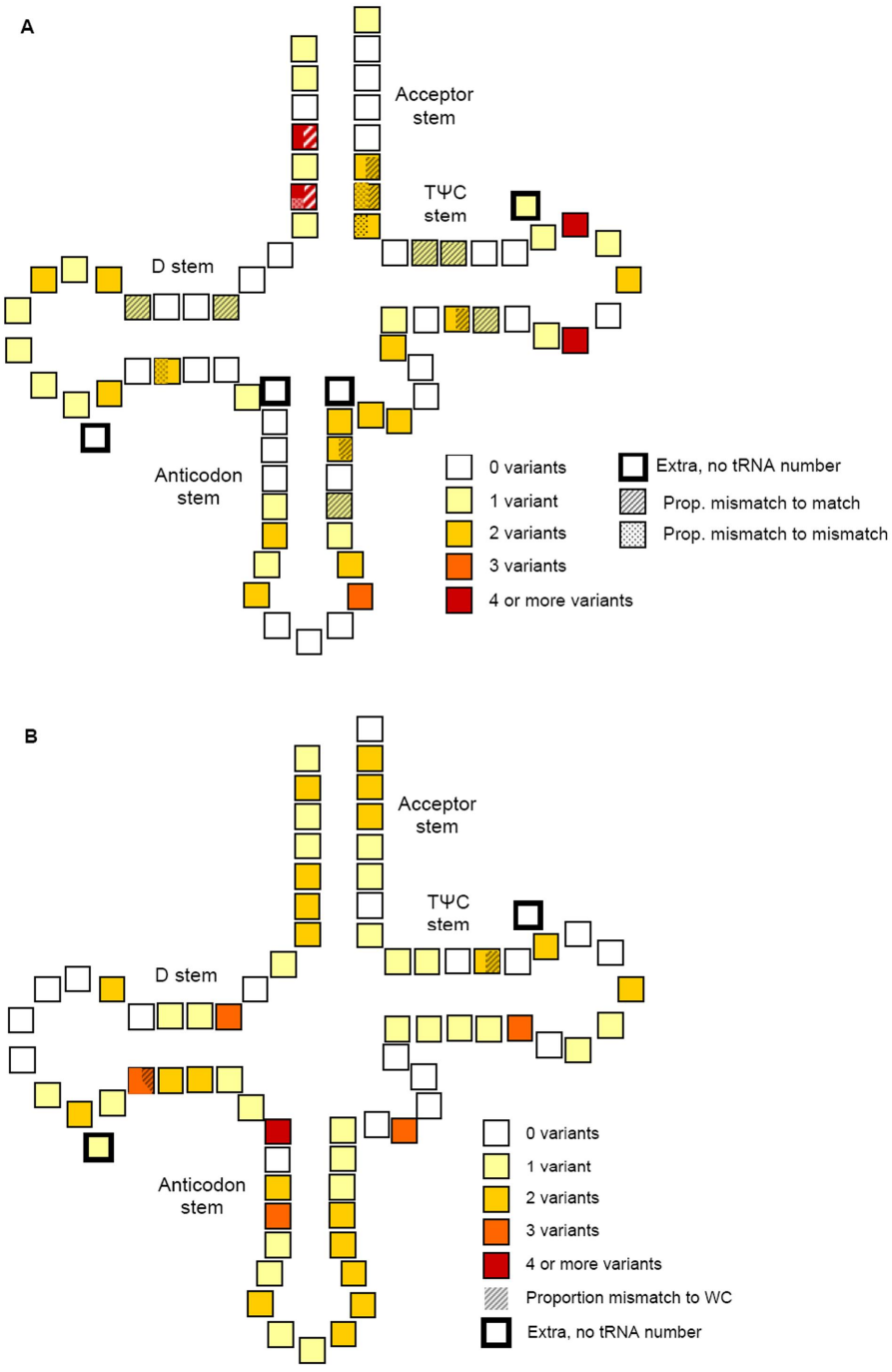
A
Acceptor stem
TΨC stem
D stem
Anticodon stem
0 variants
1 variant
2 variants
3 variants
4 or more variants
Extra, no tRNA number
Prop. mismatch to match
Prop. mismatch to mismatch
B
Acceptor stem
TΨC stem
D stem
Anticodon stem
0 variants
1 variant
2 variants
3 variants
4 or more variants
Proportion mismatch to WC
Extra, no tRNA number

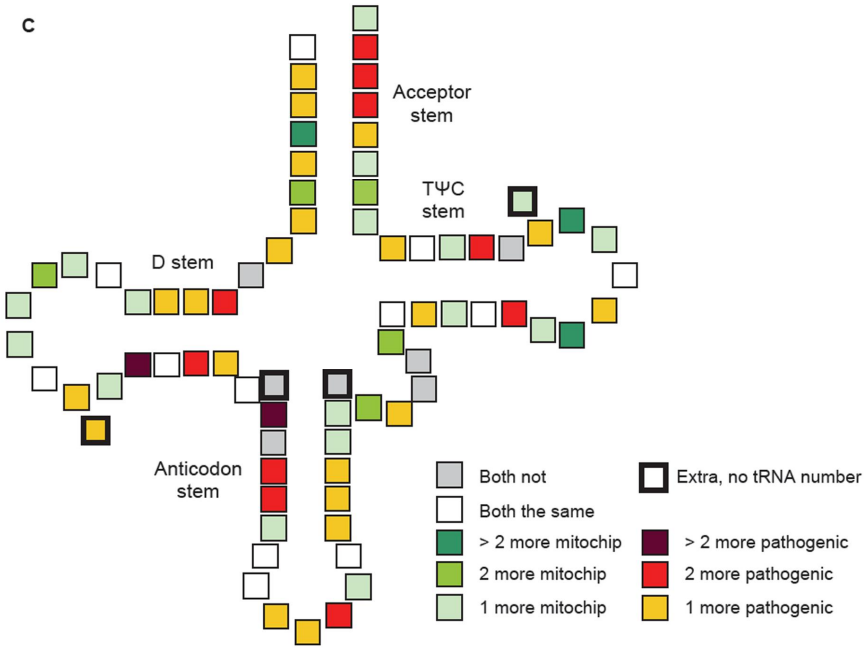

Figure 2.5. Composite of all 22 tRNA secondary structures with variant/mutation locations. All tRNAs are merged into one figure according to tRNA number. Frequencies of homoplasmic variants (**A**) and pathogenic mutations (**B**) are appointed to each tRNA position with different colors. Stripes and dots represent the proportion of mismatch to WC or mismatch to mismatch changes, respectively, comparable to the area that is indicated. No indication means WC to mismatch change. **C** depicts the difference in number of homoplasmic variants and pathogenic mutations for each tRNA position.

rRNA variants and non-coding regions

The *12S* and *16S* rRNA genes showed variants with a density of 0.041 and 0.051 different variants/base pair, respectively. These numbers are only half of the average protein coding genes but are in the same range as the average variant density in tRNA genes and codon position 1 and 2 of the protein coding genes (figure 2.3), indicating a comparable selective pressure. Non-coding nucleotides (n=58) between protein coding, rRNA and tRNA genes showed the highest number of variants with an average of 0.345 different variants per position (figure 2.3).

Discussion

In this study, the mtDNA of 730 subjects was analyzed using the Affymetrix MitoChip v2.0. Sequence data analysis was improved to increase the call rate without increasing the number of false positives or false negatives significantly. Homoplasmic mtDNA variants were scored to explore variable and evolutionary conserved regions.

Pipeline for identifying and analyzing mtDNA mutations

Compared with conventional sequencing, MitoChip resequencing is a fast and cost effective method to screen the whole mtDNA for homoplasmic and heteroplasmic mutations [13]. The mtDNA of 730 subjects was resequenced using the Affymetrix MitoChip v2.0 and base calling was performed by the GSEQ software. It has been shown previously [19] that the MitoChip has lower sensitivity and specificity in the detection of heteroplasmic variants. In our diagnostic experience (data not shown) the call rate of the MitoChip is >98% and the sensitivity to detect heteroplasmic mutation ranges from 5 to 30%, which may differ for different nucleotide positions. This implies that the in muscle DNA most relevant causal heteroplasmic mutations will be detectable. Massive parallel sequencing technology will provide an alternative, especially when prices will drop and the required coverage can be reached in a cost-effective way. By massively parallel sequencing-by-synthesis, it was observed that in nearly all of the normal tissues, somatic low level heteroplasmic variants (>1.6% heteroplasmy) were present [28]. However, the relevance of detecting such low heteroplasmy levels in relation to phenotypic expression is debatable. The MitoChip has been used in studies concerning the influence of homoplasmic polymorphisms on disease (progression) [29, 30] and anthropological studies [19]. We also concentrated on homoplasmic variants only [4]. Highly deleterious pathogenic mutations will very rarely reach homoplasmy because homoplasmy is likely to be lethal at the cellular level [18]. This is in contrast to neutral or adaptive heteroplasmic variants, which become homoplasmic or are lost within 70 cell divisions [31].

GSEQ has been reported to generate very few false negatives and false positives but a high number of no calls [19, 32], as was also observed in this study. The alternative local context probes on the MitoChip v2.0 did not provide a solution for this problem, since these probes were mainly located in the D-loop. The use of additional algorithms or masks following GSEQ analysis has been shown to improve the average call rate [19-21, 32]. In our study, the combination of the haploid model of GSEQ followed by analysis using SeqC (with a higher call rate [33]) turned out to be a sensitive and efficient approach. A key difference between the software programs with respect to the number of no-calls is the ability of SeqC to call a position based on one strand, where as GSEQ requires consistent calls on both strands. Furthermore, SeqC uses all previously analyzed samples as controls for the actual samples which enables a statistically validated continuous software learning process. To control for false positives, we used both software tools and all additional variants called by SeqC were checked visually. Conclusively, the current protocol was feasible for the number of

MitoChips studied, making this method applicable for the analysis of MitoChip data in a large cohort of subjects.

Characterization of mtDNA variants

General features

In 730 subjects, 12,063 homoplasmic variants were detected in the mtDNA excluding the D-loop. D-loop variations (especially the hypervariable segments) have been characterized extensively to study variation within and between human populations [34-37] and were not considered further in this study. The variant intensity analysis indicated that nucleotides G and C proportionally presented with the highest and lowest variant intensities compared with A and T, respectively. This is in agreement with previously published results that showed guanine to be the least stable nucleotide and cytosine the most stable nucleotide while adenine and thymine had intermediate stability [26, 38]. Differences in variant intensity however can only occur when there are strand-specific biases in substitution rates. This theory is reinforced by the deviation from the theoretical A=T and G=C nucleotide composition within each strand when no strand-specific bias would exist [39]. Multiple other studies have shown strand asymmetry in mutation rates [40]; this is probably due to periods of separation of the two DNA strands during replication, which may lead to increased mutability, and transcription-coupled repair [41, 42].

Protein coding variants

Our data confirmed not unexpectedly the strong negative selection against variants on codon position 1 and 2 due to the non-synonymous nature of variants at these positions [43, 44]. Not all protein coding genes accumulated the same number of variants which was correlated with a heterogeneous guanine mutation rate. Previously, it was suggested that different mutation rates of mitochondrial genes are at least partly independent of protein structure and function and a property of the mtDNA itself [26]. The authors based their theory on segmentation of the mtDNA by differences in nucleotide composition and that the segments showed a heterogeneous guanine mutation rate. Our study indicated that the heterogeneous guanine mutation rate not only applies to the different mtDNA segments described previously [26], but also plays a role in the individual genes. The protein coding gene results largely correspond with a previous study using data from the mtDNA mutator mice and the human mtDB database [43].

The differences in variant accumulation in the protein coding genes may also be due to differences in selective pressure at the functional (amino acid) level. For the highly conserved *COI* gene, variants were mainly located on less conserved positions whereas the less well conserved *ATP6* gene showed weaker preference for variants on these positions. If only third codon positions were considered in the analysis, then no differences were observed between the genes. Conclusively, the hypothesis of stronger selection against variants in genes with a high level of sequence conservation and more tolerance for variants in less well conserved genes [43], seems valid in this data set but it only applies for functionally relevant first and second codon positions. In

agreement with this, differences in variant numbers between the different genes are reflected by differences in variant numbers on codon positions 1 and 2, whereas variant numbers on positions with minor effect on protein function (codon position 3) are more or less comparable among all genes. The role of functional preservation and conservation is further emphasized by the location of the filtered list of pathogenic mutations (supplementary table 2.2) of which most were on highly conserved functionally relevant positions.

tRNA, rRNA and non-coding region variants (except D-loop)

The position and effect of the 78 different tRNA variants in the present data set were compared with the position and effect of the known pathogenic mutations (supplementary table 2.2). As mentioned previously [11, 45], for many mtDNA variants listed as pathogenic mutations in the MITOMAP database, insufficient evidence is presented to confidently ascribe pathogenicity to these variants. For example, 40 of the 171 different mutations listed as pathogenic, also appeared to be polymorphisms in the same database and original source data should be checked [10, 45]. The major differences between the pathogenic mutation and homoplasmic variant sets were that the different homoplasmic variants (a) were located more often in the tRNA loops (41/78 compared with 29/90 for pathogenic mutations), (b) changed less WCs into mismatches in the tRNA stems (19/78 compared with 59/90 for the pathogenic mutations) and (c) affected less conserved base pairs (7/78 compared with 34/90 for the pathogenic mutations). Smaller studies based on database sequences also pointed to these differences between polymorphisms and pathogenic mutations [11, 18, 46]. The relation between conservation and pathogenicity was further demonstrated by evolutionary selection in 14 different primate species [46]. Pathogenic loop and stem mutations were under higher evolutionary pressure than polymorphisms. For the latter, the stem was under greater selective constraint than the loop. Additionally, the mismatches in the tRNA stem were under lower selective constraint than WCs and it has been proposed that mismatch to WC changes might be adaptive in nature [46]. The tRNA secondary structure heat map showed that pathogenic mutations were dominating the D stem, acceptor stem, anticodon stem and anticodon but the homoplasmic variants showed also some hot spots in these regions. The D loop and T loop were predominantly targeted by homoplasmic variants. Others also showed hotspots for pathogenic mutations in the acceptor and anticodon stems in smaller studies [11]. In contrast, another group [18] reported a random distribution of pathogenic mutations and polymorphisms across the tRNA structure. The different results of the latter publication may be due to the inclusion of different or more ‘pathogenic’ mutations in their analysis compared with ours. Although the amount of data on tRNA variants in the mtDNA has increased during the past years, absolute conclusions regarding the pathogenicity of mitochondrial tRNA molecules can still not be provided for every variant in those genes.

The rRNA genes showed a frequency of variants in the same range of tRNA genes and codon position 1 and 2 of the protein coding genes. From this and the relatively low number of pathogenic rRNA mutations published, it appears that homoplasmic variants

in these genes are not tolerated, which would increase the likelihood that a rRNA variant is pathogenic. However, this is in contrast with results from a mice study [43]. There, in offspring from mtDNA mutator mice, purifying selection against non-synonymous mutations in protein coding genes was evident after two generations. The rRNA and tRNA genes experienced less intense germline selection, comparable with the third codon position in protein coding genes [43]. The difference between the studies is probably due to the inclusion of heteroplasmic mutations in the mice study. The authors suggest that tRNA mutations at low heteroplasmy levels are more compatible with life than some protein coding mutations and are therefore subjected to a less rapid form of purifying selection. Although less rapid, the mechanism of purification seems to be equally important as this study showed comparable selection against variants in tRNAs, rRNAs and first and second codon positions on the population level. Since the rRNA results are comparable with the tRNA results in these studies, the same mechanism might be acting on both, although in contrast to tRNAs not many pathogenic heteroplasmic rRNA mutations have been reported. Examining if heteroplasmy is more tolerated in RNA genes than protein coding genes will give valuable information in the near future.

As expected, the 58 non-coding nucleotides in between the protein coding, rRNA and tRNA genes experienced the lowest selective pressure with the highest number of variants per base pair. This means that even the third codon position of genes is not entirely free of selection. Probably this is due to amino acids that do not allow for synonymous substitution (methionine and tryptophan) or have only limited third codon position possibilities (cysteine, aspartic acid, glutamic acid, phenylalanine, histidine, lysine, asparagine, glutamine, and tyrosine). So, based on functional conservation, it could be expected that for part of the changes on the third codon position selection occurs.

Conclusion

Factors such as guanine mutation rate and (functional) conservation have been shown to affect the amount and location of homoplasmic variants in the different mitochondrial genes. All coding sequences, including the third codon position, showed evidence of negative selection against variants when compared with the non-coding nucleotides between the genes. This meta analysis provided valuable information for the improvement of pathogenicity criteria and for minimizing the amount of variants that require functional follow-up. However, larger cohorts are still necessary to classify novel variants solely using mutation screening. Extension of our approach in the future, will lead to a detailed map of the mtDNA with regions and positions that are targeted by polymorphisms or pathogenic mutations or never show variation. The latter situation probably points to mutations that are not compatible with life and will never be detected. Altogether, this will provide valuable information for evaluating the pathogenicity of mtDNA variants and counseling families.

Supplementary data

Supplementary table 2.1. Subject information (origin and haplogroup).
Supplementary table 2.2. Variants used to determine the haplogroup of the samples.
Supplementary table 2.3. Pathogenic tRNA and protein mtDNA mutations according to the criteria that are listed in the Material and methods.
Supplementary table 2.4. All homoplasmic variants that were detected in 730 subjects according to the revised Cambridge reference sequence.
Supplementary table 2.5. Comparison of the haplogroup distribution of the different cohorts.
Supplementary figure 2.1. Conservation of total gene sequence and variant positions in *COII*, *COIII*, *ND3* and *ATP8* for all codon positions (**A**) and third codon positions (**B**).

Supplementary tables are available online at doi:10.1016/j.mito.2011.09.003

References

1. Anderson, S., et al., *Sequence and organization of the human mitochondrial genome.* Nature, 1981. **290**(5806): p. 457-65.
2. Schmiedel, J., et al., *Mitochondrial cytopathies.* J Neurol, 2003. **250**(3): p. 267-77.
3. DiMauro, S. and E.A. Schon, *Mitochondrial respiratory-chain diseases.* N Engl J Med, 2003. **348**(26): p. 2656-68.
4. Chinnery, P.F. and E.A. Schon, *Mitochondria.* J Neurol Neurosurg Psychiatry, 2003. **74**(9): p. 1188-99.
5. Lucioli, S., et al., *Introducing a novel human mtDNA mutation into the Paracoccus denitrificans COX I gene explains functional deficits in a patient.* Neurogenetics, 2006. **7**(1): p. 51-7.
6. Valente, L., et al., *Identification of novel mutations in five patients with mitochondrial encephalomyopathy.* Biochim Biophys Acta, 2009. **1787**(5): p. 491-501.
7. Elliott, H.R., et al., *Pathogenic mitochondrial DNA mutations are common in the general population.* Am J Hum Genet, 2008. **83**(2): p. 254-60.
8. Jacobs, H.T., *Disorders of mitochondrial protein synthesis.* Hum Mol Genet, 2003. **12 Spec No 2**: p. R293-301.
9. Leveque, M., et al., *Whole mitochondrial genome screening in maternally inherited non-syndromic hearing impairment using a microarray resequencing mitochondrial DNA chip.* Eur J Hum Genet, 2007. **15**(11): p. 1145-55.
10. Bhardwaj, A., et al., *MtSNPscore: a combined evidence approach for assessing cumulative impact of mitochondrial variations in disease.* BMC Bioinformatics, 2009. **10 Suppl 8**: p. S7.
11. McFarland, R., et al., *Assigning pathogenicity to mitochondrial tRNA mutations: when "definitely maybe" is not good enough.* Trends Genet, 2004. **20**(12): p. 591-6.
12. van Den Bosch, B.J., et al., *Mutation analysis of the entire mitochondrial genome using denaturing high performance liquid chromatography.* Nucleic Acids Res, 2000. **28**(20): p. E89.
13. van Eijsden, R.G., et al., *Chip-based mtDNA mutation screening enables fast and reliable genetic diagnosis of OXPHOS patients.* Genet Med, 2006. **8**(10): p. 620-7.
14. White, H.E., et al., *Accurate detection and quantitation of heteroplasmic mitochondrial point mutations by pyrosequencing.* Genet Test, 2005. **9**(3): p. 190-9.

15. Wong, L.J., T.J. Chen, and D.J. Tan, *Detection of mitochondrial DNA mutations using temporal temperature gradient gel electrophoresis.* Electrophoresis, 2004. **25**(15): p. 2602-10.
16. Xiu-Cheng Fan, A., et al., *A rapid and accurate approach to identify single nucleotide polymorphisms of mitochondrial DNA using MALDI-TOF mass spectrometry.* Clin Chem Lab Med, 2008. **46**(3): p. 299-305.
17. Dobrowolski, S.F., et al., *Identifying sequence variants in the human mitochondrial genome using high-resolution melt (HRM) profiling.* Hum Mutat, 2009. **30**(6): p. 891-8.
18. Florentz, C. and M. Sissler, *Disease-related versus polymorphic mutations in human mitochondrial tRNAs. Where is the difference?* EMBO Rep, 2001. **2**(6): p. 481-6.
19. Hartmann, A., et al., *Validation of microarray-based resequencing of 93 worldwide mitochondrial genomes.* Hum Mutat, 2009. **30**(1): p. 115-22.
20. Pandya, G.A., et al., *A bioinformatic filter for improved base-call accuracy and polymorphism detection using the Affymetrix GeneChip whole-genome resequencing platform.* Nucleic Acids Res, 2007. **35**(21): p. e148.
21. Thieme, M., et al., *ReseqChip: automated integration of multiple local context probe data from the MitoChip array in mitochondrial DNA sequence assembly.* BMC Bioinformatics, 2009. **10**: p. 440.
22. Van Eyken, E., et al., *Contribution of the N-acetyltransferase 2 polymorphism NAT2*6A to age-related hearing impairment.* J Med Genet, 2007. **44**(9): p. 570-8.
23. Baudouin, S.V., et al., *Mitochondrial DNA and survival after sepsis: a prospective study.* Lancet, 2005. **366**(9503): p. 2118-21.
24. Cutler, D.J., et al., *High-throughput variation detection and genotyping using microarrays.* Genome Res, 2001. **11**(11): p. 1913-25.
25. Mitchell, A.L., et al., *Sequence variation in mitochondrial complex I genes: mutation or polymorphism?* J Med Genet, 2006. **43**(2): p. 175-9.
26. Samuels, D.C., et al., *A compositional segmentation of the human mitochondrial genome is related to heterogeneities in the guanine mutation rate.* Nucleic Acids Res, 2003. **31**(20): p. 6043-52.
27. Helm, M., et al., *Search for characteristic structural features of mammalian mitochondrial tRNAs.* RNA, 2000. **6**(10): p. 1356-79.
28. He, Y., et al., *Heteroplasmic mitochondrial DNA mutations in normal and tumour cells.* Nature, 2010. **464**(7288): p. 610-4.
29. Mithani, S.K., et al., *Mitochondrial mutations in adenoid cystic carcinoma of the salivary glands.* PLoS One, 2009. **4**(12): p. e8493.
30. Rollins, B., et al., *Mitochondrial variants in schizophrenia, bipolar disorder, and major depressive disorder.* PLoS One, 2009. **4**(3): p. e4913.
31. Coller, H.A., et al., *High frequency of homoplasmic mitochondrial DNA mutations in human tumors can be explained without selection.* Nat Genet, 2001. **28**(2): p. 147-50.
32. Kothiyal, P., et al., *High-throughput detection of mutations responsible for childhood hearing loss using resequencing microarrays.* BMC Biotechnol. **10**: p. 10.
33. Schroeder, C., et al., *High-throughput resequencing in the diagnosis of BRCA1/2 mutations using oligonucleotide resequencing microarrays.* Breast Cancer Res Treat, 2009.
34. Salas, A., et al., *mtDNA hypervariable region II (HVII) sequences in human evolution studies.* Eur J Hum Genet, 2000. **8**(12): p. 964-74.
35. Sigurgardottir, S., et al., *The mutation rate in the human mtDNA control region.* Am J Hum Genet, 2000. **66**(5): p. 1599-609.
36. Galtier, N., et al., *Mutation hot spots in mammalian mitochondrial DNA.* Genome Res, 2006. **16**(2): p. 215-22.
37. Stoneking, M., *Hypervariable sites in the mtDNA control region are mutational hotspots.* Am J Hum Genet, 2000. **67**(4): p. 1029-32.

38. Tanaka, M. and T. Ozawa, *Strand asymmetry in human mitochondrial DNA mutations.* Genomics, 1994. **22**(2): p. 327-35.
39. Lobry, J.R. and N. Sueoka, *Asymmetric directional mutation pressures in bacteria.* Genome Biol, 2002. **3**(10): p. RESEARCH0058.
40. Faith, J.J. and D.D. Pollock, *Likelihood analysis of asymmetrical mutation bias gradients in vertebrate mitochondrial genomes.* Genetics, 2003. **165**(2): p. 735-45.
41. Green, P., et al., *Transcription-associated mutational asymmetry in mammalian evolution.* Nat Genet, 2003. **33**(4): p. 514-7.
42. Majewski, J., *Dependence of mutational asymmetry on gene-expression levels in the human genome.* Am J Hum Genet, 2003. **73**(3): p. 688-92.
43. Stewart, J.B., et al., *Strong purifying selection in transmission of mammalian mitochondrial DNA.* PLoS Biol, 2008. **6**(1): p. e10.
44. Soares, P., et al., *Correcting for purifying selection: an improved human mitochondrial molecular clock.* Am J Hum Genet, 2009. **84**(6): p. 740-59.
45. Bandelt, H.J., et al., *Exaggerated status of "novel" and "pathogenic" mtDNA sequence variants due to inadequate database searches.* Hum Mutat, 2009. **30**(2): p. 191-6.
46. Ruiz-Pesini, E. and D.C. Wallace, *Evidence for adaptive selection acting on the tRNA and rRNA genes of human mitochondrial DNA.* Hum Mutat, 2006. **27**(11): p. 1072-81.

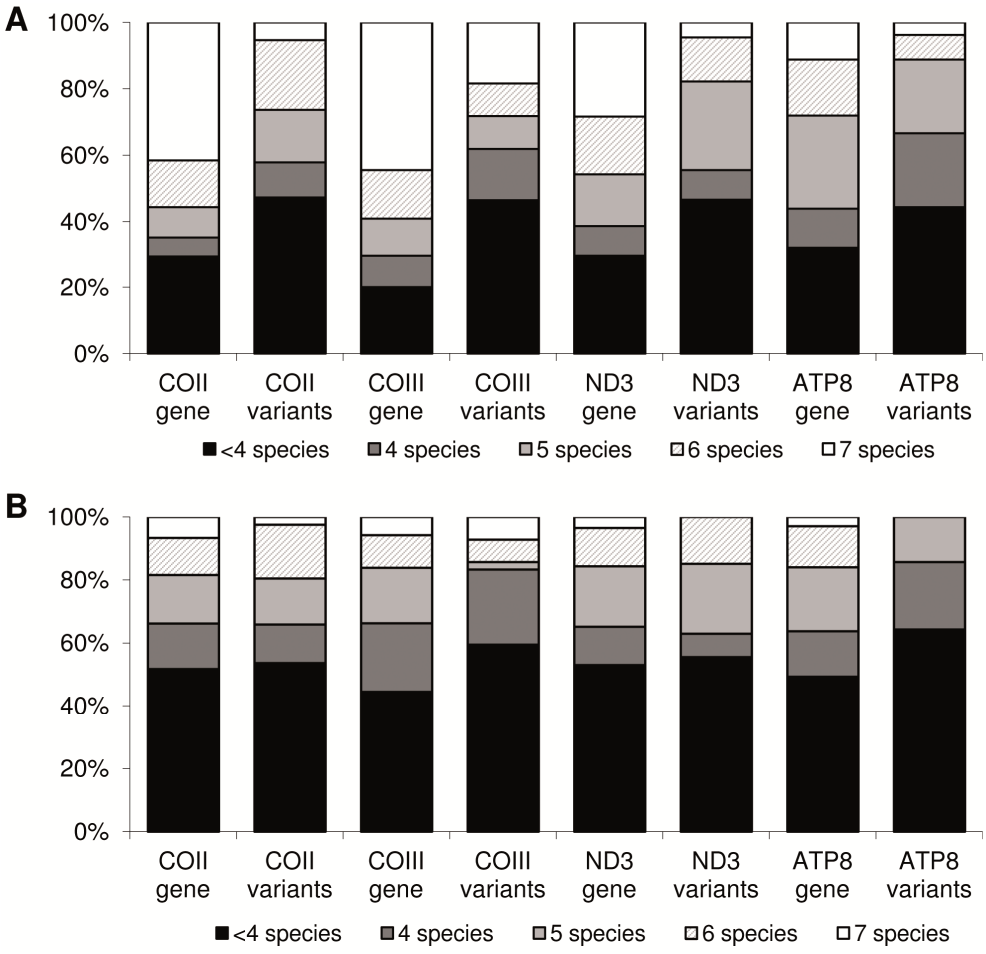

Supplementary figure 2.1. Conservation of total gene sequence and variant positions in *COII*, *COIII*, *ND3* and *ATP8* for all codon positions (**A**) and third codon positions (**B**). The human sequence of both genes was aligned with the sequence of six other species: G. gallus, C. lupus, B. taurus, M. musculus, R. norvegicus and D. melanogaster.

Chapter 3

***POLG1* defects lead to muscle abnormalities, oxidative stress in fibroblasts and apoptosis in brain and liver.**

A.M. Voets, B.J.C. van den Bosch, P.J. Lindsey, R.M. Verdijk, F.K. Verheyen, G.C. Schoonderwoerd, S.J.V. Vanherle, J.J. Esseling, P.H.G.M. Willems, W.J.H. Koopman, C.E.M. de Die-Smulders, B.T. Poll-The, M. de Visser, C.G. Faber, I.F.M. de Coo, H.J.M. Smeets

Submitted

Abstract

Background. DNA polymerase gamma (pol γ) is the only polymerase responsible for the replication and maintenance of mitochondrial DNA (mtDNA). Mutations in the catalytic subunit of pol γ (*POLG1* gene) are associated with a broad variety of clinical symptoms. Fatal complications usually involve brain and liver but muscle abnormalities have also been observed. The pathogenic mechanism of *POLG1* mutation is only partly understood. We intend to characterize molecular pathways in *POLG1* pathology.
Methods. Light and electron microscopy, mtDNA copy number and rearrangements and whole genome gene expression (Affymetrix) profiles were evaluated in skeletal muscle biopsies of *POLG1* patients. Apoptosis and oxidative stress were examined in different human tissues.
Results. Most patients showed decreased mtDNA copy number, accumulation of mtDNA deletions and/or decreased OXPHOS activity in skeletal muscle. Morphological changes were observed in the majority of patients' skeletal muscles biopsies. Transcriptomics revealed lower expression of fatty acid beta oxidation, increased expression of electron transport chain subunits and decreased expression of uncoupling proteins 2 and 3. Increased apoptosis was shown in the brain and liver and increased oxidative stress was measured in fibroblast cultures in part of the patients.
Conclusion. Except for two patients, all *POLG1* patients showed muscle abnormalities for at least one of the investigated parameters, indicating that any of these observations can be suggestive for defects in *POLG1*. Oxidative stress and apoptosis were identified as pathological processes in part of the patients and may be counterbalanced by a genetic-background-dependent yet unidentified mechanism.

Key words

POLG1, oxidative stress, apoptosis, gene expression

Introduction

Mitochondrial diseases are among the most frequently inherited neurological disorders [1]. DNA polymerase gamma (pol γ) is the sole DNA polymerase involved in the replication and maintenance of the mtDNA. *POLG1* mutations have been reported to cause a broad variety of phenotypes, such as Alpers-Huttenlocher syndrome, ataxia neuropathy syndrome (ANS), epilepsy and chronic progressive external ophtalmoplegia (CPEO) [2]. Phenotypes involving hepatopathy usually manifest early in life, while isolated myopathy affects older individuals and brain abnormalities can occur at any age [3]. The correlation between genotype and phenotype in patients with *POLG1* mutations is sometimes tight but more often variable [3]. The pathological mechanism explaining the diverse clinical manifestations of *POLG1* mutations is only partly understood. Human studies have focused on *in vitro* characterization of purified or recombinant enzyme [4], *in vivo* analysis of the functions of the pol γ protein and its domains in cultured cells [5] and large scale screening of mtDNA molecules in skeletal muscle and fibroblasts [6, 7]. These studies showed a higher probability of accumulating mtDNA mutations and/or depletion of mtDNA when *POLG1* is mutated.
The aim of this study is to identify molecular mechanisms involved in human *POLG1* pathogenesis by examining skeletal muscle, fibroblast cultures and (post mortem) liver and brain specimens of *POLG1* patients. This is the first study combining gene expression analysis with physiological measurements and staining in human patients. Identification of pathology associated processes is important to decipher the clinical heterogeneity, to identify new treatment approaches and improve prognosis.

Material and methods

POLG1 patients

Characteristics of eleven patients homozygous or compound heterozygous for *POLG1* mutations are described in table 3.1. Blood lactate levels of the patients at rest and enzyme activities of the OXPHOS complexes derived from muscle biopsies are presented when available (table 3.1). Not all assays could be performed for all patients due to the limited material available. Ethics approval was not required according to Dutch legislation as residual material of previous diagnostic investigations has been studied.

Skeletal muscle morphology

Muscle biopsies were taken from the quadriceps muscle. Samples were split for light microscopy (LM) and electron microscopy (EM). Skeletal muscle histology - HE (haematoxolin and eosin), trichrome, periodic acid–Schiff (PAS) and ORO (oil red O) staining - and enzyme histochemistry - acid phosphatase, ATPase (adenosine triphosphatase), NADH (nicotinamide adenine dinucleotide), SDH (succinate dehydrogenase) and COX (cytochrome oxidase) - were evaluated. Ultrastructural studies were performed as described previously [8].

Mitochondrial DNA copy number and large scale deletions

DNA was isolated using the Wizard Genomic DNA Purification Kit (Promega, Leiden, NL). Mitochondrial DNA copy number was determined as described previously [8]. To detect mtDNA deletions, 50 ng of DNA was amplified into two overlapping fragments of 16.1 (I) and 16.0 (II) kb using Phusion Hot Start DNA polymerase (Finnzymes) and 100 ng forward and reverse primer corresponded to nucleotide positions (nt, 5' to 3', according to Cambridge sequence) FwdI 314-343 ; RevI 16382- 16411; FwdII 1330-1355; RevII 756- 778). The PCR conditions were as follows : 30 sec at 98°C ; 30 cycles of 10 sec at 98°C and 8 min 15 sec at 72°C ; 10 min at 72°C. PCR products were first analyzed on a 1% agarose gel and next for 32h on a 0.7% agarose gel.

Microarray procedure

Skeletal muscle needle biopsies were immediately frozen in liquid nitrogen from six subjects carrying a *POLG1* mutation and twelve controls (table 3.2). Total RNA was isolated using the TRIzol reagent (Invitrogen, Carlsbad, CA, USA) and purified with the RNeasy clean-up kit (Qiagen, Hilden, DE). RNA quantity and purity were determined spectrophotometrically using the Nanodrop ND-1000 (Nanodrop Technologies) and RNA integrity was assessed by determining the RNA 28S/18S ratio using the Bioanalyser 2100 (Agilent Technologies, Santa Clara, CA, USA). 150 ng of muscle RNA was reverse transcribed into cDNA and amplified in a two-round amplification reaction according to the manufacturer's protocol (Affymetrix, Santa Clara, CA, USA). A mixture of cDNA and added hybridization controls was hybridized on Affymetrix HG-U133 Plus 2.0 chips, followed by staining and washing steps in the GeneChip fluidics station 400 (Affymetrix) according to the manufacturer's procedures. To assess the raw probe signal intensities, chips were scanned using the GeneChip scanner 3000 (Affymetrix).

Microarray data analysis

Images of the Human Genome U133 Plus 2.0 arrays were quantified with GCOS software (Affymetrix). The microarray data reported in this manuscript have been deposited in NCBI Gene expression omnibus (GEO), accession number GSE18715. The chip description file (CDF) used for the analysis was an update created and freely distributed by the microarray lab of the university of Michigan (http://brainarray.mbni.med.umich.edu; [9]) based on UniGenes (version 9). This resulted in the analysis of 17215 gene-transcripts out of the 54613 commonly obtained using the Human Genome U133 Plus 2.0 CDF provided by Affymetrix. All genes were analyzed using a Gaussian linear regression (N (μ, σ^2) where μ is the mean and σ^2 is the variance) including the best hybridization and best labeling spike, the age, and sex. The inference criterion used for comparing the models is their ability to predict the observed data, i.e. models are compared directly through their minimized minus log-likelihood. When the numbers of parameters in models differ, they are penalized by adding the number of estimated parameters, a form of the Akaike information criterion (AIC) [10]. For each gene, a model containing the relevant covariates (E(y) = Hyb. Spike + Lab. Spike + Age + Sex) was fitted in order to obtain a reference AIC. Then a model containing the group was fitted (E (y) = Hyb. Spike + Lab. Spike + Age + Sex +

Grp). The gene under consideration was found to be differentially expressed if the AIC of this second model was smaller when compared to the AIC of the model not containing the group effect. The genes analyzed and fold changes were loaded into GenMapp (version 2.1, build 20080507) and MAPPFinder (version 2.0, build 20041218) software packages to evaluate the transcripts in relation to known biological processes. The gene database version "Hs-Std_20070817" and the Mapps version "Hs_Contributed_20080619" were used for both programs. Only gene-transcripts with either their average intensities for the control and patient groups above 500 or average intensities for one of these groups above 1000 (background signal criteria) and a 10 percent fold change were used to obtain a ranked list of pathways with differentially expressed genes.

Quantification of reactive oxygen species

Reactive oxygen species (ROS) levels were measured in four patient (P54, P194, P382 and P504) and three control fibroblast cultures by dihydroethidine (DHE) oxidation as described previously [11]. All cell lines were cultured in parallel. Similarly to the microarray data, the ROS data were analyzed using a Gaussian linear regression including the day, medium, group, and medium-group interactions if required. As previously, the Akaike Information Criteria (AIC) was used to compare models without and with the group effect. The model with the smallest AIC was selected as the model best fitting the observed data.

Histology and apoptosis in liver and brain

Histological and immunohistochemical analysis was performed on formalin fixed paraffin embedded sections (4µm) of liver and brain of patients (P30, P382 and P504) and controls. Anonymous control liver (n=3) and brain (n=3) sections (age 15 or older) were used for comparison. Subsequent sections were used for HE staining and the detection of apoptosis using immunohistochemistry (IHC) with rabbit-anti cleaved caspase 3 primary antibody (Cell Signalling, Danvers, MA, USA). IHC was performed according to the manufacturer's protocol. In short, endogenous peroxidase was blocked by incubation with 0.3% H_2O_2 in methanol for 20 minutes, tissue antigenicity was recovered using heat-based retrieval (10mM citrate buffer, pH 6, 95°C, 10 min), sections were blocked with 4% normal swine serum (DAKO) in phosphate buffered saline containing 1% BSA and 0.1% tween (PBT) and incubated overnight with 1:100 primary antibody in 5% foetal calve serum in PBT. After washing, 1:1000 biotin-conjugated swine anti-rabbit secondary antibody (DAKO) in PBT was applied for 30 minutes, followed by 30 minutes of Vectastain ABC reagent (Vector Laboratories, Burlingame, CA, USA). 3'3-diaminobenzidine (DAB, DAKO) was applied as a color substrate and hematoxylin for nuclear counterstaining. Sections were dehydrated in a graded ethanol solution and xylene, subsequently enclosed with Entellan (Merck) and evaluated with a Nikon Eclipse E800 microscope. Pictures were taken with a Nikon Digital Camera DXM 1200F and analyzed using the Lucia G version 4.81 (Laboratory Imaging) software. Cleaved caspase 3 positive (apoptotic) cells were counted in six random pictures and expressed as percentage of all cells.

Table 3.1. Patient characteristics, muscle mtDNA measurements and OXPHOS complex activities.

Subject code	Mutation(s)	Sex	Age (y)	Prominent clinical features	mtDNA deletions	mtDNA copy number[a]	Enzyme measurement[b]	Blood lactate[d]
P30	A467T HOM	F	23 †	Migraine, sensory ataxia, seizures, status epilepticus, liver insufficiency; VPA treatment	ND	11158	CI 103, CII 84, CIII 168, CIV 122, CS 54	ND
P38	A467T / W748S + E1143G	M	36	Ptosis, CPEO, polyneuropathy, cerebellar ataxia, dysarthria	**multiple**	6478	ND	1.6
P54	A467T HOM	F	29	Cerebellar ataxia, axonal neuropathy, migraine, initial external ophthalmoplegia, epilepsy, myoclonic seizures, mild mental retardation	no	3321	CI 102, CII 108, CIII 77, CIV 121, CS 90	**1.9**
P194	R227P / A467T	F	0 †	Failure to thrive, died after status epilepticus	no	3644	**CI 9, CII 39**, CIII 69, CIV 66, CS 79	**3.9**
P253	T251I + P587L / A467T	F	47	Cataract, myopathy	ND	ND	CI 103, CII 75, CIII 107, CIV 108, CV 68, CS 94	1.6
P382	A467T / A957P	F	1 †	Growth retardation, occipital strokes, focal epilepsy, liver failure, died of heart failure	ND	ND	**CI 34**, CII 77, CIII 59, CIV 75, CV 125, CS 59	**3.5**
P423	R943H	F	68	POF and CPEO	**multiple**	**3174**	ND	ND

P477	T251I + P587L / G848S	F	50	Ptosis	**multiple**	6092	ND	0.9
P497	A467T / Lys925ArgfsX42	F	1 †	Prematurity, epilepsy, deafness, retinitis pigmentosa, status epilepticus, hemiparesis, liver failure	ND	2030	CI 62, CII 65, CIII 70, CIV 87, CV 94, CS 182	**>10**
P504	A467T HOM	F	15 †	Focal seizures, Alpers syndrome; trauma and VPA treatment	ND	ND	CI 67, CII75, CIII 42, **CIV 13**, CV 85, CS 29	**>10**
P509	S1095R / D1184N	F	3 †	Feeding problems, intestinal pseudo-obstruction, failure to thrive, congenital deafness, demyelinating sensomotor neuropathy, impaired liver function	no	**692**	CI 118, CII+CIII 51, CIV 513, CS 158[c]	**1.7-5.6**

Effects of the *POLG1* defect on the mtDNA; defects are in bold. HOM = homozygous, M = male, F = female, POF = premature ovarian failure, CPEO = chronic progressive external ophthalmoplegia, VPA = valproic acid treatment, n.a. = not applicable, ND = not determined, no material left for analysis; * Siblings; † deceased

[a] Reference copy numbers for depletion, as determined in 370 sample of various ages: Low (10-30% of controls): 0-2y 150-500; 3-9y 300-1000; above 10y 600-2000; Possibly low (30-50% of controls): 0-2y 500-800; 3-9y 1000-1600; above 10y 2000-3200;

[b] Expressed as percentage of control, except for P509. CI complex I, CII complex II, CIII complex III, CIV complex IV, CS citrate synthase, complex activities were considered decreased when below 40 percent of control to account for variability in control values;

[c] expressed as mU/U CS, control range CI 84-273, CII+CIII 40-285, CIV 520-2080, CS 45-187;

[d] normal values lactate 0.5-1.7 mmol/l

Results

In total, eleven patients with *POLG1* mutations were included in the study (table 3.1). Three patients were homozygous for p.A467T, five patients were compound heterozygous for this mutation and another mutation, two patients were compound heterozygote for other mutations and one patient had an autosomal dominant mutation (P423). Eight patients presented with neurological problems, five patients suffered from impaired liver function and three patients had chronic PEO and/or ptosis. Four patients died within their first years of life, one patient (P504) was diagnosed incidentally after death of valproic acid (VPA) treatment of post traumatic epileptic seizures and one patient (P30) experienced clinical symptoms for a prolonged time but deceased after VPA treatment. Based on these data, no obvious genotype-phenotype association could be observed.

Muscle mtDNA and morphology

In total, four out of eight patients showed either reduced mtDNA copy number (P509) or the presence of multiple deletions in skeletal muscle (P38, P423 and P477, table 3.1). Normal values were observed in the younger patients ageing 0 to 23 years. In three out of eight patients the activity of one or more OXPHOS complexes was decreased in muscle biopsies (table 3.1). Seven out of eight patients showed morphologic abnormalities in muscle. Four patients showed myopathic changes with ragged red fibers and multiple cytochrome *c* oxidase negative muscle fibers (patients P38, P194, P253 and P509; figure 3.1A-C). Another three patients (P497, P382 and P504) exhibited a striped positive staining of the muscle fibers in the trichrome stain in the absence of ragged red fibers. One patient (P54) did not show any changes of the muscle morphology. Ultrastructural changes were observed in all five patients (P194, P253, P497, P504 and P509) evaluated on electron microscopy with aberrant shape, size and distribution of the mitochondria. The mitochondria appeared elongated in shape or rounded with tubular cristae. Mitochondria were frequently aggregated and localized in the subsarcolemmal and A-band areas. One in five patients showed mitochondria with paracristalline inclusions (patient P253; figure 3.1D).

Muscle gene expression analysis

Gene expression levels of 17,215 transcripts were measured in skeletal muscle samples of six *POLG1* patients and twelve age matched controls (table 3.2). Transcripts of 3,718 genes passed the background signal criteria. The expression of 1,193 transcripts was significantly different between controls and *POLG1* patients (Appendix). Of the differentially expressed genes, 247 transcripts were increased and 946 were decreased, respectively. These results indicated mostly small (fold change < 1.5) gene expression changes. QPCR confirmed nine out of ten microarray results (data not shown).

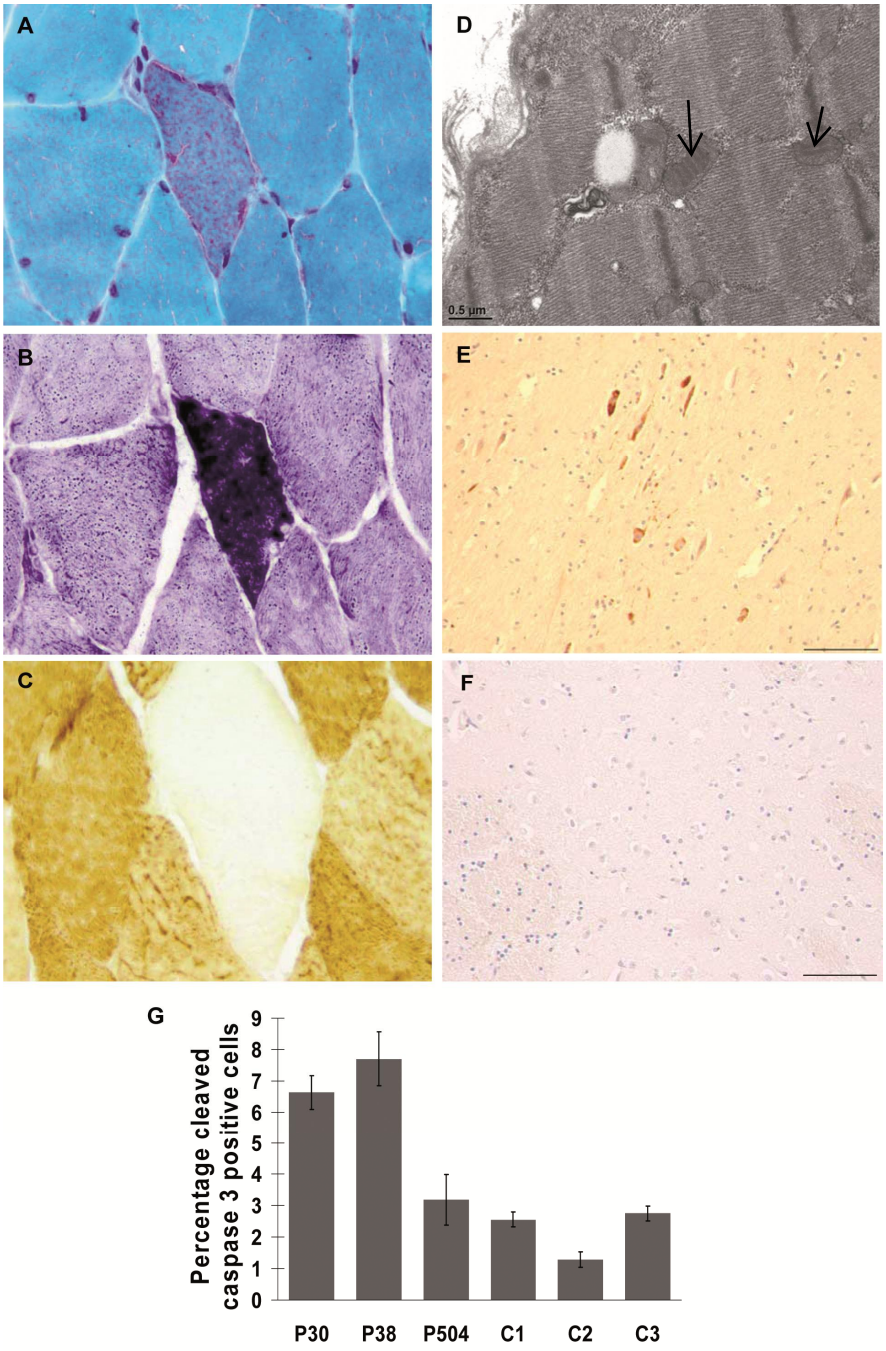

Figure 3.1. Histology and apoptosis in tissues of *POLG1* patients. Muscle biopsy**:** Modified Gomori trichrome (**A**), NADH (**B**) and cytochrome c oxidase (**C**) stain (400x) and electron microscopy (**D**). Clustered apoptotic cells in the brain of patient P30 (**E**), which are absent in controls (**F**) and the summarized results of apoptosis detection in liver of patients (P) and controls (C) (**G**). Bars in E and F are 100 µm. Arrows in panel D indicate paracristalline inclusions.

Table 3.2. Patients and controls for gene expression analysis.

Patient code	Sex	Age at biopsy	Control code	Sex	Age at biopsy
Age group: young					
P194	F	0	C11	M	0
P509	F	3	C12	M	1
			C13	M	9
			C14	M	2
			C15	F	5
			C16	M	2
Age group: middle					
P38	M	36	C3	F	34
P54	F	29	C5	F	17
			C7	F	22
			C9	M	25
Age group: old					
P423	F	68	C4	F	64
P477	F	50	C8	M	53

Overview of patients and controls used for the microarray gene expression analysis. P = patient, C = control, M = male, F = female; * Age groups: young (0 – 10 years old), middle (11 – 49 years old), old (≥ 50 years old)

Pathway analysis, using MAPPFinder, showed ten significantly altered pathways ($p<0.05$; table 3.3). In patient cells, the electron transport chain showed higher gene expression levels for 75% of its differentially expressed transcripts, whereas uncoupling protein 2 (*UCP2*) transcripts were decreased. In contrast, the expression of almost all differentially expressed genes in the fatty acid beta oxidation pathway was decreased (table 3.3). Transcripts of carnitine palmitoyltransferase 1 (*CPT1*) B, which is the rate-limiting step in beta oxidation, were decreased. This indicated reduced fatty acid catabolism. In the triglyceride synthesis pathway, the expression of most changed genes was decreased (table 3.3). Gene expression levels of NAD^+ dependent enzymes *SIRT2* and poly-(ADP-ribose) polymerase 1 (*PARP1*) were decreased (both fold change 0.79). Based on the observed changes, we performed an additional QPCR for *SIRT1* and *UCP3*, which had intensity levels in the background range of the microarray analysis. In the QPCR analysis, both were significantly decreased with fold changes 0.74 and 0.43, respectively. *POLG1* itself also showed intensity levels in the background range.

Overall, oxidative stress or apoptosis pathways were not significantly altered in muscle of *POLG1* patients. Nevertheless, in the oxidative stress pathway, superoxide dismutase 1 (*SOD1*) and glutathione peroxidase 4 (*GPX4*) gene expression levels were changed significantly with fold changes 0.91 and 1.46, respectively. Many genes in the apoptosis pathway did not reach significance due to low signal intensities. However, for the expression of 31 genes there was a tendency to be increased (n=16) or decreased (n=15) with an inconclusive effect on the total pathway. There were no significant

changes in the expression level of genes involved in mitochondrial biogenesis - peroxisome proliferator-activated receptor gamma coactivator 1-alpha/beta (*PGC1-α/β*), nuclear respiratory factor 1 (*NRF-1*) and mitochondrial transcription factor A (*TFAM*). Only minor changes were observed in the expression of genes involved in mitochondrial fusion and fission (*OPA1* fold change 0.81 and *MFN2* fold change 0.83).

Table 3.3. MAPPFinder results grouped into related categories.

MAPP Name	Changed	Up	Down	Measured	On MAPP	P-value
Metabolism and energy production						
Electron Transport Chain	20	15	5	97	105	0.000
Triglyceride Synthesis	9	2	7	23	24	0.000
Fatty Acid Beta Oxidation Meta	7	1	6	32	32	0.020
Transcription/translation						
mRNA processing Reactome	29	10	19	119	127	0.000
Translation Factors	12	1	11	42	50	0.000
RNA transcription Reactome	9	2	7	36	40	0.008
Others						
IL-9 NetPath 20	6	0	6	23	24	0.012
Nucleotide Metabolism	4	1	3	16	17	0.043
Circadian Exercise	8	1	7	46	48	0.046
Striated Muscle Contraction	7	1	6	38	38	0.048

Number of differentially expressed genes in the significantly changed ($p<0.05$) pathways according to MAPPFinder.

Increased ROS levels in POLG1 patient fibroblasts

Reactive oxygen species (ROS) levels were significantly increased in fibroblasts of patients P54, P194 and P382 (136% (confidence interval (c.i.) 114-163), 117% (c.i. 104-133) and 251% (c.i. 213-295) of controls, respectively), but not of patient P504 (112% of controls (c.i. 96-130)).

Histology and apoptosis in liver and brain

Histology of liver specimens of three investigated patients (P504, P382 and P30) showed a microvesicular steatosis with marked fibrosis, ductular proliferation and cholestasis as described before [12]. Hepatocyte mitochondria of patient P509 appeared aberrant in shape and size and often contained crystalloid inclusions. Post mortem examination of the brain of patient P504, exhibited typical Alpers-Huttenlocher like changes with ischemia and gliosis of the occipital cortex combined with spongiosis and gliosis of cortical and deep gray matter regions with a subtle and generalized decrease of neuronal numbers. The brain of patient P30 on the other hand did not exhibit changes of the occipital cortex. In this patient a degeneration with decrease of neuronal numbers and gliosis at all levels of the corticospinal tracts was observed, compatible with a phenotype of Friedreichs ataxia. Immunohistochemistry identified a

higher percentage of cleaved caspase 3 positive cells in liver of two (2/3) *POLG1* patients compared with three controls (figure 3.1G). In *POLG1* brain sections, a few apoptotic hot spots could be seen (figure 3.1E), which were not present in control brain sections (figure 3.1F).

Discussion

This study provides the first comprehensive characterization of molecular genetic, biochemical and morphological processes in human *POLG1* patients.

Muscle abnormalities in *POLG1* patients

This study revealed variable muscle aberrations in virtually all *POLG1* patients investigated. All patients tested showed ultrastructural changes on electron microscopy, which is in this study the most sensitive test. Other aberrations were related to the mtDNA (multiple deletions or decreased copy number), the activity of OXPHOS enzymes or were morphological changes. The three adult *POLG1* patients over 35 years old, for which mtDNA rearrangements could be analyzed, showed multiple deletions. Decreased activity of respiratory chain enzymes was observed in three out of eight patients. The presence of multiple deletions, mtDNA depletion or decreased OXPHOS function is suggestive for defects in the mtDNA maintenance and *POLG1*, but the absence of these features does not exclude mtDNA maintenance or *POLG1* defects, especially in young patients (P30 and P54 [13]). Nevertheless, because muscle biopsies will not always be available and based on clinical manifestations *POLG1* sequencing can be the first step, especially if an urgent diagnosis is required for treatment.

Changes in tissues of POLG1 patients

Metabolic switch in skeletal muscle

Transcription of genes in the beta oxidation pathway was significantly decreased. This might be explained by increased NADH levels as previously observed in fibroblasts from patients with isolated mitochondrial complex I (CI) deficiency [14]. Three of the patients in this study indeed showed a decreased OXPHOS function. Decreased OXPHOS-derived ATP production can stimulate glycolysis. This is associated with higher lactate production, inhibition of carnitine palmitoyltransferase 1 (CPT1) and thus also beta oxidation [15] (figure 3.2). Excess NADH in the cytosol can be oxidized by lactate dehydrogenase. Increased lactate levels are therefore often measured in patients with mitochondrial disease, including *POLG1* patients [16]. In this study, six out of nine patients showed increased lactate levels in serum. The increased transcription of the OXPHOS complexes could be a rescue attempt to process excess NADH and supply the cell of sufficient energy. This is supported by the decreased transcription of *UCP2* and *UCP3* leading to increased coupling of proton pumping and ATP production. The expected higher levels of point mutations and deletions in the mtDNA associated with defect pol γ [5] will only allow for increased quantity but not quality of the OXPHOS subunits when their transcription is increased. Therefore, the compensatory mechanism

might only partially be effective in tissues in which the OXPHOS system is not maximally used (*e.g.* fibroblasts), but would not meet the energy demand of highly active tissues such as muscle, liver and brain, leading to disease symptoms.
In this study, no significant effect was detected on mitochondrial or mtDNA biogenesis and its key regulator PGC1-α, even though two patients showed decreased mtDNA copy number. However, *SIRT1* transcripts were decreased. SIRT1 normally stimulates mitochondrial biogenesis and fatty acid β oxidation through post-translational activation of PGC1-α by deacetylation [17]. The NAD^+/NADH ratio has been shown to regulate transcription of the *SIRT1* gene [17], emphasizing additional cellular consequences of disturbed NADH metabolism.

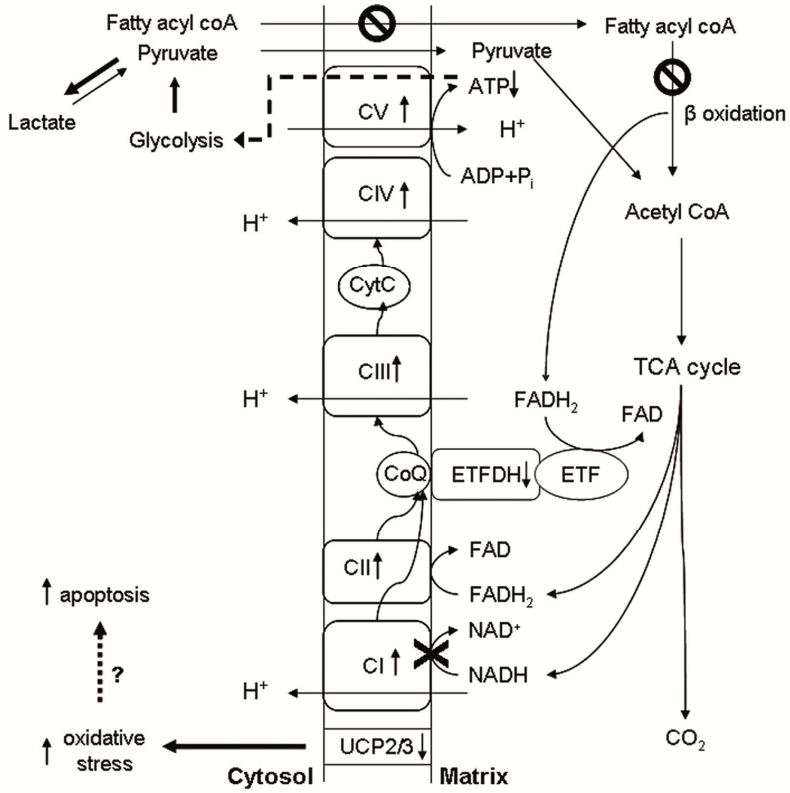

Figure 3.2. Pathophysiological processes in *POLG1* patients. Processes differentially expressed in *POLG1*patients: decreased beta oxidation, increased expression of OXPHOS subunits and decreased expression of uncoupling proteins. These changes suggest increased glycolysis, oxidative stress and apoptosis.

Mitochondrial fusion and fission

Only two genes associated with mitochondrial fusion and fission (*OPA1* and *MFN2*) showed minor gene expression changes. Recent literature states that mitochondrial fusion is essential for the equilibration of nuclear-encoded mitochondrial proteins over all organelles but leads to clonal expansion of mitochondrial deletion mutants with replicative advantage. Therefore, fusion is normally coupled to fission which enables

selective degradation of damaged mitochondria with decreased membrane potential by mitophagy [18]. The gene expression analysis does not provide convincing evidence for a role of mitochondrial fission and fusion in *POLG1* pathology. However, given the post-translational regulation of these processes [19], this should still be investigated on the protein level when patient material is available.

Increased ROS levels in fibroblast cultures

The involvement of oxidative stress in *POLG1* pathology is controversial. The overall oxidative stress pathway expression was not significantly changed, but particular genes such as *SOD1* and *GPX4* transcripts showed altered expression levels. Also *UCP3* expression was decreased. In the setting of doxorubicin-induced heart failure in rats, compensatory down-regulation of myocardial UCP2 and UCP3 lead to increased mitochondrial ROS production [20]. ROS levels were measured in fibroblast cultures of four patients and found to be increased in three (P54, P194 and P382) of them compared with controls, but not in patient P504. Increased ROS levels in OXPHOS disease are usually believed to originate from complex I or III sites. However, only fibroblasts of P194 showed a significant biochemical defect (data not shown). The method used cannot distinguish the exact cellular localization of hydroethidine oxidation [11], thus, another explanation for increased ROS levels could be the activation of alpha-ketoglutarate dehydrogenase in the tricarboxylic acid cycle. This enzyme can be stimulated to produce ROS by increased NADH levels [21]. The fact that one patient with and another patient without oxidative stress are both homozygous for the p.A467T mutation implies that it is not only the POLG defect that triggers ROS production. The patients may differ in the mtDNA defects resulting from the *POLG1* mutations, but we could not test this, because no muscle was left for one of the patients (P504). On the other hand, other genetic (protective or exacerbating) factors could be involved in controlling ROS levels. Altogether, the current results correspond with the unclear and controversial involvement of ROS in *POLG1* pathogenesis today.

Different transgenic mouse models are discordant on the presence [22] or absence [23] of increased oxidative stress due to pol γ defects. Furthermore, increased oxidative protein damage in the heart of these mice could be reduced by cardial mCAT overexpression, leading to attenuated cardiomyopathy [22]. Our results in human patients indicated that oxidative stress probably plays a role in part, but not all, of the *POLG1* patients. Divergent results in the different mouse models and patients could possibly be related to alternative effects of different *POLG1* mutations, mtDNA defects or different genetic backgrounds (*i.e*. antioxidant expression levels).

Apoptosis in liver and brain

The expression of only few apoptosis-related genes was significantly changed in muscle. Nevertheless, multiple other apoptosis genes showed a trend towards altered expression. Therefore, the presence of apoptotic cells in liver and brain, the most severely affected tissues in *POLG1* patients, was assessed. In the liver, apoptosis was distributed relatively evenly across the section and two out of three patients showed a more than twofold increase of apoptotic cells compared with controls. Different from the liver, there were only a few clusters of apoptotic cells in the brain of patients but not of

controls. In agreement, results from transgenic POLG mice showed the induction of apoptosis in the duodenum, liver, testis, thymus and skeletal muscle by measuring caspase 3 cleavage and TUNEL staining [23]. Strikingly, the two patients with increased liver apoptosis (P30 and P382) also showed increased oxidative stress in fibroblasts cultures, whereas both were not seen in the third patient (P504). This may suggest that apoptosis, possibly associated with increased ROS levels, contributes to *POLG1* related pathology (P30 and P382). However, the acute effect of trauma or drugs (*e.g.* VPA treatment) seems a much stronger trigger of acute organ failure in a previously disease-free individual (P504).

Conclusions

Even though muscle, liver and brain material of *POLG1* patients is scarce, this study elucidated a number of processes involved in *POLG1* pathogenesis. The heterogeneity in clinical presentation is reflected in the variable morphological, molecular and biochemical findings that were obtained. Increased oxidative stress and increased apoptosis appear to be related to the severity of the phenotype although trauma and/or drugs can shortcut this pathological route and lead to acute organ failure. In the future, measuring oxidative damage and apoptosis in liver and brain of additional patients is necessary to establish the link between ROS levels and apoptosis induction.

Acknowledgements

This work was supported by the Dutch IOP Genomics grant IGE5003C1 and the Kerry foundation (Maastricht, the Netherlands). We would like to thank A. Hendrickx, G. Konings, R. Kamps and M. Gijbels for technical expertise and help and H.R. Scholte for carefully reading the manuscript.

Supplementary material

Supplementary table 1 (in Appendix) – Significantly differentially expressed genes in muscle of *POLG1* patients

References

1. McFarland, R., R.W. Taylor, and D.M. Turnbull, *A neurological perspective on mitochondrial disease.* Lancet Neurol, 2010. **9**(8): p. 829-40.
2. Wong, L.J., et al., *Molecular and clinical genetics of mitochondrial diseases due to POLG mutations.* Hum Mutat, 2008. **29**(9): p. E150-E172.
3. Milone, M. and R. Massie, *Polymerase gamma 1 mutations: clinical correlations.* Neurologist, 2010. **16**(2): p. 84-91.

4. Chan, S.S. and W.C. Copeland, *Functional analysis of mutant mitochondrial DNA polymerase proteins involved in human disease.* Methods Mol Biol, 2009. **554**: p. 59-72.
5. Spelbrink, J.N., et al., *In vivo functional analysis of the human mitochondrial DNA polymerase POLG expressed in cultured human cells.* J Biol Chem, 2000. **275**(32): p. 24818-28.
6. Ashley, N., et al., *Depletion of mitochondrial DNA in fibroblast cultures from patients with POLG1 mutations is a consequence of catalytic mutations.* Hum Mol Genet, 2008. **17**(16): p. 2496-506.
7. Del Bo, R., et al., *Remarkable infidelity of polymerase gammaA associated with mutations in POLG1 exonuclease domain.* Neurology, 2003. **61**(7): p. 903-8.
8. van Tienen, F.H., et al., *Prolonged Nrf1 overexpression triggers adipocyte inflammation and insulin resistance.* J Cell Biochem, 2010. **111**(6): p. 1575-85.
9. Dai, M., et al., *Evolving gene/transcript definitions significantly alter the interpretation of GeneChip data.* Nucleic Acids Res, 2005. **33**(20): p. e175.
10. Akaike, H. *Information theory and an extension of the maximum likelihood principle*. in *Second International Symposium on Inference Theory*. 1973. Budapest: Akadémiai Kiadó.
11. Verkaart, S., et al., *Superoxide production is inversely related to complex I activity in inherited complex I deficiency.* Biochim Biophys Acta, 2007. **1772**(3): p. 373-81.
12. Muller-Hocker, J., et al., *Mitochondrial DNA depletion and fatal infantile hepatic failure due to mutations in the mitochondrial polymerase gamma (POLG) gene A combined morphological/enzyme histochemical and immunocytochemical/biochemical and molecular genetic study.* J Cell Mol Med, 2009.
13. Blok, M.J., et al., *The unfolding clinical spectrum of POLG mutations.* J Med Genet, 2009. **46**(11): p. 776-85.
14. Verkaart, S., et al., *Mitochondrial and cytosolic thiol redox state are not detectably altered in isolated human NADH:ubiquinone oxidoreductase deficiency.* Biochim Biophys Acta, 2007. **1772**(9): p. 1041-51.
15. Sahlin, K., et al., *Turning down lipid oxidation during heavy exercise--what is the mechanism?* J Physiol Pharmacol, 2008. **59 Suppl 7**: p. 19-30.
16. de Vries, M.C., et al., *Multiple oxidative phosphorylation deficiencies in severe childhood multi-system disorders due to polymerase gamma (POLG1) mutations.* Eur J Pediatr, 2007. **166**(3): p. 229-34.
17. Fulco, M. and V. Sartorelli, *Comparing and contrasting the roles of AMPK and SIRT1 in metabolic tissues.* Cell Cycle, 2008. **7**(23): p. 3669-79.
18. Kowald, A. and T.B. Kirkwood, *Evolution of the mitochondrial fusion-fission cycle and its role in aging.* Proc Natl Acad Sci U S A, 2011. **108**(25): p. 10237-42.
19. Han, X.J., et al., *Regulation of mitochondrial dynamics and neurodegenerative diseases.* Acta Med Okayama, 2011. **65**(1): p. 1-10.
20. Bugger, H., et al., *Uncoupling protein downregulation in doxorubicin-induced heart failure improves mitochondrial coupling but increases reactive oxygen species generation.* Cancer Chemother Pharmacol, 2010.
21. Starkov, A.A., et al., *Mitochondrial alpha-ketoglutarate dehydrogenase complex generates reactive oxygen species.* J Neurosci, 2004. **24**(36): p. 7779-88.
22. Dai, D.F., et al., *Age-dependent cardiomyopathy in mitochondrial mutator mice is attenuated by overexpression of catalase targeted to mitochondria.* Aging Cell, 2010. **9**(4): p. 536-44.
23. Kujoth, G.C., et al., *Mitochondrial DNA mutations, oxidative stress, and apoptosis in mammalian aging.* Science, 2005. **309**(5733): p. 481-4.

Chapter 4

Transcriptional changes in OXPHOS complex I deficiency are related to anti-oxidant pathways and could explain the disturbed calcium homeostasis.

A.M. Voets, M. Huigsloot, P.J. Lindsey, A.M. Leenders, W.J.H. Koopman, P.H.G.M. Willems, R.J. Rodenburg, J.A.M. Smeitink, H.J.M Smeets

Biochimica et Biophysica Acta (BBA) – Molecular Basis of Disease,
In press

Abstract

Defective complex I (CI) is the most common type of oxidative phosphorylation disease, with an incidence of 1 in 5,000 live births. Here, whole genome expression profiling of fibroblasts from CI deficient patients was performed to gain insight into the cell pathological mechanism. Our results suggest that patient fibroblasts responded to oxidative stress by Nrf2-mediated induction of the glutathione antioxidant system and Gadd45-mediated activation of the DNA damage response pathway. Furthermore, the observed reduced expression of selenoproteins, might explain the disturbed calcium homeostasis previously described for the patient fibroblasts and might be linked to endoplasmic reticulum stress. These results suggest that both glutathione and selenium metabolism are potentially therapeutic targets in CI deficiency.

Key words

Gene expression, complex I deficiency, mitochondria, oxidative stress, selenoproteins, Nrf2

Introduction

Mitochondria produce most of the cellular ATP through the process of oxidative phosphorylation (OXPHOS). The OXPHOS system is comprised of four multisubunit electron transport chain (ETC) complexes (Complex I-IV) and the F_0/F_1-ATP-synthase (Complex V). Complex I (CI) is the largest of the OXPHOS complexes and one of the entry points of electrons into the ETC. CI deficiency is the most frequently encountered defect in mitochondrial energy metabolism [1] and is associated with *e.g.* Leigh disease, Leber hereditary optic neuropathy (LHON), fatal infantile acidosis, neonatal cardiomyopathy with lactic acidosis, leucodystrophy with macrocephaly and hepatopathy with renal tubulopathy [2, 3]. Although children usually have a normal prenatal development, symptoms start occurring during their first year of life after which the disease deteriorates rapidly and may become fatal [4].
Disease-causing mutations have been described in both the mitochondrial DNA (mtDNA)-encoded (*ND1* to *ND6*, and *ND4L* genes) and nuclear DNA-encoded structural CI subunits (*e.g.* NDUFS1, NDUFS2, NDUFS4, NDUFS7, NDUFS8) and CI assembly factors (*e.g.* B17.2L, NDUFA12L, C20ORF7) [5-26]. The cellular consequences of CI deficiency have been extensively studied in patient fibroblasts. CI deficiency leads to a slightly depolarized mitochondrial membrane potential [27], increased reactive oxygen species (ROS) levels [28], increased NAD(P)H levels [29], changes in mitochondrial morphology [30] and disturbed calcium homeostasis [31, 32]. However, increased ROS production and mitochondrial fragmentation was not always detectable [33]. A first study investigating transcriptional responses in CI deficient fibroblasts cultured with glucose and galactose using a mitochondria-targeted microarray detected the induction of metallothioneins and heat shock proteins and the decreased expression of mtDNA-encoded transcripts [34]. To get an unbiased overview of the underlying pathological processes (not restricted to mitochondria) in CI deficiency, we performed whole genome gene expression and additional pathway analysis in fibroblasts of a homogeneous group of CI deficient patients with a defect in one of the nuclear encoded structural subunits. The CI deficiency might not stress the cell to such an extent that relevant disease-associated gene expression changes can be picked up. Therefore, fibroblasts were deprived of glucose to stimulate energy production through oxidative phosphorylation. In galactose medium, the flow of galactose to glucose-1-phosphate is very slow which obliges cells to obtain ATP from mitochondrial oxidation of pyruvate and glutamine [35].

Material and methods

Fibroblast cell lines

Fibroblasts were derived from skin biopsies of five patients homozygous or compound heterozygous for nuclear complex I mutations and five controls. The groups were matched for age and sex. All patients have been described previously (#8807 see [26], #7898 see [24], #5175 see [15], #6613 see [30], #8382 see [25]). Table 4.1 provides an

overview of the subjects and physiological parameters in the patient cell lines [4, 28, 29, 32]. The age- and sex-matched control group consisted of four male subjects, ages 6 months (mo), 1 year (y) 7mo, 1y 6mo, 3y 6mo respectively and one female subject of 1y 11mo.
Fibroblasts were routinely cultured in medium 199 (Gibco, Paisley, UK) supplemented with 10% fetal calf serum and penicillin/streptomycin (respectively 100U/ml and 100 µg/ml). To stimulate energy production by oxidative phosphorylation, fibroblasts were cultured in galactose medium for 48 hours. Galactose medium consisted of DMEM without glucose, without pyruvate and with 4 mM L-glutamine (Invitrogen, Paisley, UK), 5.5 mM D-galactose (Sigma, Zwijndrecht, Netherlands), 1 mM uridine (Acros, Geel, BE), 10% dialyzed fetal calf serum (Invitrogen) and penicillin/streptomycin, Glucose medium was identical to galactose medium except that D-glucose was present at 5.5 mM instead of galactose. The stability of the mtDNA was preserved during the course of the experiment in all cell lines under both conditions as no mtDNA deletions or group/treatment specific differences in mtDNA copy number (supplementary table 4.1) could be detected.

Microarray procedure

Total RNA was isolated using the TRIzol reagent (Invitrogen) and purified with the RNeasy clean-up kit (Qiagen, Hilden, DE). RNA quantity and purity were determined spectrophotometrically using the Nanodrop ND-1000 (Nanodrop Technologies, Wilmington, DE, USA). RNA integrity was assessed by determining the RNA 28S/18S ratio using the Bioanalyser 2100 (Agilent Technologies, Santa Clara, CA, USA). Fibroblast RNA (150 ng) was reverse transcribed into cDNA and amplified in a two-round amplification reaction according to the manufacturer's protocol (Affymetrix, Santa Clara, CA, USA). A mixture of cDNA and added hybridization controls was hybridized on Affymetrix HG-U133 Plus 2.0 chips, followed by staining and washing steps in the GeneChip fluidics station 400 (Affymetrix) according to the manufacturer's procedures. To assess the raw probe signal intensities, chips were scanned using the GeneChip scanner 3000 (Affymetrix).

Microarray data analysis

Images of the Human Genome U133 Plus 2.0 arrays were quantified with GCOS software (Affymetrix). The microarray data reported in this manuscript have been deposited in NCBI Gene expression omnibus (GEO), accession number GSE27041. The chip description file (CDF) used for the analysis was an update created and freely distributed by the microarray lab of the university of Michigan (http://brainarray.mbni.med.umich.edu; [36]) based on Ensembl (version 10). A more detailed description of this analysis is shown in the supplementary data. Briefly, the genes were analyzed using Gaussian linear regression including the hybridization and labeling spikes, age, sex, passage, mtDNA copy number, and medium. The inference criterion used for comparing the models is their ability to predict the observed data, i.e. models are compared directly through their minimized minus log-likelihood. When the numbers of parameters in models differ, they are penalized by adding the number of estimated parameters, a form of the Akaike information criterion (AIC) [37]. For each

gene, the group was then added to the model. Then, the group-medium interaction was also added to the model. The gene under consideration was found to be differentially expressed if the AIC of either of these two models decreased compared to the model containing no group effect at all. The genes analyzed and fold changes were loaded into the Pathvisio (version 2.0.8) [38] software package to evaluate the transcripts in relation to known biological processes. The gene database version "Hs_Derby_20090509" was used. Only gene-transcripts with either their average intensities for the control and patient groups above 150 or average intensities for one of these groups above 300 and a 10 percent up or down regulation fold change were used to obtain a ranked list of pathways with differentially expressed genes. Pathvisio software was used to select the pathways with a Z score larger than 1.96 and thus containing relatively high numbers of differentially expressed genes.

Quantitative PCR

Differentially expressed genes were validated by real-time quantitative PCR (QPCR) with the same RNA samples used for the microarrays. Primers were designed using the NCBI Primer-BLAST tool (NCBI home page; http://www.ncbi.nlm.nih.gov/). cDNA was prepared from 1 µg of RNA in a standard reverse transcriptase reaction. PCR was performed in a 7900HT Fast Real-Time PCR System (Applied Biosystems, Foster City, CA, USA) using SensiMixPlus SYBR (Quantace, Finchley, UK). Cycling conditions were: an initial step of 2 minutes at 50°C, activation of the polymerase at 95°C for 10 minutes, and 40 cycles of 15 seconds at 95°C followed by 1 minute at 60°C. The TATA-box binding protein (TBP) gene was used as an internal reference. Genes for which QPCR was performed and the primers used for amplification are listed in supplementary table 4.2. Results were analyzed using Gaussian linear regression, similar to the microarray analysis. The housekeeping gene (TBP), age, sex, passage, mtDNA copy number, RNA integrity number (RIN) and medium were included during the analysis. The AIC was used to assess whether there was a difference between the controls and patients (group effect). All statistical analyses presented were performed using the freely available program R [39] and the publicly available library 'growth' [40].

Western blot analysis

Protein expression was monitored by Western blot analysis of 12% SDS-PAGE gels loaded with 40 µg of whole cell extract. The following primary antibodies were used: Complex I (NDUFA9; Mitosciences, Oregon, USA), HMOX1 (Abcam, Cambridge, UK), GCLM (Sigma), GSR (Santa Cruz, Heidelberg, DE), and TrxR1 (Santa Cruz). Complex II (70kDa Fp; Mitosciences) was used as a loading control. Secondary antibodies used were polyclonal goat anti-mouse IgG/HRP (Dako, DK) and immunoPure goat anti-rabbit IgG/Peroxidase (Pierce Biotechnology, Rockford, IL, USA). Detection of the signal was performed using ECL Western Blotting Substrate (Thermo Scientific, Amsterdam, NL) following the manufacturer's instructions.

Table 4.1. Patient characteristics and physiological cell line parameters

Cell line	group	Age	sex	Affected subunit and mutation	CI	HEt	CM-H_2DCF	GSH	GSSG	ER_{Ca}	$[Ca]_C$ peak	$[Ca]_M$ peak
8328	patient	1y	m	NDUFS1-211delE/V288A	**24**	N/A	N/A	N/A	N/A	N/A	N/A	N/A
8807	patient	7mo	f	NDUFS2 – D445N	**26**	**191**	**244**	N/A	N/A	**82**	**91**	**87**
7898	patient	<7mo	m	NDUFS4 – R106X	**36**	**174**	**187**	18.8	0.587	**77**	**84**	**79**
5175	patient	3y	m	NDUFS7 – V122M	**68**	**151**	**212**	21.3	0.630	**73**	**80**	**76**
6613	patient	<1mo	m	NDUFS8 – R94C	**18**	**222**	**275**	28.5	1.017	**85**	**91**	**89**

Physiological parameters have been published previously [4, 28, 29, 32]; values in bold are significantly different from control (see respective publications); mutations are given at the protein level; CI = residual CI activity (% of lowest control); HEt = rate of ethidium formation as a measure of ROS levels (% of control); CM-DCF = rate of 5-[and -6]-chloromethyl-2',7'-dichlorofluorescein formation as a measure of ROS levels (% of control); GSH = reduced glutathione levels (average control value 26.1±1.8 nmol/mg protein); GSSG = oxidized glutathione levels (average control value 0.793±0.033 nmol/mg protein); ER_{Ca} = resting calcium content of the endoplasmic reticulum (% of control); $[Ca]_C$ peak = bradykinin(Bk)-induced peak in crease in cytosolic free Ca^{2+} concentration (% of control); $[Ca]_M$ peak = Bk-induced peak increase in mitochondrial free Ca^{2+} concentration (% of control); in previous publications, cell lines 8807, 7898 and 6613 correspond to cell lines 7276, 5260 and 6603 respectively; m = male, f = female, N/A = not available.

Results

Global gene expression profiles of fibroblast cell lines from five CI deficient patients with a mutation in a nuclear CI gene were characterized in glucose and galactose medium to identify processes involved in pathogenesis, novel biomarkers for CI deficiency and potential future targets for therapeutic interventions. In order to gain insight into the changes in essential cellular processes rather than single genes, genes were clustered based on cellular function and analyzed by pathway analysis using Pathvisio software [38].

Gene expression analysis

In total, disease state, culture condition and their interaction significantly altered the expression of 3,279 genes by more than 10 percent. The disease state induced fold changes between 0.08 and 6.89 (of which 79% between 0.66 and 1.5 (10-50% change)) in the glucose condition and between 0.08 and 12.18 (69% between 0.66 and 1.5) in the galactose condition. Furthermore, the different culture conditions caused gene expression changes of 0.32 to 2.91 (90% between 0.66 and 1.5) and 0.11 to 29.74 fold (46% between 0.66 and 1.5) in controls and patients respectively. Pathway analysis was performed to identify processes that were altered due to the cumulative effect of differentially expressed genes (table 4.2, supplementary table 4.3). The sum of the differentially expressed genes in a pathway can lead to increased expression, decreased expression or a miscellaneous effect (both inhibition and stimulation), which is indicated for each pathway.

Changes due to culture condition only

The metabolic switch due to glucose deprivation of the cells in galactose medium changed the expression of 2,888 genes. This included genes with a larger/smaller fold change or an opposite fold change in patients compared with controls. If only genes were included that showed the same effect on galactose compared with glucose for both groups, 1,304 genes were changed and these could be mapped to the pathways cholesterol biosynthesis (increased in galactose), proteasome degradation (miscellaneous effect) and prostaglandin synthesis and regulation (increased in galactose) (figure 4.1B).

Changes due to complex I deficiency

Between patients and controls, 1,407 and 2,335 genes were significantly changed in glucose and galactose, respectively, with an overlap of 1,199 genes. Pathways that showed a significant change only in the normal glucose condition included the pentose phosphate pathway (increased in patients), heme biosynthesis (decreased in patients), alanine and aspartate metabolism (increased in patients), urea cycle and metabolism of amino groups (increased in patients) and ganglio spingolipid metabolism (decreased in patients). Furthermore, some pathways were significantly altered in both normal glucose and galactose condition: senescence and autophagy (miscellaneous effect), selenium (decreased in patients), mismatch repair (decreased in patients) and nucleotide metabolism (increased in patients) (figure 4.1A).

Table 4.2. Pathway analysis results

Pathway	patients vs controls glucose		patients vs controls galactose		galactose vs glucose identical in patients and controls		galactose vs glucose different in patients and controls	
	% changed	Z score	% changed	Z score	% changed	Z score	% changed	Z score
Changes due to culture condition only								
Cholesterol Biosynthesis	14.29	0.53	14.29	-0.32	**57.14**	**5.92**	0.00	-1.34
Proteasome Degradation	13.33	0.85	25.00	1.53	**18.33**	**2.20**	15.00	0.89
Prostaglandin Synthesis and Regulation	13.33	0.60	20.00	0.36	**23.33**	**2.47**	6.67	-0.81
Changes due to disease, notable in normal condition								
Pentose Phosphate Pathway	**57.14**	**4.15**	42.86	1.76	28.57	1.65	14.29	0.24
Heme Biosynthesis	**44.44**	**3.43**	33.33	1.25	22.22	1.24	0.00	-1.08
Alanine and aspartate metabolism	**33.33**	**2.69**	33.33	1.44	25.00	1.75	8.33	-0.33
Urea cycle and metabolism of amino groups	**26.32**	**2.36**	31.58	1.61	**31.58**	**3.17**	10.53	-0.12
Ganglio Sphingolipid Metabolism	**26.67**	**2.14**	33.33	1.61	**33.33**	**3.04**	6.67	-0.57
Adipogenesis	**15.70**	**2.10**	23.14	1.65	11.57	0.62	12.40	0.36
Changes due to disease, notable in normal and selective condition								
Senescence and Autophagy	**22.58**	**4.07**	**27.96**	**2.68**	15.05	1.68	13.98	0.80
Selenium	**17.57**	**2.17**	**29.73**	**2.78**	9.46	-0.13	17.57	1.70
Mismatch repair	**33.33**	**2.32**	**44.44**	**2.12**	11.11	0.12	22.22	1.03
Nucleotide Metabolism	**27.78**	**2.51**	**38.89**	**2.39**	22.22	1.75	22.22	1.45
Changes due to disease that interact with culture condition								
Oxidative Stress	**22.22**	**2.11**	**48.15**	**4.20**	14.81	0.85	**37.04**	**4.22**
Selenium metabolism/ Selenoproteins	**28.13**	**3.41**	**40.63**	**3.45**	15.63	1.08	**28.13**	**3.00**
TGF Beta Signaling Pathway	**19.23**	**2.22**	**34.62**	**3.26**	11.54	0.39	**26.92**	**3.56**
Translation Factors	**21.43**	**2.46**	26.19	1.48	**19.05**	**1.99**	**21.43**	**2.07**
Changes due to interaction disease-culture condition only								
Cell cycle	14.12	1.26	**32.94**	**3.78**	10.59	0.21	**24.71**	**3.92**
G1 to S cell cycle control	12.31	0.61	**27.69**	**2.17**	9.23	-0.19	**21.54**	**2.61**
Androgen Receptor Signaling Pathway	8.41	-0.57	**25.23**	**2.12**	6.54	-1.19	**21.50**	**3.35**
Glutathione metabolism	6.25	-0.51	**37.50**	**2.10**	0.00	-1.33	**37.50**	**3.30**
Keap1-Nrf2	7.69	-0.28	**46.15**	**2.72**	15.38	0.66	**38.46**	**3.08**
DNA damage response	11.94	0.52	**31.34**	**3.00**	11.94	0.56	**23.88**	**3.26**
Glycogen Metabolism	11.43	0.27	**31.43**	**2.17**	14.29	0.87	**25.71**	**2.69**
TGF-beta Receptor Signaling Pathway	10.27	0.09	22.60	1.64	10.96	0.43	**17.12**	**2.24**
Id Signaling Pathway	6.12	-0.92	22.45	0.91	10.20	0.07	**20.41**	**2.01**
TNF-alpha/NF-kB Signaling Pathway	8.00	-0.93	20.00	0.88	8.57	-0.61	**16.00**	**1.98**

Every pathway counts at least 7 genes measured by the microarray. A Z score of more than 1.96 indicates that a pathway is significantly changed (shown in bold).

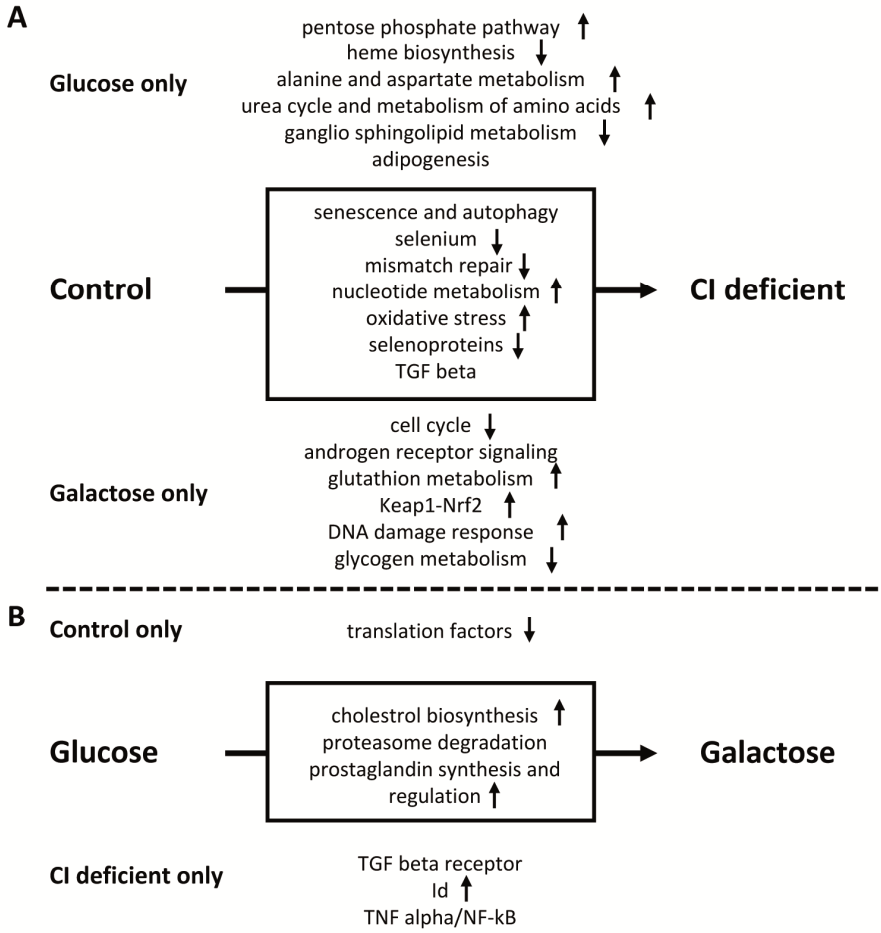

Figure 4.1. Pathways significantly different (A) in controls and patients and (B) in glucose and galactose conditions. Pathways in the box are changed in both culture conditions (A) or groups (B). Pathways above and below the box are only changed in the indicated condition (A) or group (B). Arrows indicate increased or decreased expression; for pathways without arrow, the direction of the change is not clear.

<u>Changes due to disease and interacting with the culture condition</u>

There were 1,584 genes that differed between patients and controls in the glucose and/or galactose culture condition, but for which patients showed a different response to the galactose condition compared with the controls. A different response could be a response to galactose in only the patients or the controls, a quantitative difference or an opposite effect. When considering these genes, part of them were altered as a result of the CI deficiency, but additionally showed an interaction between this deficiency and the culture condition. Altered pathways included oxidative stress (increased in patients and further increased in galactose medium), selenium metabolism and selenoproteins (decreased in patients and further decreased in galactose medium), the TGF beta

signaling pathway (miscellaneous effect) and translation factors (decreased in patients). The remainder of the genes was only altered in patient cells relative to control cells on galactose medium but not in glucose medium. This last group of genes was mapped to pathways involved in cell cycle progression (decreased in patients), oxidative stress (increased in patients; Keap1-NRF2, glutathione metabolism, DNA damage response) and signaling (miscellaneous effect; androgen receptor, TGF beta receptor, Id, TNF alpha/NF-κB). A general overview of all significantly changed pathways is shown in figure 4.1.

QPCR and western blot validation of microarray data

From the pathway analysis, representative genes with fold changes of more than fifty percent were selected and validated by QPCR (table 4.3). For all except one gene (*C-MYC*), the QPCR method detected a difference between patients and controls comparable with the microarray analysis. Furthermore, to correlate gene expression and protein levels, western blot analysis was performed for proteins selected from the genes with relatively high gene expression fold changes in significantly altered pathways for patients versus controls in galactose medium. Significantly increased expression was confirmed for HMOX and GCLC, a similar trend in protein expression was observed for TXNRD1 but no change was detected for GSR (figure 4.2). Additionally, western blot analysis also revealed that complex I deficiency in the cell lines was accompanied by reduced protein levels of complex I (figure 4.2).

Discussion

During the last decade, studies have generated extensive knowledge on the pathogenesis of CI deficiency [4, 28, 29, 32]. In spite of these advances in physiological, biochemical and genetic insights, the total picture is far from complete. In the present study, gene expression analysis was performed for a more general overview of the processes involved in CI deficiency in fibroblasts. According to recent models of complex I assembly, the selected patients all had mutations in structural CI subunits of the dehydrogenase and hydrogenase modules of the hydrophilic peripheral arm of complex I protruding in the matrix. These modules are involved in oxidation of NADH to NAD^+ and electron transfer to ubiquinone [41] and mutations in their proteins disturb these fluxes, leading to CI deficiency. Therefore, we consider these patients as a group with a common pathophysiological basis, making them suitable for genome-wide gene expression approaches.

Differential expression of a number of genes and proteins in relevant pathways was validated and related to available physiological and biochemical data.

Legend Table 4.3. Genes in italics did not show an interaction between disease effect and medium effect with QPCR analysis (in contrast to microarray analysis) but are still able to distinguish patients from controls in both culture media.

Table 4.3. Selected genes for the QPCR signature

Gene symbol	Disease effect				Medium effect			
	Glucose condition		Galactose condition		Controls		Patients	
	Array	QPCR	Array	QPCR	Array	QPCR	Array	QPCR
Keap1-Nrf2								
NRF2		0.77	1.30	1.42	0.82	0.77	1.25	1.42
KEAP1		0.77	1.28	1.27			1.68	1.58
Oxidative stress								
CYBA		*0.56*	*0.63*	*0.56*		*0.62*	*0.63*	*0.62*
FOS	0.44	0.48	1.55	2.10	0.62		2.19	2.85
HMOX1			7.23	17.58			9.76	28.95
Glutathione metabolism								
GSR			1.96	2.46			2.31	3.23
IDH1			1.50	1.79		1.27	1.88	2.61
GCLC			1.90	1.82			2.38	2.66
GCLM			1.94	2.67			1.91	2.81
Selenium metabolism/Selenoproteins								
SELK			2.14	2.30			2.01	2.36
SEPP1	*0.38*	*0.33*	*0.21*	*0.33*	*0.59*	*0.39*	*0.32*	*0.39*
Pentose phosphate pathway								
PGD			1.75	1.55			2.10	2.36
DNA damage response								
GADD45A		1.86	2.25	3.20			1.89	2.08
GADD45B	*1.71*	*3.56*	*3.40*	*3.56*		*1.81*	*1.84*	*1.81*
TNFRSF10B			2.05	1.69			2.12	2.11
C-MYC			1.90			1.78	1.75	1.78
Cell cycle - anaphase regulation								
ESPL1			0.60	0.35	1.69	2.04		
CDC20		*0.48*	*0.38*	*0.48*	*2.55*			
Nucleotide metabolism								
PRPS1	1.77	1.79		0.59			0.50	0.29
Glycogen metabolism								
GBE1	0.87		1.43	1.74			1.63	1.70
Senescence and autophagy								
ING1		0.71	1.60				1.91	1.69
TGF Beta signaling pathway								
LTBP1	1.70		0.60	0.23		1.97	0.44	0.54
TGIF			1.46	1.65			1.71	2.60
Adipogenesis								
RORA		1.49	1.86	2.59			1.84	2.41
DDIT3			2.61	2.50		1.65	2.24	3.46
LMNA			0.45	0.44			0.45	0.46
ADFP		0.66	1.41				1.95	1.84

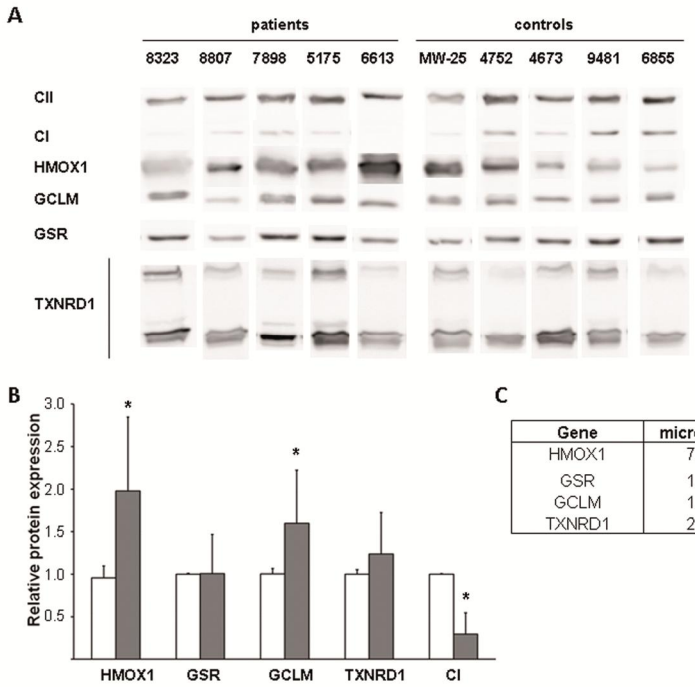

C

Gene	microarray	QPCR	western blot
HMOX1	7.23	17.58	1.98
GSR	1.96	2.46	1.01
GCLM	1.94	2.67	1.6
TXNRD1	2.24	N/A	1.24

Figure 4.2. Western blot validation of mRNA results. (**A**) Original western blot results and (**B**) a graphical representation of differences in protein levels for complex I (CI), HMOX, GSR, GCLM and TXNRD1 between controls (white bars) and patients (grey bars) fibroblasts cultured with galactose medium, normalized for the expression in controls (* $p < 0.05$ patients versus controls galactose). Complex II (CII) was used as a reference. In panel **C**, microarray, QPCR and western blot results for these genes in patients versus controls in galactose medium were compared.

Experimental set-up

To be able to examine the consequences of CI deficiency in fibroblasts (which are mainly glycolytic), cell lines were challenged to use their OXPHOS system for energy production by culturing in galactose medium in the absence of glucose [33, 34]. Our analytical model corrected for a number of potential 'noise' factors (biological e.g. age, sex and passage; technical e.g. chip effect), in contrast to a previous study [34]. The approach differed further from this study [34] by type and scope of the array (Affymetrix GeneCHIPS versus home-made two-color cDNA microarrays with selected mitochondria-related genes). The current study provides a well-controlled and more complete picture of the molecular processes in fibroblasts of CI patients. These differences can explain why only eleven genes showing differential expression in the previous study could be confirmed [34] (supplementary table 4.4). Unfortunately, nine additional genes could not be analyzed due to the use of the more accurate updated probe set definitions [36] and thirteen genes had low signal intensities, which made comparison impossible. However, the eleven confirmed results included multiple metallothionein transcripts, which were key elements in the previous study [34].

General gene expression analysis results

Linear regression analysis showed significantly altered expression of in total 3,279 genes due to disease, culture medium or a combination of both. As expected, gene expression differences were the highest when comparing patient and control cells cultured in galactose medium and when comparing the glucose and galactose condition in patient fibroblasts. Both the number of differentially expressed genes and the expression difference were higher. In control cells, less than 10% of the differentially expressed genes showed fold changes of more than 50% in galactose compared with glucose indicating that control cells were better capable of handling the galactose challenge. The altered expression of a number of genes was validated by QPCR and all of these, except for one gene (*C-MYC*), showed a response similar to the microarray thus confirming the overall reliability of the microarray data. Furthermore, for two genes, increased gene expression was accompanied by increased protein expression, validating the biological relevance of the detected differences in gene and pathway expression.

Differentially expressed processes

To identify processes that were altered due to the cumulative effect of differentially expressed genes in such a process, pathway analysis was performed. Pathways that were only changed in patient versus control fibroblasts both cultured in the presence of glucose were mainly involved in metabolism and included in most cases only a small number of genes with limited fold changes. This suggests that under glycolytic conditions, fibroblasts can adapt relatively easily to alternative energy sources. Therefore, we focused on processes that were changed due to the combination of disease and galactose culturing when the cells are forced to use their oxidative phosphorylation system.

Oxidative stress

Although the oxidative stress pathway was significantly changed when comparing patient and control cells on glucose, the difference was more significant (higher Z score) and more genes were involved on galactose medium. This is consistent with the observation of increased ROS levels in the CI deficient fibroblasts (table 4.1; [4, 28]). Furthermore, in an independent study with fibroblasts from OXPHOS (including CI deficient) patients, we observed higher ROS levels when fibroblasts (including controls) were cultured with galactose compared with glucose (manuscript in preparation). Transcripts of genes involved in glutathione homeostasis were increased, but transcription of the other antioxidant enzymes, catalase and superoxide dismutase (mitochondrial and extracellular), was decreased. Although enzyme activity measurements should confirm these results, this suggests that the glutathione antioxidant system is the main defense mechanism counterbalancing increased ROS production in CI fibroblasts. Additionally, the induction of the DNA damage response through increased expression of *GADD45A* and *GADD45B* could further emphasize cellular stress. Gadd45-mediated growth arrest [42] might explain why fibroblasts of CI deficient patients proliferate at a slower rate than healthy control fibroblasts.

A number of redox-sensitive genes that were significantly changed in this study (*HMOX1*, *CAT* and *SOD3*) were not reported in a previous study [34], most likely due to a different analytical approach. However, the induction of a number of metallothionein genes was detected in both studies (supplementary table 4.4). Metallothioneins are considered potent antioxidants of which the expression is induced by ROS, heavy metals and other forms of cellular stress [34]. Another study with different genetically characterized CI deficient patient fibroblast cell lines (*NDUFV1* p.W51X + p.T423M and *NDUFA1* p.R37S + G8R) did not detect differences in catalase and glutathione reductase protein expression and only one of the three patient cell lines showed the induction of mitochondrial superoxide dismutase protein [33]. This could be explained by the fact that, in contrast to our cell lines (table 4.1; [4, 28]), their cell lines did not show increased ROS production, explaining the lack of increased antioxidant defense. It also suggests that the CI mutations of these patients might have different consequences than the ones studied here.

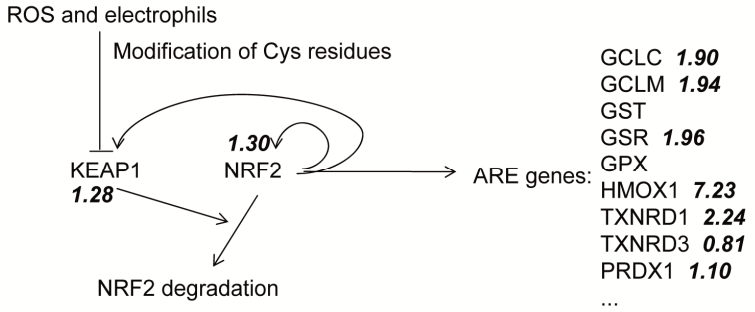

Figure 4.3. Activation of the KEAP1-NRF2 pathway in patient fibroblasts cultured with galactose. Fold changes of the significantly changed genes (patients versus control cultured with galactose) are shown in bold italics.

KEAP1-NRF2-glutathione

One of the most obvious differentially expressed pathways was the *KEAP1-NRF2* pathway, leading to the activation of a large number of genes involved in glutathione homeostasis and the thioredoxin and peroxiredoxin antioxidant defense (figure 4.3). ROS-mediated modification of cysteine (Cys) residues in Keap1 is known to result in diminished binding of Nrf2, leading to decreased Nrf2 degradation, its translocation to the nucleus and transcription of genes containing the antioxidant response element (ARE) in their promoter region [43, 44]. Activation of *NRF2* signaling was described previously in fibroblasts of patients with a mutation in the mitochondrial *ATP6* gene [45]. Consistent with a lack of *NRF2* signaling, glutathione levels in patient fibroblasts were not significantly different from controls in de glucose situation (table 4.1; [29]). However, reduced glutathione (GSH) levels of cell lines 7898 and 5175 were at the lower limit of control values and oxidized glutathione (GSSG) levels were at the higher limit of control values for cell line 6613 [29]. It has been suggested previously that antioxidants present in the culture medium may quench ROS [46], which might make up-regulation of the

antioxidants unnecessary. With the induction of glutathione homeostasis genes, it can be expected that glutathione levels are increased in the galactose situation to buffer the additional free radicals and prevent oxidative damage. Up-regulation of GCLC was confirmed at the protein level.

Selenium and selenoproteins

Pathway analysis revealed significant differences in the expression of the selenium (metabolism) and selenoprotein genes in control and patient fibroblasts. Although some overlap exists between these pathways and the oxidative stress pathway, the functions of many of the selenoproteins are unknown [47]. Selenoproteins are a group of proteins that contain selenocystein as an integral part of their polypeptide chain and include different protein families such as the thioredoxin reductases (TXNRDs) and glutathione peroxidases (GPXs), and a number of alphabetically annotated selenoproteins (SelK, SelM, SelN…) [47, 48]. While some classes are definitely involved in antioxidant pathways (GPXs) and redox pathways (TXNRDs), others have been implicated to play a role in calcium homeostasis (SelN) [47]. Recently, it was shown that association of SelN with the ryanodine receptor was necessary to control release of calcium from intracellular endoplasmic reticulum stores [49]. Thus, a decrease of *SEPN1* transcripts, might correlate with the decreased calcium fluxes measured in the studied patient cell lines (table 4.1; [31, 32]). If confirmed this might provide a new lead in the pathogenesis of CI deficiency. In HepG2 cells, SelK was induced by endoplasmic reticulum stress and protected the cells from stress induced apoptosis [50]. The increased mRNA expression of *TXNRD1* and *SelK*, opposed to the decreased expression of multiple other selenoproteins, might suggest the preferential expression of selenoproteins involved in stress reduction in oxidative CI deficient patient fibroblasts. The expression of selenoproteins is depending on the cellular selenium status [51]. Selenium deficiency has been shown to induce the expression of Nrf2 target genes [51, 52], providing a link between the observed induction of the Keap1-Nrf2 pathway and the decreased expression of selenoproteins. Therefore, monitoring and adjusting selenium levels might be beneficial for patients with complex I deficiency. Dietary selenium has been supplemented for the treatment or prevention of cancer [53] and Alzheimer's disease [54]. This study emphasizes the relevance of testing the applicability and efficiency of selenium supplementation also for CI deficiency, which should be tested first *in vitro* and in animal models and later in clinical trials.

Conclusion

The gene expression analysis supports the changes in oxidative stress levels previously measured in fibroblasts of CI deficient patients. It was shown that the cells adapt to and protect themselves against a higher oxidative state through transcriptional regulation of the *NRF2* pathway. Additionally, altered expression of selenoproteins provided a new way to explain diminished calcium fluxes in the CI deficient fibroblasts. Altogether, the glutathione and selenium pathways might be considered as (new) targets for future therapeutic interventions. Extending our approach to other CI deficient

patient groups with functionally different defects (assembly factor or mtDNA defects affecting the CI proton translocation) in different genes will elucidate if the mechanisms identified are common to all complex I patients or if heterogeneity of pathophysiological processes exist .

Acknowledgements
This work was supported by the Dutch IOP Genomics grant IGE05003. We would like to thank S. Vanherle for technical expertise and help.

Supplementary data

Supplementary table 4.1. mtDNA copy number results
Supplementary table 4.2. QPCR primers for microarray validation
Supplementary table 4.3. Differentially expressed genes in significantly changed pathways.
Supplementary table 4.4. Differentially expressed genes in the mitochondria-targeted study.
Supplementary material – Microarray statistical analysis

Supplementary material is available online at doi:10.1016/j.bbadis.2011.10.009

References

1. Smeitink, J., L. van den Heuvel, and S. DiMauro, *The genetics and pathology of oxidative phosphorylation.* Nat Rev Genet, 2001. **2**(5): p. 342-52.
2. Loeffen, J.L., et al., *Isolated complex I deficiency in children: clinical, biochemical and genetic aspects.* Hum Mutat, 2000. **15**(2): p. 123-34.
3. Pitkanen, S., et al., *NADH-coenzyme Q reductase (complex I) deficiency: heterogeneity in phenotype and biochemical findings.* J Inherit Metab Dis, 1996. **19**(5): p. 675-86.
4. Distelmaier, F., et al., *Mitochondrial complex I deficiency: from organelle dysfunction to clinical disease.* Brain, 2009. **132**(Pt 4): p. 833-42.
5. Dunning, C.J., et al., *Human CIA30 is involved in the early assembly of mitochondrial complex I and mutations in its gene cause disease.* EMBO J, 2007. **26**(13): p. 3227-37.
6. Benit, P., et al., *Mutant NDUFV2 subunit of mitochondrial complex I causes early onset hypertrophic cardiomyopathy and encephalopathy.* Hum Mutat, 2003. **21**(6): p. 582-6.
7. Benit, P., et al., *Large-scale deletion and point mutations of the nuclear NDUFV1 and NDUFS1 genes in mitochondrial complex I deficiency.* Am J Hum Genet, 2001. **68**(6): p. 1344-52.
8. Benit, P., et al., *Mutant NDUFS3 subunit of mitochondrial complex I causes Leigh syndrome.* J Med Genet, 2004. **41**(1): p. 14-7.
9. Berger, I., et al., *Mitochondrial complex I deficiency caused by a deleterious NDUFA11 mutation.* Ann Neurol, 2008. **63**(3): p. 405-8.

10. Fernandez-Moreira, D., et al., *X-linked NDUFA1 gene mutations associated with mitochondrial encephalomyopathy.* Ann Neurol, 2007. **61**(1): p. 73-83.
11. Hoefs, S.J., et al., *NDUFA2 complex I mutation leads to Leigh disease.* Am J Hum Genet, 2008. **82**(6): p. 1306-15.
12. Kirby, D.M., et al., *NDUFS6 mutations are a novel cause of lethal neonatal mitochondrial complex I deficiency.* J Clin Invest, 2004. **114**(6): p. 837-45.
13. Loeffen, J., et al., *The first nuclear-encoded complex I mutation in a patient with Leigh syndrome.* Am J Hum Genet, 1998. **63**(6): p. 1598-608.
14. Loeffen, J., et al., *Mutations in the complex I NDUFS2 gene of patients with cardiomyopathy and encephalomyopathy.* Ann Neurol, 2001. **49**(2): p. 195-201.
15. Triepels, R.H., et al., *Leigh syndrome associated with a mutation in the NDUFS7 (PSST) nuclear encoded subunit of complex I.* Ann Neurol, 1999. **45**(6): p. 787-90.
16. Schuelke, M., et al., *Mutant NDUFV1 subunit of mitochondrial complex I causes leukodystrophy and myoclonic epilepsy.* Nat Genet, 1999. **21**(3): p. 260-1.
17. van den Heuvel, L., et al., *Demonstration of a new pathogenic mutation in human complex I deficiency: a 5-bp duplication in the nuclear gene encoding the 18-kD (AQDQ) subunit.* Am J Hum Genet, 1998. **62**(2): p. 262-8.
18. Barghuti, F., et al., *The unique neuroradiology of complex I deficiency due to NDUFA12L defect.* Mol Genet Metab, 2008. **94**(1): p. 78-82.
19. Lazarou, M., et al., *Assembly of mitochondrial complex I and defects in disease.* Biochim Biophys Acta, 2009. **1793**(1): p. 78-88.
20. Ogilvie, I., N.G. Kennaway, and E.A. Shoubridge, *A molecular chaperone for mitochondrial complex I assembly is mutated in a progressive encephalopathy.* J Clin Invest, 2005. **115**(10): p. 2784-92.
21. Pagliarini, D.J., et al., *A mitochondrial protein compendium elucidates complex I disease biology.* Cell, 2008. **134**(1): p. 112-23.
22. Sugiana, C., et al., *Mutation of C20orf7 disrupts complex I assembly and causes lethal neonatal mitochondrial disease.* Am J Hum Genet, 2008. **83**(4): p. 468-78.
23. Gerards, M., et al., *Defective complex I assembly due to C20orf7 mutations as a new cause of Leigh syndrome.* J Med Genet, 2009. **47**(8): p. 507-12.
24. Budde, S.M., et al., *Clinical heterogeneity in patients with mutations in the NDUFS4 gene of mitochondrial complex I.* J Inherit Metab Dis, 2003. **26**(8): p. 813-5.
25. Hoefs, S.J., et al., *Novel mutations in the NDUFS1 gene cause low residual activities in human complex I deficiencies.* Mol Genet Metab, 2010. **100**(3): p. 251-6.
26. Visch, H.J., et al., *Decreased agonist-stimulated mitochondrial ATP production caused by a pathological reduction in endoplasmic reticulum calcium content in human complex I deficiency.* Biochim Biophys Acta, 2006. **1762**(1): p. 115-23.
27. Koopman, W.J., et al., *Computer-assisted live cell analysis of mitochondrial membrane potential, morphology and calcium handling.* Methods, 2008. **46**(4): p. 304-11.
28. Verkaart, S., et al., *Superoxide production is inversely related to complex I activity in inherited complex I deficiency.* Biochim Biophys Acta, 2007. **1772**(3): p. 373-81.
29. Verkaart, S., et al., *Mitochondrial and cytosolic thiol redox state are not detectably altered in isolated human NADH:ubiquinone oxidoreductase deficiency.* Biochim Biophys Acta, 2007. **1772**(9): p. 1041-51.
30. Koopman, W.J., et al., *Mitochondrial network complexity and pathological decrease in complex I activity are tightly correlated in isolated human complex I deficiency.* Am J Physiol Cell Physiol, 2005. **289**(4): p. C881-90.
31. Valsecchi, F., et al., *Calcium and ATP handling in human NADH:ubiquinone oxidoreductase deficiency.* Biochim Biophys Acta, 2009. **1792**(12): p. 1130-7.
32. Willems, P.H., et al., *Mitochondrial Ca2+ homeostasis in human NADH:ubiquinone oxidoreductase deficiency.* Cell Calcium, 2008. **44**(1): p. 123-33.
33. Moran, M., et al., *Mitochondrial bioenergetics and dynamics interplay in complex I-deficient fibroblasts.* Biochim Biophys Acta, 2010. **1802**(5): p. 443-53.

34. van der Westhuizen, F.H., et al., *Human mitochondrial complex I deficiency: investigating transcriptional responses by microarray.* Neuropediatrics, 2003. **34**(1): p. 14-22.
35. Reitzer, L.J., B.M. Wice, and D. Kennell, *Evidence that glutamine, not sugar, is the major energy source for cultured HeLa cells.* J Biol Chem, 1979. **254**(8): p. 2669-76.
36. Dai, M., et al., *Evolving gene/transcript definitions significantly alter the interpretation of GeneChip data.* Nucleic Acids Res, 2005. **33**(20): p. e175.
37. Akaike, H. *Information theory and an extension of the maximum likelihood principle*. in *Second International Symposium on Inference Theory*. 1973. Budapest: Akadémiai Kiadó.
38. van Iersel, M.P., et al., *Presenting and exploring biological pathways with PathVisio.* BMC Bioinformatics, 2008. **9**: p. 399.
39. Ihaka, R. and R. Gentleman, *"R: a language for data analysis and graphics".* Journal of Computational Graphics and Statistics, 1996. **5**(3): p. 299-314.
40. Lindsey, J., *Models for repeated measurements, 2nd edition*. 1999, Oxford: Oxford University Press. 536.
41. Fernandez-Vizarra, E., V. Tiranti, and M. Zeviani, *Assembly of the oxidative phosphorylation system in humans: what we have learned by studying its defects.* Biochim Biophys Acta, 2009. **1793**(1): p. 200-11.
42. Gao, M., et al., *Diverse roles of GADD45alpha in stress signaling.* Curr Protein Pept Sci, 2009. **10**(4): p. 388-94.
43. Nguyen, T., P. Nioi, and C.B. Pickett, *The Nrf2-antioxidant response element signaling pathway and its activation by oxidative stress.* J Biol Chem, 2009. **284**(20): p. 13291-5.
44. Singh, S., et al., *Nrf2-ARE stress response mechanism: A control point in oxidative stress-mediated dysfunctions and chronic inflammatory diseases.* Free Radic Res, 2010.
45. Dassa, E.P., et al., *The mtDNA NARP mutation activates the actin-Nrf2 signaling of antioxidant defenses.* Biochem Biophys Res Commun, 2008. **368**(3): p. 620-4.
46. von Kleist-Retzow, J.C., et al., *Impaired mitochondrial Ca2+ homeostasis in respiratory chain-deficient cells but efficient compensation of energetic disadvantage by enhanced anaerobic glycolysis due to low ATP steady state levels.* Exp Cell Res, 2007. **313**(14): p. 3076-89.
47. Bellinger, F.P., et al., *Regulation and function of selenoproteins in human disease.* Biochem J, 2009. **422**(1): p. 11-22.
48. Papp, L.V., et al., *From selenium to selenoproteins: synthesis, identity, and their role in human health.* Antioxid Redox Signal, 2007. **9**(7): p. 775-806.
49. Jurynec, M.J., et al., *Selenoprotein N is required for ryanodine receptor calcium release channel activity in human and zebrafish muscle.* Proc Natl Acad Sci U S A, 2008. **105**(34): p. 12485-90.
50. Du, S., et al., *SelK is a novel ER stress-regulated protein and protects HepG2 cells from ER stress agent-induced apoptosis.* Arch Biochem Biophys, 2010. **502**(2): p. 137-43.
51. Muller, M., et al., *Nrf2 target genes are induced under marginal selenium-deficiency.* Genes Nutr, 2010. **5**(4): p. 297-307.
52. Burk, R.F., et al., *Selenium deficiency activates mouse liver Nrf2-ARE but vitamin E deficiency does not.* Free Radic Biol Med, 2008. **44**(8): p. 1617-23.
53. Klein, E.A., et al., *SELECT: the selenium and vitamin E cancer prevention trial.* Urol Oncol, 2003. **21**(1): p. 59-65.
54. Kryscio, R.J., et al., *Designing a large prevention trial: statistical issues.* Stat Med, 2004. **23**(2): p. 285-96.

Chapter 5

Patient-derived fibroblasts indicate oxidative stress status and may justify antioxidant therapy in OXPHOS disorders.

A.M. Voets, P.J. Lindsey, S.J. Vanherle, E.D. Timmer, J.J. Esseling, W.J.H. Koopman, P.H.G.M. Willems, G.C. Schoonderwoerd, D. De Groote, B.T. Poll-The, I.F.M. de Coo, H.J.M. Smeets

Submitted

Abstract

Oxidative phosphorylation (OXPHOS) disorders are often associated with increased oxidative stress and antioxidant therapy is frequently given as treatment. However, the role of oxidative stress in OXPHOS disorders or patients is far from clear and consequently the preventive or therapeutic effect of antioxidants is highly anecdotic. Therefore, we performed a systematic study of a panel of oxidative stress parameters (ROS levels, damage and defense) in fibroblasts of twelve well-characterized OXPHOS patients with a defect in the *POLG1* gene, in the mitochondrial DNA (mtDNA)-encoded tRNA-Leu gene (3243A>G or 3302A>G) and in one of the mtDNA-encoded NADH dehydrogenase complex I (CI) subunits. All except two cell lines (one POLG1 and one tRNA-Leu) showed increased ROS levels compared with controls, but only four (two CI and two tRNA-Leu) cell lines provided evidence for increased oxidative protein damage. The absence of a correlation between ROS levels and oxidative protein damage implies differences in damage prevention or correction. This was investigated by gene expression studies, which showed adaptive and compensating changes involving antioxidants and the unfolded protein response, especially in the *POLG1* group. This study indicated that patient fibroblasts enable the identification of patients that potentially benefit from antioxidant therapy. Furthermore, the fibroblast model can also be used to search for and test novel, more specific antioxidants or explore ways to stimulate compensatory mechanisms.

Key words

oxidative stress, POLG1, CI deficiency, MELAS, ROS levels, protein carbonyls, glutathione

Introduction

Oxidative phosphorylation (OXPHOS) disorders are the most common group of inherited metabolic disorders characterized by a primary dysfunction of the OXPHOS system. The clinical and biochemical heterogeneity of OXPHOS disorders is partly due to the dual (mitochondrial and nuclear DNA) genetic control of mitochondrial energy production. Other factors that could explain this heterogeneity are only partly resolved, awaiting further insight in the pathophysiological processes. Recently, a number of papers have addressed the issue of oxidative stress in OXPHOS disorders (*e.g.* [1-8]). The electron transport chain in the mitochondria is considered the major source of reactive oxygen species (ROS), which are by-products of the redox reactions necessary to reduce NADH to NAD^+ [9]. At low levels, ROS behave as signaling molecules [10], but increased levels are damaging for DNA, proteins and lipids as well as detrimental for cellular function [11-14]. Therefore, cells are well equipped with antioxidant systems to control ROS levels. Oxidative stress occurs when the balance between pro-oxidants (ROS) and antioxidants is disturbed and antioxidants are no longer able to maintain normal physiological ROS levels.

Increased ROS production has been described in patients with clinically, biochemically [4, 15, 16] and/or genetically [17-19] diagnosed OXPHOS disorders, in cybrid models [6-8] and in cell lines where the respiratory chain was inhibited by chemicals [20]. The antioxidant status of tissues or cell cultures from OXPHOS patients [1, 5, 6, 16, 19, 21] was investigated with variable and sometimes contradictory results. Only few studies report the total picture of oxidative stress in these patients, including ROS production, antioxidant defense and the eventual oxidative damage [6, 19, 22]. The goal of this study was to investigate the role of oxidative stress in three different genetically characterized OXPHOS disorders: patients with mutations in the *POLG1* gene, patients with a tRNA leucine (tRNA-Leu) mutation in the mtDNA (3243A>G and 3302A>G) causing mitochondrial encephalomyopathy, lactic acidosis and stroke-like episodes (MELAS) and patients with a mutation in one of the mtDNA encoded complex I subunits. Complex I deficiency and tRNA-Leu mutations have been associated with increased oxidative stress previously [19, 23], although not all studies could confirm this [24]. Importantly, different parameters have been characterized to determine oxidative stress, including increased probe oxidation [23] combined with antioxidant expression [24] and increased oxidative damage, or combinations of the three [19]. For *POLG1* mutations, a couple of studies were performed in transgenic mice, but again with conflicting conclusions: transgenic mouse models carrying the D257A mutation in the exonuclease domain of pol γ did not increase oxidative stress [25, 26] whereas transgenic mice with cardiac-targeted human mutant Y955C pol γ, affecting the polymerase domain, did [27].

Our study aimed at investigating parameters including ROS levels, ROS detoxification (glutathione levels, antioxidant gene expression) and oxidative damage (protein carbonyls) in patient-derived fibroblasts as a model system. Because the genetic defect might not stress the cells to such an extent that relevant disease-associated changes

can be picked up, fibroblasts were deprived of glucose to stimulate energy production through oxidative phosphorylation. Nevertheless, our main focus is on changes due to the genetic defect and not the difference between the two culture conditions. This model will help to resolve the underlying adaptive mechanisms, identify the subgroup of patients that will most likely benefit from antioxidant treatments and test the efficacy of new targeted candidate antioxidants.

Materials and methods

Patient fibroblast cell lines

Fibroblasts were derived from skin biopsies of five patients with a *POLG1* mutation, four with a tRNA-Leu (m.3243A>G or m.3302A>G) MELAS mutation, three with a mutation in an mtDNA encoded complex I subunit, and three controls (table 5.1). Fibroblasts were routinely cultured in Dulbecco's modified Eagle medium (DMEM; Gibco, Paisley, UK) supplemented with 10% fetal bovine serum, 0.2 mM uridine (Acros, Geel, BE), penicillin and streptomycin. To stimulate energy production by oxidative phosphorylation, fibroblasts were cultured for 72 hours without glucose in de presence of galactose. Galactose medium consisted of DMEM without glucose supplemented with 5.5mM galactose (Sigma, Zwijndrecht, Netherlands), 20% FBS, 0.2 mM uridine, penicillin and streptomycin [28]. Measurements were performed in primary cell cultures between passage 7 and 20. Except for the quantification of reactive oxygen species, cultures from the same cell line and condition were pooled and the cell pellet was divided for the different assays.

Quantification of reactive oxygen species

Reactive oxygen species (ROS) levels were measured as described previously [23]. In short, fibroblasts were incubated in HEPES-Tris medium (132 mM NaCl, 4.2 mM KCl, 1 mM $CaCl_2$, 1 mM $MgCl_2$, 10 mM HEPES and 5.5 mM D-glucose or galactose, pH 7.4), containing 10 µM hydroethidine (HEt; Molecular Probes, Paisley, UK) for 10 minutes at 37°C. The reaction was stopped by thorough washing of the cells with PBS. Culture dishes were mounted in an incubation chamber placed on the stage of an inverted microscope (Axiovert 200M, Carl Zeiss, Jena, DE) equiped with a Zeiss 40x/1.3 NA fluor objective. The cells were excited at 490 nm using a monochromator (Polychrome IV, TILL Photonics, Gräfelfing, DE). Fluorescence emission light was directed by a 525DRLP dichroic mirror filter (Omega) onto a CoolSNAP HQ monochrome CCD-camera (Roper Scientific, Vianen, NL) with an acquisition time of 100 ms. Hardware was controlled with Metafluor 6.0 software (Universal Imaging Corporation, Downingtown, PA, USA). Processing and analysis of fluorescence images was performed with MetaMorph 6.1 (Universal Imaging Corporation). All cell lines were examined on at least two but possibly up to four different days. In total, at least 50 cells (range 52-407) were analyzed on each day for each cell line and condition, resulting in a total of at least 150 cells (range 156-568) analyzed for each cell line and condition.

Table 5.1. Patient characteristics for primary fibroblast cell lines.

Cell line	Sex	Age at biopsy (years)	Group[a]	Mutation(s)[b]	OXPHOS complex activity[c]
2862S	F	24	POLG	p.467A>T HOM	CI 67, CII 125, CIII 108, CIV 87, CS 93
06E0703	F	16	POLG	p.467A>T HOM	CI 54, CII 141, CIII 79, CIV 84, CS 71
00E0741	F	<1	POLG	p.227R>P + p.467A>T	CI 34, CII 76,CIII 31, CIV 50, CS 227
3591	M	8	POLG	p.305S>R + p.467A>T	CI 50, CII 86, CIII 57, CIV 89, CS 142
05E0536	F	1	POLG	p.467A>T + p.957A>P	CI 63, CII 81, CIV 57, CS 150
2400	M	27	tRNA-Leu	m.3243A>G (80%)	CI 43, CII 86, CIII 67, CIV 80, CS 125
1933	M	27	tRNA-Leu	m.3243A>G (90%)	CI 50, CII 84, CIII 60, CIV 79, CS 117
2830	F	19	tRNA-Leu	m.3243A>G (83%)	CI 57, CII 86, CIII 77, CIV 60, CS 100
1330	M	34	tRNA-Leu	m.3302A>G (50%)	CI 62, CII 100, CIII 79, CIV 83, CS 108
3765	M	5	CI	ND1, m.3890G>A (80%)	CI 34, CII 69, CIII 72, CIV 114, CS 160
2181	M	3	CI	ND5, m.13042G>A (86%)	CI 50, CII 90, CIII 59, CIV 70, CS 110
1682	F	4	CI	ND5, m.13511A>T (60%)	CI 52, CII 94, CIII 91, CIV 115, CS 105
C0388			Control	-	n.a.
C0407			Control	-	n.a.
C2244			Control	-	n.a.

[a] Patient cell lines are grouped according to their genetic defect: polymerase gamma mutations (POLG), mtDNA tRNA leucine mutation with MELAS phenotype (MELAS) and mtDNA complex I subunit mutation (CI). [b] Mutations are given at the protein level for POLG and at the mtDNA level for MELAS and CI, the mutation percentage of the mtDNA mutations is given between ( ). [c]The activities of the different OXPHOS complexes is expressed as the percentage of a control population, normalized to citrate synthase (CS) activity. CI=complex I, CII=complex II, CIII=complex III, CIV=complex IV. n.a. = not applicable.

Preparation of lysates for glutathione measurements and protein carbonyls

Cell pellets were resuspended in ice-cold extraction buffer (0.1% Triton X-100 and 0.6% sulfosalicylic acid in 0.1M potassium phosphate buffer with 5mM EDTA disodium salt, pH 7.5) and homogenized with a Teflon pestle. After sonication and 2 freeze-thaw cycles, the suspension was centrifuged for 4 min at 3000g (4 degrees) and the supernatant was stored at -70 degrees until further use. Protein concentrations were determined using the Bio-Rad Protein Assay.

Glutathione measurement

Total glutathione (reduced (GSH) + oxidized (GSSG)) was measured in the cell lysates as described in [29]. In short, freshly prepared 5,5'-dithio-bis(2-nitrobenzoic acid) (Sigma) and glutathione reductase (Sigma) solutions were mixed and added to the cell lysates (40µg protein in 20 microliter). After 30s, NADPH (Sigma) was added and the rate of change in absorbance at 412nm was proportional to the concentration of total GSH ([GSH] + 2 x [GSSG]) in the sample. The concentration of total GSH was deduced from the regression curve generated from several standards of GSH. Data were analyzed using the univariate analysis of variance in the SPSS software package.

Protein carbonyl detection

To detect oxidative modifications of proteins, the Oxyblot™ Protein Oxidation Detection kit (Millipore, Amsterdam, NL) was used. After derivatization of the carbonyl groups in the cell lysates with di-nitrophenylhydrazone, oxidatively modified proteins were detected by immunoblotting according to the manufacturer's protocol in two replicates. Results were normalized to beta-actin protein levels in different lanes of the same gels.

Oxidative stress related gene expression

The expression levels of genes involved in oxidative stress and inflammation were measured using the OxyGenes™ microarrays (Probiox SA, Liege, BE) [30]. RNA was isolated from cell pellets with the High Pure RNA Isolation kit (Roche, Woerden, NL). RNA quantity and purity were determined spectrophotometrically using the Nanodrop ND-1000 (Nanodrop Technologies, Wilmington, DE, USA) and RNA integrity was assessed by determining the RNA 28S/18S ratio using the Bioanalyser 2100 (Agilent Technologies, Santa Clara, CA, USA). 2 µg of RNA was reverse transcribed into cDNA according to the 3DNA Array 900 protocol (Genisphere, Hatfield, PA, USA). Next, cDNA was hybridized on the OxyGenes™ slides overnight, followed by washing steps and hybridization of Cy™3-labeled 3DNA capture reagent according to the manufacturer's procedures (Genisphere). To assess the raw probe signal intensities, slides were scanned using the LS Reloaded laser scanner (Tecan, Männedorf, CH) with gain settings 160, 180 and 200 and analyzed using Array-Pro analyzer software (MediaCybernetics, Bethesda, USA) or scanned using the Agilent High-Resolution Microarray Scanner (Agilent Technologies, Amstelveen, NL) and analyzed using Feature Extraction 10.7 software (Agilent Technologies).

Data analysis

The data were analyzed using multivariate Gaussian linear regression including a one (protein carbonyls and Oxygenes™) or two level (ROS levels) random effect to take into account the dependence among observations from the same subject (all assays) and the dependence among the different measurement days (ROS levels). For the ROS level analysis, the medium (glucose and galactose) and the group (control, complex I, tRNA-Leu and POLG) were included during the analysis, as well as interactions among these when required. For the protein carbonyl analysis, the reference protein (beta-actin), concentration, day, gel number, medium and group were included. The inference criterion used for comparing the models reflects their ability to predict the observed data, *i.e.* models are compared directly through their minimized minus log-likelihood. When the numbers of parameters in models differ, they are penalized by adding the number of estimated parameters, a form of the Akaike information criterion (AIC) [31]. First, all cell lines were analyzed together and then each one was also considered separately. In each case, the relevant group differences were reported if the model with the smallest AIC contained any combination of one or more groups.

For the Oxygenes™ analysis, one of the 30 housekeeping genes, the pooled sample, the background intensity, the scanner used, the medium and group were included during the analysis as well as interactions among these when required. Similarly to the ROS levels and protein carbonyl analysis, the AIC was used to assess whether there was a group effect. First, each gene was analyzed for all cell lines in the patient groups together and then the analysis was also repeated for all genes but considering each cell line separately. In each analysis, the relevant group differences were reported if the model with the smallest AIC contained any combination of one or more groups.

Importantly, the reported fold changes are estimated values by the models, taking into account both the effect of the mutation and the medium.

Results

Increased ROS levels in most of the patient cell lines

ROS levels, quantified by the oxidation rate of hydroethidine (HEt), were assessed in the control and patient cell lines under glucose and galactose conditions (table 5.2). Unlike the estimated fold changes for the patient group differences, analysis of individual cell lines and controls did not always estimate a medium effect, *i.e.* a different fold change for the glucose and galactose condition, due to low power. In these cases, the estimated fold changes represent the difference between the specific patient and control fibroblasts regardless of the medium.

Except for two cell lines, one *POLG1* mutant (06E0703; p.467A>T homozygote) and one tRNA-Leu mutant (1330; m.3302A>G), all other cell lines showed increased HEt oxidation compared with control cell lines in glucose and galactose medium. HEt oxidation was highest in the CI group, although one of the *POLG1* cell lines (05E0536; p.467A>T + p.957A>P) presented with the highest HEt oxidation rate. Although the main focus was on changes due to the mutation and not the differences between

culture conditions, six cell lines showed a larger fold change for HEt oxidation (versus controls) in galactose compared with glucose. Galactose medium also induced a 1.53 fold increase in HEt oxidation in controls (table 5.2).

Table 5.2. ROS levels as measured by HEt oxidation.

Cell line	Glucose mean (C.I.)	Galactose mean (C.I.)
Average control	1.00	**1.53** (1.49-1.57)
(3 cell lines)		
Average POLG	**1.47** (1.12-1.82)	**1.71** (1.34-2.18)
2862S	**1.36** (1.14-1.63)	**1.96** (1.65-2.34)
06E0703	1.12 (0.96-1.30)	
00E0741	**1.18** (1.04-1.33)	
3591	**1.51** (1.35-1.70)	
05E0536	**2.51** (2.13-2.95)	**4.80** (4.08-5.65)
Average tRNA-Leu	**1.48** (1.14-1.83)	**1.72** (1.35-2.19)
2400	**1.45** (1.28-1.64)	
1933	**1.30** (1.12-1.51)	**1.92** (1.65-2.23)
2830	**1.74** (1.46-2.08)	**2.52** (2.10-3.03)
1330	1.10 (0.96-1.25)	
Average CI	**1.87** (1.47-2.27)	**2.28** (1.73-3.01)
3765	**1.61** (1.37-1.90)	**2.38** (2.01-2.83)
2181	**2.31** (1.98-2.69)	
1682	**1.36** (1.20-1.54)	

HEt oxidation expressed as fold change compared with control in the respective culture medium. Values are estimated fold changes for patients versus controls provided by the model, taking into account both the effect of the mutation and the medium. Values for the patient groups and the individual cell lines were estimated in separate analyses. If the fold change was not significantly different for a cell line between both media, the fold change of the best fitting model was estimated for glucose and galactose together. Values in bold differ significantly from control in the respective medium or glucose and galactose together. # versus control glucose, only applies for the patient groups comparison.

Oxidative damage

The levels of protein carbonyls, an index for oxidative protein damage, were significantly elevated in three patient cell lines cultured with glucose and galactose: tRNA-Leu cell lines 2400 (80% m.3243A>G) and 1933 (90% m.3243A>G) and CI cell

line 3765 (80% m.3890G>A). CI cell line 1682 (60% m.13511A>T) only showed increased levels of protein carbonyls compared with controls when cultured with galactose medium (table 5.3).

Table 5.3. Oxidative protein damage (protein carbonyls).

Cell line	Glucose mean (C.I.)	Galactose mean (C.I.)
Average control	1.00	
(3 cell lines)		
Average POLG	1.07 (0.94-1.21)	
2862S	1.07 (0.76-1.50)	
06E0703	0.93 (0.81-1.08)	
00E0741	1.14 (0.96-1.35)	
3591	1.15 (0.92-1.43)	
05E0536	0.92 (0.73-1.66)	
Average tRNA-Leu	**1.30** (1.13-1.48)	
2400	**1.25** (1.06-1.47)	
1933	**1.56** (1.29-1.89)	
2830	1.26 (0.90-1.77)	
1330	1.14 (0.94-1.39)	
Average CI	**1.22** (1.06-1.41)	
3765	**1.36** (1.07-1.74)	
2181	1.08 (0.96-1.22)	
1682	1.12 (0.76-1.65)	**2.22** (1.79-2.75)

Protein carbonyls as measured using the Oxyblot assay, expressed as fold change compared with control in the respective culture medium. Values are estimated fold changes for patients versus controls provided by the model, taking into account both the effect of the mutation and the medium. Values for the patient groups and the individual cell lines were estimated in separate analyses. If the fold change was not significantly different for a cell line or group between both media (due to less power compared with the analysis of the groups), the fold change of the best fitting model was estimated for glucose and galactose together. Values in bold differ significantly from control.

Stress-related gene expression and antioxidant defense

To examine ROS-related gene expression changes, the transcription levels of stress-related genes were determined using OxyGenes™ microarrays. Of the 165 genes on the microarray, 38 genes showed more than 20% difference in expression above the background level in at least one of the groups and one of the culture media. Of these 38 genes, 10 were altered due to the genetic defect only, as their expression was not influenced by the culture medium in controls and patients (table 5.4). Therefore these were considered specific for the genetic defects and included, amongst others, heat shock protein (*HSPA1A*), oxidative stress related (*SOD1*, *PON2*, *MT1M*) and inflammatory (*ICAM1*, *IL2RG*, *TNFRSF1B*) genes. The expression of the remaining 28 genes was altered due to both the culture medium and genetic defect (supplementary table 5.1). The POLG group showed the highest number of differentially expressed genes compared with controls, both in glucose and galactose medium. The galactose

medium induced larger expression changes of 17 stress-related genes in the POLG group (supplementary table 5.1). In contrast, the tRNA-Leu and CI groups showed less differentially expressed genes, both in glucose and galactose (supplementary table 5.1). A closer examination of the gene expression changes of classical antioxidant genes in the individual cell lines (table 5.5) revealed an inconsistent picture. On the one hand, genes could behave comparable in multiple cell lines of one or more patient groups in one or both culture conditions (*e.g. GSR* in POLG glucose and galactose, *GPX1* in tRNA-Leu galactose, *SOD1* in tRNA-Leu and CI galactose). Whereas, on the other hand, their expression changed differently, either up or down, in cell lines of the same group in one or both culture conditions (*e.g. GPX1* in POLG glucose and galactose, *SOD1* in tRNA-Leu and CI glucose) (table 5.5).

Table 5.4. Stress-related gene expression changes due to disease without medium effect.

Gene	FC CI vs control	FC POLG vs control	FC tRNA-Leu vs control	FC All vs control
HSPA1A				3.39 (2.80-4.09)
ICAM1		1.58 (1.33-1.87)		
IGFBP3		1.40 (1.35-1.45)		
IL2RG	0.68 (0.56-0.82)	1.27 (1.03-1.56)	0.68 (0.56-0.82)	
MT1M		2.36 (2.07-2.69)		
PON2				0.58 (0.38-0.89)
SIRT1		2.60 (1.36-4.96)		
SOD1		1.99 (1.71-2.31)		
SOS2		1.38 (1.27-1.50)		
TNFRSF1B	0.67 (0.59-0.76)			

Fold changes of stress-related genes in patients versus controls as measured by the OxyGenes™ microarrays. Fold changes were the same for glucose and galactose medium. Values are estimated fold changes for patient groups versus controls provided by the model, taking into account both the effect of the mutation and the medium. If the fold change was not significantly different for all patient groups, the fold change of the best fitting model was estimated for three groups together and provided in the 'All vs control' column. Only significant results are shown.

Total glutathione levels were measured to evaluate the oxidative status of the cell lines (figure 5.1). Univariate analysis of variance did not detect any significant difference between the groups or culture conditions. As can be appreciated from figure 5.1, there was a large variation between cell lines of patients within one group. Eight patient cell lines showed total glutathione values below the control range in the glucose situation. Additionally, the total glutathione levels in galactose were increased compared with the glucose levels in seven of these same cell lines, making them similar to control levels in galactose. On the contrary a decrease or no change at all was observed in the control cell lines or the remaining patient cell lines.

Correlations between different parameters

To search for correlations between the different parameters (ROS levels, oxidative protein damage, total GSH levels and classic antioxidant gene expression) and between these parameters and sex and age, a correlation matrix was created

(supplementary table 5.2). Statistical significant correlations (p value < 0.05) were only detected between ROS levels and *CAT* expression fold changes (Pearson's r -0.508) and protein carbonyl levels and *GPX1* expression fold changes (Pearson's r 0.454).

Discussion

The goal of this study was to characterize different oxidative stress parameters in three groups of patients with a genetically characterized mitochondrial disorder caused by mutations either in the *POLG1* gene or in mtDNA encoded complex I and tRNA leucine genes. Fibroblast cells predominantly use glycolysis for energy production when cultured with high glucose availability [24, 32, 33]. Hence, cell lines were forced to derive ATP from OXPHOS using glucose-free galactose medium [34]. An overview of the results is shown in table 5.6.

Table 5.5. Antioxidant gene expression for each cell line.

Gene	CAT		SOD1		GSR		GPX1	
Cell line	**glu**	**gal**	**glu**	**gal**	**glu**	**gal**	**glu**	**gal**
POLG								
2862S		1.37	2.35	19.05		2.42	0.77	2.50
06E0703		1.36			1.21			
00E0741	1.29				1.22		1.51	0.58
3591						1.46		
05E0536							0.73	
tRNA-Leu								
2400			14.35	0.64	1.75			0.54
1933								0.67
2830				0.56		2.64		0.42
1330							0.75	0.51
CI								
3765		1.40						
2181			4.11	0.54		1.17		0.79
1682				0.61				1.29

Fold changes are given relative to the average control (glucose or galactose). Values are estimated fold changes for patients versus controls provided by the model, taking into account both the effect of the mutation and the medium. If the fold change was not significantly different for a cell line between both media, the fold change of the best fitting model was estimated for glucose and galactose together. Blanc cells indicate no (<10% change) or a non-significant difference compared with controls.

Oxidative stress in patients with mutations in mtDNA encoded complex I subunits

The fibroblast cell lines with mutations in mtDNA encoded complex I subunits presented the highest ROS levels, accompanied with most oxidative protein damage (2/3 cell lines) and only few changes in antioxidant gene expression (table 5.6). Interestingly, the CI cell line with the highest ROS levels was the cell line without oxidative damage, indicating adaptation to or compensation of the defect. The other two cell lines seemed less capable to adapt to or compensate for increased ROS levels, resulting in oxidative stress and damage. Possible consequences of extensive oxidative stress are cell cycle arrest, senescence and apoptosis [35]. Increased ROS levels have been detected previously in cells or tissues of patients with a genetically (nuclear [23] or mitochondrial DNA [16]) and/or functionally [4] characterized CI deficiency. The finding is not surprising as CI is one of the major ROS sources in mitochondria [36]. Luo *et al* observed increased lipid peroxidation in fibroblasts of patients with CI deficiency [37], but this was not detected in another study by Verkaart *et al* [15]. The only publication reporting on oxidative protein damage in CI deficiency involved cybrids carrying the 3460, 11778 and 14484 Leber mutations showing increased protein carbonylation [38]. This nicely supports our results. In contrast to the lymphoblast cell lines from biochemically characterized CI deficient patients with predominantly (5/6 cell lines) homoplasmic mtDNA mutations [16], we did not detect consistently increased expression of *SOD*, *CAT*, *GPX* and *GST* in our patients with a genetic defect in mtDNA CI genes [16]. However, in their study, increased expression of the genes in the presence of elevated ROS levels was not correlated with increased expression of the corresponding proteins and they actually measured lower antioxidant activity of these enzymes, except for SOD1. In spite of the inconsistency between RNA and protein data, they concluded, mainly based on the enzyme data, that ROS levels and alteration of ROS scavenging enzymes were good parameters to assign antioxidant therapy. However, oxidative damage parameters were not examined, which in our study seemed to be an appropriate biomarker to estimate the eventual consequences of increased ROS levels in fibroblasts.

Oxidative stress in patients with mutations in tRNA leucine genes

All three cell lines with the m.3243A>G mutation (80-90% heteroplasmy) experienced increased ROS levels, whereas the cell line with the m.3302A>G mutation (60%) did not (table 5.6). In this study with primary patient fibroblast cell lines, the lack of increased ROS levels in the m.3302A>G cell line is likely due to the lower mutation percentage but a different molecular mechanism compared with the m. 3243A>G tRNA-Leu mutation cannot be excluded [39]. The m.3302A>G and m.3243A>G tRNA-Leu mutations have been shown to increase superoxide production in homoplasmic cybrid models with deficiencies of OXPHOS complexes I, III, IV and V [40], whereas in our group complex I deficiency was most prominent, and in muscle of patients with the m.3243A>G mutation [19]. Oxidative protein damage was observed in two m.3243A>G cell lines. Again, the cell line with the highest ROS levels did not show oxidative damage in galactose. For the tRNA-Leu patients, only few studies previously reported on oxidative damage. One study detected increased protein carbonylation in muscle biopsies [19] while two other studies did not observe increased oxidative damage in

cybrids carrying the homoplasmic 3243A>G [6, 39] or 3302A>G [39] mutations. There have been no reports on oxidative stress/damage in mutant tRNA-Leu fibroblasts so far.

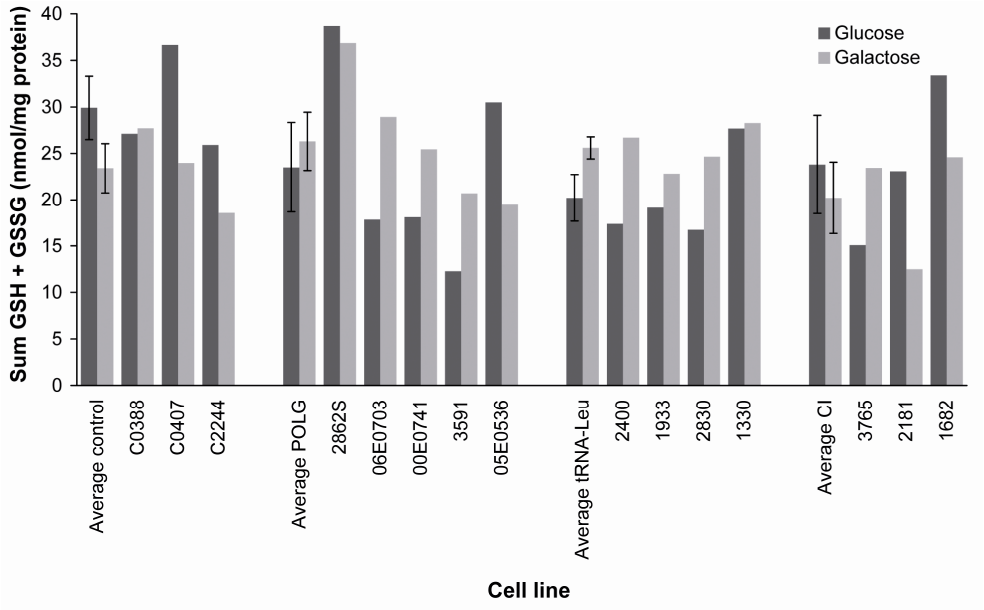

Figure 5.1. Total glutathione (GSH+GSSG) levels.

Our results differ partly from previous studies on antioxidant enzymes in MELAS patients, reporting increased gene expression and activities of SOD, CAT and GPX, although studies are difficult to compare due to differences in cell types, mutation load and analytical approaches [5, 6, 41]. In one study, the mutation load was considerably lower (<45% heteroplasmy) than in our fibroblasts, and myoblast cultures were used [5]. This might indicate that antioxidant defenses are triggered at lower ROS levels in muscle-derived cells, compared with fibroblasts, to prevent accumulation of oxidative damage in post-mitotic tissues; however, ROS levels, which could support this hypothesis, were not determined in the myoblast cultures. Therefore, it is not certain that the gene expression changes resulted from increased ROS production related to the mtDNA mutations. A second study did not quantify their immunohistochemical results in muscle [41], making it difficult to judge and compare the results. Finally, a third study used homoplasmic mutation load and cybrid models [6] instead of primary patient material. Although there is a possible interference of the nuclear cancer background here, the increased expression of antioxidant genes nicely correlates with the lack of oxidative damage. Altogether, all studies point to increased ROS production, whether or not compensated by antioxidant defenses. These studies emphasize the importance of standardization and examining different aspects of oxidative stress to be

able to compare the results of different studies, especially if heterogeneous patient populations or different model systems with different adaptive capacities are being used.

Oxidative stress in patients with mutations in the *POLG1* gene

All except one *POLG1* cell line showed increased ROS levels. *POLG1* cell line 06E0703 has the same mutation as cell line 2862S, while only the latter showed increased ROS levels (table 5.6). This suggests that other factors in addition to or apart from the primary genetic defect(s) play a role in ROS levels in the POLG group (and possibly also in the other groups). This might involve intrinsic individual differences in ROS scavenging capacity due to *e.g.* genetic polymorphisms or environmental factors [42]. It may also be related to the random effect of pol γ on mtDNA stability and point mutations leading to many, random low level heteroplasmy mutations in contrast to the high heteroplasmic CI and tRNA-Leu mutations. Even though the POLG and tRNA-Leu group experienced similar ROS levels, the former group seemed less vulnerable to accumulate oxidative protein damage in fibroblasts. As suggested by the multiple gene expression changes, this is possibly correlated with an adaptive activation of the antioxidant or repair systems associated with increased endogenous ROS levels in our patient lines [43]. No human cells or tissues with *POLG1* mutations have been evaluated for oxidative stress parameters so far. In POLG mutator mice with proofreading deficient D268A polymerase resulting in the random accumulation of mtDNA mutations, no or only mildly increased ROS production and no oxidative damage could be detected in several tissues (liver, heart, muscle) by two groups [25, 26]. Contrastingly, a third group examining the same mice, did observe increased oxidative protein damage in the heart which could be attenuated by overexpression of mitochondrial catalase [44]. Additionally, in transgenic mice with cardiac-targeted human mutant Y955C pol γ, affecting the polymerase domain, increased oxidative DNA damage associated with decreased mtDNA copy number was observed [27]. In concordance with the latter publications, the current study implies that ROS levels are increased in most *POLG1* patients and therefore their antioxidant levels and oxidative damage markers should be followed up to supplement them with antioxidants when their endogeneous system starts failing.

Increased ROS levels in the majority of primary fibroblasts of OXPHOS patients

One of the general observations in this study is that ROS levels were increased in most patient-derived cell lines, both when cultured with glucose and galactose medium (table 5.6). The moderate increase in ROS levels in control fibroblasts due to the replacement of glucose by galactose might reflect increased basal OXPHOS-related ROS production due to the switch from glycolysis to OXPHOS for energy production. Our results indicated that ROS levels could already be increased by quite moderate OXPHOS deficiencies (*e.g.* CI activity lower than 70% of the average control activity), as shown for most fibroblasts in this study, *e.g.* due to disturbed electron fluxes in the mutated complexes. In support of this theory, increased superoxide production was measured in fibroblasts of patients with a mutation in a nuclear DNA-encoded CI gene and residual CI activities up to 75% of controls [23]. A drawback is that the method

applied cannot distinguish the exact site(s) of HEt oxidation and that the exact mechanism therefore remains speculative [23]. Other proteins that might influence the measured ROS levels are alpha-ketoglutarate dehydrogenase in the tricarboxylic acid cycle [45, 46] and NADPH oxidases (NOX) [47], all suggested to be influenced by the redox status of cells [48]. Therefore, genetically defined OXPHOS deficiencies might not only increase ROS levels by electron leakage at the OXPHOS complexes but also by altering the NAD^+/NADH ratio.

Adaptive processes in fibroblasts of OXPHOS patients

Most cell lines showed increased ROS levels but no increased oxidative protein damage. Stress-induced adaptive gene expression changes, especially in the *POLG1* cell lines, might account for these findings. The existence of such a delicate balance is supported by the presence of oxidative damage in one CI mutant fibroblast cell line in galactose but not glucose medium, associated with higher ROS levels. The increased expression of stress-inducible *HSPA1A, DNAJB1* and *HSF2* in the glucose and/or galactose condition in patient cell lines pointed to a stress condition induced by the genetic defect. Heat shock proteins function as chaperones for correct folding of other proteins. The induction of these genes indicates activation of the unfolded protein response and possibly increased endoplasmic reticulum stress. Defects in protein synthesis have been associated with the 3243A>G mutation previously [49]. The activation of the unfolded protein response in the patients of this study might be related to prevention or repair of oxidative protein damage. Other compensatory mechanisms such as protein regeneration and muscle regeneration have also been observed in muscle biopsies of m.3243A>G mutation carriers [19]. However, repair and regenerative processes are highly energy demanding. Therefore, probably also the remaining energy capacity of a defect OXPHOS system plays a role in the faith of cells. Recently, exercise training has been shown to be beneficial for improving oxidative metabolism in muscle [50] and to induce antioxidant-related adaptations, enhancing the ability to cope with oxidative stress [51]. Thus, possibly also the physical activity or training of patients plays a role in how well their antioxidant systems will be able to cope with or adapt to the increased ROS levels caused by their genetic defect.

A consistent correlation was observed between classic antioxidant genes and the other oxidative stress parameters. ROS levels were inversely correlated with *CAT* expression and protein carbonyl levels were correlated with *GPX1* gene expression. Superoxide has been shown previously to inhibit catalase directly [52], whereas *GPX1* was crucial for protection against protein oxidation in mice [53], both of which might explain the observed correlations. Therefore, the expression of these genes might serve as biological biomarkers, although this remains to be confirmed in a larger patient cohort.

Table 5.6. Summarizing overview of oxidative stress parameters for each cell line.

Cell line	Mutation	OXPHOS complexes	Culture	ROS levels	Oxidative damage	Antioxidant response	Benefit from antioxidant therapy?*
POLG							
2862S	p.467A>T HOM		glu	↑		↑ SOD1, ↓ GPX1	Follow-up endogenous protection
			gal	↑↑		↑ CAT, ↑↑ SOD1, ↑ GSR, ↑ GPX1	
06E0703	p.467A>T HOM		glu			↑ GSR	No
			gal			↑ CAT, ↑ GSR	
00E0741	p.227R>P p.467A>T	↓	glu	↑		↑ CAT, ↑ GSR, ↑ GPX1	Follow-up endogenous protection
			gal	↑		↓ GPX1	
3591	p.305S>R p.467A>T		glu	↑			Follow-up endogenous protection
			gal	↑		↑ GSR	
05E0536	p.467A>T p.957A>P		glu	↑↑		↓ GPX1	Probably
			gal	↑↑↑		↓ GPX1	
tRNA-Leu							
2400	80% m.3243A>G	↓	glu	↑	↑	↑↑ SOD1, ↑ GSR	Yes
			gal	↑	↑	↓ SOD1, ↓ GPX1	
1933	90% m.3243A>G		glu	↑	↑		Yes
			gal	↑↑	↑	↓ GPX1	
2830	83% m.3243A>G		glu	↑		↓ SOD1	Probably
			gal	↑↑		↓ SOD1, ↑ GSR, ↓ GPX1	
1330	60% m.3302A>G		glu			↓ GPX1	No
			gal			↓ GPX1	

Cell line	Mutation	OXPHOS complexes	Culture	ROS levels	Oxidative damage	Antioxidant response	Benefit from antioxidant therapy?*
CI							
3765	80% m.3890G>A	↓	glu	↑	↑		Yes
			gal	↑↑	↑	↑ CAT	
2181	86% m.13042G>A		glu	↑↑		↑ SOD1	Probably
			gal	↑↑		↓ SOD1, ↑ GSR, ↓ GPX1	
1682	60% m.13511A>T		glu	↑		↓ SOD1	Yes
			gal	↑	↑	↓ SOD1, ↑ GPX1	

* based on the combination of ROS levels, oxidative damage and antioxidant gene expression in fibroblasts

Conclusions

In this study using fibroblasts of patients with different genetically characterized OXPHOS disease, it was shown that in the majority ROS was increased and could lead to oxidative damage in different OXPHOS disorders, although not in every patient-derived fibroblast. This has to be determined individually. Whether this also applies to more clinically relevant tissues, like brain and muscle of those patients, is not clear, but is not unlikely given data from literature involving other tissues [19, 54, 55] and mouse studies [27, 56] illustrating that fibroblasts are not the most sensitive system. Therefore, patient-derived fibroblasts can be used to identify patients with increased risk for oxidative damage, who will most likely benefit from boosting their antioxidant defense and energy capacity (training), possibly leading to patient-tailored prevention and antioxidant therapy in the future. Nevertheless, even in these patients, efficacy and toxicity of antioxidant supplementation should be evaluated carefully as side-effects can occur [57].

Acknowledgements

This work was supported by the Dutch IOP Genomics grant IGE05003 and the Interreg IV program (project EMR.INT4). We would like to thank I. Kuipers and N. Reynaert for technical expertise and help.

Supplementary data

Supplementary table 5.1. Significantly changed genes with medium effect on the OxyGenes array.
Supplementary table 5.2. Correlation matrix for ROS levels, protein carbonyl levels, total GSH levels and fold changes of classic antioxidant genes.

References

1. Floreani, M., et al., *Antioxidant defences in cybrids harboring mtDNA mutations associated with Leber's hereditary optic neuropathy.* FEBS J, 2005. **272**(5): p. 1124-35.
2. Pang, C.Y., H.C. Lee, and Y.H. Wei, *Enhanced oxidative damage in human cells harboring A3243G mutation of mitochondrial DNA: implication of oxidative stress in the pathogenesis of mitochondrial diabetes.* Diabetes Res Clin Pract, 2001. **54 Suppl 2**: p. S45-56.
3. Piccolo, G., et al., *Biological markers of oxidative stress in mitochondrial myopathies with progressive external ophthalmoplegia.* J Neurol Sci, 1991. **105**(1): p. 57-60.
4. Pitkanen, S. and B.H. Robinson, *Mitochondrial complex I deficiency leads to increased production of superoxide radicals and induction of superoxide dismutase.* J Clin Invest, 1996. **98**(2): p. 345-51.

5. Rusanen, H., K. Majamaa, and I.E. Hassinen, *Increased activities of antioxidant enzymes and decreased ATP concentration in cultured myoblasts with the 3243A-->G mutation in mitochondrial DNA.* Biochim Biophys Acta, 2000. **1500**(1): p. 10-6.
6. Vives-Bauza, C., et al., *Enhanced ROS production and antioxidant defenses in cybrids harbouring mutations in mtDNA.* Neurosci Lett, 2006. **391**(3): p. 136-41.
7. Wei, Y.H., et al., *Oxidative stress in human aging and mitochondrial disease-consequences of defective mitochondrial respiration and impaired antioxidant enzyme system.* Chin J Physiol, 2001. **44**(1): p. 1-11.
8. Wojewoda, M., J. Duszynski, and J. Szczepanowska, *Antioxidant defence systems and generation of reactive oxygen species in osteosarcoma cells with defective mitochondria: Effect of selenium.* Biochim Biophys Acta, 2010. **1797**(6-7): p. 890-6.
9. Balaban, R.S., S. Nemoto, and T. Finkel, *Mitochondria, oxidants, and aging.* Cell, 2005. **120**(4): p. 483-95.
10. Powers, S.K., et al., *Reactive oxygen species are signalling molecules for skeletal muscle adaptation.* Exp Physiol, 2010. **95**(1): p. 1-9.
11. Hawkins, C.L., P.E. Morgan, and M.J. Davies, *Quantification of protein modification by oxidants.* Free Radic Biol Med, 2009. **46**(8): p. 965-88.
12. Sekiguchi, M. and T. Tsuzuki, *Oxidative nucleotide damage: consequences and prevention.* Oncogene, 2002. **21**(58): p. 8895-904.
13. Bayeva, M. and H. Ardehali, *Mitochondrial Dysfunction and Oxidative Damage to Sarcomeric Proteins.* Curr Hypertens Rep, 2010.
14. Stark, G., *Functional consequences of oxidative membrane damage.* J Membr Biol, 2005. **205**(1): p. 1-16.
15. Verkaart, S., et al., *Mitochondrial and cytosolic thiol redox state are not detectably altered in isolated human NADH:ubiquinone oxidoreductase deficiency.* Biochim Biophys Acta, 2007. **1772**(9): p. 1041-51.
16. Wani, A.A., et al., *Analysis of reactive oxygen species and antioxidant defenses in complex I deficient patients revealed a specific increase in superoxide dismutase activity.* Free Radic Res, 2008. **42**(5): p. 415-27.
17. Lu, C.Y., et al., *Increased expression of manganese-superoxide dismutase in fibroblasts of patients with CPEO syndrome.* Mol Genet Metab, 2003. **80**(3): p. 321-9.
18. Ma, Y.S., et al., *Upregulation of matrix metalloproteinase 1 and disruption of mitochondrial network in skin fibroblasts of patients with MERRF syndrome.* Ann N Y Acad Sci, 2005. **1042**: p. 55-63.
19. van Eijsden, R.G., et al., *Termination of damaged protein repair defines the occurrence of symptoms in carriers of the m.3243A > G tRNA(Leu) mutation.* J Med Genet, 2008. **45**(8): p. 525-34.
20. Koopman, W.J., et al., *Inhibition of complex I of the electron transport chain causes O2-. -mediated mitochondrial outgrowth.* Am J Physiol Cell Physiol, 2005. **288**(6): p. C1440-50.
21. Li, J., et al., *Increased ROS generation and SOD activity in heteroplasmic tissues of transmitochondrial mice with A3243G mitochondrial DNA mutation.* Genet Mol Res, 2008. **7**(4): p. 1054-62.
22. Quinzii, C.M., et al., *Respiratory chain dysfunction and oxidative stress correlate with severity of primary CoQ10 deficiency.* FASEB J, 2008. **22**(6): p. 1874-85.
23. Verkaart, S., et al., *Superoxide production is inversely related to complex I activity in inherited complex I deficiency.* Biochim Biophys Acta, 2007. **1772**(3): p. 373-81.
24. Moran, M., et al., *Mitochondrial bioenergetics and dynamics interplay in complex I-deficient fibroblasts.* Biochim Biophys Acta, 2010. **1802**(5): p. 443-53.
25. Kujoth, G.C., et al., *Mitochondrial DNA mutations, oxidative stress, and apoptosis in mammalian aging.* Science, 2005. **309**(5733): p. 481-4.
26. Trifunovic, A., et al., *Somatic mtDNA mutations cause aging phenotypes without affecting reactive oxygen species production.* Proc Natl Acad Sci U S A, 2005. **102**(50): p. 17993-8.

27. Lewis, W., et al., *Decreased mtDNA, oxidative stress, cardiomyopathy, and death from transgenic cardiac targeted human mutant polymerase gamma.* Lab Invest, 2007. **87**(4): p. 326-35.
28. van der Westhuizen, F.H., et al., *Human mitochondrial complex I deficiency: investigating transcriptional responses by microarray.* Neuropediatrics, 2003. **34**(1): p. 14-22.
29. Rahman, I., A. Kode, and S.K. Biswas, *Assay for quantitative determination of glutathione and glutathione disulfide levels using enzymatic recycling method.* Nat Protoc, 2006. **1**(6): p. 3159-65.
30. De Groote, D., et al., *Effects of oral contraception with ethinylestradiol and drospirenone on oxidative stress in women 18-35 years old.* Contraception, 2009. **80**(2): p. 187-93.
31. Akaike, H. *Information theory and an extension of the maximum likelihood principle*. in *Second International Symposium on Inference Theory*. 1973. Budapest: Akadémiai Kiadó.
32. Rossignol, R., et al., *Energy substrate modulates mitochondrial structure and oxidative capacity in cancer cells.* Cancer Res, 2004. **64**(3): p. 985-93.
33. Guillery, O., et al., *Modulation of mitochondrial morphology by bioenergetics defects in primary human fibroblasts.* Neuromuscul Disord, 2008. **18**(4): p. 319-30.
34. Robinson, B.H., et al., *Nonviability of cells with oxidative defects in galactose medium: a screening test for affected patient fibroblasts.* Biochem Med Metab Biol, 1992. **48**(2): p. 122-6.
35. Unterluggauer, H., et al., *Senescence-associated cell death of human endothelial cells: the role of oxidative stress.* Exp Gerontol, 2003. **38**(10): p. 1149-60.
36. Rigoulet, M., E.D. Yoboue, and A. Devin, *Mitochondrial ROS generation and its regulation: mechanisms involved in H(2)O(2) signaling.* Antioxid Redox Signal, 2011. **14**(3): p. 459-68.
37. Luo, X., et al., *Excessive formation of hydroxyl radicals and aldehydic lipid peroxidation products in cultured skin fibroblasts from patients with complex I deficiency.* J Clin Invest, 1997. **99**(12): p. 2877-82.
38. Beretta, S., et al., *Leber hereditary optic neuropathy mtDNA mutations disrupt glutamate transport in cybrid cell lines.* Brain, 2004. **127**(Pt 10): p. 2183-92.
39. Maniura-Weber, K., et al., *Molecular dysfunction associated with the human mitochondrial 3302A>G mutation in the MTTL1 (mt-tRNALeu(UUR)) gene.* Nucleic Acids Res, 2006. **34**(22): p. 6404-15.
40. von Kleist-Retzow, J.C., et al., *Impaired mitochondrial Ca2+ homeostasis in respiratory chain-deficient cells but efficient compensation of energetic disadvantage by enhanced anaerobic glycolysis due to low ATP steady state levels.* Exp Cell Res, 2007. **313**(14): p. 3076-89.
41. Filosto, M., et al., *Antioxidant agents have a different expression pattern in muscle fibers of patients with mitochondrial diseases.* Acta Neuropathol, 2002. **103**(3): p. 215-20.
42. Di Pietro, A., et al., *Ex vivo study for the assessment of behavioral factor and gene polymorphisms in individual susceptibility to oxidative DNA damage metals-induced.* Int J Hyg Environ Health, 2011. **214**(3): p. 210-8.
43. Kulkarni, R., et al., *Mitochondrial gene expression changes in normal and mitochondrial mutant cells after exposure to ionizing radiation.* Radiat Res, 2010. **173**(5): p. 635-44.
44. Dai, D.F., et al., *Age-dependent cardiomyopathy in mitochondrial mutator mice is attenuated by overexpression of catalase targeted to mitochondria.* Aging Cell, 2010. **9**(4): p. 536-44.
45. Tretter, L. and V. Adam-Vizi, *Generation of reactive oxygen species in the reaction catalyzed by alpha-ketoglutarate dehydrogenase.* J Neurosci, 2004. **24**(36): p. 7771-8.

46. Starkov, A.A., et al., *Mitochondrial alpha-ketoglutarate dehydrogenase complex generates reactive oxygen species.* J Neurosci, 2004. **24**(36): p. 7779-88.
47. Bedard, K. and K.H. Krause, *The NOX family of ROS-generating NADPH oxidases: physiology and pathophysiology.* Physiol Rev, 2007. **87**(1): p. 245-313.
48. Pendyala, S. and V. Natarajan, *Redox regulation of Nox proteins.* Respir Physiol Neurobiol, 2010. **174**(3): p. 265-71.
49. Chomyn, A., et al., *MELAS mutation in mtDNA binding site for transcription termination factor causes defects in protein synthesis and in respiration but no change in levels of upstream and downstream mature transcripts.* Proc Natl Acad Sci U S A, 1992. **89**(10): p. 4221-5.
50. Hassani, A., R. Horvath, and P.F. Chinnery, *Mitochondrial myopathies: developments in treatment.* Curr Opin Neurol, 2010. **23**(5): p. 459-65.
51. De Lisio, M., et al., *Exercise training enhances the skeletal muscle response to radiation-induced oxidative stress.* Muscle Nerve, 2011. **43**(1): p. 58-64.
52. Kono, Y. and I. Fridovich, *Superoxide radical inhibits catalase.* J Biol Chem, 1982. **257**(10): p. 5751-4.
53. Cheng, W., et al., *Selenium-dependent cellular glutathione peroxidase protects mice against a pro-oxidant-induced oxidation of NADPH, NADH, lipids, and protein.* FASEB J, 1999. **13**(11): p. 1467-75.
54. Umaki, Y., et al., *Apoptosis-related changes in skeletal muscles of patients with mitochondrial diseases.* Acta Neuropathol, 2002. **103**(2): p. 163-70.
55. Katayama, Y., et al., *Accumulation of oxidative stress around the stroke-like lesions of MELAS patients.* Mitochondrion, 2009. **9**(5): p. 306-13.
56. Quintana, A., et al., *Complex I deficiency due to loss of Ndufs4 in the brain results in progressive encephalopathy resembling Leigh syndrome.* Proc Natl Acad Sci U S A, 2010. **107**(24): p. 10996-1001.
57. Bjelakovic, G., et al., *Mortality in randomized trials of antioxidant supplements for primary and secondary prevention: systematic review and meta-analysis.* JAMA, 2007. **297**(8): p. 842-57.

Supplementary table 5.1. Significantly changed genes with medium effect on the OxyGenes array.

Medium	GLUCOSE									GALACTOSE											
	CI vs control			POLG vs control			tRNA-Leu vs control			control vs control			CI vs control			POLG vs control			tRNA-Leu vs control		
Gene	LL	FC	UL	LL	FC	UL	LL	FC	UL	LL	FC	UL	LL	FC	UL	LL	FC	UL	LL	FC	UL
CCL2	3.35	3.37	3.39				3.35	3.37	3.39	0.98	0.99	0.99	1.03	1.04	1.05	3.24	3.44	3.65	1.03	1.04	1.05
CCL8				0.54	0.55	0.57				1.07	1.08	1.09				2.32	3.10	4.15			
CCR6	0.24	0.29	0.35	0.47	0.50	0.52				0.78	0.88	0.99	2.02	2.09	2.15	1.65	2.22	3.00			
CCR7				0.40	0.62	0.97				0.26	0.37	0.52				3.67	4.00	4.37			
CRP				1.02	1.08	1.15				0.59	0.73	0.89				1.02	1.08	1.15			
CXCR4	0.51	0.55	0.60	0.78	0.79	0.81				0.40	0.42	0.45	1.06	1.26	1.49	1.71	2.40	3.35			
DNAJB1	0.74	0.79	0.84	0.66	0.68	0.71	0.66	0.68	0.71	0.47	0.60	0.76	0.77	0.78	0.79	1.66	2.07	2.59	1.66	2.07	2.59
FOS							6.16	6.40	6.64	1.18	1.29	1.42							0.05	0.09	0.16
FTH1				1.87	2.09	2.33				3.22	3.85	4.60				1.51	2.09	2.88			
FTL							1.23	1.24	1.25	9.59	17.33	31.32							0.31	0.33	0.35
FXN				0.81	0.82	0.83	0.49	0.50	0.51	0.16	0.18	0.20				2.50	3.10	3.85	3.38	4.26	5.35
GCLC	1.66	1.69	1.71	1.25	1.28	1.30				0.60	0.63	0.66	0.57	0.59	0.62	2.57	2.59	2.62			
GLRX2				0.66	0.68	0.71				0.86	0.89	0.92				2.41	2.49	2.57			
HMOX1	0.16	0.20	0.24	0.16	0.20	0.24	0.16	0.20	0.24	0.00	0.01	0.02	8.70	9.15	9.64	8.70	9.15	9.64	8.70	9.15	9.64
HSF2	0.69	0.72	0.74	0.62	0.63	0.64	0.62	0.63	0.64	0.50	0.55	0.61	0.73	0.74	0.75	2.70	3.12	3.60	2.70	3.15	3.60
IL10				1.17	1.22	1.27				0.50	0.54	0.58				1.93	2.29	2.70			
IL1B				0.91	0.92	0.94				1.01	1.04	1.06				1.81	1.87	1.93			
IL3	0.66	0.67	0.68	1.06	1.09	1.12				0.21	0.24	0.26	1.54	1.74	1.97	2.52	2.66	2.80			
MMP9	1.01	1.45	2.08	1.02	1.19	1.39				0.67	0.73	0.80	0.59	0.60	0.62	2.33	2.57	2.84			
NFKB1				0.71	0.74	0.77				0.06	0.08	0.11				2.69	2.79	2.89			
PDIA3				1.07	1.58	2.34				0.16	0.24	0.36				1.57	1.58	1.59			
PPAT				0.25	0.26	0.27				0.40	0.45	0.49				4.86	4.96	5.06			
PRDX1							1.02	1.03	1.04	1.17	1.42	1.74							0.48	0.53	0.58
PTGS2	1.13	1.16	1.19	1.56	1.70	1.86	1.13	1.16	1.19	0.65	0.75	0.86	0.43	0.55	0.71	1.42	1.75	2.14	0.43	0.55	0.71
TNF							2.02	3.10	4.77	2.58	3.56	4.92							0.23	0.25	0.28
TXN	0.91	0.92	0.94	0.66	0.72	0.78	0.60	0.72	0.87	1.41	1.56	1.72	0.83	0.89	0.96	0.69	0.72	0.75	0.69	0.72	0.75
UBC	3.49	5.63	9.09							0.49	0.50	0.51	0.94	0.95	0.96						
UCP2										2.06	3.52	6.04									

Supplementary table 5.2. Correlation matrix

	ROS levels	Protein carbonyl level	Total GSH level	*CAT* expression FC	*SOD1* expression FC	*GSR* expression FC	*GPX1* expression FC
ROS levels							
Protein carbonyl level	-0.158						
Total GSH level	-0.093	-0.032					
CAT expression FC	**-0.508**	-0.197	-0.005				
SOD1 expression FC	-0.001	-0.050	0.246	0.227			
GSR expression FC	0.258	-0.170	-0.120	-0.160	0.400		
GPX1 expression FC	0.225	**0.454**	0.046	-0.177	0.327	0.234	

Correlation matrix for ROS levels, protein carbonyl levels, total GSH levels and fold changes of classic antioxidant genes. The Pearson correlation values produced by SPSS are shown; significant correlations are depicted in bold.

Chapter 6

General Discussion

Mitochondrial enchephalomyopathies are a clinically and genetically highly heterogeneous group of diseases. They are also referred to as oxidative phosphorylation (OXPHOS) disorders, because of the causative role of deficiencies of the OXPHOS system in the pathology of most cases. The pathophysiology of these disorders is only partly understood and efficient therapies are not available for the vast majority of patients. The aims of this thesis were:
1. to facilitate diagnostics of mtDNA-based OXPHOS disorders by determining the non-pathogenic variation of mtDNA in the general population;
2. to gain knowledge on primary and secondary biological processes involved in OXPHOS disorders which have an impact on prognosis and therapy;
3. to explore the extent to which different pathogenic mtDNA and nuclear DNA mutations induce oxidative stress and the consequences of this in a cell line model.
The general discussion elaborates on the most significant findings and models and puts them in a broader perspective of strategies to unravel pathophysiology and evaluate therapy.

Mitochondrial DNA: evolution and disease

The mitochondrial DNA (mtDNA) codes for 13 subunits of complex I, III, IV and V of the OXPHOS chain and 22 tRNAs and 2 rRNAs necessary for mRNA translation. Therefore, it is not surprising that mtDNA mutations or variants can affect OXPHOS function. Some variants cause disease themselves but others only influence the risk of developing disease or affect the course of the disease (so-called risk factors and modifiers). There are also neutral variants that do not have disease-related consequences. An additional factor in determining the effect of variants is the multi-copy nature of the mtDNA with a threshold of expression for heteroplasmic pathogenic mtDNA mutations. In order to understand the presence and the consequences of mtDNA variants, it is necessary to understand how mtDNA variants arise, how they are maintained and why some variants are tolerated whereas others are not.

According to the endosymbiotic hypothesis, eukaryotic mitochondria evolved from endocytosed aerobic bacteria more than 1 billion years ago, when oxygen entered the atmosphere. During eukaryotic evolution, most (but not all) of the bacterial genome encoded genes have been transferred to the nuclear genome, leading to the present dual genetic control of the OXPHOS system [1]. Interestingly, the number of transferred genes differs between eukaryotic species as exemplified in table 6.1. Although in vertebrates there is an almost invariant gene content, other species show considerable mtDNA plasticity, mostly attributable to differences in the number of tRNA genes [2]. This suggests some form of stabilization in more evolved species and a flexibility of eukaryotic mitochondria regarding their ability to import tRNAs from the cytoplasm. Even though the number of protein coding genes is rather stable, loss of ATP8 was shown in five evolutionary-distant fast-evolving taxa (Nematoda, Rotifera, Chaetognatha, Platyhelminthes and Bivalvia). This might indicate that ATP8 is

'dispensable' in the mtDNA [2] and might also have consequences for the tolerance of variation within this gene.

Table 6.1. Genes encoded by the mtDNA in eukaryotic species.

Species	Number of mtDNA genes	Number of protein coding genes
H. sapiens (human)	37	13
M. musculus (mouse)	37	13
G. gallus (chicken)	37	13
D. rerio (zebra fish)	37	13
D. melanogaster (fruit fly)	37	13
P. megacephalus (frog)	35	11
C. elegans (worm)	36	12
S. cephaloptera (worm)	13	11
A. aurita (jelly fish)	19	15
M. occidentalis (mite)	53	21
S. cerevisiae (yeast)	46	19
A. thaliana (plant)	131	117

According to NCBI Genome.

The mtDNA has a higher mutation rate compared to the nuclear DNA. Presumably due to the proximity of the mtDNA to the electron transport chain, a major ROS production site, and the lack of protective histones, the mtDNA is more prone to oxidative damage [3, 4]. Although originally it was suggested that mitochondria have no or only a limited DNA repair capacity [5], efficient base excision repair in mitochondria was detected afterwards [6, 7]. Furthermore, mitochondrial dynamics, characterized by mitochondrial fusion and fission, has been shown to be important for mitochondrial genomic stability through intramitochondrial exchange of mutant mtDNA and stimulation of autophagy of damaged mitochondria [8]. However, the uniparental (maternal) inheritance, the mitochondrial bottleneck (random unbalanced partitioning of the cytoplasm during gamete formation) and possibly low recombination, lead to accumulation of mutations that escape the repair machinery [9] even though their original goal might be the maintenance of mitochondrial genomic integrity [10]. This is not necessarily negative, as the genetic variation is the driving force of evolution, providing a species the possibility to adapt to environmental changes. For example, there is evidence of natural selection on mtDNA variants by temperature [11, 12]. When the human population started expanding and migrated from tropical Africa to more northern and colder climates, variants that decrease coupling efficiency and ATP production but increase heat production would be advantageous for survival [11, 12]. A correlation between two non-synonymous mtDNA variants in *ND3* and *ATP6* and temperature has been described recently [11]. Additional evidence for an adaptive role of ancient mtDNA polymorphisms comes from the presence of the same mtDNA variant on different mtDNA haplogroup backgrounds [13]. Contrastingly, the same beneficial ancient

mtDNA adaptations might be correlated with complex bioenergetic disorders related to the sedentary life-style and increasing age of the human population today (e.g. obesity, diabetes, cardiovascular disease) [12, 14]. Obviously, pathogenic mutations are under strong negative selection to prevent fixation of the mutation in the population. No advantage for disease-causing mtDNA mutations has been observed at the population level [14]. Altogether, after ages of evolution, the human mtDNA sequence will consist of conserved positions, which are identical among most species, and variable positions. Mutation of conserved positions will probably be associated with (*in utero*) mortality and disease (pathogenic mutations) while mutation of variable positions will have minor consequences and will be detected more frequently in the human population.

To study the strength and consequences of natural/purifying selection on mtDNA variation, offspring of the so-called mtDNA mutator mouse was studied [15]. The mutator mice accumulate high levels of mtDNA mutations randomly across their mtDNA due to their proofreading deficient polymerase gamma [15, 16]. However, already after a few generations, a strong selection against non-synonymous changes in protein coding was reported. The strongest selection was observed in genes with high sequence conservation (*COX1*, *COX2*). Similar results were obtained for selective forces on the human mtDNA when resequencing the mitochondrial genome of 730 subjects (**chapter 2**). In agreement with the presumed evolutionary dispensability, also in this study *ATP8* was among the genes with most tolerated variation. Until recently, the study of mtDNA and nuclear DNA variants on a large scale by PCR, DHPLC analysis and/or Sanger sequencing was laborious and time-consuming. Now, the use of next generation whole genome sequencing leads to high throughput analysis of whole genomes and will lead to a detailed map of both genomes. This map will consist of positions that are targeted by tolerated polymorphisms (occurring in healthy individuals) or pathogenic mutations (in diseased but not healthy individuals) or positions that never show variation. The latter situation probably points to mutations that are not compatible with life and will never be detected. Detailed and complete knowledge on tolerance and natural selection in large numbers of individuals will provide valuable information for evaluating the pathogenicity of DNA variants in patients and their families. Furthermore, as mitochondria have been implicated to play a role in a plethora of diseases (*e.g.* diabetes, Alzheimer's disease and cancer), the significance of mtDNA variation in these pathologies can also be judged more adequately. In addition to *in silico* predictions, functional assays can be applied for those pathogenic variants leading to enzyme deficiencies. Cytosolic hybrids (cybrids) carrying the mutant mtDNA in a cancer nuclear background (*e.g.* osteosarcoma) can be used for this purpose [17-19]. However, this approach does not apply to variants with subtle defects with no measurable effect on enzyme activities.

Models to study pathophysiology and/or test compounds: suitability/applicability

When disease-causing mutations are identified, the pathogenic mechanism has to be unraveled in order to investigate potential therapeutic strategies. There will be no single model able to deal with all follow-up investigations and high-throughput analyses in cell lines and simple model organisms will be complemented with studies in more laborious mammalian models. The same applies for intervention studies. Several potential models exist, including human (post-mitotic tissue), human primary cell culture, rodents and small animals (*e.g.* Caenorhabditis elegans [worm], Drosophila melanogaster [fruit fly], Danio rerio [zebrafish]). Each of the models has its own advantages, disadvantages and applications (figure 6.1).

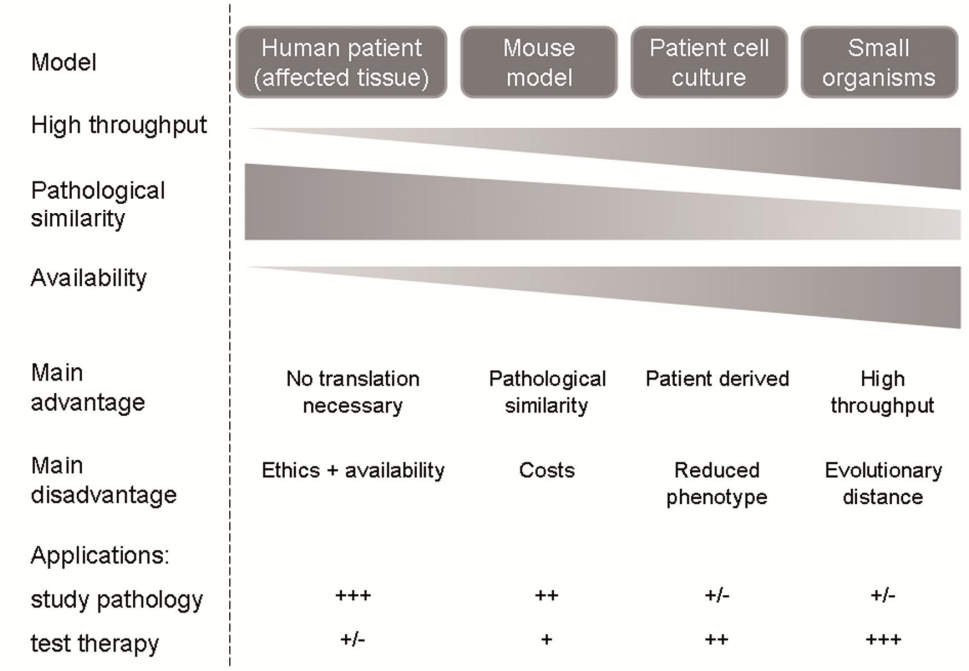

Figure 6.1. Different models to study inherited disorders with characteristics and applications.

For pathophysiological studies, affected tissues from patients would allow the most relevant and specific disease processes to be identified. However, for diseases affecting non-dividing tissues (*e.g.* brain), the availability and amount of material is limited. In **chapter 3**, we circumvented this by studying morphological, genetic (mtDNA) and gene expression changes in muscle of *POLG1* patients to unravel biological processes involved in *POLG1* pathogenesis. Gene expression analysis in muscle hinted towards a possible association of ROS production and apoptosis with patient phenotypes, which was subsequently confirmed in liver and brain of part of the patients.

This study demonstrates how only mildly sub-pathologically affected but better available tissues (such as muscle) can be the surrogate tissue for the identification of pathological processes in more severely affected tissues (such as brain and liver).

Due to the limited availability of post-mitotic patient material, primary cell cultures of dividing patient tissues (*e.g.* fibroblasts) are often used to study pathophysiology and to test therapies *in vitro* [20, 21]. Although this model type allows for high-throughput *in vitro* screening assays, the complex *in vivo* interactions and physiological conditions are not comparable with *in vitro* conditions and often the consequences of the primary defect are less outspoken, especially in the case of OXPHOS disorders [22], where e.g. fibroblast can switch from oxidative to glycolytic energy production. Furthermore, it is important to check the genetic and biochemical stability of the cell lines over time in case they are used as tester panels for compound screening. A panel of fibroblasts cell lines of complex I deficient patients was characterized for this purpose (**chapter 4**). The primary goal was to characterize a complex I deficient cell culture system that could be used for high-throughput screening of small compounds for beneficial effects on complex I activity and energy production. The use of fibroblasts was complicated by the mainly (~70%) glycolytic energy production in fibroblasts under standard (glucose) culture conditions [23]. To induce OXPHOS-derived (oxidative) energy production, and thus stress the primary OXPHOS defect, fibroblast cell lines were cultured in glucose-lacking galactose-containing medium in the presence of glutamine (an essential amino acid for cell growth [24]). Although in HeLa cells, it has been shown that ATP production in galactose medium occurs mainly (98%) through glutaminolysis [25], others did not detect a glutamine dependency of fibroblasts in glucose and galactose medium [26]. Nevertheless, possible energy production through other non-glytolytic pathways has to be kept in mind. Only minor gene expression changes and no signs of mtDNA instability (large scale rearrangements and copy number) were detected, suggesting that cultured complex I deficient fibroblasts have an inherent genetic stability. This makes these parameters less suitable for testing interventions, but they can be used to check stability of the model in time. Other parameters such as biochemical indicators (*e.g.* posttranslational modification of pyruvate dehydrogenase), mitochondrial morphology, mitochondrial membrane potential and calcium fluxes [27-29] have been tested as well and are better indicators to test the effect of adding compounds to the cell culture medium (B. Wieringa and P. Willems, personal communication). The primary patient cell cultures are not only suitable for manipulating the primary defect of complex I deficiency, they can also be used to explore secondary manifestations of OXPHOS deficiency, like for example oxidative stress, which is considered a major contributing factor to OXPHOS pathology. By an in-depth analysis of the level of oxidative stress in different genetically characterized OXPHOS patients, we were able to identify patients with increased ROS levels and evaluate their risk for acquiring oxidative damage in relevant tissues (**chapter 5**). This information gives an indication which patients will be more likely to benefit from antioxidant therapy.
However, biological processes or responses identified by *in vitro* assays should be carefully translated to the patients. Especially when screening compounds or drugs, one must keep in mind that the *in vitro* results do not always correlate with *in vivo*

effects. Validation of candidate compounds in animal models is necessary to examine their pharmacokinetic and toxic properties before going into clinical trials. For some compounds already on the market, like ROS-scavenger or stimulators of mitochondrial biogenesis, the toxic properties have been established, but the positive effect should be carefully judged. This may be difficult as the patients are often unique and grouping is not possible, implying that drug administration is based on individual evaluation and not on a group effect. For better insight in this, mice models are often used because of the high homology between the human and murine genes but also due to the similar phenotypes they develop. For example, mice expressing mutant proofreading deficient D257A polymerase gamma [16, 30] and mice with complex I deficiency by knocking out (KO) or mutating complex I subunit NDUFS4 [31, 32] have been created. The POLG mutator mice presented with increased accumulation of mtDNA mutations and deletions and premature ageing-related phenotypes (*e.g.* reduced fertility, heart enlargement, sarcopenia, hearing loss) [16, 30]. Some of these features also occur as a phenotype in *POLG1* patients [33]. *NDUFS4*-KO mice manifested a lethal phenotype, similar to the Leigh-like symptoms in human patients carrying *NDUFS4* mutations [31]. Heterozygous dominant-negative mutant *NDUFS4* mice were viable and also presented with biochemical changes similar to human Leigh patients [32]. Nevertheless, it is obvious that strain specific differences exist and that it is not possible to make a mouse for each complex human phenotype. The main disadvantages of mouse or other higher organism models are the high costs and the laborious and time-consuming nature of the experiments. In finding a balance between a high-throughput analysis and matching phenotypes, small animal models come into sight. These vertebrate (*D. rerio*) or invertebrate animals (*D. melanogaster*, *C. elegans*) usually have a rapid development, are easy to manipulate genetically and can be phenotyped in a high-throughput fashion. Mutants are often available and compounds can be administered by adding directly to the food, medium or water, making these models suitable for the study of pathophysiology as well as compound screening. Their main disadvantage is their evolutionary distance to humans and the fact that not all of these small organisms contain the organs that are affected in human disease. In the end, there is not a single model optimal for every application. Therefore, the most appropriate mode of action would be to use the models interdependently in a continuum, exploiting all of their individual advantages (figure 6.1).

Pathological processes in genetically characterized OXPHOS disorders

The clinical symptoms/syndromes associated with OXPHOS dysfunction and their ages of onset are extremely variable. There is often no clear genotype:phenotype correlation [34]. One may say that the step from gene to phenotype is too big and ‘genomes speak biochemistry, not phenotypes’ [35] but even that is not always straightforward in case of OXPHOS disorders. Patients with exactly the same mutation(s) can have different biochemistry results in muscle [36], which challenges the concept of monogenic disorders and suggests that in mitochondrial disorders genetic complexity is the rule. During the last decades, the molecular basis of OXPHOS pathology has been

intensively studied. This research has been primarily focused on genetically characterized OXPHOS patients. However, it should be emphasized that half of the patients with a diagnostic OXPHOS deficiency do not have a genetic diagnosis yet [37]. Therefore, family studies using linkage analysis and/or next generation or exome sequencing are applied to identify new genes associated with mitochondrial function or reveal new OXPHOS-related functions for a previously known gene. In rare cases, this approach can lead from a genetic mutation directly to therapy (*e.g.* CoQ10 supplementation for patients with *CABC1* [38] or *ETFDH* [39] mutation). However, most often, the molecular consequences of a novel mutation are not so straightforward and primary and secondary consequences have to be unraveled to identify targets for therapeutic interventions.

The primary consequence of an OXPHOS disorder is generally considered to be the inability of mitochondria to supply sufficient ATP to meet cellular needs, which often becomes manifest when large amounts of energy are required, for example in case of an infection [40]. However, different gene defects lead to OXPHOS deficiency and disease in different ways. There are mutations in the protein-coding genes of the OXPHOS system itself, in genes coding for OXPHOS system assembly factors, in genes responsible for the replication and maintenance of the mtDNA and in genes more indirectly related to OXPHOS function. Furthermore, the negative effect on tissues or organs relates also to their dependence on OXPHOS instead of glycolysis for energy supply and the residual capacity they have. A summary of common processes in OXPHOS patients, partly identified and described in this thesis, is presented in figure 6.2. Interventions directed at these processes should be beneficial for the larger group of patients.

Bioenergetics

Increased lactate levels in *POLG1* patients (**chapter 3**) and in OXPHOS patients in general [41], indicate a metabolic switch from OXPHOS to glycolysis derived ATP production and pyruvate to lactate oxidation for NAD^+ regeneration. Increased concentrations of lactate and tricarboxylic acid cycle intermediates are frequently encountered in patients with OXPHOS disease [42, 43] as a measure of disturbed bioenergetics. Reinecke *et al* recently reviewed the limited literature on RNA expression changes of metabolic genes in a variety of disease phenotypes and models for OXPHOS deficiency [44]. Even though a disturbance of energy metabolism genes is most often apparent in OXPHOS patients [40], expression changes of the genes involved in the different studies are highly diverse and inconsistent [44]. This is a further reflection of the extreme heterogeneic pathogenicity of the disorders, illustrating that multiple pathways and processes are playing a role. Characterization of gene expression changes, contributing to disease manifestation and progression, at the individual level is important to obtain more insight in personal consequences of and adaptations to OXPHOS deficiency.

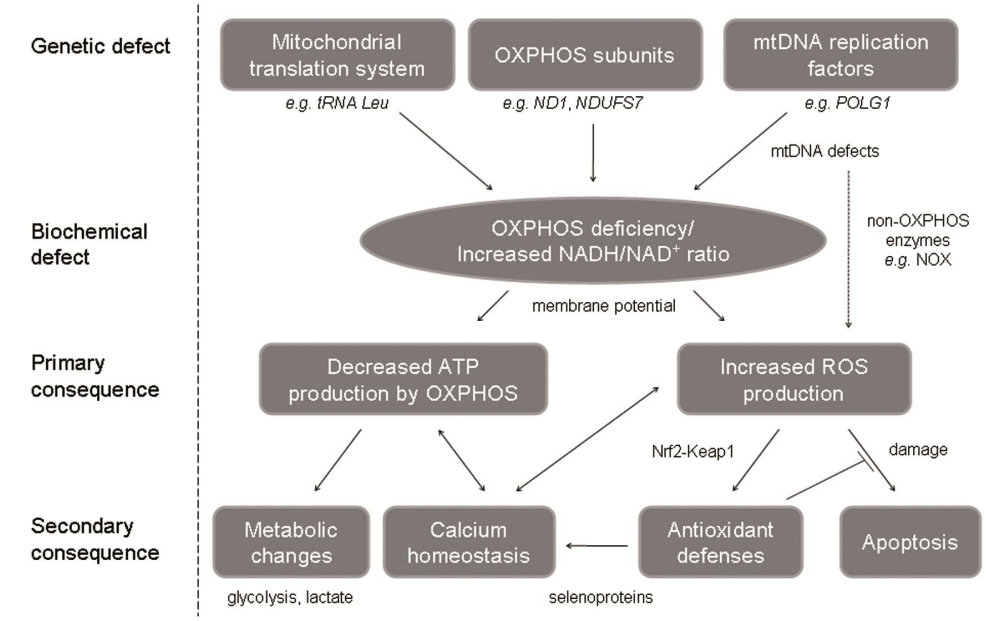

Figure 6.2. Pathophysiological processes involved in OXPHOS disease.

Mitochondrial ATP production is essential for transport of key metabolites across membranes. Cellular ionic calcium is an important second messenger, regulating many cellular processes with variable spatial and temporal dynamics [45]. Calcium homeostasis, which is normally maintained within a very narrow range around ~100 nM [45], has often been shown to be aberrant in mitochondrial diseases [46-48]. Impaired sequestration of calcium in intracellular calcium stores (mitochondria, sarcoplasmic/endoplasmic reticulum) can be secondary to ATP depletion [28] and ROS [49] due to their effect on the ATP-dependent Ca^{2+} pumps. Calcium has been shown to be a physiological stimulator of mitochondrial OXPHOS function, although at high concentration it changes to a pathological enhancer of ROS production [50]. Other potential pathological effects following deregulated calcium homeostasis are the opening of mitochondrial permeability transition pore, resulting in cytochrome *c* release and apoptosis [50]. Recently, the protein responsible for mitochondrial calcium pumping, the mitochondrial calcium uniporter (MCU), was identified and characterized [51, 52]. Future studies are necessary to establish the exact mechanism and the regulation of mitochondrial calcium transport by MCU.

OXPHOS defects are also associated with changes in the mitochondrial membrane potential [53, 54]. Altered mitochondrial membrane potential influences mitochondrial dynamics (fission and fusion) [55]. Depolarized mitochondria are not able to fuse with the network after fission and are targeted for autophagy/mitophagy [56]. This bioenergetic quality control mechanism has to monitor that dysfunctional mitochondria are selectively removed from the mitochondrial network. Increased stimulation or

activation of autophagy has been described for mtDNA point mutations [57] and deletions [58] before and are expected to apply also for other OXPHOS disorders with altered mitochondrial membrane potential. The processes mentioned above are generally reported in OXPHOS disorders. Nevertheless, specific gene mutations can lead to more specific metabolic consequences such as reduced flavine adenine dinucleotide (FAD) binding due to *ACAD9* mutation [59], (secondary) CoQ10 deficiency due to ETFDH deficiency associated with *ETFDH* mutation [39] or mutation of *CABC1*, involved in CoQ10 synthesis [38].

Oxidative stress and apoptosis

ROS production

ROS production has predominantly been considered a secondary factor following dysfunction of one of the OXPHOS complexes (especially complex I or III [60, 61]) or changes in the mitochondrial membrane potential [62, 63]. Fibroblasts of patients with a *POLG1*, mitochondrial *tRNA Leu* or mtDNA encoded complex I subunit mutation showed increased ROS production with a moderate OXPHOS deficiency (**chapter 5**). This could indicate that moderately decreased (lower than 65% activity of average control) OXPHOS function already increases ROS levels. In support of this theory, at least for complex I deficiency, increased superoxide production was measured in fibroblasts of patients with a mutation in a nuclear DNA-encoded CI gene and residual CI activities up to 75% of control [61]. However, the methods applied (HEt oxidation) do not distinguish the exact site(s) of ROS production [61] and therefore, other proteins might be responsible for the increased ROS levels measured. Genetic OXPHOS defects have been associated with a shift in the intramitochondrial NAD^+/NADH ratio towards NADH [44, 64]. This can stimulate ROS production (superoxide and H_2O_2) by alpha-ketoglutarate dehydrogenase in the tricarboxylic acid cycle [65, 66]. The NADPH oxidases (NOX) are another class of proteins that mainly function in ROS production [67] and have also been suggested to be regulated by the redox status of cells [68]. Therefore, ROS should also be considered as a pathological process in genetically characterized OXPHOS patients without diagnostic OXPHOS deficiency in fibroblasts.

One therapeutic strategy that is often applied is antioxidant supplementation to scavenge increased ROS. However, up to now, the efficacy of such therapy has been highly anecdotic as patients have not been carefully evaluated for amount and origin of ROS production. The most recent evidence of a positive therapeutic effect of antioxidants for mitochondrial disease comes from a small double-blind cross-over study involving 27 mitochondrial patients and 42 controls showing that a 30-day supplementation with a cysteine donor reduced exercise-induced oxidative damage levels in blood [69]. The cell culture models established in this thesis (**chapter 4 and 5**) enable detailed analysis of the ROS factor in the pathology observed and could be used to measure the (beneficial) effects of soluble cell permeable antioxidant compounds by simply adding them to the cell culture and monitoring the characterized parameters. Future addition of measurements related to cellular repair capacity to this pipeline would be relevant since repair is highly energy dependent. These studies might reveal differences in oxidative damage in cell lines with similar ROS levels and antioxidant defenses and ways to prevent and treat them. Nevertheless, although

difficult in a small and diverse patient group as this, the effect of antioxidant therapy should be evaluated critically as existing evidence also suggests a harmful effect, *i.e.* increased mortality, of particular antioxidant supplementation in the general population [70]. Our cell culture model can actually help in selecting patients to enroll in such an evaluation study.

Antioxidant defense

ROS have also a central physiological signaling character, inducing antioxidant pathways. This was observed by the induction of the Nrf2-Keap1 pathway (**chapter 4**) and the changed gene expression of classic antioxidant genes (*SOD1*, *GPX1*, *GSR*; **chapter 5**) in fibroblasts with increased ROS levels. The Nrf2-Keap1 pathway is one of the major redox-sensitive signaling systems in the cell and acts as a molecular sensor of disturbances in cellular homeostasis [71]. Activation of Nrf2 signaling was described previously in fibroblasts of patients with a mutation in the mitochondrial *ATP6* gene [72], indicating a potential general therapeutic relevance for OXPHOS diseases. The Nrf2-Keap1 pathway has been mentioned before as a therapeutic target for neurovascular protection in stroke [73] and has been shown to ameliorate neurodegenerative phenotypes in a Drosophila model of Parkinson's disease [74]. However, care should be taken when stimulating this pathway since deregulation of the Nrf2-Keap1 system has been implicated in carcinogenesis [75]. The consequences of modulating Nrf2, but preferentially also of more specific downstream targets can be evaluated using the cell culture models described in this thesis before translating it to animal models and eventually human patients.

Whereas the effectiveness of activation of the antioxidant system against the accumulation of oxidative damage has been shown in **chapter 5**, increasing antioxidant defenses can be detrimental for other cellular functions. This was shown by the preferential expression of selenoproteins involved in (oxidative) stress reduction (thioredoxins, SelK) which probably led to decreased expression of multiple other selenoproteins (**chapter 4**). Some of these proteins have been associated with the control of calcium fluxes (*e.g.* SelN, SelK, SelM) [76-78]. The decreased gene expression of these proteins in our analysis provides a new hypothesis for the decreased calcium fluxes measured previously in the studied patient cell lines [28, 29]. In these studies, decreased endoplasmic reticulum (ER) calcium content and slower calcium removal from the cytosol were observed [28]. Apart from the hypothesized role of decreased ATP delivery [28], the associations of SelN [77] and SelK [78] with the ER membrane and its receptors point to a contribution of selenoproteins to the disturbed calcium homeostasis. Furthermore, the expression of selenoproteins is dependent on the cellular selenium status [79] and therefore, monitoring and adjusting selenium levels might eventually prove to be a new therapeutic lead for CI deficient patients. The beneficial effect of selenium has also been reported for mtDNA defects [48] and therefore, this pathway is probably implicated in OXPHOS defects in more general.

Apoptosis

The process of programmed cell death, or apoptosis, plays an important role in the regulation of normal cell populations and focal apoptosis is involved in many normal embryonic processes such as the development of organs and digits [80]. However, when apoptosis is triggered abnormally in post-mitotic tissues, the functionality of those tissues might become compromised. When antioxidant systems fail and cellular (oxidative) damage is beyond repair, apoptosis is often triggered. This was observed in liver and brain, the most affected tissues, of patients with *POLG1* mutations (**chapter 3**). Therefore, loss of non-replaceable cells by apoptosis can be regarded as a marker of disease severity and/or progression in *POLG1* pathogenesis and possibly in other OXPHOS diseases [81].

Therapeutic considerations

As a consequence of the extreme clinical, biochemical and genetic diversity in patients, it is unlikely that one single therapy could treat all OXPHOS diseases [82]. The current rationale is that slightly increasing compromised OXPHOS activity above a certain threshold may already be beneficial, even if you stimulate a dysfunctional system. Stimulation of mitochondrial biogenesis by for example controlled exercise training is currently suggested as a general approach in patients with OXPHOS disease [83]. Although the initial feeling might be that rest is better for an already compromised muscle, controlled training has been shown to induce muscle regeneration in patients with mtDNA disease from satellite cells with generally lower mutation levels, to maximize muscle function and to prevent disuse atrophy [83, 84]. Nevertheless, additional, more specific treatments will be required for patients in a form of 'personalized medicine'. Pathological processes should be characterized in each OXPHOS patient, leading to a patient profile that indicates which treatment(s) best suit(s) that patient. For example, antioxidants should only be administered to patients that really suffer from oxidative damage and would therefore benefit from this kind of therapy. Additionally, when drugs are administered to patients, it should be proven that the drug reaches the affected tissue(s). For most organs (liver, muscle), this usually does not seem to be a problem, but when the brain is involved, the capacity of a drug to penetrate the blood brain barrier must be considered. Exogenous antioxidants of varying chemical structures have been investigated, but most of them poorly cross the blood brain barrier [85]. In this thesis, a standardized and extensive cell line panel has been developed for fast and large-scale screening of compounds (new chemical substances as well as known nutritional supplements) with therapeutic potential in OXPHOS disorders. Default parameters have been documented extensively to evaluate the effect of the candidate compounds reliably and in detail. Furthermore, monitoring the amount of oxidative (protein) damage and/or apoptosis have been pointed out as valuable markers in OXPHOS pathology and can possibly also be considered to assess the effect of compounds on disease outcome.

Therapeutic approaches

Current therapy approaches are based on specific treatment of particular mitochondrial diseases, treatment of symptoms of mitochondrial disease, (prevention by) exercise therapy and inhibition of ROS damage and prevention of germline transmission as explained below. Specific treatments include CoQ10 replacement therapy for patients with *CABC1* [38] or *ETFDH* [39] mutation, L-arginine supplementation in MELAS patients [86, 87] and peritoneal dialysis or allogeneic hematopoietic stem cell transplantation in patients with *TYMP* mutations and mitochondrial neurogastrointestinal encephalomyopathy [MNGIE] [88]. Furthermore, more than a decade ago, riboflavin supplementation has been shown to be beneficial for certain patients with complex I deficiency by Scholte *et al [89]*, while recently the genetic basis for this finding (*ACAD9* mutation) has been elucidated in these patients [59]. Although not proven, it is striking that untreated patients with ACAD9 mutations die at young age of cardiomyopathies [90, 91].

Symptomatic therapy

Current symptomatic pharmacological therapy includes, amongst others, sodium bicarbonate and dichloroacetate for lactic acidosis, anticonvulsants for epileptic seizures and beta blockers for cardiomyopathy [84, 92]. Despite that the effectiveness is not clear for most compounds, various treatment cocktails of vitamins and cofactors (e.g. riboflavin, thiamine, folic acid, L-carnitine, creatine monohydrate and idebenone) are administrated to patients with OXPHOS disease because they are presumed harmless [93]. Non-pharmacological treatment options include organ transplantation (*e.g.* kidney or heart with single organ involvement), corrective ptosis surgery, gastrostomy and deep brain stimulation [84].

Prevention of transmission

Instead of treating the disease itself, one might also choose for the prevention of mtDNA disease segregation in families. A number of approaches currently available are prenatal diagnosis using chorionic villus sampling, preimplantation genetic diagnosis (PGD), or nuclear transfer, which is still in the experimental phase [94]. Prenatal diagnosis (PND) is applicable for nuclear gene defects. For mtDNA disease this is not reliable, as the clinical severity of the phenotype after birth cannot reliably be predicted for most mtDNA mutations, based on the mutation percentage in chorionic villus [95]. At present, PGD is the better alternative for carriers of heteroplasmic mtDNA mutations [95]. In PGD, embryos are generated by in vitro fertilization and tested for the mitochondrial DNA mutations. Only the embryos with low or undetectable amounts of mutant DNA are transferred to the uterus, which unlike PND, avoids the dilemma of pregnancy termination. Although it cannot guarantee that a child will be unaffected, PGD aims at reducing the risk of having an affected child [95]. Because of this suboptimal testing, a number of ethical questions have arisen on the selection of embryos, the setting of safe margins for mtDNA mutations and the wishes of the parents [96]. In the future, nuclear transfer might be promising. This involves the fusion of a nucleus from a fertilized oocyte with an enucleated donor oocyte. Although recent

studies have shown the feasibility hereof in apes *in vivo* [97] and in humans *in vitro* [94, 98], the technique is still experimental, implies many unknowns (e.g. the effect on nucleo-mitochondrial interactions) and brings about even more ethical issues [99].

Gene therapy

In the last decade, a number of approaches in gene therapy, especially for long-term treatment of mtDNA related OXPHOS disorders, have been explored [93]. One strategy focuses on introducing a wild type copy of the mutated mitochondrial gene into the nucleus, translating the protein in the cytosol and importing normal copies of the protein into the mitochondria (allotopic expression). Although elegant, this method involves some obstacles to overcome. The protein has to be targeted to the mitochondria (by adding a targeting signal), imported into the mitochondria and assembled into a multi-subunit complex. In addition, translation in the cytosol requires the use of the standard genetic code instead of the mitochondrial code [100]. Some successes have been reported with the NARP m.T8993G mutation in *ATP6*, the LHON mutations m.G3460A and m.G11778A in *ND1* and *ND4* respectively and the MERRF m.A8344G mutation in *tRNALys* [101-103]. Allotopic expression of the wild type genes in cybrid cell lines or patient fibroblasts carrying the (nearly, >95%) homoplasmic mutations (partially) rescued the biochemical defect [101-103]. Another promising long-term therapy is to selectively inhibit replication of mutant mtDNA molecules (antigenomic therapy). The challenge is to find an agent that discriminates between wild type and mutant mtDNA, that can be imported into the mitochondria and binds the mutant mtDNA irreversibly to prevent its release when natural replication is occurring [100]. In vitro experiments with peptide nucleic acids showed their ability to selectively inhibit replication of the m.A8344G MERRF mutant mtDNA [104]. However, problems related with the import of the antigenomic molecules into the mitochondria still have to be resolved [100]. So far, these approaches have only been tested *in vitro*. Due to the current lack of pathogenic heteroplasmic mtDNA mouse models, further development and translation to human patients will not be for the near future [105].

Even though few OXPHOS disorders can be treated because of a specific metabolic defect inherent to a certain mutation, most cannot. The phenotypic diversity of patients with the same genetic defect and the genetic heterogeneity of patients with the same syndrome or symptoms emphasize that therapy is better not based on the patients' phenotype and/or genotype but on the molecular pathways, some of which are described in this thesis that are triggered or changed in the patients' tissues. Therefore, the future strategy would be to systematically monitor key pathways in tissues of OXPHOS patients, irrespective of their genetic or biochemical diagnosis, and from this build a personal therapy plan to optimize the treatment effect and reduce the amount of ineffective medication.

References

1. Alberts B, J.A., Lewis J, Raff M, Roberts K, Walter P, *Molecular Biology of the Cell, 4th edition*. 2002, New York: Garland Science.
2. Gissi, C., F. Iannelli, and G. Pesole, *Evolution of the mitochondrial genome of Metazoa as exemplified by comparison of congeneric species.* Heredity, 2008. **101**(4): p. 301-20.
3. Croteau, D.L. and V.A. Bohr, *Repair of oxidative damage to nuclear and mitochondrial DNA in mammalian cells.* J Biol Chem, 1997. **272**(41): p. 25409-12.
4. Wallace, D.C., *A mitochondrial paradigm of metabolic and degenerative diseases, aging, and cancer: a dawn for evolutionary medicine.* Annu Rev Genet, 2005. **39**: p. 359-407.
5. Clayton, D.A., J.N. Doda, and E.C. Friedberg, *The absence of a pyrimidine dimer repair mechanism in mammalian mitochondria.* Proc Natl Acad Sci U S A, 1974. **71**(7): p. 2777-81.
6. Takao, M., et al., *Mitochondrial targeting of human DNA glycosylases for repair of oxidative DNA damage.* Nucleic Acids Res, 1998. **26**(12): p. 2917-22.
7. Pinz, K.G. and D.F. Bogenhagen, *Efficient repair of abasic sites in DNA by mitochondrial enzymes.* Mol Cell Biol, 1998. **18**(3): p. 1257-65.
8. Seo, A.Y., et al., *New insights into the role of mitochondria in aging: mitochondrial dynamics and more.* J Cell Sci, 2010. **123**(Pt 15): p. 2533-42.
9. Neiman, M. and D.R. Taylor, *The causes of mutation accumulation in mitochondrial genomes.* Proc Biol Sci, 2009. **276**(1660): p. 1201-9.
10. Jansen, R.P., *Germline passage of mitochondria: quantitative considerations and possible embryological sequelae.* Hum Reprod, 2000. **15 Suppl 2**: p. 112-28.
11. Balloux, F., et al., *Climate shaped the worldwide distribution of human mitochondrial DNA sequence variation.* Proc Biol Sci, 2009. **276**(1672): p. 3447-55.
12. Mishmar, D., et al., *Natural selection shaped regional mtDNA variation in humans.* Proc Natl Acad Sci U S A, 2003. **100**(1): p. 171-6.
13. Wallace, D.C., *Bioenergetics and the epigenome: interface between the environment and genes in common diseases.* Dev Disabil Res Rev, 2010. **16**(2): p. 114-9.
14. Mishmar, D. and I. Zhidkov, *Evolution and disease converge in the mitochondrion.* Biochim Biophys Acta, 2010. **1797**(6-7): p. 1099-104.
15. Stewart, J.B., et al., *Strong purifying selection in transmission of mammalian mitochondrial DNA.* PLoS Biol, 2008. **6**(1): p. e10.
16. Trifunovic, A., et al., *Premature ageing in mice expressing defective mitochondrial DNA polymerase.* Nature, 2004. **429**(6990): p. 417-23.
17. Vazquez-Memije, M.E., et al., *Cellular and functional analysis of four mutations located in the mitochondrial ATPase6 gene.* J Cell Biochem, 2009. **106**(5): p. 878-86.
18. Trounce, I.A. and C.A. Pinkert, *Cybrid models of mtDNA disease and transmission, from cells to mice.* Curr Top Dev Biol, 2007. **77**: p. 157-83.
19. Smits, P., et al., *Functional consequences of mitochondrial tRNA Trp and tRNA Arg mutations causing combined OXPHOS defects.* Eur J Hum Genet, 2010. **18**(3): p. 324-9.
20. van der Westhuizen, F.H., et al., *Human mitochondrial complex I deficiency: investigating transcriptional responses by microarray.* Neuropediatrics, 2003. **34**(1): p. 14-22.
21. Valsecchi, F., et al., *Complex I disorders: causes, mechanisms, and development of treatment strategies at the cellular level.* Dev Disabil Res Rev, 2010. **16**(2): p. 175-82.
22. van den Heuvel, L.P., J.A. Smeitink, and R.J. Rodenburg, *Biochemical examination of fibroblasts in the diagnosis and research of oxidative phosphorylation (OXPHOS) defects.* Mitochondrion, 2004. **4**(5-6): p. 395-401.

23. Moran, M., et al., *Mitochondrial bioenergetics and dynamics interplay in complex I-deficient fibroblasts.* Biochim Biophys Acta, 2010. **1802**(5): p. 443-53.
24. Eagle, H., A.E. Freeman, and M. Levy, *The amino acid requirements of monkey kidney cells in first culture passage.* J Exp Med, 1958. **107**(5): p. 643-52.
25. Rossignol, R., et al., *Energy substrate modulates mitochondrial structure and oxidative capacity in cancer cells.* Cancer Res, 2004. **64**(3): p. 985-93.
26. Wolfrom, C., et al., *Glutamine dependency of human skin fibroblasts: modulation by hexoses.* Exp Cell Res, 1989. **183**(2): p. 303-18.
27. Koopman, W.J., et al., *Computer-assisted live cell analysis of mitochondrial membrane potential, morphology and calcium handling.* Methods, 2008. **46**(4): p. 304-11.
28. Willems, P.H., et al., *Mitochondrial Ca2+ homeostasis in human NADH:ubiquinone oxidoreductase deficiency.* Cell Calcium, 2008. **44**(1): p. 123-33.
29. Valsecchi, F., et al., *Calcium and ATP handling in human NADH:ubiquinone oxidoreductase deficiency.* Biochim Biophys Acta, 2009. **1792**(12): p. 1130-7.
30. Kujoth, G.C., et al., *Mitochondrial DNA mutations, oxidative stress, and apoptosis in mammalian aging.* Science, 2005. **309**(5733): p. 481-4.
31. Kruse, S.E., et al., *Mice with mitochondrial complex I deficiency develop a fatal encephalomyopathy.* Cell Metab, 2008. **7**(4): p. 312-20.
32. Ingraham, C.A., et al., *NDUFS4: creation of a mouse model mimicking a Complex I disorder.* Mitochondrion, 2009. **9**(3): p. 204-10.
33. Saneto, R.P. and R.K. Naviaux, *Polymerase gamma disease through the ages.* Dev Disabil Res Rev, 2010. **16**(2): p. 163-74.
34. Tuppen, H.A., et al., *Mitochondrial DNA mutations and human disease.* Biochim Biophys Acta, 2010. **1797**(2): p. 113-28.
35. Plasterk, R.H., *Hershey heaven and Caenorhabditis elegans.* Nat Genet, 1999. **21**(1): p. 63-4.
36. de Vries, M.C., et al., *Normal biochemical analysis of the oxidative phosphorylation (OXPHOS) system in a child with POLG mutations: A cautionary note.* J Inherit Metab Dis, 2008.
37. Thorburn, D.R., et al., *Biochemical and molecular diagnosis of mitochondrial respiratory chain disorders.* Biochim Biophys Acta, 2004. **1659**(2-3): p. 121-8.
38. Gerards, M., et al., *Nonsense mutations in CABC1/ADCK3 cause progressive cerebellar ataxia and atrophy.* Mitochondrion, 2010. **10**(5): p. 510-5.
39. Gempel, K., et al., *The myopathic form of coenzyme Q10 deficiency is caused by mutations in the electron-transferring-flavoprotein dehydrogenase (ETFDH) gene.* Brain, 2007. **130**(Pt 8): p. 2037-44.
40. Smeitink, J.A., et al., *Mitochondrial medicine: a metabolic perspective on the pathology of oxidative phosphorylation disorders.* Cell Metab, 2006. **3**(1): p. 9-13.
41. Robinson, B.H., *Lactic acidemia and mitochondrial disease.* Mol Genet Metab, 2006. **89**(1-2): p. 3-13.
42. Smeitink, J.A., *Mitochondrial disorders: clinical presentation and diagnostic dilemmas.* J Inherit Metab Dis, 2003. **26**(2-3): p. 199-207.
43. Esteitie, N., et al., *Secondary metabolic effects in complex I deficiency.* Ann Neurol, 2005. **58**(4): p. 544-52.
44. Reinecke, F., J.A. Smeitink, and F.H. van der Westhuizen, *OXPHOS gene expression and control in mitochondrial disorders.* Biochim Biophys Acta, 2009. **1792**(12): p. 1113-21.
45. Berridge, M.J., M.D. Bootman, and H.L. Roderick, *Calcium signalling: dynamics, homeostasis and remodelling.* Nat Rev Mol Cell Biol, 2003. **4**(7): p. 517-29.
46. Brini, M., et al., *A calcium signaling defect in the pathogenesis of a mitochondrial DNA inherited oxidative phosphorylation deficiency.* Nat Med, 1999. **5**(8): p. 951-4.

47. Visch, H.J., et al., *Decreased agonist-stimulated mitochondrial ATP production caused by a pathological reduction in endoplasmic reticulum calcium content in human complex I deficiency.* Biochim Biophys Acta, 2006. **1762**(1): p. 115-23.
48. Wojewoda, M., et al., *Effect of selenite on basic mitochondrial function in human osteosarcoma cells with chronic mitochondrial stress.* Mitochondrion, 2011.
49. Kaminishi, T. and K.J. Kako, *Sensitivity to oxidants of mitochondrial and sarcoplasmic reticular calcium uptake in saponin-treated cardiac myocytes.* Basic Res Cardiol, 1989. **84**(3): p. 282-90.
50. Brookes, P.S., et al., *Calcium, ATP, and ROS: a mitochondrial love-hate triangle.* Am J Physiol Cell Physiol, 2004. **287**(4): p. C817-33.
51. De Stefani, D., et al., *A forty-kilodalton protein of the inner membrane is the mitochondrial calcium uniporter.* Nature, 2011. **476**(7360): p. 336-40.
52. Baughman, J.M., et al., *Integrative genomics identifies MCU as an essential component of the mitochondrial calcium uniporter.* Nature, 2011. **476**(7360): p. 341-5.
53. James, A.M., et al., *Altered mitochondrial function in fibroblasts containing MELAS or MERRF mitochondrial DNA mutations.* Biochem J, 1996. **318 (Pt 2)**: p. 401-7.
54. Distelmaier, F., et al., *Mitochondrial complex I deficiency: from organelle dysfunction to clinical disease.* Brain, 2009. **132**(Pt 4): p. 833-42.
55. Iglewski, M., et al., *Mitochondrial fission and autophagy in the normal and diseased heart.* Curr Hypertens Rep, 2010. **12**(6): p. 418-25.
56. Twig, G. and O.S. Shirihai, *The interplay between mitochondrial dynamics and mitophagy.* Antioxid Redox Signal, 2011. **14**(10): p. 1939-51.
57. Chen, C.Y., et al., *Decreased heat shock protein 27 expression and altered autophagy in human cells harboring A8344G mitochondrial DNA mutation.* Mitochondrion, 2011. **11**(5): p. 739-49.
58. Alemi, M., et al., *Mitochondrial DNA deletions inhibit proteasomal activity and stimulate an autophagic transcript.* Free Radic Biol Med, 2007. **42**(1): p. 32-43.
59. Gerards, M., et al., *Riboflavin-responsive oxidative phosphorylation complex I deficiency caused by defective ACAD9: new function for an old gene.* Brain, 2011. **134**(Pt 1): p. 210-9.
60. Selivanov, V.A., et al., *Reactive oxygen species production by forward and reverse electron fluxes in the mitochondrial respiratory chain.* PLoS Comput Biol, 2011. **7**(3): p. e1001115.
61. Verkaart, S., et al., *Superoxide production is inversely related to complex I activity in inherited complex I deficiency.* Biochim Biophys Acta, 2007. **1772**(3): p. 373-81.
62. Huttemann, M., et al., *Regulation of oxidative phosphorylation, the mitochondrial membrane potential, and their role in human disease.* J Bioenerg Biomembr, 2008. **40**(5): p. 445-56.
63. Korshunov, S.S., V.P. Skulachev, and A.A. Starkov, *High protonic potential actuates a mechanism of production of reactive oxygen species in mitochondria.* FEBS Lett, 1997. **416**(1): p. 15-8.
64. Munnich, A. and P. Rustin, *Clinical spectrum and diagnosis of mitochondrial disorders.* Am J Med Genet, 2001. **106**(1): p. 4-17.
65. Tretter, L. and V. Adam-Vizi, *Generation of reactive oxygen species in the reaction catalyzed by alpha-ketoglutarate dehydrogenase.* J Neurosci, 2004. **24**(36): p. 7771-8.
66. Starkov, A.A., et al., *Mitochondrial alpha-ketoglutarate dehydrogenase complex generates reactive oxygen species.* J Neurosci, 2004. **24**(36): p. 7779-88.
67. Bedard, K. and K.H. Krause, *The NOX family of ROS-generating NADPH oxidases: physiology and pathophysiology.* Physiol Rev, 2007. **87**(1): p. 245-313.
68. Pendyala, S. and V. Natarajan, *Redox regulation of Nox proteins.* Respir Physiol Neurobiol, 2010. **174**(3): p. 265-71.
69. Mancuso, M., et al., *Oxidative stress biomarkers in mitochondrial myopathies, basally and after cysteine donor supplementation.* J Neurol, 2010. **257**(5): p. 774-81.

70. Bjelakovic, G., et al., *Mortality in randomized trials of antioxidant supplements for primary and secondary prevention: systematic review and meta-analysis.* JAMA, 2007. **297**(8): p. 842-57.
71. Tkachev, V.O., E.B. Menshchikova, and N.K. Zenkov, *Mechanism of the Nrf2/Keap1/ARE signaling system.* Biochemistry (Mosc), 2011. **76**(4): p. 407-22.
72. Dassa, E.P., et al., *The mtDNA NARP mutation activates the actin-Nrf2 signaling of antioxidant defenses.* Biochem Biophys Res Commun, 2008. **368**(3): p. 620-4.
73. Alfieri, A., et al., *Targeting the Nrf2-Keap1 antioxidant defence pathway for neurovascular protection in stroke.* J Physiol, 2011.
74. Barone, M.C., G.P. Sykiotis, and D. Bohmann, *Genetic activation of Nrf2 signaling is sufficient to ameliorate neurodegenerative phenotypes in a Drosophila model of Parkinson's disease.* Dis Model Mech, 2011.
75. Muscarella, L.A., et al., *Frequent epigenetics inactivation of KEAP1 gene in non-small cell lung cancer.* Epigenetics, 2011. **6**(6): p. 710-9.
76. Reeves, M.A., F.P. Bellinger, and M.J. Berry, *The neuroprotective functions of selenoprotein M and its role in cytosolic calcium regulation.* Antioxid Redox Signal, 2010. **12**(7): p. 809-18.
77. Jurynec, M.J., et al., *Selenoprotein N is required for ryanodine receptor calcium release channel activity in human and zebrafish muscle.* Proc Natl Acad Sci U S A, 2008. **105**(34): p. 12485-90.
78. Verma, S., et al., *Selenoprotein K knockout mice exhibit deficient calcium flux in immune cells and impaired immune responses.* J Immunol, 2011. **186**(4): p. 2127-37.
79. Muller, M., et al., *Nrf2 target genes are induced under marginal selenium-deficiency.* Genes Nutr, 2010. **5**(4): p. 297-307.
80. Kerr, J.F., A.H. Wyllie, and A.R. Currie, *Apoptosis: a basic biological phenomenon with wide-ranging implications in tissue kinetics.* Br J Cancer, 1972. **26**(4): p. 239-57.
81. Aure, K., et al., *Apoptosis in mitochondrial myopathies is linked to mitochondrial proliferation.* Brain, 2006. **129**(Pt 5): p. 1249-59.
82. Dimauro, S. and P. Rustin, *A critical approach to the therapy of mitochondrial respiratory chain and oxidative phosphorylation diseases.* Biochim Biophys Acta, 2009. **1792**(12): p. 1159-67.
83. Zeviani, M., *Train, train, train! No pain, just gain.* Brain, 2008. **131**(Pt 11): p. 2809-11.
84. McFarland, R., R.W. Taylor, and D.M. Turnbull, *A neurological perspective on mitochondrial disease.* Lancet Neurol, 2010. **9**(8): p. 829-40.
85. Gilgun-Sherki, Y., E. Melamed, and D. Offen, *Oxidative stress induced-neurodegenerative diseases: the need for antioxidants that penetrate the blood brain barrier.* Neuropharmacology, 2001. **40**(8): p. 959-75.
86. Lekoubou, A., et al., *Effect of long-term oral treatment with L-arginine and idebenone on the prevention of stroke-like episodes in an adult MELAS patient.* Rev Neurol (Paris), 2011. **167**(11): p. 852-5.
87. Koga, Y., et al., *Molecular pathology of MELAS and l-arginine effects.* Biochim Biophys Acta, 2011.
88. Halter, J., et al., *Allogeneic hematopoietic SCT as treatment option for patients with mitochondrial neurogastrointestinal encephalomyopathy (MNGIE): a consensus conference proposal for a standardized approach.* Bone Marrow Transplant, 2011. **46**(3): p. 330-7.
89. Scholte, H.R., et al., *Riboflavin-responsive complex I deficiency.* Biochim Biophys Acta, 1995. **1271**(1): p. 75-83.
90. Haack, T.B., et al., *Exome sequencing identifies ACAD9 mutations as a cause of complex I deficiency.* Nat Genet, 2010. **42**(12): p. 1131-4.
91. Nouws, J., et al., *Acyl-CoA dehydrogenase 9 is required for the biogenesis of oxidative phosphorylation complex I.* Cell Metab, 2010. **12**(3): p. 283-94.
92. Chinnery, P., et al., *Treatment for mitochondrial disorders.* Cochrane Database Syst Rev, 2006(1): p. CD004426.

93. Horvath, R., G. Gorman, and P.F. Chinnery, *How can we treat mitochondrial encephalomyopathies? Approaches to therapy.* Neurotherapeutics, 2008. **5**(4): p. 558-68.
94. Craven, L., et al., *Pronuclear transfer in human embryos to prevent transmission of mitochondrial DNA disease.* Nature, 2010. **465**(7294): p. 82-5.
95. Poulton, J., et al., *Preventing transmission of maternally inherited mitochondrial DNA diseases.* BMJ, 2009. **338**: p. b94.
96. Jacobs, L.J., et al., *The transmission of OXPHOS disease and methods to prevent this.* Hum Reprod Update, 2006. **12**(2): p. 119-36.
97. Tachibana, M., et al., *Mitochondrial gene replacement in primate offspring and embryonic stem cells.* Nature, 2009. **461**(7262): p. 367-72.
98. Heindryckx, B., et al., *Embryo development after successful somatic cell nuclear transfer to in vitro matured human germinal vesicle oocytes.* Hum Reprod, 2007. **22**(7): p. 1982-90.
99. Bredenoord, A.L., G. Pennings, and G. de Wert, *Ooplasmic and nuclear transfer to prevent mitochondrial DNA disorders: conceptual and normative issues.* Hum Reprod Update, 2008. **14**(6): p. 669-78.
100. Smith, P.M., et al., *Strategies for treating disorders of the mitochondrial genome.* Biochim Biophys Acta, 2004. **1659**(2-3): p. 232-9.
101. Manfredi, G., et al., *Rescue of a deficiency in ATP synthesis by transfer of MTATP6, a mitochondrial DNA-encoded gene, to the nucleus.* Nat Genet, 2002. **30**(4): p. 394-9.
102. Bonnet, C., et al., *The optimized allotopic expression of ND1 or ND4 genes restores respiratory chain complex I activity in fibroblasts harboring mutations in these genes.* Biochim Biophys Acta, 2008. **1783**(10): p. 1707-17.
103. Kolesnikova, O.A., et al., *Nuclear DNA-encoded tRNAs targeted into mitochondria can rescue a mitochondrial DNA mutation associated with the MERRF syndrome in cultured human cells.* Hum Mol Genet, 2004. **13**(20): p. 2519-34.
104. Taylor, R.W., et al., *Selective inhibition of mutant human mitochondrial DNA replication in vitro by peptide nucleic acids.* Nat Genet, 1997. **15**(2): p. 212-5.
105. Smith, P.M. and R.N. Lightowlers, *Altering the balance between healthy and mutated mitochondrial DNA.* J Inherit Metab Dis, 2011. **34**(2): p. 309-13.

Summary

Mitochondrial disorders are often fatal multisystem disorders or syndromes, associated with abnormalities of the terminal component of mitochondrial energy metabolism, *i.e.* oxidative phosphorylation (OXPHOS). These diseases mainly manifest in tissues with high energy demands such as the heart, brain, liver and muscle and are further referred to as OXPHOS disorders. It is estimated that OXPHOS disorders affect about 1 in 5000 individuals. The OXPHOS system is responsible for cellular aerobic energy production and its subunits are encoded by over 80 genes of which 37 are located in the mitochondrial DNA (mtDNA). However, more than 1000 nuclear DNA (nDNA) genes are involved OXPHOS function, assembly and maintenance. Accordingly, mutations in the mtDNA or nDNA genes encoding structural OXPHOS elements or nDNA encoded factors involved in the maintenance or assembly often lead to OXPHOS disorders. The extreme genetic and phenotypic heterogeneity and the lack of consistent genotype-phenotype correlations complicate genetic testing of these disorders. Moreover, the underlying pathological mechanisms of these diseases are only partly understood and there is a lack of efficient therapies. The aim of this thesis is to create and evaluate models and approaches to facilitate diagnostics of mtDNA-based OXPHOS disorders, study OXPHOS pathophysiology and as a consequence identify new potential targets for therapeutic interventions. In that respect, mitochondrial DNA resequencing chips (**chapter 2**), microarray gene expression profiling (**chapter 3 and 4**) and a set of oxidative stress markers (**chapter 5**) have been applied to obtain new information on the distribution of mtDNA variation in the general population and pathological and/or adaptive processes involved in OXPHOS disease, respectively. **Chapter 6** discusses the validity and relevance of the different models for the study of OXPHOS disorders.

Evaluating pathogenicity of new unclassified variants identified in patients with symptoms related to OXPHOS disorders is not straightforward. Improved insight in the presence, tolerance, negative selection and consequences of mtDNA variation in the human population will give valuable information for the diagnostic classification of these mtDNA variants. In **chapter 2**, the mtDNA of 730 subjects was resequenced and compared with the revised reference sequence. The locations of non-pathogenic variants identified in this study and known pathogenic mtDNA mutations were evaluated in terms of functional importance and conservation. For the non-pathogenic variation, there was a preferential selection against variants in protein coding genes with high sequence conservation. Also for tRNA genes, neutral variants and pathogenic mutations showed differences in functional location (loop or stem) and sequence or base pair conservation. Thus, evaluating the conservation and functional importance of a newly identified variant remain the most important parameters. It can be expected that this approach combined with the data generated by next generation sequencing will lead to a detailed map of all variants ever detected, both for the mitochondrial and nuclear DNA.

When a genetic diagnosis for an OXPHOS disorder is established, the pathogenic process has to be unraveled in order to determine cause and mechanism of the disease symptoms for proper prognosis and to explore potential therapeutic strategies. For pathophysiological studies, affected tissues from patients would allow the most

relevant and specific disease processes to be identified. However, for diseases affecting non-dividing tissues (*e.g.* brain), the availability and amount of material is obviously limited. Therefore, model systems such as other patient derived tissues (*e.g.* muscle biopsies, fibroblasts) can be used. Even though these tissues might be less or not affected in OXPHOS patients, they can still provide clues for pathological processes in other affected tissues.

To identify new biomarkers or potential therapeutic targets, whole genome gene expression profiling and pathway analysis have been applied to explore the underlying molecular processes in patients with *POLG1* mutations and patients with complex I (CI) deficiency, the largest patient groups with mitochondrial disease. DNA polymerase gamma (pol γ; *POLG1* gene) is the only DNA polymerase involved in maintenance of the mtDNA. *POLG1* mutations have been reported to cause a broad variety of phenotypes involving hepatopathy usually early in life, isolated myopathy in older individuals or brain abnormalities at any age. The correlation between genotype and phenotype in patients with *POLG1* mutations is sometimes tight but more often variable. In **chapter 3**, skeletal muscle from patients with mutations in the *POLG1* gene was used as a model for pathological changes in liver and brain. The majority of these patients exhibited subtle morphological skeletal muscle changes and gene expression analysis mainly pointed to an energy metabolism switch (decreased beta oxidation, increased coupling of electron transfer and ATP production) and hinted towards changes in oxidative stress and apoptosis. The latter increased processes were further validated in fibroblast cultures, liver and brain and were shown to be increased in part of the patients. Ultimately, this study revealed the involvement of these processes in the pathology of at least part of human *POLG1* patients for the first time and emphasizes the previously described heterogeneity in this patient group, requesting an individual-based approach. In **chapter 4**, primary fibroblast cultures of CI deficient patients with a nuclear mutation were used as a model to study pathology. CI deficiency is the most frequently encountered defect in mitochondrial energy metabolism and is associated with *e.g.* Leigh and LHON disease, fatal infantile acidosis, neonatal cardiomyopathy with lactic acidosis, leucodystrophy with macrocephaly and hepatopathy with renal tubulopathy. Although children usually have a normal prenatal development, symptoms start occurring during their first year of life after which the disease deteriorates rapidly and may become fatal. Because fibroblasts primarily (~70%) produce ATP by glycolysis, fibroblasts were experimentally stimulated to use OXPHOS (and express the defect) by culturing them without glucose in the presence of galactose. Whole genome expression profiling showed that patient fibroblasts responded to oxidative stress by Nrf2-mediated induction of the glutathione antioxidant system and Gadd45-mediated activation of the DNA damage response pathway. Furthermore, the observed reduced expression of selenoproteins could explain the disturbed calcium homeostasis previously described for the patient fibroblasts and might be linked to endoplasmic reticulum stress. These results indicate that both glutathione and selenium metabolism are potentially therapeutic targets in CI deficiency.

Oxidative stress was observed in both the *POLG1* and CI deficiency models (**chapter 3** and **4**) and has been implicated to play a role in OXPHOS disorders in literature. However, most studies did not report on the full spectrum of ROS levels, ROS detoxification (antioxidant status) and oxidative damage. Nevertheless, OXPHOS patients are often supplemented with antioxidants, even though their efficacy is highly anecdotic. Therefore, a pipe-line for the characterization of ROS levels, stress induced (antioxidant) gene expression and oxidative protein damage in fibroblasts was established (**chapter 5**). Using this approach, the level of oxidative stress in fibroblasts of three different patient groups (*POLG1* patients and patients with mtDNA *tRNA-Leu* or CI mutations) was compared. Whereas almost all cell lines showed increased ROS levels compared with wild type fibroblasts, only few concomitantly exhibited increased oxidative protein damage. The absence of oxidative damage in the other cell lines could partially be explained by increased stress-related (antioxidant) gene expression. Even though fibroblasts are better able to adapt to a genetic or biochemical defect than severely affected post-mitotic tissues, the current study demonstrated the ability to measure altered ROS levels and oxidative damage in these cells. Therefore, the fibroblast model provides an indication for the oxidative status of a patient and information on which adaptive processes are therapeutically relevant. The characterized fibroblasts models in **chapter 4** and **5** can also be used for high-throughput screening of potentially beneficial compounds using the same read-out parameter, as used for establishing the pathophysiological processes.

In this thesis, models and methodologies have been developed for the improvement of diagnostics, prognostics, understanding and therapy of specific OXPHOS disorders, for which the genetic defect was known. Comparable models can be established for other OXPHOS disorders as well, applying the same methodologies. However, as discussed in **chapter 6**, no single model system can cover every aspect from the identification of pathological processes to the screening of therapeutic compounds. Our *in vitro* data based on patient material should be validated and followed-up in more advanced (animal) models before eventually translating them into patient care.

Samenvatting

Mitochondriële afwijkingen zijn vaak dodelijke afwijkingen of syndromen in meerdere organen die geassocieerd zijn met abnormaliteiten van de laatste component van het mitochondriële energiemetabolisme, oxidatieve fosforylering (OXPHOS). Deze ziekten treffen voornamelijk weefsels met een hoge energiebehoefte zoals het hart, de hersenen, de lever en spier. Dezen zullen verder OXPHOS ziekten genoemd worden. Naar schatting wordt 1 op 5000 individuen getroffen door een OXPHOS ziekte. Het OXPHOS systeem is verantwoordelijk voor de cellulaire aërobe energie productie en de afzonderlijke subeenheden worden door meer dan 80 genen gecodeerd waarvan er 37 gelegen zijn in het mitochondrieel DNA (mtDNA). Er zijn echter meer dan 1000 genen in het nucleaire DNA (nDNA) betrokken bij OXPHOS functie, assemblage en onderhoud. Daarom leiden mutaties in mtDNA of nDNA genen die coderen voor structurele OXPHOS elementen of in nDNA gecodeerde factoren betrokken bij OXPHOS onderhoud en de assemblage vaak tot OXPHOS ziekten. De extreme genetische en fenotypische heterogeniteit en het gebrek aan consistente genotype-fenotype correlaties maken het genetische testen van deze ziekten complex. Verder wordt het onderliggende pathologische mechanisme slechts gedeeltelijk begrepen en is er een gebrek aan efficiënte therapieën. Het doel van deze thesis is de creatie en evaluatie van modellen en strategieën om de diagnostiek van mtDNA-gebaseerde OXPHOS ziekten makkelijker te maken, de pathofysiologie van OXHPOS ziekten te bestuderen en bijgevolg nieuwe potentiële doelen voor therapie te identificeren. Daarom werden mtDNA *resequencing* chips (**hoofdstuk 2**), *microarray* genexpressie analyse (**hoofdstuk 3 en 4**) en een set van oxidatieve stress merkers (**hoofdstuk 5**) ingezet om nieuwe informatie te verkrijgen over de verdeling van mtDNA variatie in de normale populatie en over de pathologische en/of adaptieve processen betrokken bij OXPHOS ziekten. **Hoofdstuk 6** bediscussieert de validiteit en de relevantie van de verschillende modellen voor het bestuderen van OXPHOS ziekten.

De evaluatie van de pathogeniciteit van nieuwe ongeclassificeerde varianten in patiënten met symptomen gerelateerd aan OXPHOS ziekten is niet eenvoudig. Een verbeterd inzicht in de aanwezigheid van, de tolerantie van, negatieve selectie tegen en de gevolgen van mtDNA variatie in de menselijke populatie zal waardevolle informatie verschaffen voor de diagnostische classificatie van deze mtDNA varianten. In **hoofdstuk 2** werd het mtDNA van 730 individuen geanalyseerd en vergeleken met de gereviseerde referentiesequentie. De locatie van niet-pathogene varianten die geïdentificeerd werden in deze studie en bekende pathogene mutaties werd geëvalueerd met betrekking tot functioneel belang en conservering. Voor de niet-pathogene variatie was er een preferentiële selectie tegen varianten in eiwitcoderende genen met een sterke conservering. Ook voor de tRNA genen toonden de neutrale varianten en pathogene mutaties verschillen in functionele locatie (loop of stam) en sequentie of basenpaar conservering. Dus, de evaluatie van de conservering en het functionele effect van een nieuw geïdentificeerde variant blijven de meest belangrijke parameters. Verwacht wordt dat deze aanpak, in combinatie met de data van *next generation seqeuncing*, zal leiden tot een gedetailleerde kaart van alle varianten die ooit gedetecteerd werden, zowel voor het mitochondriële als het nucleaire DNA.

Wanneer er een genetische diagnose voor een OXPHOS ziekte is, moet het pathogene process nog ontrafeld worden om de oorzaak en het mechanisme dat leidt tot de symptomen te bepalen zodat de juiste prognose en het onderzoeken van mogelijke therapieën mogelijk is. Voor pathofysiologische studies, zouden de aangedane weefsels van patiënten toelaten de meest relevante en specifieke processen te identificeren. Echter, voor aandoeningen van niet-delende weefsels (bijvoorbeeld hersenen) is de beschikbaarheid en hoeveelheid van materiaal beperkt. Daarom kunnen modelsystemen zoals andere weefsels (bijvoorbeeld spierbiopsies, fibroblasten) van de patiënten gebruikt worden. Hoewel deze weefsels minder of niet aangedaan kunnen zijn in OXPHOS patiënten, kunnen ze nog steeds aanwijzingen voor pathologische processen in andere aangedane weefsels opleveren.

Genexpressie-analyse van het volledige genoom en process-gebaseerde analyse werden toegepast om de onderliggende moleculaire processen in patiënten met *POLG1* mutaties en patiënten met complex I (CI) deficiëntie te bestuderen en mogelijk nieuwe biomerkers of potentiële therapeutische doelwitten te identificeren. DNA polymerase gamma (pol γ; *POLG1* gen) is het enige DNA polymerase dat betrokken is bij het onderhoud van het mtDNA. *POLG1* mutaties veroorzaken een brede waaier aan fenotypes inclusief hepatopathie op jonge leeftijd, geïsoleerde myopathie in oudere individuen en hersenafwijkingen op elke leeftijd. De correlatie tussen genotype en fenotype in patiënten met *POLG1* mutaties is soms eenduidig maar meestal variabel. In **hoofdstuk 3** werd skeletspier van patiënten met mutaties in het *POLG1* gen gebruikt als model voor pathologische veranderingen in lever en hersenen. De meerderheid van deze patiënten hadden subtiele morfologische skeletspier veranderingen. Genexpressie-analyse wees voornamelijk op een omschakeling van het energie metabolisme (vermindere beta oxidatie, versterkte koppeling van elektronentransport en ATP productie) en suggereerde veranderingen in oxidatieve stress en apoptose. Deze laatste processen werden verder gevalideerd in fibroblastkweken, lever en hersenen en bleken verhoogd te zijn in een gedeelte van de patiënten. Uiteindelijk heeft deze studie voor het eerst aangetoond dat deze processen betrokken zijn bij de pathologie van minstens een gedeelte van de humane *POLG1* patiënten. Voorts wordt de eerder beschreven heterogeniteit van deze patiëntengroep en de nood aan een individuele aanpak nogmaals benadrukt.
In **hoofdstuk 4** werden primaire fibroblast kweken van CI deficiënte patiënten met een nucleaire mutatie gebruikt als model om CI pathologie te bestuderen. CI deficiëntie is het meeste frequente defect in mitochondrieel energie metabolisme en is geassocieerd met bvb. Leigh en LHON ziekte, fatale infantiele acidose, neonatale cardiomyopathie met lactaat acidose, leukodystrofie met macrocefalie en hepatopathie met renale tubulopathie. Hoewel kinderen meestal een normale prenate ontwikkeling doormaken, beginnen de eerste symptomen te verschijnen tijdens hun eerste levensjaar waarna de ziekte snel verergert en tot overlijden kan leiden. Omdat fibroblasten voornamelijk (~70%) ATP produceren via glycolyse, werden de fibroblasten experimenteel gestimuleerd om OXPHOS te gebuiken (en het defect tot expressie te brengen) door hen te kweken zonder glucose in aanwezigheid van galactose. Genexpressie-analyse van het volledige genoom toonde aan dat patiëntfibroblasten op oxidatieve stress

reageerden door Nrf2-gemedieerde inductie van het glutathion antioxidant systeem en Gadd45-gemedieerde activatie van de DNA schade respons. Verder kan de geobserveerde verminderde expressie van seleno-eiwitten de eerder beschreven verstoorde calcium homeostase in deze patiënten fibroblasten verklaren en kan dit ook gelinkt zijn aan endoplasmatisch reticulum stress. Deze resultaten tonen aan dat zowel glutathion als selenium metabolisme potentiële therapeutische kandidaten zijn bij CI deficiëntie.
Oxidatieve stress werd in beide (*POLG1* en CI deficiëntie) modellen geobserveerd en wordt ook in de literatuur genoemd als een speler in OXPHOS ziekten. De meeste studies rapporteerden echter niet over het volledige spectrum van reactieve zuurstof soorten (ROS) niveaus, ROS detoxificatie (antioxidant status) en oxidatieve schade. Desalniettemin krijgen OXPHOS patiënten vaak antioxidant supplementen, ook al is hun efficiëntie sterk anecdotisch. Daarom werd een pijplijn opgezet voor de characterisatie van ROS niveaus, stress geïnduceerde (antioxidant) genexpressie en oxidatieve eiwit schade in fibroblasten (**hoofdstuk 5**). Met deze aanpak werd de mate van oxidatieve stress in fibroblasten van drie verschillende patiënten groepen (*POLG1* patiënten en patiënten met mtDNA *tRNA-Leu* of CI mutaties) vergeleken. Hoewel bijna alle cellijnen verhoogde ROS niveaus vertoonden vergeleken met controle fibroblasten, waren er slechts enkele met verhoogde oxidatieve eiwitschade. De afwezigheid van oxidatieve schade in de andere cellijnen kon gedeeltelijk verklaard worden door verhoogde stress-gerelateerde (antioxidant) genexpressie. Ook al zijn fibroblasten beter in staat om zich aan te passen aan een genetisch of biochemisch defect dan ernstig aangedane post-mitotische weefsel, de huidige studie laat zien dat het mogelijk is verhoogde ROS niveaus en oxidatieve schade in de cellen te meten. Daarom geeft het fibroblast model een indicatie voor de oxidatieve status van een patiënt en tevens ook informatie over welke adaptieve processen mogelijk van therapeutisch belang kunnen zijn. De gekarakteriseerde fibroblastmodellen in **hoofdstuk 4 en 5** kunnen voorts ook gebruikt worden voor het *high throughput* screenen van potentiële therapeutische stoffen, gebruik makend van dezelfde uitleesparameters als voor de studie van de pathofysiologische processen.

In deze thesis werden modellen en methods ontwikkeld voor de verbetering van diagnose, prognose, het begrip en de therapie van specifieke OXPHOS ziekten waarvoor het genetisch defect gekend was. Vergelijkbare modellen kunnen ook opgezet worden andere OXPHOS ziekten. Echter, zoals aangehaald in **hoofdstuk 6**, zal geen enkel modelsysteem in staat zijn om elk aspect, van de identificatie van de pathologische processen tot de screening van therapeutische stoffen, te omvatten. Onze *in vitro* data, gebaseerd op patiëntenmateriaal, moet daarom ook gevalideerd en opgevolgd worden in meer geavanceerde (dier)modellen voordat ze vertaald kan worden naar patiëntenzorg.

Dankwoord

Is het dan eindelijk zover? Ik kan het bijna niet geloven... mijn boekje is klaar! En dat na 5 jaar die parodoxaal soms traag en soms snel leken om te vliegen. Natuurlijk werd ik gedurende deze tijd bijgestaan, geholpen, vermaakt... door een hele hoop mensen die ik hieronder wat uitgebreider wil bedanken. Ik zal me voor het grotendeels Nederlandse publiek alvast verontschuldigen voor de Vlaamse termen die hieronder wel eens de revue zouden kunnen passeren en andersom natuurlijk ook ☺.

Eerst en vooral wil ik Bert bedanken. Simpelweg, zonder jou zou dit boekje er niet zijn. Dank je dat je me de kans gegeven hebt om deze ervaringen op te doen. Als mijn promotor, en tevens enige begeleider, zorgde je ervoor dat ik de rode draad in het verhaal niet kwijt raakte. Op momenten dat ik wel eens minder gemotiveerd was, wist je toch weer de juiste dingen te zeggen. Van jou heb ik verder geleerd dat je in Nederland een mail begint met 'Beste' en eindigt met 'Groeten' (wat in jouw mails – zelfs héle korte – zelden tot nooit ontbreekt) in plaats van het Vlaamse 'Geachte' en 'Met vriendelijke groet'. Ik vond het ook heel fijn dat ik over alles open met je kon praten, zowel de leuke als de minder leuke dingen.
Volgende in rij is René. Dankjewel dat je mijn co-promotor wilde zijn. Ondanks dat Rotterdam en Maastricht ver van elkaar liggen, stond je altijd klaar om te helpen als dat mogelijk was. Ik vergeet nooit dat je ons (Auke, jij en ik) als 1 groep, met jou in Rotterdam en Auke en ik in Maastricht, voorstelde aan anderen tijdens een symposium in Nijmegen. Dat geeft wel aan dat de RoMa-mensen een clubje vormen van onderzoekers die graag samenwerken.

In Rotterdam zijn er nog meer mensen die ik graag zou willen bedanken: Kees, Rob en Wim. Kees, bedankt voor de vele OXPHOS activiteit metingen en dat je me hebt ingewijd in de wondere wereld van de biochemie. Rob, jou ken ik het kortst in Rotterdam, maar jouw bijdrage aan het POLG verhaal heeft het echt naar een hoger niveau gebracht. En Wim, jammer dat we elkaar al een tijd niet meer gezien hebben, maar dankjewel voor mijn eerste ervaring met ROS-kleuringen!

Naast Rotterdam en Maastricht heb ik nog een andere stad in Nederland ontdekt: Nijmegen. Jan, Be, Merei, Richard, Peter, Werner, John en alle anderen van het IOP Genomics project: dank jullie voor de leuke samenwerking! Ik heb echt genoten van de halfjaarlijkse projectmeetings en de discussies die daar plaatsvonden (ook al moesten we vanuit Maastricht soms wel héél vroeg vertrekken s'ochtends). Merei en Richard, ik denk dat het toch nog een mooi verhaal geworden is, niet? De moeite van de vele uren celkweek wel waard. Peter, Werner en John, bedankt voor het helpen met de ROS-metingen en de hartelijke ontvangst voor de paar weken die ik bij jullie in het lab heb doorgebracht.

Hoog tijd om even dichter bij huis te komen. De paranimfen: Florence, als voorganger heb ik veel van je geleerd, niet enkel wijsheden over het hele AIO-traject/gebeuren maar ook dagdagelijkse gebeurtenissen kwamen op de AIO-kamer vaak aan bod. Na een half jaartje afwezigheid, was ik blij dat je er toch weer terug bent zodat ik je kon lastig vallen met al mijn vragen over promotie/verdediging/paperassen. Maar uiteraard

vind ik het gewoon ook leuk om die gelijkgestemde ziel weer in de buurt te hebben! Zullen we eens een keertje gaan dansen? ☺ Gonda, ik heb iedere keer genoten van onze reisjes, terrasjes, filmpjes... Hopelijk hebben we binnenkort weer terug wat meer tijd om wat vaker af te spreken (met 2 of met 4 aan tafel ;))! Ook jij heel veel succes met je promotietraject. Dank jullie wel dat jullie mijn paranimfen wilden zijn!

De andere (oud)-AIO's/postdocs: Nicole, jij weet als geen ander dat je met mij geen grapjes moet uithalen want voordat je het weet ben je carnavalsprinses bij Klinische Genetica ☺; Bianca, jij zorgde ervoor dat ik snel ingewerkt was in het mito/POLG-wereldje; Lars, Mr. MSN-afkortingen, net gemist op de kamer maar dat betekent niet dat we geen leuke carnaval en pinkpop momenten hebben beleefd; Rudy, heeft mijn Vlaamse invloed je wat kunnen voorbereiden op je baan in Leuven?; Ruben, Mr. Parafilm-fetisj en 'Harry Potter with the magic wand', I will keep the pussies, you can stick with the balls ☺; Rita, I'm glad everything returned to normal in the end, good luck finishing your thesis; Mike, Mr. Ochtendhumeur, hopelijk geraak je nog een keertje in de Alpen, de vakantie was (afgezien van die gips) echt super, succes in Finland!; Auke, Mr. Ochtendhumeur 2, als ik nu van voetbal zou houden, was ik altijd up-to-date met jou op de kamer... maar ik hou niet van voetbal!!! ☺; Abhishek, you were here only shortly but I learned a lot about the Indian way of life, for example... Indian people can appreciate a joke or two (hundred) ☺; Minh, you only started your PhD training recently, good luck and enjoy life in the Netherlands! With lots of spring rolls and Vietnamese noodles ☺. Allemaal heel erg bedankt! Ze zeggen wel eens, gedeelde smart is halve smart en gedeelde vreugde is dubbele vreugde.

Niet te vergeten zijn natuurlijk alle andere mensen van de afdeling, zowel in UNS50 als in het 3X/Noordgebouw. Rosy, bedankt voor het regelen van allerlei afspraken, papierwerk enzovoort; Patrick, thanks for all the analyses, I know they were not always straight-forward; Fons, zonder jouw hulp met de SeqC data was ik nu waarschijnlijk nog altijd aan het tellen, dankjewel!; Bieke, Erika en Rik, bedankt voor de hulp bij de experimenten en labdingen in het algemeen; Torik, Roselie, Wanwisa, Ellen, Iris, Frank, Barbie, Bart, Jo, Jos, Marion, Sabine, Miroslav, Rob, Ton en Marij, ik zal de afgelopen jaren wel minstens een keer om hulp gevraagd hebben, dank je voor jullie tijd. Robin en Kelly, ik vond het heel leuk om jullie als stagiaires te (mogen) begeleiden. Bedankt voor jullie inzet en veel succes met jullie verdere loopbaan!
Alexandra, ik denk dat ik jouw nummer wel het meest van allemaal heb ingetoetst. Voor mijn gevoel wist jij gewoon bijna altijd alle antwoorden op mijn vragen. Heel erg bedankt! Chantal, Eveline en Debby, jullie horen eveneens tot het mito-clubje en konden ook wel eens door mij gespamd worden. Bedankt voor alle hulp!

Eigenlijk is het al een tijdje geleden dat ik mijn echte AIO-periode heb afgesloten. Daarom wil ik toch nog even alle 'nieuwe' collega's bij Clinical Genomics en Maastro Lab/Clinic willen bedanken voor hun hulp, kennis, collegialiteit en de kansen die ze mij de afgelopen maanden gegeven hebben.
Alle andere co-auteurs die ik nog niet vermeld heb of mensen die ik onbewust vergeten ben: heel erg bedankt, thanks a lot, merci beaucoup!

De afgelopen jaren draaiden natuurlijk niet enkel om werk. Op de universiteit waren er de koffie pauzes. Antoine, jij bent een aantal jaar mijn koffiemaatje geweest, het zullen inderdaad wel ettelijke liters geweest zijn alles tesamen. Veel succes met je opleiding en niet te vergeten je onmiskenbare observatievermogen, vooral voor vrouwelijk schoon ☺ Maar eerlijk gezegd, zonder Papendal had ik je misschien nooit leren kennen. Aanbeland in het Arnhemse zou ik toch ook nog de andere mensen willen bedanken die die 3 weekjes (over)leefbaar gemaakt hebben: kamergenootjes Hilde en Jelly, Kris, Anneleen en Bart, Olivier, en alle anderen... bedankt voor de leuke avonden! Erik, ook jij bedankt voor de leuke BBQ's, PhD parties, borrels...
Ik heb verder het privilege gehad om ondergedompeld te worden in de karatewereld. Sensei Peter (R.I.P.), sensei Ramon en sensei Tamara, ik heb ZO veel van jullie geleerd, karate is zoveel meer dan enkel een gevechtssport, het is een manier van leven. Jullie club voelt aan als een hele hechte groep vrienden, bijna als een familie. Jullie hadden precies in de gaten wanneer ik even een dipje had en konden dan precies de juiste woorden gebruiken om dat weer te overwinnen (ja, motiveren en oppeppen is een van jullie sterke punten). Samen met alle andere karateka, waaronder Charlotte, Irene, Samefko, Vasken... dank jullie wel voor de hele leuke tijd!
Naast de karateclub was er nog een ander clubje dat ik niet mag vergeten. Meisjes die elkaar kennen van de universiteit. Maar kleine meisjes worden groot! Ann, Kim, Katrien en Greet, ik vond het echt leuk dat we zijn blijven afspreken, dank jullie voor de gezellige momenten. Ook al is het de laatste tijd wat minder geweest door omstandigheden, we moeten dit zeker in ere houden!
Ine, een zoveelste prettig gestoorde Belg in Maastricht. Ach ja, gek zijn doet geen pijn he ☺ Het klikte meteen tussen ons en woorden waren vaak niet nodig om duidelijk te maken wat we bedoelden. Ook al woon je nu in Washington, ik hoop dat we regelmatig contact zullen blijven houden. Dankjewel voor de leuke tijd!
Lisanne en Dennis: het is echt wel gezellig dat we van het nieuwjaarsetentje een (twee) maandelijks evenement hebben kunnen maken. Dank jullie voor de gekke toestanden en niet-voor-publicatie foto's!

Er zijn twee mensen zonder wie dit hele verhaal niet mogelijk was geweest: mama en papa. Bedankt dat jullie me de kans gegeven hebben om te gaan studeren en erna nog even te blijven plakken totdat ik op mijn eigen benen kon staan. Ook al begrijpen jullie waarschijnlijk niet veel van wat er in dit boekje allemaal staat, ik ben jullie heel erg dankbaar voor alle wijsheid die jullie mij tot nog toe hebben bijgebracht en alle steun die ik aan jullie gehad heb. Hopelijk zijn jullie even trots op mij als ik ben op jullie! Ben, grote kleine broer, ook al kwamen we niet altijd even goed overeen, ik weet dat ik toch altijd bij je terecht kon/kan als dat nodig was/is.

Als laatste maar zeker niet de minste, Ben(jamin), je hebt me leren kennen in een (voor mij) nogal stressvolle periode waarin ik waarschijnlijk niet altijd even veel tijd voor je had. Dankjewel voor je geduld en je steun! Nu meer tijd voor ons.

An

Curriculum vitae

List of publications

Curriculum Vitae

An Mieke Voets werd geboren op 8 juni 1984 te Bilzen. Van 1996 tot 2002 doorliep zij het Algemeen Secundair Onderwijs (ASO) aan de Onze Lieve Vrouwe Humaniora te Tongeren. Na het behalen van haar middelbare school diploma in de richting Wetenschappen-Wiskunde in 2002, startte ze datzelfde jaar met de Bacheloropleiding Biomedische Wetenschappen aan de Universiteit Hasselt/transnationale Universiteit Limburg. In 2005 liep ze korte stages bij het Biomedisch Onderzoeksinstituut van de Universiteit Hasselt en de afdeling Gezondheidsrisicoanalyse en Toxicologie van de Universiteit Maastricht en behaalde ze haar Bachelor diploma met grote onderscheiding. Gedurende het volgende jaar volgde ze de Masteropleiding Biomedische Wetenschappen aan de Universiteit Hasselt/transnationale Universiteit Limburg. Haar afstudeerstage bij het Biomedisch Onderzoeksinstituut situeerde zich rond het identificeren van nieuwe diagnostische merkers voor Multiple Sclerose en leidde tot het behalen van het Master diploma Biomedische Wetenschappen met onderscheiding in 2006. Geprikkeld door moleculaire levenswettenschappen, met name genetica, en met de wil onderzoekservaring op te doen, startte ze haar promotietraject aan de Universiteit Maastricht bij de afdeling Clinical Genomics (voormalig Populatiegenetica), verbonden aan de Cardiovascular Research School CARIM. Het promotieonderzoek was gericht op genetische mitochondriële aandoeningen met het doel modellen te creëren ter bestudering van de pathofysiologie van deze aandoeningen en/of ter evaluatie van kandidaat therapeutische stoffen. Tijdens deze periode heeft ze tevens meerdere cursussen gevolgd ter behaling van o.a. het CARIM certificaat voor promovendi en deskundigheidsniveau 5b voor stralingshygiëne. Sinds het voorjaar 2011 is zij betrokken bij een gezamelijke studie van de afdeling Klinische Genetica en Maastro Lab/Clinic die de link tussen mitochondria/mitochondrieel DNA en stralingsgevoeligheid moet verduidelijken. Vanaf september 2011 combineerde zij dit onderzoek met DNA-diagnostiek van erfelijke (borst)kanker.

Publications

Bonneux S, Fransen E, Van Eyken E, Van Laer L, Huyghe J, Van de Heyning P, Voets A, Gerards M, Stassen AP, Hendrickx AT, Smeets HJ, Van Camp G. Inherited mitochondrial variants are not a major cause of age-related hearing impairment in the European population. *Mitochondrion 2011; 11:729-734.*

Voets AM, van den Bosch BJC, Stassen AP, Hendrickx AT, Hellebrekers DM, Van Laer L, Van Eycken E, Van Camp G, Pyle A, Baudouin SV, Chinnery PF, Smeets HJM. Large scale mtDNA sequencing reveals sequence and functional conservation as major determinants of homoplasmic mtDNA variant distribution. *Mitochondrion 2011; 11: 964-972.*

Voets AM, Huigsloot M, Lindsey PJ, Leenders AM, Rodenburg RJ, Koopman WJ, Willems PH, Smeitink JA, Smeets HJ. Transcriptional changes in OXPHOS complex I deficiency are related to antioxidant pathways and could explain the disturbed calcium homeostasis. *In press, BBA – Molecular basis of disease*.

Voets AM, van den Bosch BJC, Lindsey PJ, Verdijk R, Verheyen F, Vanherle SJ, Schoonderwoerd GC, de Die-Smulders CE, Poll-The BT, de Visser M, Faber CG, de Coo IFM, Smeets HJM. *POLG1* defects lead to mitochondrial muscle abnormalities, oxidative stress in fibroblasts and apoptosis in brain and liver. *Submitted.*

Voets AM, Esseling JJ, Lindsey PJ, Schoonderwoerd GC, Godschalk RW, Koopman W, Willems P, de Coo IFM, Smeets HJM. Patient-derived fibroblasts indicate oxidative stress status and may justify antioxidant therapy in OXPHOS disorders. *Submitted*.

Voets AM, Dehing-Oberije C, Struijk RB, De Ruyck K, Thierens H, Vandecasteele K, De Neve W, De Ruysscher D, Smeets HJM, Lambin P. No association between TGF-β1 polymorphisms and radiation-induced lung toxicity in a European cohort of lung cancer patients. *Submitted*.

Abstracts

Voets AM, van den Bosch BJC, Blok MJ, de Coo IFM, Smeets HJM. Mutations in the polymerase gamma 1 gene negatively influence energy production and lead to compensatory mechanisms in human and mouse.
Poster presentation VLAG Nutrigenomics Master Class 2007, Wageningen, NL
Poster presentation NHS PhD training course 2007, Papendal, NL
Oral presentation Genetica Retraite 2008, Rolduc Kerkrade, NL

Voets AM, van den Bosch BJC, de Coo IFM, Smeets HJM. Pathophysiological processes involved in mitochondrial disorders and ageing.
Poster presentation NHS PhD training course 2008, Papendal, NL

Voets AM, Cleutjens JP, Lindsey PL, de Coo IFM, Smeets HJM. Oxidative stress in OXPHOS disorders depends on the genetic defect.
Poster presentation NHS PhD training course 2009, Papendal, NL
Poster presentation FEBS advanced lecture course 2009, Antalya, TR

Voets AM, Otten ABC, van den Bosch BJC, van Eijsden RGE, Lindsey P, Winandy M, de Coo IFM, Smeets HJM. Human and zebrafish models to study cardiac mitochondrial disease from cause to treatment.
Poster presentation CARIM external cluster review, Maastricht, NL
Poster presentation CARIM symposium 2010, Maastricht, NL

Abbreviations

ADP	adenosine di-phosphate
AIC	Akaike information criterion
ATP	adenosine tri-phosphate
CAT	catalase
CI	complex I
COX	cytochrome C oxidase
D-loop	displacement loop
DNA	deoxyribonucleic acid
EM	electron microscopy
ETC	electron transport chain
FAD^+/FADH2	flavin adenine dinucleotide
GSEQ	Genechip Sequence Analysis Software (Affymetrix)
H_2O_2	hydrogen peroxide
IHC	immunohistochemistry
KSS	Kearns Sayre syndrome
LHON	Leber hereditery optic neuropathy
LS	Leigh syndrome
MDS	mitochondrial depletion syndrome
MELAS	mitochondrial encephalomyopathy, lactic acidosis and stroke-like episodes
MERRF	myoclonus epilepsy with ragged red fibers
MNGIE	mitochondrial neurogastrointestinal encephalomyopathy
mRNA	messenger ribonucleic acid
mtDNA	mitochondrial DNA
NAD^+/NADH	nicotinamide adenine dinucleotide
NARP	neuropathy, ataxia and retinitis pigmentosa
nDNA	nuclear DNA
$O_2^{\cdot\cdot}$	superoxide
$OH^{\cdot}$	hydroxyl radical
OXPHOS	oxidative phosphorylation
PEO	progressive external ophtalmoplegia
Pol γ	polymerase gamma
QPCR	quantitative polymerase chain reaction
rCRS	revised Cambridge Reference Sequence
ROS	reactive oxygen species
RRF	ragged red fibers
rRNA	ribosomal ribonucleic acid
SDH	succinate dehydrogenase
SeqC	Sequence Pilot – module C (JSI)
SOD	superoxide dismutase
tRNA	transfer ribosomal ribonucleic acid
VPA	valproic acid
WC	Watson-Crick

Appendix

Supplementary table 3.1. Significantly differentially expressed genes in muscle of *POLG1* patients.

Ensemble ID	fc	GeneSymbol	Description
ENSG00000130600	0.37	H19	H19, imprinted maternally expressed transcript (non-protein coding)
ENSG00000165312	0.42	OTUD1	OTU domain containing 1
ENSG00000175567	0.45	UCP2	Uncoupling protein 2 (mitochondrial, proton carrier)
ENSG00000124588	0.49	NQO2	NAD(P)H dehydrogenase, quinone 2
ENSG00000129250	0.49	KIF1C	Kinesin family member 1C
ENSG00000169047	0.53	IRS1	Insulin receptor substrate 1
ENSG00000198925	0.56	ATG9A	ATG9 autophagy related 9 homolog A (S. cerevisiae)
ENSG00000204574	0.56	ABCF1	ATP-binding cassette, sub-family F (GCN20), member 1
ENSG00000177731	0.56	FLII	Flightless I homolog (Drosophila)
ENSG00000133454	0.56	MYO18B	Myosin XVIIIB
ENSG00000120709	0.56	FAM53C	Family with sequence similarity 53, member C
ENSG00000197905	0.56	TEAD4	TEA domain family member 4
ENSG00000114999	0.57	TTL	Tubulin tyrosine ligase
ENSG00000108823	0.57	SGCA	Sarcoglycan, alpha (50kDa dystrophin-associated glycoprotein)
ENSG00000103264	0.57	FBXO31	F-box protein 31
ENSG00000144868	0.58	TMEM108	Transmembrane protein 108
ENSG00000164068	0.58	RNF123	Ring finger protein 123
ENSG00000079999	0.58	KEAP1	Kelch-like ECH-associated protein 1
ENSG00000204463	0.59	BAT3	HLA-B associated transcript 3
ENSG00000089693	0.59	MLF2	Myeloid leukemia factor 2
ENSG00000143321	0.60	HDGF	Hepatoma-derived growth factor (high-mobility group protein 1-like)
ENSG00000148229	0.60	POLE3	Polymerase (DNA directed), epsilon 3 (p17 subunit)
ENSG00000106070	0.60	GRB10	Growth factor receptor-bound protein 10
ENSG00000034152	0.60	MAP2K3	Mitogen-activated protein kinase kinase 3
ENSG00000123700	0.61	KCNJ2	Potassium inwardly-rectifying channel, subfamily J, member 2
ENSG00000156804	0.61	FBXO32	F-box protein 32
ENSG00000102935	0.61	ZNF423	Zinc finger protein 423
ENSG00000129245	0.62	FXR2	Fragile X mental retardation, autosomal homolog 2
ENSG00000134644	0.62	PUM1	Pumilio homolog 1 (Drosophila)
ENSG00000141965	0.62	FEM1A	Fem-1 homolog a (C. elegans)
ENSG00000182446	0.62	NPLOC4	Nuclear protein localization 4 homolog (S. cerevisiae)
ENSG00000111046	0.63	MYF6	Myogenic factor 6 (herculin)
ENSG00000165916	0.63	PSMC3	Proteasome (prosome, macropain) 26S subunit, ATPase, 3
ENSG00000197746	0.63	PSAP	Prosaposin
ENSG00000087191	0.63	PSMC5	Proteasome (prosome, macropain) 26S subunit, ATPase, 5
ENSG00000186350	0.63	RXRA	Retinoid X receptor, alpha
ENSG00000103994	0.63	ZFP106	Zinc finger protein 106 homolog (mouse)
ENSG00000189091	0.63	SF3B3	Splicing factor 3b, subunit 3, 130kDa
ENSG00000136247	0.63	ZDHHC4	Zinc finger, DHHC-type containing 4

Ensemble ID	fc	GeneSymbol	Description
ENSG00000111276	0.63	CDKN1B	Cyclin-dependent kinase inhibitor 1B (p27, Kip1)
ENSG00000112245	0.64	PTP4A1	Protein tyrosine phosphatase type IVA, member 1
ENSG00000102572	0.64	STK24	Serine/threonine kinase 24 (STE20 homolog, yeast)
ENSG00000092607	0.64	TBX15	T-box 15
ENSG00000122971	0.64	ACADS	Acyl-Coenzyme A dehydrogenase, C-2 to C-3 short chain
ENSG00000130749	0.64	CS007_HUMAN	Zinc finger CCCH domain-containing protein C19orf7
ENSG00000182108	0.64	MYLE_HUMAN	Protein MYLE (Dexamethasone-induced protein)
ENSG00000165795	0.65	NDRG2	NDRG family member 2
ENSG00000107829	0.65	FBXW4	F-box and WD repeat domain containing 4
ENSG00000036448	0.65	MYOM2	Myomesin (M-protein) 2, 165kDa
ENSG00000119242	0.65	CCDC92	Coiled-coil domain containing 92
ENSG00000145901	0.65	TNIP1	TNFAIP3 interacting protein 1
ENSG00000198954	0.66	KIAA1279	KIAA1279
ENSG00000179364	0.66	PACS2	Phosphofurin acidic cluster sorting protein 2
ENSG00000144579	0.66	CTDSP1	CTD (carboxy-terminal domain, RNA polymerase II, polypeptide A) small phosphatase 1
ENSG00000125827	0.66	TXNDC13	Thioredoxin domain-containing protein 13 precursor
ENSG00000143761	0.66	ARF1	ADP-ribosylation factor 1
ENSG00000134590	0.66	FAM127A	Family with sequence similarity 127, member A
ENSG00000107372	0.66	ZFAND5	Zinc finger, AN1-type domain 5
ENSG00000171497	0.66	PPID	Peptidylprolyl isomerase D
ENSG00000159692	0.67	CTBP1	C-terminal binding protein 1
ENSG00000138668	0.67	HNRPD	Heterogeneous nuclear ribonucleoprotein D0
ENSG00000169564	0.67	PCBP1	Poly(rC) binding protein 1
ENSG00000095139	0.67	ARCN1	Archain 1
ENSG00000084463	0.67	WBP11	WW domain binding protein 11
ENSG00000107959	0.67	PITRM1	Pitrilysin metallopeptidase 1
ENSG00000115677	0.67	HDLBP	High density lipoprotein binding protein
ENSG00000099942	0.67	CRKL	Crk-like protein
ENSG00000168575	0.67	SLC20A2	Solute carrier family 20 (phosphate transporter), member 2
ENSG00000173545	0.67	ZNF622	Zinc finger protein 622
ENSG00000100714	0.67	MTHFD1	Methylenetetrahydrofolate dehydrogenase (NADP+ dependent) 1, methenyltetrahydrofolate cyclohydrolase, formyltetrahydrofolate synthetase
ENSG00000101400	0.67	SNTA1	Syntrophin, alpha 1 (dystrophin-associated protein A1, 59kDa, acidic component)
ENSG00000123815	0.67	ADCK4	AarF domain containing kinase 4
ENSG00000159720	0.67	ATP6V0D1	ATPase, H+ transporting, lysosomal 38kDa, V0 subunit d1
ENSG00000122884	0.67	P4HA1	Prolyl 4-hydroxylase, alpha polypeptide I
ENSG00000130957	0.67	FBP2	Fructose-1,6-bisphosphatase 2
ENSG00000182533	0.67	CAV3	Caveolin 3
ENSG00000185052	0.68	SLC24A3	Solute carrier family 24 (sodium/potassium/calcium exchanger), member 3
ENSG00000078804	0.68	TP53INP2	Tumor protein p53 inducible nuclear protein 2
ENSG00000160094	0.68	ZNF362	Zinc finger protein 362
ENSG00000065675	0.68	PRKCQ	Protein kinase C, theta

Ensemble ID	fc	GeneSymbol	Description
ENSG00000096384	0.68	HSP90AB1	Heat shock protein 90kDa alpha (cytosolic), class B member 1
ENSG00000104341	0.68	LAPTM4B	Lysosomal protein transmembrane 4 beta
ENSG00000197043	0.68	ANXA6	Annexin A6
ENSG00000204310	0.68	AGPAT1	1-acylglycerol-3-phosphate O-acyltransferase 1 (lysophosphatidic acid acyltransferase, alpha)
ENSG00000004142	0.68	POLDIP2	Polymerase (DNA-directed), delta interacting protein 2
ENSG00000015676	0.68	NUDCD3	NudC domain containing 3
ENSG00000082641	0.68	NFE2L1	Nuclear factor (erythroid-derived 2)-like 1
ENSG00000103319	0.68	EEF2K	Eukaryotic elongation factor-2 kinase
ENSG00000065060	0.68	C6orf107	UHRF1-binding protein 1
ENSG00000107140	0.68	TESK1	Testis-specific kinase 1
ENSG00000188636	0.69	LDOC1L	Leucine zipper, down-regulated in cancer 1-like
ENSG00000102974	0.69	CTCF	CCCTC-binding factor (zinc finger protein)
ENSG00000164062	0.69	APEH	N-acylaminoacyl-peptide hydrolase
ENSG00000197321	0.69	SVIL	Supervillin
ENSG00000130764	0.69	LRRC47	Leucine rich repeat containing 47
ENSG00000167182	0.69	SP2	Sp2 transcription factor
ENSG00000174243	0.69	DDX23	DEAD (Asp-Glu-Ala-Asp) box polypeptide 23
ENSG00000177728	0.69	KIAA0195	KIAA0195
ENSG00000007314	0.69	SCN4A	Sodium channel, voltage-gated, type IV, alpha subunit
ENSG00000185909	0.69	KLHDC8B	Kelch domain containing 8B
ENSG00000159346	0.69	ADIPOR1	Adiponectin receptor 1
ENSG00000109775	0.69	C4orf20	CDNA FLJ11200 fis, clone PLACE1007725
ENSG00000125304	0.69	TM9SF2	Transmembrane 9 superfamily member 2
ENSG00000108639	0.69	SYNGR2	Synaptogyrin 2
ENSG00000078618	0.69	NRD1	Nardilysin (N-arginine dibasic convertase)
ENSG00000111481	0.69	COPZ1	Coatomer protein complex, subunit zeta 1
ENSG00000113141	0.69	IK	IK cytokine, down-regulator of HLA II
ENSG00000114853	0.69	ZBTB47	Zinc finger and BTB domain containing 47
ENSG00000103502	0.69	CDIPT	CDP-diacylglycerol--inositol 3-phosphatidyltransferase (phosphatidylinositol synthase)
ENSG00000158828	0.69	PINK1	PTEN induced putative kinase 1
ENSG00000105968	0.69	H2AFV	H2A histone family, member V
ENSG00000073969	0.69	NSF	N-ethylmaleimide-sensitive factor
ENSG00000134686	0.69	PHC2	Polyhomeotic homolog 2 (Drosophila)
ENSG00000136891	0.69	TEX10	Testis expressed 10
ENSG00000090097	0.70	PCBP4	Poly(rC) binding protein 4
ENSG00000132471	0.70	WBP2	WW domain binding protein 2
ENSG00000185000	0.70	DGAT1	Diacylglycerol O-acyltransferase 1
ENSG00000132383	0.70	RPA1	Replication protein A1, 70kDa
ENSG00000136451	0.70	VEZF1	Vascular endothelial zinc finger 1
ENSG00000133606	0.70	MKRN1	Makorin ring finger protein 1
ENSG00000004487	0.70	AOF2	Flavin-containing amine oxidase domain-containing protein 2
ENSG00000125534	0.70	C20orf149	Chromosome 20 open reading frame 149

Ensemble ID	fc	GeneSymbol	Description
ENSG00000135624	0.70	CCT7	Chaperonin containing TCP1, subunit 7 (eta)
ENSG00000161202	0.70	DVL3	Dishevelled, dsh homolog 3 (Drosophila)
ENSG00000036257	0.70	CUL3	Cullin 3
ENSG00000103150	0.70	MLYCD	Malonyl-CoA decarboxylase
ENSG00000120438	0.70	TCP1	T-complex 1
ENSG00000176087	0.70	SLC35A4	Solute carrier family 35, member A4
ENSG00000156515	0.70	HK1	Hexokinase 1
ENSG00000180304	0.70	OAZ2	Ornithine decarboxylase antizyme 2
ENSG00000144028	0.70	ASCC3L1	Activating signal cointegrator 1 complex subunit 3-like 1
ENSG00000178764	0.70	ZHX2	Zinc fingers and homeoboxes protein 2
ENSG00000119335	0.70	SET	Protein SET (Phosphatase 2A inhibitor I2PP2A) (I-2PP2A)
ENSG00000141699	0.70	NP_835227.1	NA
ENSG00000108270	0.70	AATF	Apoptosis antagonizing transcription factor
ENSG00000047249	0.70	ATP6V1H	ATPase, H+ transporting, lysosomal 50/57kDa, V1 subunit H
ENSG00000138363	0.70	ATIC	5-aminoimidazole-4-carboxamide ribonucleotide formyltransferase/IMP cyclohydrolase
ENSG00000163431	0.70	LMOD1	Leiomodin 1 (smooth muscle)
ENSG00000204619	0.70	PPP1R11	Protein phosphatase 1, regulatory (inhibitor) subunit 11
ENSG00000114867	0.70	EIF4G1	Eukaryotic translation initiation factor 4 gamma, 1
ENSG00000126457	0.71	PRMT1	Protein arginine methyltransferase 1
ENSG00000006125	0.71	AP2B1	Adaptor-related protein complex 2, beta 1 subunit
ENSG00000104848	0.71	KCNA7	Potassium voltage-gated channel, shaker-related subfamily, member 7
ENSG00000153827	0.71	TRIP12	Thyroid hormone receptor interactor 12
ENSG00000136813	0.71	KIAA0368	Proteasome-associated protein ECM29 homolog
ENSG00000162104	0.71	ADCY9	Adenylate cyclase 9
ENSG00000124299	0.71	PEPD	Peptidase D
ENSG00000177105	0.71	RHOG	Ras homolog gene family, member G (rho G)
ENSG00000111897	0.71	SERINC1	Serine incorporator 1
ENSG00000177189	0.71	RPS6KA3	Ribosomal protein S6 kinase, 90kDa, polypeptide 3
ENSG00000185551	0.71	NR2F2	Nuclear receptor subfamily 2, group F, member 2
ENSG00000108515	0.71	ENO3	Enolase 3 (beta, muscle)
ENSG00000012822	0.71	CALCOCO1	Calcium binding and coiled-coil domain 1
ENSG00000078061	0.71	ARAF	A-Raf proto-oncogene serine/threonine-protein kinase
ENSG00000113048	0.71	MRPS27	Mitochondrial ribosomal protein S27
ENSG00000198676	0.71	Q7Z4H1_HUMAN	HBeAg-binding protein 1
ENSG00000197451	0.72	HNRPAB	Heterogeneous nuclear ribonucleoprotein A/B
ENSG00000065970	0.72	FOXJ2	Forkhead box J2
ENSG00000077549	0.72	CAPZB	Capping protein (actin filament) muscle Z-line, beta
ENSG00000115806	0.72	GORASP2	Golgi reassembly stacking protein 2, 55kDa
ENSG00000122203	0.72	KIAA1191	KIAA1191
ENSG00000188130	0.72	MAPK12	Mitogen-activated protein kinase 12
ENSG00000188677	0.72	PARVB	Parvin, beta
ENSG00000198837	0.72	DENND4B	DENN/MADD domain containing 4B

Ensemble ID	fc	GeneSymbol	Description
ENSG00000100632	0.72	ERH	Enhancer of rudimentary homolog (Drosophila)
ENSG00000119950	0.72	MXI1	MAX interactor 1
ENSG00000114544	0.72	SLC41A3	Solute carrier family 41, member 3
ENSG00000185883	0.72	ATP6V0C	ATPase, H+ transporting, lysosomal 16kDa, V0 subunit c
ENSG00000104812	0.72	GYS1	Glycogen synthase 1 (muscle)
ENSG00000100109	0.72	TFIP11	Tuftelin interacting protein 11
ENSG00000100412	0.72	ACO2	Aconitase 2, mitochondrial
ENSG00000115657	0.72	ABCB6	ATP-binding cassette, sub-family B (MDR/TAP), member 6
ENSG00000131462	0.72	TUBG1	Tubulin, gamma 1
ENSG00000115840	0.72	SLC25A12	Solute carrier family 25 (mitochondrial carrier, Aralar), member 12
ENSG00000137073	0.72	UBAP2	Ubiquitin associated protein 2
ENSG00000167671	0.72	UBXD1	UBX domain-containing protein 1
ENSG00000022840	0.72	RNF10	Ring finger protein 10
ENSG00000185651	0.73	UBE2L3	Ubiquitin-conjugating enzyme E2L 3
ENSG00000102225	0.73	PCTK1	PCTAIRE protein kinase 1
ENSG00000143365	0.73	LRRN6D	Nuclear receptor ROR-gamma
ENSG00000141646	0.73	SMAD4	SMAD family member 4
ENSG00000102900	0.73	NUP93	Nucleoporin 93kDa
ENSG00000140718	0.73	NP_001073901.1	NA
ENSG00000142186	0.73	SCYL1	SCY1-like 1 (S. cerevisiae)
ENSG00000179262	0.73	RAD23A	RAD23 homolog A (S. cerevisiae)
ENSG00000187446	0.73	CHP1_HUMAN	Calcium-binding protein p22
ENSG00000011007	0.73	TCEB3	Transcription elongation factor B polypeptide 3
ENSG00000143621	0.73	ILF2	Interleukin enhancer binding factor 2, 45kDa
ENSG00000169221	0.73	TBC1D10B	TBC1 domain family, member 10B
ENSG00000139990	0.73	WDR22	WD repeat domain 22
ENSG00000186204	0.73	CYP4F12	Cytochrome P450, family 4, subfamily F, polypeptide 12
ENSG00000107404	0.73	DVL1L1	Segment polarity protein dishevelled homolog DVL-1
ENSG00000111652	0.73	COPS7A	COP9 constitutive photomorphogenic homolog subunit 7A (Arabidopsis)
ENSG00000112305	0.73	SMAP1	Small ArfGAP 1
ENSG00000182500	0.73	TMEM142A	Calcium release-activated calcium channel protein 1
ENSG00000144659	0.73	SLC25A38	Solute carrier family 25, member 38
ENSG00000099821	0.73	POLRMT	Polymerase (RNA) mitochondrial (DNA directed)
ENSG00000204389	0.73	HSPA1A	Heat shock 70 kDa protein 1
ENSG00000099622	0.73	CIRBP	Cold inducible RNA binding protein
ENSG00000100220	0.73	C22orf28	Chromosome 22 open reading frame 28
ENSG00000130821	0.73	SLC6A8	Solute carrier family 6 (neurotransmitter transporter, creatine), member 8
ENSG00000100347	0.73	SAMM50	Sorting and assembly machinery component 50 homolog (S. cerevisiae)
ENSG00000111540	0.73	RAB5B	RAB5B, member RAS oncogene family
ENSG00000100242	0.73	UNC84B	Unc-84 homolog B (C. elegans)
ENSG00000170153	0.73	RNF150	Ring finger protein 150
ENSG00000138814	0.74	PPP3CA	Protein phosphatase 3 (formerly 2B), catalytic subunit, alpha isoform

Ensemble ID	fc	GeneSymbol	Description
ENSG00000185721	0.74	DRG1	Developmentally regulated GTP binding protein 1
ENSG00000132716	0.74	WDR42A	WD repeat domain 42A
ENSG00000167986	0.74	DDB1	Damage-specific DNA binding protein 1, 127kDa
ENSG00000157020	0.74	SEC13	SEC13 homolog (S. cerevisiae)
ENSG00000102007	0.74	PLP2	Proteolipid protein 2 (colonic epithelium-enriched)
ENSG00000077522	0.74	ACTN2	Actinin, alpha 2
ENSG00000126247	0.74	CAPNS1	Calpain, small subunit 1
ENSG00000092203	0.74	KIAA0737	Epidermal Langerhans cell protein LCP1
ENSG00000145945	0.74	FAM50B	Family with sequence similarity 50, member B
ENSG00000006704	0.74	GTF2IRD1	GTF2I repeat domain containing 1
ENSG00000196230	0.74	TUBB	Tubulin beta chain
ENSG00000159069	0.74	FBXW5	F-box and WD repeat domain containing 5
ENSG00000197081	0.74	IGF2R	Insulin-like growth factor 2 receptor
ENSG00000155189	0.74	AGPAT5	1-acylglycerol-3-phosphate O-acyltransferase 5 (lysophosphatidic acid acyltransferase, epsilon)
ENSG00000181929	0.74	PRKAG1	Protein kinase, AMP-activated, gamma 1 non-catalytic subunit
ENSG00000062485	0.74	CS	Citrate synthase
ENSG00000179889	0.74	NP_055842.1	NA
ENSG00000164024	0.74	METAP1	Methionyl aminopeptidase 1
ENSG00000087365	0.74	SF3B2	Splicing factor 3b, subunit 2, 145kDa
ENSG00000162413	0.74	KLHL21	Kelch-like 21 (Drosophila)
ENSG00000129116	0.74	PALLD	Palladin, cytoskeletal associated protein
ENSG00000006757	0.74	PNPLA4	Patatin-like phospholipase domain containing 4
ENSG00000187555	0.74	USP7	Ubiquitin specific peptidase 7 (herpes virus-associated)
ENSG00000013455	0.74	ARPC1A	Actin related protein 2/3 complex, subunit 1A, 41kDa
ENSG00000123992	0.74	DNPEP	Aspartyl aminopeptidase
ENSG00000049245	0.74	VAMP3	Vesicle-associated membrane protein 3 (cellubrevin)
ENSG00000124422	0.74	USP22	Ubiquitin specific peptidase 22
ENSG00000143870	0.74	PDIA6	Protein disulfide isomerase family A, member 6
ENSG00000184007	0.75	PTP4A2	Protein tyrosine phosphatase type IVA, member 2
ENSG00000186187	0.75	ZNRF1	Zinc and ring finger 1
ENSG00000100462	0.75	PRMT5	Protein arginine methyltransferase 5
ENSG00000168610	0.75	STAT3	Signal transducer and activator of transcription 3 (acute-phase response factor)
ENSG00000166974	0.75	MAPRE2	Microtubule-associated protein, RP/EB family, member 2
ENSG00000079246	0.75	XRCC5	X-ray repair complementing defective repair in Chinese hamster cells 5 (double-strand-break rejoining)
ENSG00000013374	0.75	NUB1	Negative regulator of ubiquitin-like proteins 1
ENSG00000124214	0.75	STAU1	Staufen, RNA binding protein, homolog 1 (Drosophila)
ENSG00000197170	0.75	PSMD12	Proteasome (prosome, macropain) 26S subunit, non-ATPase, 12
ENSG00000110025	0.75	SNX15	Sorting nexin 15
ENSG00000166685	0.75	COG1	Component of oligomeric golgi complex 1
ENSG00000135424	0.75	ITGA7	Integrin alpha-7 precursor
ENSG00000183386	0.75	FHL3	Four and a half LIM domains 3
ENSG00000095637	0.75	SORBS1	Sorbin and SH3 domain containing 1

Ensemble ID	fc	GeneSymbol	Description
ENSG00000175806	0.75	MSRA	Methionine sulfoxide reductase A
ENSG00000169184	0.75		NA
ENSG00000180900	0.75	SCRIB	Scribbled homolog (Drosophila)
ENSG00000126368	0.75	NR1D1	Nuclear receptor subfamily 1, group D, member 1
ENSG00000115525	0.75	ST3GAL5	ST3 beta-galactoside alpha-2,3-sialyltransferase 5
ENSG00000151327	0.75	C14orf24	NA
ENSG00000146457	0.75	WTAP	Wilms' tumor 1-associating protein
ENSG00000175591	0.75	P2RY2	Purinergic receptor P2Y, G-protein coupled, 2
ENSG00000166337	0.75	TAF10	TAF10 RNA polymerase II, TATA box binding protein (TBP)-associated factor, 30kDa
ENSG00000145990	0.75	GFOD1	Glucose-fructose oxidoreductase domain containing 1
ENSG00000176171	0.75	BNIP3	BCL2/adenovirus E1B 19kDa interacting protein 3
ENSG00000163125	0.75	KIAA0460	NA
ENSG00000163866	0.75	C1orf212	NA
ENSG00000148498	0.75	PARD3	Par-3 partitioning defective 3 homolog (C. elegans)
ENSG00000143702	0.75	CEP170	Centrosomal protein 170kDa
ENSG00000108468	0.75	CBX1	Chromobox homolog 1 (HP1 beta homolog Drosophila)
ENSG00000011638	0.75	TMEM159	Transmembrane protein 159
ENSG00000164054	0.75	NP_057563.3	scotin
ENSG00000185787	0.75	MORF4L1	Mortality factor 4 like 1
ENSG00000172731	0.76	LRRC20	Leucine rich repeat containing 20
ENSG00000188554	0.76	NBR1	neighbor of BRCA1 gene 1
ENSG00000170296	0.76	GABARAP	GABA(A) receptor-associated protein
ENSG00000170027	0.76	YWHAG	Tyrosine 3-monooxygenase/tryptophan 5-monooxygenase activation protein, gamma polypeptide
ENSG00000185896	0.76	LAMP1	Lysosomal-associated membrane protein 1
ENSG00000118639	0.76	RNF103	Ring finger protein 103
ENSG00000171503	0.76	ETFDH	Electron-transferring-flavoprotein dehydrogenase
ENSG00000143457	0.76	GOLPH3L	Golgi phosphoprotein 3-like
ENSG00000111716	0.76	LDHB	Lactate dehydrogenase B
ENSG00000171867	0.76	PRNP	Major prion protein precursor
ENSG00000184678	0.76	HIST2H2BE	Histone cluster 2, H2be
ENSG00000060762	0.76	BRP44L	Brain protein 44-like
ENSG00000115216	0.76	NRBP1	Nuclear receptor binding protein 1
ENSG00000119953	0.76	SMNDC1	Survival motor neuron domain containing 1
ENSG00000106105	0.76	GARS	Glycyl-tRNA synthetase
ENSG00000142046	0.76	TMEM91	Transmembrane protein 91
ENSG00000144043	0.76	TEX261	Testis expressed 261
ENSG00000117450	0.76	PRDX1	Peroxiredoxin 1
ENSG00000167987	0.76	VPS37C	Vacuolar protein sorting 37 homolog C (S. cerevisiae)
ENSG00000163159	0.76	VPS72	Vacuolar protein sorting 72 homolog (S. cerevisiae)
ENSG00000156471	0.76	PTDSS1	Phosphatidylserine synthase 1
ENSG00000157916	0.76	RER1	RER1 retention in endoplasmic reticulum 1 homolog (S. cerevisiae)
ENSG00000184916	0.76	JAG2	Jagged 2

Ensemble ID	fc	GeneSymbol	Description
ENSG00000113657	0.76	DPYSL3	Dihydropyrimidinase-like 3
ENSG00000084090	0.76	STARD7	StAR-related lipid transfer (START) domain containing 7
ENSG00000099875	0.76	MKNK2	MAP kinase interacting serine/threonine kinase 2
ENSG00000131507	0.76	NDFIP1	Nedd4 family interacting protein 1
ENSG00000170745	0.76	KCNS3	Potassium voltage-gated channel, delayed-rectifier, subfamily S, member 3
ENSG00000184489	0.76	PTP4A3	Protein tyrosine phosphatase type IVA, member 3
ENSG00000135723	0.76	FHOD1	Formin homology 2 domain containing 1
ENSG00000157881	0.76	PANK4	Pantothenate kinase 4
ENSG00000168066	0.76	SF1	Splicing factor 1
ENSG00000174132	0.76	TMEM157	Transmembrane protein 157 precursor
ENSG00000005243	0.76	COPZ2	Coatomer protein complex, subunit zeta 2
ENSG00000198355	0.76	PIM3	Pim-3 oncogene
ENSG00000162980	0.76	ARL5A	ADP-ribosylation factor-like 5A
ENSG00000068383	0.76	INPP5A	Inositol polyphosphate-5-phosphatase, 40kDa
ENSG00000157450	0.76	RNF111	Ring finger protein 111
ENSG00000100522	0.76	GNPNAT1	Glucosamine-phosphate N-acetyltransferase 1
ENSG00000115484	0.76	CCT4	Chaperonin containing TCP1, subunit 4 (delta)
ENSG00000047315	0.76	POLR2B	Polymerase (RNA) II (DNA directed) polypeptide B, 140kDa
ENSG00000130962	0.76	PRRG1	Proline rich Gla (G-carboxyglutamic acid) 1
ENSG00000148468	0.76	C10orf38	NA
ENSG00000146007	0.76	ZMAT2	Zinc finger, matrin type 2
ENSG00000197324	0.77	LRP10	Low density lipoprotein receptor-related protein 10
ENSG00000145495	0.77	Mar-06	membrane-associated ring finger
ENSG00000100897	0.77	WDR23	WD repeat domain 23
ENSG00000103274	0.77	NUBP1	Nucleotide binding protein 1 (MinD homolog, E. coli)
ENSG00000087111	0.77	PIGS	Phosphatidylinositol glycan anchor biosynthesis, class S
ENSG00000145916	0.77	RMND5B	Required for meiotic nuclear division 5 homolog B (S. cerevisiae)
ENSG00000162144	0.77	CYBASC3	Cytochrome b, ascorbate dependent 3
ENSG00000103342	0.77	GSPT1	G1 to S phase transition 1
ENSG00000109971	0.77	HSPA8	Heat shock 70kDa protein 8
ENSG00000116350	0.77	SFRS4	Splicing factor, arginine/serine-rich 4
ENSG00000142684	0.77	ZNF593	Zinc finger protein 593
ENSG00000119318	0.77	RAD23B	RAD23 homolog B (S. cerevisiae)
ENSG00000145391	0.77	SETD7	SET domain containing (lysine methyltransferase) 7
ENSG00000106554	0.77	CHCHD3	Coiled-coil-helix-coiled-coil-helix domain containing 3
ENSG00000137996	0.77	RTCD1	RNA terminal phosphate cyclase domain 1
ENSG00000109332	0.77	UBE2D3	Ubiquitin-conjugating enzyme E2D 3 (UBC4/5 homolog, yeast)
ENSG00000175216	0.77	CKAP5	Cytoskeleton associated protein 5
ENSG00000140497	0.77	SCAMP2	Secretory carrier membrane protein 2
ENSG00000084754	0.77	HADHA	Hydroxyacyl-Coenzyme A dehydrogenase/3-ketoacyl-Coenzyme A thiolase/enoyl-Coenzyme A hydratase (trifunctional protein), alpha subunit
ENSG00000132405	0.77	TBC1D14	TBC1 domain family, member 14

Ensemble ID	fc	GeneSymbol	Description
ENSG00000198786	0.77	MT-ND5	NADH-ubiquinone oxidoreductase chain 5
ENSG00000149100	0.77	PCID1	B5 receptor
ENSG00000006695	0.77	COX10	COX10 homolog, cytochrome c oxidase assembly protein, heme A: farnesyltransferase (yeast)
ENSG00000136238	0.77	RAC1	Ras-related C3 botulinum toxin substrate 1 (rho family, small GTP binding protein Rac1)
ENSG00000031698	0.77	SARS	Seryl-tRNA synthetase
ENSG00000179632	0.77	MAF1	MAF1 homolog (S. cerevisiae)
ENSG00000157306	0.77	THTPA	Thiamine triphosphatase
ENSG00000058600	0.77	POLR3E	Polymerase (RNA) III (DNA directed) polypeptide E (80kD)
ENSG00000152642	0.77	GPD1L	Glycerol-3-phosphate dehydrogenase 1-like
ENSG00000185950	0.77	IRS2	Insulin receptor substrate 2
ENSG00000160917	0.77	CPSF4	Cleavage and polyadenylation specific factor 4, 30kDa
ENSG00000100902	0.77	PSMA6	Proteasome (prosome, macropain) subunit, alpha type, 6
ENSG00000124486	0.77	USP9X	Ubiquitin specific peptidase 9, X-linked
ENSG00000178952	0.77	TUFM	Tu translation elongation factor, mitochondrial
ENSG00000198771	0.77	RCSD1	RCSD domain containing 1
ENSG00000185262	0.77	FAM100B	Family with sequence similarity 100, member B
ENSG00000196792	0.77	STRN3	Striatin, calmodulin binding protein 3
ENSG00000101605	0.77	MYOM1	Myomesin 1, 185kDa
ENSG00000175826	0.77	DULLARD	Dullard homolog (Xenopus laevis)
ENSG00000188021	0.77	UBQLN2	Ubiquilin 2
ENSG00000170310	0.77	STX8	Syntaxin 8
ENSG00000170881	0.77	RNF139	Ring finger protein 139
ENSG00000125821	0.77	HARS2	Histidyl-tRNA synthetase 2, mitochondrial (putative)
ENSG00000168802	0.77	Q71E72_HUMAN	chromosome transmission fidelity factor 8 homolog (S. cerevisiae)
ENSG00000129084	0.78	PSMA1	Proteasome (prosome, macropain) subunit, alpha type, 1
ENSG00000134775	0.78	FHOD3	Formin homology 2 domain containing 3
ENSG00000131446	0.78	MGAT1	Mannosyl (alpha-1,3-)-glycoprotein beta-1,2-N-acetylglucosaminyltransferase
ENSG00000134014	0.78	ELP3	Elongation protein 3 homolog (S. cerevisiae)
ENSG00000075568	0.78	TMEM131	Transmembrane protein 131
ENSG00000162923	0.78	WDR26	WD repeat domain 26
ENSG00000165704	0.78	HPRT1	Hypoxanthine phosphoribosyltransferase 1
ENSG00000151240	0.78	DIP2C	DIP2 disco-interacting protein 2 homolog C (Drosophila)
ENSG00000172765	0.78	TMCC1	Transmembrane and coiled-coil domain family 1
ENSG00000132388	0.78	UBE2G1	Ubiquitin-conjugating enzyme E2G 1 (UBC7 homolog, yeast)
ENSG00000148834	0.78	GSTO1	Glutathione S-transferase omega 1
ENSG00000113360	0.78	RNASEN	Ribonuclease type III, nuclear
ENSG00000118564	0.78	FBXL5	F-box and leucine-rich repeat protein 5
ENSG00000171603	0.78	CLSTN1	Calsyntenin 1
ENSG00000178537	0.78	SLC25A20	Solute carrier family 25 (carnitine/acylcarnitine translocase), member 20
ENSG00000168216	0.78	LMBRD1	LMBR1 domain containing 1
ENSG00000168884	0.78	TNIP2	TNFAIP3 interacting protein 2
ENSG00000111666	0.78	CHPT1	Choline phosphotransferase 1

Ensemble ID	fc	GeneSymbol	Description
ENSG00000176871	0.78	WSB2	WD repeat and SOCS box-containing 2
ENSG00000064601	0.78	CTSA	Cathepsin A
ENSG00000146872	0.78	TLK2	Tousled-like kinase 2
ENSG00000154945	0.78	ANKRD40	Ankyrin repeat domain 40
ENSG00000180758	0.78	GPR157	G protein-coupled receptor 157
ENSG00000068120	0.78	COASY	Coenzyme A synthase
ENSG00000090615	0.78	GOLGA3	Golgi autoantigen, golgin subfamily a, 3
ENSG00000196507	0.78	TCEAL3	Transcription elongation factor A (SII)-like 3
ENSG00000197157	0.78	SND1	Staphylococcal nuclease and tudor domain containing 1
ENSG00000136758	0.78	YME1L1	YME1-like 1 (S. cerevisiae)
ENSG00000158470	0.78	B4GALT5	UDP-Gal:betaGlcNAc beta 1,4- galactosyltransferase, polypeptide 5
ENSG00000169083	0.78	AR	Androgen receptor
ENSG00000173692	0.78	PSMD1	Proteasome (prosome, macropain) 26S subunit, non-ATPase, 1
ENSG00000004776	0.78	HSPB6	Heat shock protein, alpha-crystallin-related, B6
ENSG00000013583	0.78	HEBP1	Heme binding protein 1
ENSG00000085377	0.78	PREP	Prolyl endopeptidase
ENSG00000105711	0.78	SCN1B	Sodium channel, voltage-gated, type I, beta
ENSG00000101457	0.78	DNTTIP1	Deoxynucleotidyltransferase, terminal, interacting protein 1
ENSG00000140350	0.78	ANP32A	Acidic (leucine-rich) nuclear phosphoprotein 32 family, member A
ENSG00000110958	0.78	PTGES3	Prostaglandin E synthase 3 (cytosolic)
ENSG00000054793	0.78	ATP9A	ATPase, class II, type 9A
ENSG00000167674	0.79	NP_001001520.1	hepatoma-derived growth factor-related protein 2 isoform 1
ENSG00000126945	0.79	HNRPH2	Heterogeneous nuclear ribonucleoprotein H'
ENSG00000068903	0.79	SIRT2	Sirtuin (silent mating type information regulation 2 homolog) 2 (S. cerevisiae)
ENSG00000186298	0.79	PPP1CC	Protein phosphatase 1, catalytic subunit, gamma isoform
ENSG00000061676	0.79	NCKAP1	NCK-associated protein 1
ENSG00000090621	0.79	PABPC4	Poly(A) binding protein, cytoplasmic 4 (inducible form)
ENSG00000116871	0.79	RPRC1	arginine/proline rich coiled-coil 1
ENSG00000150459	0.79	SAP18	Sin3A-associated protein, 18kDa
ENSG00000130021	0.79	HDHD1A	Haloacid dehalogenase-like hydrolase domain containing 1A
ENSG00000197724	0.79	PHF2	PHD finger protein 2
ENSG00000088833	0.79	NSFL1C	NSFL1 (p97) cofactor (p47)
ENSG00000148335	0.79	C9orf32	NA
ENSG00000025800	0.79	KPNA6	Karyopherin alpha-6
ENSG00000121440	0.79	PDZRN3	PDZ domain containing ring finger 3
ENSG00000168734	0.79	PKIG	Protein kinase (cAMP-dependent, catalytic) inhibitor gamma
ENSG00000100288	0.79	CPT1B	Carnitine palmitoyltransferase 1B (muscle)
ENSG00000116096	0.79	SPR	Sepiapterin reductase (7,8-dihydrobiopterin:NADP+ oxidoreductase)
ENSG00000196455	0.79	PIK3R4	Phosphoinositide-3-kinase, regulatory subunit 4
ENSG00000204560	0.79	DHX16	DEAH (Asp-Glu-Ala-His) box polypeptide 16
ENSG00000116521	0.79	SCAMP3	Secretory carrier membrane protein 3
ENSG00000156026	0.79	CCDC109A	Coiled-coil domain containing 109A

Ensemble ID	fc	GeneSymbol	Description
ENSG00000160967	0.79	CUTL1	NA
ENSG00000101266	0.79	CSNK2A1	Casein kinase 2, alpha 1 polypeptide
ENSG00000138629	0.79	UBL7	Ubiquitin-like 7 (bone marrow stromal cell-derived)
ENSG00000028203	0.79	VEZT	Vezatin, adherens junctions transmembrane protein
ENSG00000108349	0.79	CASC3	Cancer susceptibility candidate 3
ENSG00000131378	0.79	RFTN1	Raftlin, lipid raft linker 1
ENSG00000149929	0.79	HIRIP3	HIRA interacting protein 3
ENSG00000146731	0.79	CCT6A	Chaperonin containing TCP1, subunit 6A (zeta 1)
ENSG00000187715	0.79	KLHDC6	Kelch domain containing 6
ENSG00000071655	0.79	MBD3	Methyl-CpG binding domain protein 3
ENSG00000163346	0.79	PBXIP1	Pre-B-cell leukemia homeobox interacting protein 1
ENSG00000136478	0.79	TEX2	Testis expressed 2
ENSG00000006831	0.79	ADIPOR2	Adiponectin receptor 2
ENSG00000147416	0.79	ATP6V1B2	ATPase, H+ transporting, lysosomal 56/58kDa, V1 subunit B2
ENSG00000155506	0.79	LARP1	La ribonucleoprotein domain family, member 1
ENSG00000106290	0.79	TAF6	TAF6 RNA polymerase II, TATA box binding protein (TBP)-associated factor, 80kDa
ENSG00000071205	0.79	ARHGAP10	Rho GTPase activating protein 10
ENSG00000121210	0.79	KIAA0922	KIAA0922
ENSG00000130175	0.79	PRKCSH	Protein kinase C substrate 80K-H
ENSG00000071462	0.79	WBSCR22	Williams Beuren syndrome chromosome region 22
ENSG00000171206	0.79	TRIM8	Tripartite motif-containing 8
ENSG00000174684	0.79	B3GNT1	UDP-GlcNAc:betaGal beta-1,3-N-acetylglucosaminyltransferase 1
ENSG00000103942	0.79	HOMER2	Homer homolog 2 (Drosophila)
ENSG00000130165	0.79	ELOF1	Elongation factor 1 homolog (S. cerevisiae)
ENSG00000116649	0.79	SRM	Spermidine synthase
ENSG00000112276	0.79	BVES	Blood vessel epicardial substance
ENSG00000139405	0.79	C12orf52	Chromosome 12 open reading frame 52
ENSG00000004848	0.79	ARX	Aristaless related homeobox
ENSG00000143799	0.79	PARP1	Poly (ADP-ribose) polymerase 1
ENSG00000179041	0.79	RRS1	RRS1 ribosome biogenesis regulator homolog (S. cerevisiae)
ENSG00000171307	0.79	ZDHHC16	Zinc finger, DHHC-type containing 16
ENSG00000155463	0.80	OXA1L	Oxidase (cytochrome c) assembly 1-like
ENSG00000142864	0.80	SERBP1	SERPINE1 mRNA binding protein 1
ENSG00000115685	0.80	PPP1R7	Protein phosphatase 1, regulatory (inhibitor) subunit 7
ENSG00000079459	0.80	FDFT1	Farnesyl-diphosphate farnesyltransferase 1
ENSG00000067113	0.80	PPAP2A	Phosphatidic acid phosphatase type 2A
ENSG00000165695	0.80	C9orf98	Chromosome 9 open reading frame 98
ENSG00000156599	0.80	ZDHHC5	Zinc finger, DHHC-type containing 5
ENSG00000122068	0.80	FYTTD1	Forty-two-three domain containing 1
ENSG00000131238	0.80	PPT1	Palmitoyl-protein thioesterase 1
ENSG00000149218	0.80	ENDOD1	Endonuclease domain containing 1
ENSG00000054523	0.80	KIF1B	Kinesin family member 1B

Ensemble ID	fc	GeneSymbol	Description
ENSG00000102178	0.80	UBL4A	Ubiquitin-like 4A
ENSG00000149547	0.80	EI24	Etoposide induced 2.4 mRNA
ENSG00000126581	0.80	BECN1	Beclin 1, autophagy related
ENSG00000115241	0.80	PPM1G	Protein phosphatase 1G (formerly 2C), magnesium-dependent, gamma isoform
ENSG00000069998	0.80	CECR5	Cat eye syndrome chromosome region, candidate 5
ENSG00000105202	0.80	FBL	Fibrillarin
ENSG00000079332	0.80	SAR1A	SAR1 homolog A (S. cerevisiae)
ENSG00000152795	0.80	HNRPDL	Heterogeneous nuclear ribonucleoprotein D-like
ENSG00000023734	0.80	STRAP	Serine/threonine kinase receptor associated protein
ENSG00000204155	0.80	PARG	Poly(ADP-ribose) glycohydrolase
ENSG00000053254	0.80	CHES1	Checkpoint suppressor 1
ENSG00000110048	0.80	OSBP	Oxysterol binding protein
ENSG00000111275	0.80	ALDH2	Aldehyde dehydrogenase 2 family (mitochondrial)
ENSG00000140259	0.80	MFAP1	Microfibrillar-associated protein 1
ENSG00000174080	0.80	CTSF	Cathepsin F
ENSG00000108039	0.80	XPNPEP1	X-prolyl aminopeptidase (aminopeptidase P) 1, soluble
ENSG00000187109	0.80	NAP1L1	Nucleosome assembly protein 1-like 1
ENSG00000148541	0.80	FAM13C1	Protein FAM13C1
ENSG00000152443	0.80	ZNF776	Zinc finger protein 776
ENSG00000173933	0.80	RBM4	RNA binding motif protein 4
ENSG00000143384	0.80	MCL1	Myeloid cell leukemia sequence 1 (BCL2-related)
ENSG00000138449	0.80	SLC40A1	Solute carrier family 40 (iron-regulated transporter), member 1
ENSG00000113643	0.80	RARS	Arginyl-tRNA synthetase
ENSG00000077157	0.80	PPP1R12B	Protein phosphatase 1, regulatory (inhibitor) subunit 12B
ENSG00000111332	0.80	H2AFJ	H2A histone family, member J isoform 2
ENSG00000105393	0.80	NP_001028721.1	NA
ENSG00000143771	0.80	CNIH4	Cornichon homolog 4 (Drosophila)
ENSG00000183624	0.80	C3orf37	Chromosome 3 open reading frame 37
ENSG00000112478	0.80	VPS52	Vacuolar protein sorting 52 homolog (S. cerevisiae)
ENSG00000140543	0.80	DET1	De-etiolated homolog 1 (Arabidopsis)
ENSG00000109534	0.80	NOLA1	Nucleolar protein family A member 1
ENSG00000136205	0.80	TNS3	Tensin 3
ENSG00000147065	0.80	MSN	Moesin
ENSG00000122359	0.80	ANXA11	Annexin A11
ENSG00000196704	0.80	AMZ2_HUMAN	Archaemetzincin-2
ENSG00000167136	0.80	ENDOG	Endonuclease G
ENSG00000151929	0.80	BAG3	BCL2-associated athanogene 3
ENSG00000157600	0.80	TMEM164	Transmembrane protein 164
ENSG00000077348	0.80	EXOSC5	Exosome component 5
ENSG00000187239	0.80	FNBP1	Formin binding protein 1
ENSG00000110651	0.80	CD81	CD81 molecule
ENSG00000119280	0.80	C1orf198	Chromosome 1 open reading frame 198
ENSG00000166272	0.80	C10orf26	NA

Ensemble ID	fc	GeneSymbol	Description
ENSG00000097033	0.80	SH3GLB1	SH3-domain GRB2-like endophilin B1
ENSG00000110046	0.80	NP_055919.1	NA
ENSG00000119718	0.80	EIF2B2	Eukaryotic translation initiation factor 2B, subunit 2 beta, 39kDa
ENSG00000089289	0.80	IGBP1	Immunoglobulin (CD79A) binding protein 1
ENSG00000125835	0.80	SNRPB	Small nuclear ribonucleoprotein polypeptides B and B1
ENSG00000172939	0.81	OXSR1	Oxidative-stress responsive 1
ENSG00000104872	0.81	NOP17	NA
ENSG00000114786	0.81	ACY1	Aminoacylase 1
ENSG00000024422	0.81	EHD2	EH-domain containing 2
ENSG00000211861	0.81	TRAJ28	T-cell receptor alpha J gene segment
ENSG00000022277	0.81	C20orf43	Chromosome 20 open reading frame 43
ENSG00000069275	0.81	NUCKS1	Nuclear ubiquitous casein and cyclin-dependent kinases substrate
ENSG00000088256	0.81	GNA11	Guanine nucleotide-binding protein subunit alpha-11
ENSG00000106993	0.81	CDC37L1	Cell division cycle 37 homolog (S. cerevisiae)-like 1
ENSG00000102978	0.81	POLR2C	Polymerase (RNA) II (DNA directed) polypeptide C, 33kDa
ENSG00000067560	0.81	RHOA	Ras homolog gene family, member A
ENSG00000108592	0.81	FTSJ3	FtsJ homolog 3 (E. coli)
ENSG00000186660	0.81	ZFP91	Zinc finger protein 91 homolog (mouse)
ENSG00000102226	0.81	USP11	Ubiquitin specific peptidase 11
ENSG00000135049	0.81	AGTPBP1	ATP/GTP binding protein 1
ENSG00000113552	0.81	GNPDA1	Glucosamine-6-phosphate deaminase 1
ENSG00000175203	0.81	DCTN2	Dynactin 2 (p50)
ENSG00000088543	0.81	C3orf18	Chromosome 3 open reading frame 18
ENSG00000198836	0.81	OPA1	Optic atrophy 1 (autosomal dominant)
ENSG00000129691	0.81	ASH2L	Ash2 (absent, small, or homeotic)-like (Drosophila)
ENSG00000137492	0.81	PRKRIR	Protein-kinase, interferon-inducible double stranded RNA dependent inhibitor, repressor of (P58 repressor)
ENSG00000135211	0.81	TMEM60	Transmembrane protein 60
ENSG00000047849	0.81	MAP4	Microtubule-associated protein 4
ENSG00000198492	0.81	YTHDF2	YTH domain family, member 2
ENSG00000138107	0.81	ACTR1A	ARP1 actin-related protein 1 homolog A, centractin alpha (yeast)
ENSG00000130826	0.81	DKC1	Dyskeratosis congenita 1, dyskerin
ENSG00000065427	0.81	KARS	Lysyl-tRNA synthetase
ENSG00000057608	0.81	GDI2	GDP dissociation inhibitor 2
ENSG00000066044	0.81	ELAVL1	ELAV (embryonic lethal, abnormal vision, Drosophila)-like 1 (Hu antigen R)
ENSG00000121073	0.81	SLC35B1	Solute carrier family 35, member B1
ENSG00000138430	0.81	GTPBP9	Putative GTP-binding protein 9
ENSG00000102893	0.81	PHKB	Phosphorylase kinase, beta
ENSG00000135452	0.81	TSPAN31	Tetraspanin 31
ENSG00000141905	0.81	NFIC	Nuclear factor I/C (CCAAT-binding transcription factor)
ENSG00000116954	0.81	RRAGC	Ras-related GTP binding C
ENSG00000070770	0.81	CSNK2A2	Casein kinase 2, alpha prime polypeptide
ENSG00000156253	0.81	C21orf6	NA

Ensemble ID	fc	GeneSymbol	Description
ENSG00000115053	0.81	NCL	Nucleolin
ENSG00000089154	0.81	GCN1L1	GCN1 general control of amino-acid synthesis 1-like 1 (yeast)
ENSG00000147649	0.81	MTDH	Metadherin
ENSG00000073111	0.81	MCM2	Minichromosome maintenance complex component 2
ENSG00000162735	0.81	PEX19	Peroxisomal biogenesis factor 19
ENSG00000111144	0.81	LTA4H	Leukotriene A4 hydrolase
ENSG00000115561	0.81	VPS24	Vacuolar protein sorting 24 homolog (S. cerevisiae)
ENSG00000183576	0.81	SETD3	SET domain containing 3
ENSG00000184047	0.81	DIABLO	Diablo homolog (Drosophila)
ENSG00000185624	0.81	P4HB	Prolyl 4-hydroxylase, beta polypeptide
ENSG00000116748	0.81	AMPD1	Adenosine monophosphate deaminase 1 (isoform M)
ENSG00000152700	0.81	SAR1B	SAR1 homolog B (S. cerevisiae)
ENSG00000165678	0.81	GHITM	Growth hormone inducible transmembrane protein
ENSG00000198853	0.81	RUSC2	RUN and SH3 domain containing 2
ENSG00000078808	0.81	SDF4	Stromal cell derived factor 4
ENSG00000169446	0.82	TMEM32	transmembrane protein 32
ENSG00000161016	0.82	RPL8	Ribosomal protein L8
ENSG00000168286	0.82	THAP11	THAP domain containing 11
ENSG00000107341	0.82	UBE2R2	Ubiquitin-conjugating enzyme E2R 2
ENSG00000204564	0.82	C6orf136	Chromosome 6 open reading frame 136
ENSG00000132768	0.82	DPH2	DPH2 homolog (S. cerevisiae)
ENSG00000101126	0.82	ADNP	Activity-dependent neuroprotector homeobox
ENSG00000100804	0.82	PSMB5	Proteasome (prosome, macropain) subunit, beta type, 5
ENSG00000151208	0.82	DLG5	Discs, large homolog 5 (Drosophila)
ENSG00000142687	0.82	KIAA0319L	KIAA0319-like
ENSG00000167325	0.82	RRM1	Ribonucleotide reductase M1
ENSG00000073905	0.82	VDAC1	Voltage-dependent anion channel 1
ENSG00000168329	0.82	CX3CR1	Chemokine (C-X3-C motif) receptor 1
ENSG00000039123	0.82	SKIV2L2	Superkiller viralicidic activity 2-like 2 (S. cerevisiae)
ENSG00000100811	0.82	YY1	YY1 transcription factor
ENSG00000183207	0.82	RUVBL2	RuvB-like 2 (E. coli)
ENSG00000116273	0.82	PHF13	PHD finger protein 13
ENSG00000124201	0.82	ZNFX1	Zinc finger, NFX1-type containing 1
ENSG00000126778	0.82	SIX1	SIX homeobox 1
ENSG00000103544	0.82	NP_064710.3	esophageal cancer associated protein (MGC16824)
ENSG00000086232	0.82	EIF2AK1	Eukaryotic translation initiation factor 2-alpha kinase 1
ENSG00000160570	0.82	DEDD2	Death effector domain containing 2
ENSG00000042022	0.82	ABHD14A	Abhydrolase domain containing 14A
ENSG00000062582	0.82	MRPS24	Mitochondrial ribosomal protein S24
ENSG00000101444	0.82	AHCY	S-adenosylhomocysteine hydrolase
ENSG00000198467	0.82	TPM2	Tropomyosin 2 (beta)
ENSG00000101367	0.82	MAPRE1	Microtubule-associated protein, RP/EB family, member 1
ENSG00000142784	0.82	WDTC1	WD and tetratricopeptide repeats 1

Ensemble ID	fc	GeneSymbol	Description
ENSG00000184900	0.82	SUMO3	SMT3 suppressor of mif two 3 homolog 3 (S. cerevisiae)
ENSG00000129351	0.82	ILF3	Interleukin enhancer binding factor 3, 90kDa
ENSG00000151465	0.82	CDC123	Cell division cycle 123 homolog (S. cerevisiae)
ENSG00000185885	0.82	IFITM1	Interferon induced transmembrane protein 1 (9-27)
ENSG00000099203	0.82	TMED1	Transmembrane emp24 protein transport domain containing 1
ENSG00000067182	0.82	TNFRSF1A	Tumor necrosis factor receptor superfamily, member 1A
ENSG00000187147	0.82	C1orf164	NA
ENSG00000161714	0.82	PLCD3	Phospholipase C, delta 3
ENSG00000124789	0.82	NUP153	Nuclear pore complex protein Nup153
ENSG00000164168	0.82	TMEM34	transmembrane protein 34
ENSG00000165424	0.82	C10orf56	NA
ENSG00000203879	0.82	GDI1	GDP dissociation inhibitor 1
ENSG00000148672	0.82	GLUD1	Glutamate dehydrogenase 1
ENSG00000038274	0.82	MAT2B	Methionine adenosyltransferase II, beta
ENSG00000204580	0.82	DDR1	Discoidin domain receptor tyrosine kinase 1
ENSG00000105220	0.82	GPI	Glucose phosphate isomerase
ENSG00000132912	0.82	DCTN4	Dynactin 4 (p62)
ENSG00000184113	0.82	CLDN5	Claudin 5
ENSG00000156976	0.82	EIF4A2	Eukaryotic initiation factor 4A-II
ENSG00000180329	0.82	CCDC43	Coiled-coil domain containing 43
ENSG00000177666	0.82	PNPLA2	Patatin-like phospholipase domain containing 2
ENSG00000030582	0.82	GRN	Granulin
ENSG00000197894	0.82	ADH5	Alcohol dehydrogenase 5 (class III), chi polypeptide
ENSG00000066027	0.83	PPP2R5A	Protein phosphatase 2, regulatory subunit B', alpha isoform
ENSG00000160679	0.83	C1orf77	Chromosome 1 open reading frame 77
ENSG00000173641	0.83	HSPB7	Heat shock 27kDa protein family, member 7 (cardiovascular)
ENSG00000124104	0.83	SNX21	Sorting nexin family member 21
ENSG00000125967	0.83	APBA2BP	Amyloid beta A4 protein-binding family A member 2-binding protein
ENSG00000103266	0.83	STUB1	STIP1 homology and U-box containing protein 1
ENSG00000143815	0.83	LBR	Lamin B receptor
ENSG00000112855	0.83	HARSL	Probable histidyl-tRNA synthetase
ENSG00000115415	0.83	STAT1	Signal transducer and activator of transcription 1, 91kDa
ENSG00000072506	0.83	HSD17B10	Hydroxysteroid (17-beta) dehydrogenase 10
ENSG00000138029	0.83	HADHB	Hydroxyacyl-Coenzyme A dehydrogenase/3-ketoacyl-Coenzyme A thiolase/enoyl-Coenzyme A hydratase (trifunctional protein), beta subunit
ENSG00000136715	0.83	SAP130	Sin3A-associated protein, 130kDa
ENSG00000130706	0.83	ADRM1	Adhesion regulating molecule 1
ENSG00000131508	0.83	UBE2D2	Ubiquitin-conjugating enzyme E2D 2 (UBC4/5 homolog, yeast)
ENSG00000142444	0.83	C19orf52	Chromosome 19 open reading frame 52
ENSG00000164896	0.83	FASTK	Fas-activated serine/threonine kinase
ENSG00000116688	0.83	MFN2	Mitofusin 2
ENSG00000156261	0.83	CCT8	Chaperonin containing TCP1, subunit 8 (theta)
ENSG00000136240	0.83	KDELR2	KDEL (Lys-Asp-Glu-Leu) endoplasmic reticulum protein

Ensemble ID	fc	GeneSymbol	Description
			retention receptor 2
ENSG00000169032	0.83	MAP2K1	Mitogen-activated protein kinase kinase 1
ENSG00000173357	0.83	Q13383_HUMAN	RNA binding motif (Fragment)
ENSG00000075945	0.83	KIFAP3	Kinesin-associated protein 3
ENSG00000080503	0.83	SMARCA2	SWI/SNF related, matrix associated, actin dependent regulator of chromatin, subfamily a, member 2
ENSG00000188549	0.83	NP_997263.1	NA
ENSG00000085511	0.83	MAP3K4	Mitogen-activated protein kinase kinase kinase 4
ENSG00000116473	0.83	RAP1A	RAP1A, member of RAS oncogene family
ENSG00000172775	0.83	NIP30_HUMAN	NEFA-interacting nuclear protein NIP30
ENSG00000135862	0.83	LAMC1	Laminin, gamma 1 (formerly LAMB2)
ENSG00000197006	0.83	METTL9	Methyltransferase like 9
ENSG00000179010	0.83	MRFAP1	Mof4 family associated protein 1
ENSG00000130511	0.83	SSBP4	Single stranded DNA binding protein 4
ENSG00000077721	0.83	UBE2A	Ubiquitin-conjugating enzyme E2A (RAD6 homolog)
ENSG00000107796	0.83	ACTA2	Actin, alpha 2, smooth muscle, aorta
ENSG00000154153	0.83	NP_001030022.1	NA
ENSG00000104442	0.83	ARMC1	Armadillo repeat containing 1
ENSG00000101421	0.83	CHMP4B	Chromatin modifying protein 4B
ENSG00000205352	0.83	NP_001005354.1	proline rich 13 isoform 2
ENSG00000134440	0.83	NARS	Asparaginyl-tRNA synthetase
ENSG00000168090	0.83	COPS6	COP9 constitutive photomorphogenic homolog subunit 6 (Arabidopsis)
ENSG00000155876	0.83	RRAGA	Ras-related GTP binding A
ENSG00000100395	0.83	L3MBTL2	L(3)mbt-like 2 (Drosophila)
ENSG00000122687	0.83	FTSJ2	FtsJ homolog 2 (E. coli)
ENSG00000120265	0.83	PCMT1	Protein-L-isoaspartate (D-aspartate) O-methyltransferase
ENSG00000065150	0.83	RANBP5	Ran-binding protein 5
ENSG00000131773	0.84	KHDRBS3	KH domain containing, RNA binding, signal transduction associated 3
ENSG00000119632	0.84	FAM14A	Protein FAM14A precursor
ENSG00000078674	0.84	PCM1	Pericentriolar material 1
ENSG00000039523	0.84	FAM65A	Family with sequence similarity 65, member A
ENSG00000115234	0.84	SNX17	Sorting nexin 17
ENSG00000135636	0.84	DYSF	Dysferlin, limb girdle muscular dystrophy 2B (autosomal recessive)
ENSG00000102054	0.84	RBBP7	Retinoblastoma binding protein 7
ENSG00000171720	0.84	HDAC3	Histone deacetylase 3
ENSG00000108799	0.84	EZH1	Enhancer of zeste homolog 1 (Drosophila)
ENSG00000114686	0.84	MRPL3	Mitochondrial ribosomal protein L3
ENSG00000115548	0.84	JMJD1A	JmjC domain-containing histone demethylation protein 2A
ENSG00000168175	0.84	C14orf32	NA
ENSG00000189311	0.84	PPME1	Protein phosphatase methylesterase 1
ENSG00000050426	0.84	LETMD1	LETM1 domain containing 1
ENSG00000122042	0.84	UBL3	Ubiquitin-like 3
ENSG00000129170	0.84	CSRP3	Cysteine and glycine-rich protein 3 (cardiac LIM protein)

Ensemble ID	fc	GeneSymbol	Description
ENSG00000132581	0.84	SDF2	Stromal cell-derived factor 2
ENSG00000204427	0.84	BAT5	HLA-B associated transcript 5
ENSG00000120705	0.84	ETF1	Eukaryotic translation termination factor 1
ENSG00000196591	0.84	HDAC2	Histone deacetylase 2
ENSG00000064545	0.84	TMEM161A	Transmembrane protein 161A
ENSG00000071051	0.84	NCK2	NCK adaptor protein 2
ENSG00000117748	0.84	RPA2	Replication protein A2, 32kDa
ENSG00000023697	0.84	DERA	2-deoxyribose-5-phosphate aldolase homolog (C. elegans)
ENSG00000048392	0.84	RRM2B	Ribonucleotide reductase M2 B (TP53 inducible)
ENSG00000011523	0.84	CEP68	Centrosomal protein 68kDa
ENSG00000198218	0.84	QRICH1	Glutamine-rich 1
ENSG00000108671	0.84	PSMD11	Proteasome (prosome, macropain) 26S subunit, non-ATPase, 11
ENSG00000196781	0.84	TLE1	Transducin-like enhancer protein 1
ENSG00000104870	0.84	FCGRT	Fc fragment of IgG, receptor, transporter, alpha
ENSG00000075413	0.84	MARK3	MAP/microtubule affinity-regulating kinase 3
ENSG00000153904	0.84	DDAH1	Dimethylarginine dimethylaminohydrolase 1
ENSG00000107438	0.84	PDLIM1	PDZ and LIM domain 1
ENSG00000135617	0.84	C2orf7	Chromosome 2 open reading frame 7
ENSG00000084623	0.84	EIF3S2	Eukaryotic translation initiation factor 3 subunit 2
ENSG00000198961	0.84	PJA2	Praja ring finger 2
ENSG00000181709	0.84	Q96DH5_HUMAN	GNA11 protein
ENSG00000091164	0.84	TXNL1	Thioredoxin-like 1
ENSG00000156298	0.84	TSPAN7	Tetraspanin 7
ENSG00000137100	0.84	DCTN3	Dynactin 3 (p22)
ENSG00000085063	0.84	CD59	CD59 glycoprotein precursor
ENSG00000132688	0.84	NES	Nestin
ENSG00000134058	0.84	CDK7	Cyclin-dependent kinase 7
ENSG00000102030	0.84	TRIM23	Tripartite motif-containing 23
ENSG00000037474	0.84	NSUN2	NOL1/NOP2/Sun domain family, member 2
ENSG00000110696	0.84	C11orf58	Chromosome 11 open reading frame 58
ENSG00000125772	0.84	GDE5_HUMAN	Putative glycerophosphodiester phosphodiesterase 5
ENSG00000166619	0.84	BLCAP	Bladder cancer associated protein
ENSG00000090487	0.84	SPG21	Spastic paraplegia 21 (autosomal recessive, Mast syndrome)
ENSG00000113648	0.84	H2AFY	Core histone macro-H2A.1
ENSG00000185630	0.84	PBX1	Pre-B-cell leukemia homeobox 1
ENSG00000182551	0.85	ADI1	Acireductone dioxygenase 1
ENSG00000163344	0.85	PMVK	Phosphomevalonate kinase
ENSG00000168264	0.85	IRF2BP2	Interferon regulatory factor 2 binding protein 2
ENSG00000188725	0.85	NP_001041714.1	NA
ENSG00000100083	0.85	GGA1	Golgi associated, gamma adaptin ear containing, ARF binding protein 1
ENSG00000109919	0.85	MTCH2	Mitochondrial carrier homolog 2 (C. elegans)
ENSG00000137815	0.85	RTF1	Rtf1, Paf1/RNA polymerase II complex component, homolog (S. cerevisiae)

Ensemble ID	fc	GeneSymbol	Description
ENSG00000166439	0.85	RNF169	Ring finger protein 169
ENSG00000125733	0.85	TRIP10	Thyroid hormone receptor interactor 10
ENSG00000136842	0.85	TMOD1	Tropomodulin 1
ENSG00000130638	0.85	ATXN10	Ataxin 10
ENSG00000065183	0.85	WDR3	WD repeat domain 3
ENSG00000158864	0.85	NDUFS2	NADH dehydrogenase (ubiquinone) Fe-S protein 2, 49kDa (NADH-coenzyme Q reductase)
ENSG00000092330	0.85	TINF2	TERF1 (TRF1)-interacting nuclear factor 2
ENSG00000188895	0.85	Q68DK7_HUMAN	MSL-1 protein
ENSG00000141627	0.85	DYM	Dymeclin
ENSG00000135316	0.85	SYNCRIP	Synaptotagmin binding, cytoplasmic RNA interacting protein
ENSG00000140400	0.85	MAN2C1	Alpha-mannosidase 2C1
ENSG00000091436	0.85	MLTK_HUMAN	Mitogen-activated protein kinase kinase kinase
ENSG00000105186	0.85	ANKRD27	Ankyrin repeat domain 27 (VPS9 domain)
ENSG00000171914	0.85	TLN2	Talin 2
ENSG00000115993	0.85	TRAK2	Trafficking protein, kinesin binding 2
ENSG00000149658	0.85	YTHDF1	YTH domain family, member 1
ENSG00000106397	0.85	PLOD3	Procollagen-lysine, 2-oxoglutarate 5-dioxygenase 3
ENSG00000174282	0.85	ZBTB4	Zinc finger and BTB domain containing 4
ENSG00000180902	0.85	D2HGDH	D-2-hydroxyglutarate dehydrogenase
ENSG00000126746	0.85	ZNF384	Zinc finger protein 384
ENSG00000140750	0.85	ARHGAP17	Rho GTPase activating protein 17
ENSG00000100031	0.85	GGT1	Gamma-glutamyltransferase 1
ENSG00000157823	0.85	AP3S2	Adaptor-related protein complex 3, sigma 2 subunit
ENSG00000130741	0.85	EIF2S3	Eukaryotic translation initiation factor 2, subunit 3 gamma, 52kDa
ENSG00000105497	0.85	ZNF175	Zinc finger protein 175
ENSG00000149792	0.85	MRPL49	Mitochondrial ribosomal protein L49
ENSG00000143401	0.85	ANP32E	Acidic (leucine-rich) nuclear phosphoprotein 32 family, member E
ENSG00000122779	0.85	TRIM24	Tripartite motif-containing 24
ENSG00000067365	0.85	C16orf68	Chromosome 16 open reading frame 68
ENSG00000114784	0.85	EIF1B	Eukaryotic translation initiation factor 1B
ENSG00000167705	0.85	RILP	Rab interacting lysosomal protein
ENSG00000104980	0.85	TIMM44	Translocase of inner mitochondrial membrane 44 homolog (yeast)
ENSG00000138081	0.85	FBXO11	F-box protein 11
ENSG00000099804	0.85	CDC34	Cell division cycle 34 homolog (S. cerevisiae)
ENSG00000165119	0.85	HNRPK	Heterogeneous nuclear ribonucleoprotein K
ENSG00000177963	0.85	RIC8A	Resistance to inhibitors of cholinesterase 8 homolog A (C. elegans)
ENSG00000087269	0.85	C4orf9	NA
ENSG00000188026	0.85	NP_847884.1	NA
ENSG00000055211	0.85	C6orf72	Chromosome 6 open reading frame 72
ENSG00000132153	0.85	DHX30	DEAH (Asp-Glu-Ala-His) box polypeptide 30
ENSG00000114480	0.85	GBE1	Glucan (1,4-alpha-), branching enzyme 1
ENSG00000134108	0.85	ARL8B	ADP-ribosylation factor-like 8B

Ensemble ID	fc	GeneSymbol	Description
ENSG00000112320	0.85	NP_060483.3	NA
ENSG00000084073	0.85	ZMPSTE24	Zinc metallopeptidase (STE24 homolog, S. cerevisiae)
ENSG00000119446	0.85	RBM18	RNA binding motif protein 18
ENSG00000148143	0.85	ZNF462	Zinc finger protein 462
ENSG00000138095	0.85	LRPPRC	Leucine-rich PPR-motif containing
ENSG00000161999	0.85	NP_001005920.2	Similar to C. Elegans protein F17C8.5
ENSG00000131779	0.85	PEX11B	Peroxisomal biogenesis factor 11 beta
ENSG00000103769	0.85	RAB11A	RAB11A, member RAS oncogene family
ENSG00000196126	0.85	HLA-DRB2	HLA class II histocompatibility antigen, DRB1-1 beta chain precursor
ENSG00000108828	0.85	VAT1	Vesicle amine transport protein 1 homolog (T. californica)
ENSG00000180834	0.85	MAP6D1	MAP6 domain containing 1
ENSG00000138293	0.85	NCOA4	Nuclear receptor coactivator 4
ENSG00000140598	0.85	EFTUD1	Elongation factor Tu GTP binding domain containing 1
ENSG00000160703	0.85	NLRX1	NLR family member X1
ENSG00000149600	0.86	COMMD7	COMM domain containing 7
ENSG00000156795	0.86	C8orf32	NA
ENSG00000187838	0.86	PLSCR3	Phospholipid scramblase 3
ENSG00000116906	0.86	GNPAT	Glyceronephosphate O-acyltransferase
ENSG00000153560	0.86	UBP1	Upstream binding protein 1 (LBP-1a)
ENSG00000138279	0.86	ANXA7	Annexin A7
ENSG00000135446	0.86	CDK4	Cyclin-dependent kinase 4
ENSG00000100938	0.86	Q86T14_HUMAN	guanosine monophosphate reductase 2 (GMPR2), transcript variant 2
ENSG00000090432	0.86	C1orf166	Putative NFkB activating protein
ENSG00000101150	0.86	TPD52L2	Tumor protein D52-like 2
ENSG00000130340	0.86	SNX9	Sorting nexin 9
ENSG00000137693	0.86	YAP1	Yes-associated protein 1, 65kDa
ENSG00000175193	0.86	PARL	Presenilin associated, rhomboid-like
ENSG00000105698	0.86	USF2	Upstream transcription factor 2, c-fos interacting
ENSG00000071626	0.86	DAZAP1	DAZ associated protein 1
ENSG00000150456	0.86	N6AMT2	N-6 adenine-specific DNA methyltransferase 2 (putative)
ENSG00000170348	0.86	TMED10	Transmembrane emp24-like trafficking protein 10 (yeast)
ENSG00000105856	0.86	HBP1	HMG-box transcription factor 1
ENSG00000133706	0.86	LARS	Leucyl-tRNA synthetase
ENSG00000204218	0.86	RGL2	Ral guanine nucleotide dissociation stimulator-like 2
ENSG00000100823	0.86	APEX1	APEX nuclease (multifunctional DNA repair enzyme) 1
ENSG00000147677	0.86	EIF3S3	Eukaryotic translation initiation factor 3 subunit 3
ENSG00000104969	0.86	SGTA	Small glutamine-rich tetratricopeptide repeat (TPR)-containing, alpha
ENSG00000063978	0.86	RNF4	Ring finger protein 4
ENSG00000109911	0.86	ELP4	Elongation protein 4 homolog (S. cerevisiae)
ENSG00000114902	0.86	SPCS1	Signal peptidase complex subunit 1 homolog (S. cerevisiae)
ENSG00000148290	0.86	SURF1	Surfeit 1
ENSG00000162302	0.86	RPS6KA4	Ribosomal protein S6 kinase, 90kDa, polypeptide 4

Ensemble ID	fc	GeneSymbol	Description
ENSG00000183283	0.86	DAZAP2	DAZ associated protein 2
ENSG00000072210	0.86	ALDH3A2	Aldehyde dehydrogenase 3 family, member A2
ENSG00000126261	0.86	SAE2	SUMO-activating enzyme subunit 2
ENSG00000103507	0.86	BCKDK	Branched chain ketoacid dehydrogenase kinase
ENSG00000115816	0.86	CEBPZ	CCAAT/enhancer binding protein (C/EBP), zeta
ENSG00000198858	0.86	C19orf22	Chromosome 19 open reading frame 22
ENSG00000135486	0.86	HNRPA1	Heterogeneous nuclear ribonucleoprotein A1
ENSG00000163788	0.86	SNRK	SNF related kinase
ENSG00000164182	0.86	NDUFA12L	Mimitin, mitochondrial precursor
ENSG00000160767	0.86	C1orf2	Chromosome 1 open reading frame 2
ENSG00000153574	0.86	RPIA	Ribose 5-phosphate isomerase A
ENSG00000056050	0.87	C4orf27	Chromosome 4 open reading frame 27
ENSG00000121774	0.87	KHDRBS1	KH domain containing, RNA binding, signal transduction associated 1
ENSG00000136436	0.87	CALCOCO2	Calcium binding and coiled-coil domain 2
ENSG00000160058	0.87	BSDC1	BSD domain containing 1
ENSG00000143149	0.87	ALDH9A1	Aldehyde dehydrogenase 9 family, member A1
ENSG00000161542	0.87	PRPSAP1	Phosphoribosyl pyrophosphate synthetase-associated protein 1
ENSG00000145332	0.87	KLHL8	Kelch-like 8 (Drosophila)
ENSG00000013563	0.87	DNASE1L1	Deoxyribonuclease I-like 1
ENSG00000197879	0.87	MYO1C	Myosin IC
ENSG00000125107	0.87	CNOT1	CCR4-NOT transcription complex, subunit 1
ENSG00000074319	0.87	TSG101	Tumor susceptibility gene 101
ENSG00000105053	0.87	VRK3	Vaccinia related kinase 3
ENSG00000074590	0.87	NUAK1	NUAK family, SNF1-like kinase, 1
ENSG00000112511	0.87	PHF1	PHD finger protein 1
ENSG00000131269	0.87	ABCB7	ATP-binding cassette, sub-family B (MDR/TAP), member 7
ENSG00000204568	0.87	MRPS18B	Mitochondrial ribosomal protein S18B
ENSG00000062650	0.87	WAPAL	Wings apart-like protein homolog
ENSG00000011009	0.87	LYPLA2	Lysophospholipase II
ENSG00000162032	0.87	SPSB3	SplA/ryanodine receptor domain and SOCS box containing 3
ENSG00000084234	0.87	APLP2	Amyloid beta (A4) precursor-like protein 2
ENSG00000102931	0.87	ARL2BP	ADP-ribosylation factor-like 2 binding protein
ENSG00000166333	0.87	ILK	Integrin-linked kinase
ENSG00000103496	0.87	STX4	Syntaxin 4
ENSG00000106049	0.87	HIBADH	3-hydroxyisobutyrate dehydrogenase
ENSG00000121067	0.87	SPOP	Speckle-type POZ protein
ENSG00000135372	0.87	NAT10	N-acetyltransferase 10 (GCN5-related)
ENSG00000141447	0.87	OSBPL1A	Oxysterol binding protein-like 1A
ENSG00000139370	0.87	SLC15A4	Solute carrier family 15, member 4
ENSG00000182660	0.87	NP_001013698.1	NA
ENSG00000117614	0.87	SYF2	SYF2 homolog, RNA splicing factor (S. cerevisiae)
ENSG00000069329	0.87	VPS35	Vacuolar protein sorting 35 homolog (S. cerevisiae)
ENSG00000165660	0.87	KIAA0157	NA

Ensemble ID	fc	GeneSymbol	Description
ENSG00000147140	0.87	NONO	Non-POU domain-containing octamer-binding protein
ENSG00000161671	0.87	NP_996261.1	hematopoietic signal peptide-containing isoform 2
ENSG00000120727	0.87	PAIP2	Polyadenylate-binding protein-interacting protein 2
ENSG00000163161	0.87	ERCC3	Excision repair cross-complementing rodent repair deficiency, complementation group 3 (xeroderma pigmentosum group B complementing)
ENSG00000104679	0.87	R3HCC1	R3H domain and coiled-coil containing 1
ENSG00000102158	0.87	IAG2_HUMAN	Implantation-associated protein precursor
ENSG00000167220	0.87	HDHD2	Haloacid dehalogenase-like hydrolase domain containing 2
ENSG00000110344	0.87	UBE4A	Ubiquitination factor E4A (UFD2 homolog, yeast)
ENSG00000136521	0.87	NDUFB5	NADH dehydrogenase (ubiquinone) 1 beta subcomplex, 5, 16kDa
ENSG00000130429	0.87	ARPC1B	Actin-related protein 2/3 complex subunit 1B
ENSG00000116863	0.87	ADPRHL2	ADP-ribosylhydrolase like 2
ENSG00000135506	0.87	OS9_HUMAN	Protein OS-9 precursor
ENSG00000170248	0.87	PDCD6IP	Programmed cell death 6 interacting protein
ENSG00000101391	0.87	CDK5RAP1	CDK5 regulatory subunit associated protein 1
ENSG00000119725	0.88	ZNF410	Zinc finger protein 410
ENSG00000035141	0.88	NP_116211.1	NA
ENSG00000169180	0.88	XPO6	Exportin 6
ENSG00000120071	0.88	KIAA1267	KIAA1267
ENSG00000143549	0.88	TPM3	Tropomyosin alpha-3 chain
ENSG00000144671	0.88	SLC22A14	Solute carrier family 22, member 14
ENSG00000116685	0.88	KIAA2013	KIAA2013
ENSG00000165516	0.88	KLHDC2	Kelch domain containing 2
ENSG00000114062	0.88	UBE3A	Ubiquitin protein ligase E3A
ENSG00000138592	0.88	USP8	Ubiquitin specific peptidase 8
ENSG00000113312	0.88	TTC1	Tetratricopeptide repeat domain 1
ENSG00000163539	0.88	CLASP2	Cytoplasmic linker associated protein 2
ENSG00000158019	0.88	BRE	Brain and reproductive organ-expressed protein
ENSG00000100601	0.88	ALKBH1	AlkB, alkylation repair homolog 1 (E. coli)
ENSG00000168894	0.88	NP_057578.1	NA
ENSG00000133193	0.88	FAM104A	Family with sequence similarity 104, member A
ENSG00000182604	0.88		NA
ENSG00000115073	0.88	ACTR1B	ARP1 actin-related protein 1 homolog B, centractin beta (yeast)
ENSG00000132466	0.88	ANKRD17	Ankyrin repeat domain 17
ENSG00000163069	0.88	SGCB	Sarcoglycan, beta (43kDa dystrophin-associated glycoprotein)
ENSG00000134759	0.88	STATIP1	Stat3-interacting protein
ENSG00000186834	0.88	HEXIM1	Hexamethylene bis-acetamide inducible 1
ENSG00000113558	0.88	SKP1A	S-phase kinase-associated protein 1A
ENSG00000109445	0.88	ZNF330	Zinc finger protein 330
ENSG00000138303	0.88	ASCC1	Activating signal cointegrator 1 complex subunit 1
ENSG00000164366	0.88	CCDC127	Coiled-coil domain containing 127
ENSG00000175220	0.88	ARHGAP1	Rho GTPase activating protein 1
ENSG00000116161	0.88	CACYBP	Calcyclin binding protein

Ensemble ID	fc	GeneSymbol	Description
ENSG00000152102	0.88	NP_001009993.2	p20
ENSG00000101193	0.88	C20orf11	Chromosome 20 open reading frame 11
ENSG00000153339	0.88	KIAA1012	KIAA1012
ENSG00000168003	0.88	SLC3A2	Solute carrier family 3 (activators of dibasic and neutral amino acid transport), member 2
ENSG00000115317	0.88	HTRA2	HtrA serine peptidase 2
ENSG00000075856	0.89	SART3	Squamous cell carcinoma antigen recognized by T cells 3
ENSG00000174748	0.89	RPL15	Ribosomal protein L15
ENSG00000110442	0.89	COMMD9	COMM domain containing 9
ENSG00000095209	0.89	TMEM38B	Transmembrane protein 38B
ENSG00000078369	0.89	GNB1	Guanine nucleotide binding protein (G protein), beta polypeptide 1
ENSG00000003393	0.89	ALS2	Amyotrophic lateral sclerosis 2 (juvenile)
ENSG00000175756	0.89	AURKAIP1	Aurora kinase A interacting protein 1
ENSG00000198176	0.89	TFDP1	Transcription factor Dp-1
ENSG00000125944	0.89	HNRPR	Heterogeneous nuclear ribonucleoprotein R
ENSG00000171604	0.89	CXXC5	CXXC finger 5
ENSG00000107021	0.89	TBC1D13	TBC1 domain family, member 13
ENSG00000077097	0.89	TOP2B	Topoisomerase (DNA) II beta 180kDa
ENSG00000173011	0.89	Q86TJ2_HUMAN	NA
ENSG00000156990	0.89	RPUSD3	RNA pseudouridylate synthase domain containing 3
ENSG00000177885	0.89	GRB2	Growth factor receptor-bound protein 2
ENSG00000158417	0.89	EIF5B	Eukaryotic translation initiation factor 5B
ENSG00000165943	0.89	MOAP1	Modulator of apoptosis 1
ENSG00000173812	0.89	EIF1	Eukaryotic translation initiation factor 1
ENSG00000204439	0.89	C6orf47	Chromosome 6 open reading frame 47
ENSG00000117408	0.89	IPO13	Importin 13
ENSG00000084093	0.89	REST	RE1-silencing transcription factor
ENSG00000108840	0.89	HDAC5	Histone deacetylase 5
ENSG00000147364	0.89	FBXO25	F-box protein 25
ENSG00000068697	0.89	LAPTM4A	Lysosomal protein transmembrane 4 alpha
ENSG00000153250	0.89	RBMS1	RNA binding motif, single stranded interacting protein 1
ENSG00000119638	0.89	NEK9	NIMA (never in mitosis gene a)- related kinase 9
ENSG00000104824	0.89	HNRPL	Heterogeneous nuclear ribonucleoprotein L
ENSG00000078140	0.89	HIP2	Ubiquitin-conjugating enzyme E2-25 kDa (EC 6.3.2.19) (Ubiquitin- protein ligase) (Ubiquitin carrier protein) (E2(25K)) (Huntingtin- interacting protein 2) (HIP-2). [Source:Uniprot/SWISSPROT;Acc:P61086]
ENSG00000163320	0.89		CGG triplet repeat binding protein 1
ENSG00000180632	0.89		NA
ENSG00000154582	0.89	TCEB1	Transcription elongation factor B (SIII), polypeptide 1 (15kDa, elongin C)
ENSG00000114650	0.89	SCAP	SREBF chaperone
ENSG00000163820	0.89	FYCO1	FYVE and coiled-coil domain containing 1
ENSG00000148925	0.90	BTBD10	BTB (POZ) domain containing 10
ENSG00000111642	0.90	CHD4	Chromodomain helicase DNA binding protein 4
ENSG00000102921	0.90	N4BP1_HUMAN	NEDD4-binding protein 1

Ensemble ID	fc	GeneSymbol	Description
ENSG00000112335	0.90	SNX3	Sorting nexin 3
ENSG00000111641	0.90	NOL1	Proliferating-cell nucleolar antigen p120
ENSG00000114388	0.90	TUSC4	Tumor suppressor candidate 4
ENSG00000115307	0.90	AUP1	Ancient ubiquitous protein 1
ENSG00000114054	0.90	PCCB	Propionyl Coenzyme A carboxylase, beta polypeptide
ENSG00000142230	0.90	SAE1	SUMO1 activating enzyme subunit 1
ENSG00000168288	0.90	C2orf25	NA
ENSG00000161835	0.90	GRASP	GRP1 (general receptor for phosphoinositides 1)-associated scaffold protein
ENSG00000162734	0.90	PEA15	Phosphoprotein enriched in astrocytes 15
ENSG00000162961	0.90	DPY30_HUMAN	Dpy-30-like protein
ENSG00000108963	0.90	DPH1	DPH1 homolog (S. cerevisiae)
ENSG00000107897	0.90	ACBD5	Acyl-Coenzyme A binding domain containing 5
ENSG00000104067	0.90	TJP1	Tight junction protein 1 (zona occludens 1)
ENSG00000083454	0.90	TAX1BP3	Tax1 (human T-cell leukemia virus type I) binding protein 3
ENSG00000071889	0.90	FAM3A	Family with sequence similarity 3, member A
ENSG00000078070	0.90	MCCC1	Methylcrotonoyl-Coenzyme A carboxylase 1 (alpha)
ENSG00000105648	0.90	IFI30	Interferon, gamma-inducible protein 30
ENSG00000144647	0.90	C3orf39	Chromosome 3 open reading frame 39
ENSG00000122783	0.91	C7orf49	Chromosome 7 open reading frame 49
ENSG00000146701	0.91	MDH2	Malate dehydrogenase 2, NAD (mitochondrial)
ENSG00000123130	0.91	ACOT9	Acyl-CoA thioesterase 9
ENSG00000169217	0.91	CD2BP2	CD2 (cytoplasmic tail) binding protein 2
ENSG00000142168	0.91	SOD1	Superoxide dismutase 1, soluble
ENSG00000145362	0.91	ANK2	Ankyrin 2, neuronal
ENSG00000085871	0.91	MGST2	Microsomal glutathione S-transferase 2
ENSG00000131966	0.91	ACTR10	Actin-related protein 10 homolog (S. cerevisiae)
ENSG00000119844	1.13	AFTPH	Aftiphilin
ENSG00000082996	1.13	RNF13	Ring finger protein 13
ENSG00000144677	1.13	CTDSPL	CTD (carboxy-terminal domain, RNA polymerase II, polypeptide A) small phosphatase-like
ENSG00000166479	1.13	TXNDC10	Protein disulfide-isomerase
ENSG00000138385	1.14	SSB	Sjogren syndrome antigen B (autoantigen La)
ENSG00000105583	1.14	C19orf56	Chromosome 19 open reading frame 56
ENSG00000054267	1.14	ARID4B	AT rich interactive domain 4B (RBP1-like)
ENSG00000162694	1.14	EXTL2	Exostoses (multiple)-like 2
ENSG00000189227	1.14	LOC145853	NA
ENSG00000153037	1.14	SRP19	Signal recognition particle 19kDa
ENSG00000064726	1.15	BTBD1	BTB (POZ) domain containing 1
ENSG00000169926	1.15	KLF13	Kruppel-like factor 13
ENSG00000090266	1.15	NDUFB2	NADH dehydrogenase (ubiquinone) 1 beta subcomplex, 2, 8kDa
ENSG00000165874	1.15	FAM35A	Family with sequence similarity 35, member A
ENSG00000135698	1.16	MPHOSPH6	M-phase phosphoprotein 6
ENSG00000113387	1.16	SUB1	SUB1 homolog (S. cerevisiae)

Ensemble ID	fc	GeneSymbol	Description
ENSG00000183513	1.16	NP_001008216.1	NA
ENSG00000166710	1.16	B2M	Beta-2-microglobulin
ENSG00000104231	1.16	ZFAND1	Zinc finger, AN1-type domain 1
ENSG00000102897	1.16	LYRM1	LYR motif containing 1
ENSG00000079134	1.16	THOC1	THO complex 1
ENSG00000144785	1.16	TMEM4	MIR-interacting saposin-like protein precursor
ENSG00000205560	1.16	CHKB	Choline kinase beta
ENSG00000127184	1.16	COX7C	Cytochrome c oxidase subunit VIIc
ENSG00000182670	1.16	TTC3	Tetratricopeptide repeat domain 3
ENSG00000138035	1.16	PNPT1	Polyribonucleotide nucleotidyltransferase 1
ENSG00000115514	1.17	TXNDC9	Thioredoxin domain containing 9
ENSG00000119013	1.17	NDUFB3	NADH dehydrogenase (ubiquinone) 1 beta subcomplex, 3, 12kDa
ENSG00000166200	1.17	COPS2	COP9 constitutive photomorphogenic homolog subunit 2 (Arabidopsis)
ENSG00000164828	1.17	UNC84A	Unc-84 homolog A (C. elegans)
ENSG00000116747	1.18	TROVE2	TROVE domain family, member 2
ENSG00000161547	1.18	SFRS2	Splicing factor, arginine/serine-rich 2
ENSG00000124593	1.18	C6orf49	LIM domain-containing protein
ENSG00000127540	1.18	UQCR	Ubiquinol-cytochrome c reductase, 6.4kDa subunit
ENSG00000164898	1.18	NP_932068.1	NA
ENSG00000120333	1.18	MRPS14	Mitochondrial ribosomal protein S14
ENSG00000118939	1.18	UCHL3	Ubiquitin carboxyl-terminal esterase L3 (ubiquitin thiolesterase)
ENSG00000143198	1.18	MGST3	Microsomal glutathione S-transferase 3
ENSG00000116560	1.18	SFPQ	Splicing factor proline/glutamine-rich (polypyrimidine tract binding protein associated)
ENSG00000127720	1.19	C12orf26	Chromosome 12 open reading frame 26
ENSG00000070501	1.19	POLB	Polymerase (DNA directed), beta
ENSG00000100387	1.19	RBX1	Ring-box 1
ENSG00000115414	1.19	FN1	Fibronectin 1
ENSG00000134253	1.19	TRIM45	Tripartite motif-containing 45
ENSG00000147027	1.19	TMEM47	Transmembrane protein 47
ENSG00000100211	1.19	PGEA1	PKD2 interactor, Golgi and endoplasmic reticulum associated 1
ENSG00000066557	1.19	LRRC40	Leucine rich repeat containing 40
ENSG00000132274	1.19	TRIM22	Tripartite motif-containing protein 22
ENSG00000156467	1.20	UQCRB	Ubiquinol-cytochrome c reductase binding protein
ENSG00000138801	1.20	PAPSS1	3'-phosphoadenosine 5'-phosphosulfate synthase 1
ENSG00000167280	1.20	NP_001036038.1	endo-beta-N-acetylglucosaminidase
ENSG00000151500	1.20	THYN1	Thymocyte nuclear protein 1
ENSG00000203743	1.20	Q5J7V3_HUMAN	Migration-inducing gene 16 protein
ENSG00000076513	1.20	ANKRD13A	Ankyrin repeat domain 13A
ENSG00000181038	1.20	Q8N712_HUMAN	NA
ENSG00000204370	1.20	SDHD	Succinate dehydrogenase complex, subunit D, integral membrane protein
ENSG00000115350	1.21	POLE4	Polymerase (DNA-directed), epsilon 4 (p12 subunit)
ENSG00000163797	1.21	MRPL33	Mitochondrial ribosomal protein L33

Ensemble ID	fc	GeneSymbol	Description
ENSG00000162407	1.21	PPAP2B	Lipid phosphate phosphohydrolase 3
ENSG00000006625	1.21	C7orf24	NA
ENSG00000166147	1.21	FBN1	Fibrillin 1
ENSG00000103121	1.21	C16orf61	Chromosome 16 open reading frame 61
ENSG00000182117	1.21	NOLA3	H/ACA ribonucleoprotein complex subunit 3
ENSG00000171862	1.21	PTENP1	Phosphatase and tensin homolog pseudogene 1
ENSG00000165672	1.22	PRDX3	Thioredoxin-dependent peroxide reductase
ENSG00000100697	1.22	DICER1	Dicer 1, ribonuclease type III
ENSG00000122033	1.23	MTIF3	Mitochondrial translational initiation factor 3
ENSG00000116717	1.23	GADD45A	Growth arrest and DNA-damage-inducible, alpha
ENSG00000182600	1.23	NP_996778.1	NA
ENSG00000165264	1.23	NDUFB6	NADH dehydrogenase (ubiquinone) 1 beta subcomplex, 6, 17kDa
ENSG00000111237	1.23	VPS29	Vacuolar protein sorting 29 homolog (S. cerevisiae)
ENSG00000136161	1.23	RCBTB2	Regulator of chromosome condensation (RCC1) and BTB (POZ) domain containing protein 2
ENSG00000173027	1.23	WBP1	WW domain binding protein 1
ENSG00000023041	1.23	ZDHHC6	Zinc finger, DHHC-type containing 6
ENSG00000125676	1.24	THOC2	THO complex 2
ENSG00000196549	1.24	MME	Membrane metallo-endopeptidase
ENSG00000196233	1.24	LCOR	Ligand dependent nuclear receptor corepressor
ENSG00000160808	1.24	MYL3	Myosin, light chain 3, alkali; ventricular, skeletal, slow
ENSG00000005075	1.24	POLR2J	Polymerase (RNA) II (DNA directed) polypeptide J, 13.3kDa
ENSG00000157510	1.24	NP_689619.1	NA
ENSG00000144182	1.24	LIPT1	Lipoyltransferase 1, mitochondrial precursor (EC 6.-.-.-) (Lipoate- protein ligase) (Lipoate biosynthesis protein) (Lipoyl ligase). [Source:Uniprot/SWISSPROT;Acc:Q9Y234]
ENSG00000183617	1.24	MRPL54	Mitochondrial ribosomal protein L54
ENSG00000197335	1.24		NA
ENSG00000196683	1.24	TOMM7	Translocase of outer mitochondrial membrane 7 homolog (yeast)
ENSG00000027697	1.25	IFNGR1	Interferon gamma receptor 1
ENSG00000172171	1.25	C17orf42	Chromosome 17 open reading frame 42
ENSG00000137500	1.25	CCDC90B	Coiled-coil domain containing 90B
ENSG00000071794	1.25	HLTF	Helicase-like transcription factor
ENSG00000136147	1.25	PHF11	PHD finger protein 11
ENSG00000139617	1.25	NP_055702.1	phosphonoformate immuno-associated protein 5
ENSG00000130508	1.25	PXDN	Peroxidasin homolog (Drosophila)
ENSG00000163520	1.25	FBLN2	Fibulin 2
ENSG00000106591	1.25	MRPL32	Mitochondrial ribosomal protein L32
ENSG00000169567	1.26	HINT1	Histidine triad nucleotide binding protein 1
ENSG00000114209	1.26	PDCD10	Programmed cell death 10
ENSG00000059588	1.26	TARBP1	TAR (HIV-1) RNA binding protein 1
ENSG00000149273	1.26	RPS3	Ribosomal protein S3
ENSG00000143933	1.27	CALM2	Calmodulin 2 (phosphorylase kinase, delta)
ENSG00000173915	1.27	USMG5	Up-regulated during skeletal muscle growth 5 homolog (mouse)

Ensemble ID	fc	GeneSymbol	Description
ENSG00000112893	1.27	MAN2A1	Mannosidase, alpha, class 2A, member 1
ENSG00000204256	1.27	BRD2	Bromodomain containing 2
ENSG00000118292	1.28	C1orf54	Chromosome 1 open reading frame 54
ENSG00000173221	1.28	GLRX	Glutaredoxin (thioltransferase)
ENSG00000134490	1.28	C18orf45	Chromosome 18 open reading frame 45
ENSG00000143442	1.29	POGZ	Pogo transposable element with ZNF domain
ENSG00000205707	1.29	LYRM5	LYR motif containing 5
ENSG00000108381	1.29	ASPA	Aspartoacylase (Canavan disease)
ENSG00000169976	1.29	SF3B5	Splicing factor 3b, subunit 5, 10kDa
ENSG00000139679	1.30	P2RY5	Purinergic receptor P2Y, G-protein coupled, 5
ENSG00000099964	1.30	MIF	Macrophage migration inhibitory factor (glycosylation-inhibiting factor)
ENSG00000068615	1.31	REEP1	Receptor accessory protein 1
ENSG00000110077	1.31	MS4A6A	Membrane-spanning 4-domains, subfamily A, member 6A
ENSG00000116754	1.31	SFRS11	Splicing factor, arginine/serine-rich 11
ENSG00000189043	1.31	NDUFA4	NADH dehydrogenase (ubiquinone) 1 alpha subcomplex, 4, 9kDa
ENSG00000137210	1.32	TMEM14B	Transmembrane protein 14B
ENSG00000109270	1.32	MAP2K1IP1	Mitogen-activated protein kinase kinase 1-interacting protein 1
ENSG00000160916	1.32	ATP5J2	ATP synthase f chain, mitochondrial
ENSG00000206528	1.32	Q6ZSM0_HUMAN	NA
ENSG00000109238	1.32	COX7A3	Cytochrome c oxidase subunit VIIa 3
ENSG00000177600	1.32	RPLP2	Ribosomal protein, large, P2
ENSG00000124193	1.33	SFRS6	Splicing factor, arginine/serine-rich 6
ENSG00000107020	1.33	C9orf46	Chromosome 9 open reading frame 46
ENSG00000115963	1.33	RND3	Rho family GTPase 3
ENSG00000156411	1.33	C14orf2	Chromosome 14 open reading frame 2
ENSG00000034510	1.34	TMSB10	Thymosin beta 10
ENSG00000184575	1.34	XPOT	Exportin, tRNA (nuclear export receptor for tRNAs)
ENSG00000118418	1.34	HMGN3	High mobility group nucleosomal binding domain 3
ENSG00000122643	1.34	NT5C3	5'-nucleotidase, cytosolic III
ENSG00000005810	1.34	MYCBP2	MYC binding protein 2
ENSG00000155367	1.34	PPM1J	Protein phosphatase 1J (PP2C domain containing)
ENSG00000088448	1.34	ANKRD10	Ankyrin repeat domain 10
ENSG00000175197	1.34	DDIT3	DNA damage-inducible transcript 3
ENSG00000188447	1.35	LOC390604	NA
ENSG00000010322	1.35	NISCH	Nischarin
ENSG00000104408	1.35	EIF3S6	Eukaryotic translation initiation factor 3 subunit 6
ENSG00000039319	1.35	ZFYVE16	Zinc finger, FYVE domain containing 16
ENSG00000204820	1.35	Q96NT9_HUMAN	GR AF-1 specific protein phosphatase
ENSG00000183963	1.35	SMTN	Smoothelin
ENSG00000172172	1.35	MRPL13	Mitochondrial ribosomal protein L13
ENSG00000178449	1.35	C12orf62	Chromosome 12 open reading frame 62
ENSG00000140450	1.35	ARRDC4	Arrestin domain containing 4

Ensemble ID	fc	GeneSymbol	Description
ENSG00000111341	1.35	MGP	Matrix Gla protein
ENSG00000183648	1.35	NDUFB1	NADH dehydrogenase (ubiquinone) 1 beta subcomplex, 1, 7kDa
ENSG00000102760	1.35	C13orf15	Chromosome 13 open reading frame 15
ENSG00000198523	1.36	PLN	Phospholamban
ENSG00000165792	1.36	METT11D1	Methyltransferase 11 domain containing 1
ENSG00000198235	1.36		similar to 40S ribosomal protein S17
ENSG00000136783	1.36	NIPSNAP3A	Nipsnap homolog 3A (C. elegans)
ENSG00000129152	1.37	MYOD1	Myogenic differentiation 1
ENSG00000144476	1.37	CXCR7	Chemokine (C-X-C motif) receptor 7
ENSG00000161281	1.37	COX7A1	Cytochrome c oxidase subunit VIIa polypeptide 1 (muscle)
ENSG00000132485	1.37	ZRANB2	Zinc finger, RAN-binding domain containing 2
ENSG00000132541	1.38	HRSP12	Heat-responsive protein 12
ENSG00000121310	1.38	ECHDC2	Enoyl Coenzyme A hydratase domain containing 2
ENSG00000175768	1.38	C9orf105	NA
ENSG00000178950	1.38	GAK	Cyclin G associated kinase
ENSG00000154553	1.38	PDLIM3	PDZ and LIM domain 3
ENSG00000116791	1.39	CRYZ	Crystallin, zeta (quinone reductase)
ENSG00000112146	1.39	FBXO9	F-box protein 9
ENSG00000113240	1.40	CLK4	CDC-like kinase 4
ENSG00000156931	1.40	VPS8	Vacuolar protein sorting 8 homolog (S. cerevisiae)
ENSG00000164919	1.40	COX6C	Cytochrome c oxidase subunit VIc
ENSG00000092841	1.40	MYL6	Myosin, light chain 6, alkali, smooth muscle and non-muscle
ENSG00000163170	1.40	BOLA3	BolA homolog 3 (E. coli)
ENSG00000124370	1.40	MCEE	Methylmalonyl CoA epimerase
ENSG00000166136	1.42	NDUFB8	NADH dehydrogenase (ubiquinone) 1 beta subcomplex, 8, 19kDa
ENSG00000197969	1.42	VPS13A	Vacuolar protein sorting 13 homolog A (S. cerevisiae)
ENSG00000185222	1.42	WBP5	WW domain binding protein 5
ENSG00000100320	1.42	RBM9	RNA binding motif protein 9
ENSG00000204262	1.43	COL5A2	Collagen, type V, alpha 2
ENSG00000011465	1.43	DCN	Decorin
ENSG00000182457	1.43	Q9NWT5_HUMAN	taurine upregulated gene 1
ENSG00000122566	1.44	HNRPA2B1	Heterogeneous nuclear ribonucleoproteins A2/B1
ENSG00000176261	1.45	ZBTB8OS	Zinc finger and BTB domain containing 8 opposite strand
ENSG00000127990	1.45	SGCE	Sarcoglycan, epsilon
ENSG00000166012	1.46	SNORA32	Small nucleolar RNA, H/ACA box 32
ENSG00000167468	1.46	GPX4	Glutathione peroxidase 4 (phospholipid hydroperoxidase)
ENSG00000127914	1.46	AKAP9	A kinase (PRKA) anchor protein (yotiao) 9
ENSG00000137288	1.46	C6orf125	Chromosome 6 open reading frame 125
ENSG00000116489	1.47	CAPZA1	Capping protein (actin filament) muscle Z-line, alpha 1
ENSG00000144034	1.48	TPRKB	TP53RK binding protein
ENSG00000179085	1.48	DPM3	Dolichyl-phosphate mannosyltransferase polypeptide 3
ENSG00000186566	1.48	GPATCH8	G patch domain containing 8

Ensemble ID	fc	GeneSymbol	Description
ENSG00000173960	1.49	UBXD4	UBX domain-containing protein 4
ENSG00000125730	1.49	C3	Complement component 3
ENSG00000104213	1.49	PDGFRL	Platelet-derived growth factor receptor-like
ENSG00000148700	1.49	ADD3	Adducin 3 (gamma)
ENSG00000176718	1.50	C5orf26	Chromosome 5 open reading frame 26
ENSG00000134853	1.51	PDGFRA	Platelet-derived growth factor receptor, alpha polypeptide
ENSG00000185847	1.51	Q8IVN4_HUMAN	NA
ENSG00000198695	1.52	MT-ND6	NADH-ubiquinone oxidoreductase chain 6
ENSG00000168002	1.52	POLR2G	Polymerase (RNA) II (DNA directed) polypeptide G
ENSG00000131016	1.53	AKAP12	A kinase (PRKA) anchor protein 12
ENSG00000119927	1.53	GPAM	Glycerol-3-phosphate acyltransferase, mitochondrial
ENSG00000115934	1.54	PPIL3	Peptidylprolyl isomerase (cyclophilin)-like 3
ENSG00000100650	1.54	SFRS5	Splicing factor, arginine/serine-rich 5
ENSG00000100941	1.54	PNN	Pinin, desmosome associated protein
ENSG00000114770	1.55	ABCC5	ATP-binding cassette, sub-family C (CFTR/MRP), member 5
ENSG00000101938	1.55	CHRDL1	Chordin-like 1
ENSG00000139329	1.55	LUM	Lumican
ENSG00000147421	1.56	HMBOX1	Homeobox containing 1
ENSG00000169019	1.56	COMMD8	COMM domain containing 8
ENSG00000186166	1.56	CCDC84	Coiled-coil domain containing 84
ENSG00000166681	1.56	NGFRAP1	Nerve growth factor receptor-associated protein 1
ENSG00000171204	1.56	TMEM126B	Transmembrane protein 126B
ENSG00000125995	1.57	C20orf52	NA
ENSG00000003756	1.59	RBM5	RNA-binding protein 5
ENSG00000141338	1.60	ABCA8	ATP-binding cassette, sub-family A (ABC1), member 8
ENSG00000115592	1.60	PRKAG3	Protein kinase, AMP-activated, gamma 3 non-catalytic subunit
ENSG00000006652	1.62	IFRD1	Interferon-related developmental regulator 1
ENSG00000119705	1.62	C14orf156	Chromosome 14 open reading frame 156
ENSG00000135046	1.63	ANXA1	Annexin A1
ENSG00000106484	1.64	MEST	Mesoderm specific transcript homolog (mouse)
ENSG00000168542	1.64	COL3A1	Collagen, type III, alpha 1
ENSG00000204460	1.65	Q499Y1_HUMAN	NA
ENSG00000089335	1.65	ZNF302	Zinc finger protein 302
ENSG00000009413	1.66	REV3L	REV3-like, catalytic subunit of DNA polymerase zeta (yeast)
ENSG00000204291	1.66	COL15A1	Collagen, type XV, alpha 1
ENSG00000186594	1.67	NP_001001870.1	NA
ENSG00000154188	1.67	ANGPT1	Angiopoietin 1
ENSG00000132680	1.68	KIAA0907	KIAA0907
ENSG00000207786	1.70	hsa-mir-133a-1	NA
ENSG00000181722	1.75	ZBTB20	Zinc finger and BTB domain containing 20
ENSG00000123689	1.76	G0S2	Putative lymphocyte G0/G1 switch protein 2
ENSG00000164692	1.77	COL1A2	Collagen, type I, alpha 2
ENSG00000108773	1.79	GCN5L2	General control of amino acid synthesis protein 5-like 2

Ensemble ID	fc	GeneSymbol	Description
ENSG00000116148	1.81	CCNL2	Cyclin-L2
ENSG00000123636	1.89	BAZ2B	Bromodomain adjacent to zinc finger domain, 2B
ENSG00000121350	1.89	NP_079130.2	NA
ENSG00000188536	1.94	HBA1	Hemoglobin, alpha 1
ENSG00000132424	2.00	C6orf111	Splicing factor, arginine/serine-rich 130
ENSG00000175606	2.01	TMEM70	Transmembrane protein 70
ENSG00000198722	2.01	UNC13B	Unc-13 homolog B (C. elegans)
ENSG00000108654	2.04	DDX5	DEAD (Asp-Glu-Ala-Asp) box polypeptide 5
ENSG00000114120	2.08	SLC25A36	Solute carrier family 25, member 36
ENSG00000109920	2.09	FNBP4	Formin binding protein 4
ENSG00000129204	2.16	USP6	Ubiquitin specific peptidase 6 (Tre-2 oncogene)
ENSG00000013441	2.16	CLK1	CDC-like kinase 1
ENSG00000189058	2.29	APOD	Apolipoprotein D
ENSG00000108848	2.48	CROP_HUMAN	Cisplatin resistance-associated overexpressed protein
ENSG00000166348	2.57	USP54	Ubiquitin specific peptidase 54
ENSG00000109061	2.60	MYH1	Myosin, heavy chain 1, skeletal muscle, adult
ENSG00000184027	2.75	MALAT_HUMAN	Metastasis-associated lung adenocarcinoma transcript 1
ENSG00000109046	2.93	WSB1	WD repeat and SOCS box-containing 1
ENSG00000117616	2.98	C1orf63	Chromosome 1 open reading frame 63
ENSG00000204691	3.04	Q9H355_HUMAN	metastasis associated lung adenocarcinoma transcript 1 (non-coding RNA)
ENSG00000188170	4.01	HBB	Hemoglobin, beta